

AD-764 795

AN EVALUATION OF MATERIAL FOR INVESTIGATION OF  
TEST METHODS FOR BRITTLE MATERIALS

SOUTHERN RESEARCH INSTITUTE

PREPARED FOR  
AIR FORCE MATERIALS LABORATORY

OCTOBER 1972

Distributed By:



National Technical Information Service  
U. S. DEPARTMENT OF COMMERCE

## **DISCLAIMER NOTICE**

**THIS DOCUMENT IS BEST QUALITY  
PRACTICABLE. THE COPY FURNISHED  
TO DTIC CONTAINED A SIGNIFICANT  
NUMBER OF PAGES WHICH DO NOT  
REPRODUCE LEGIBLY.**

AD 764795

# AN EVALUATION OF MATERIAL FOR INVESTIGATION OF TEST METHODS FOR BRITTLE MATERIALS

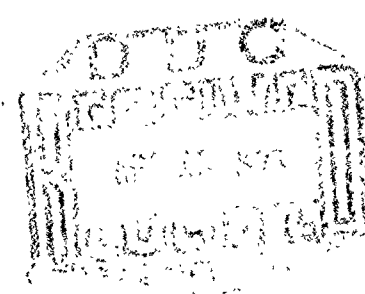
J. R. BROWN, JR.  
R. J. BICKELHAUPT  
H. S. STARRETT  
C. D. PEARS

SOUTHERN RESEARCH INSTITUTE

TECHNICAL REPORT NO. AFML-TR-72-219

Reproduced by  
NATIONAL TECHNICAL  
INFORMATION SERVICE  
U S Department of Commerce  
Springfield VA 22151

OCTOBER 1972



Approved for public release; distribution unlimited.

AIR FORCE MATERIALS LABORATORY  
AIR FORCE SYSTEMS COMMAND  
WRIGHT-PATTERSON AIR FORCE BASE, OHIO

ACCESSION NO.	
NTIS	WALL SOURCE <input checked="" type="checkbox"/>
DDO	EXT SOURCE <input type="checkbox"/>
UNCLASSIFIED	<input type="checkbox"/>
JUSTIFICATION	

BY	
DISTRIBUTION AVAILABILITY CODES	

Dist.	Avail. to / of SPECIAL
-------	------------------------

A	
---	--

## NOTICE

When Government drawings, specifications, or other data are used for any purpose other than in connection with a definitely related Government procurement operation, the United States Government thereby incurs no responsibility nor any obligation whatsoever; and the fact that the government may have formulated, furnished, or in any way supplied the said drawings, specifications, or other data, is not to be regarded by implication or otherwise as in any manner licensing the holder or any other person or corporation, or conveying any rights or permission to manufacture, use, or sell any patented invention that may in any way be related thereto.

Copies of this report should not be returned unless return is required by security considerations, contractual obligations, or notice on a specific document.



UNCLASSIFIED

Security Classification

DOCUMENT CONTROL DATA - R & D		
(Security classification of title, body of abstract and indexing annotation must be entered when the overall report is classified)		
1. ORIGINATING ACTIVITY (Corporate author) Southern Research Institute 2000 Ninth Avenue, South Birmingham, Alabama 35205		2a. REPORT SECURITY CLASSIFICATION UNCLASSIFIED
		2b. GROUP
3. REPORT TITLE An Evaluation of Material for Investigation of Test Methods for Brittle Materials		
4. DESCRIPTIVE NOTES (Type of report and inclusive dates) Final Report April 1966 through September 1971		
5. AUTHOR(S) (First name, middle initial, last name) J. R. Brown, Jr., R. J. Bickelhaupt, H. S. Starrett, C. D. Pears		
6. REPORT DATE October 1972	7a. TOTAL NO. OF PAGES 334 254	7b. NO. OF REFS 9
8a. CONTRACT OR GRANT NO. AF33(615)-3265 and F33615-70-C-1468	8b. ORIGINATOR'S REPORT NUMBER(S)	
8c. PROJECT NO. 7350		
8d. OTHER REPORT NO(S) (Any other numbers that may be assigned this report) AFML-TR-72-219		
10. DISTRIBUTION STATEMENT Approved for public release; distribution unlimited.		
11. SUPPLEMENTARY NOTES		12. SPONSORING MILITARY ACTIVITY
13. ABSTRACT This report is the final report covering work under Contract Nos. AF33(615)-3265 and F33615-70-C-1468 to perform a quantitative evaluation of test methods for brittle materials. Of primary importance for the completion of this program was the production of parts with a wide range of sizes and shapes which could be made in quantity under production conditions with a minimum of material variability. Work on this program was terminated before complete reproducibility was demonstrated for all blank shapes. The material used for this investigation was a high purity alumina, XAD997A, produced by Coors Porcelain Company. Of the 13 blank types investigated, 10 demonstrated the desired uniformity and reproducibility, 1 was slightly deficient, and 2 require additional work. Attempts at demonstrating lot to lot reproducibility were generally unsuccessful. As measured by macro specimens, the average flexural strength was 48,290 psi, and the average tensile strength was 46,300 psi. The densities of acceptable parts ranged from 3.78 to 3.83 and grain size from 3.0 to 4.1μ meters. A regression of strength on grain size and porosity fit the data quite well for a wide range of values of all three variables. Some indications were found that tighter control may be required on green density and firing parameters as well as the end properties of density and grain size to assure parts acceptable for strength. Studies of fracture source distribution indirectly indicate that surface or near surface damage is not controlling flexural strength. Indications were found that machine shop practices have an effect on strength, but other factors, grain size and porosity, seem to control. Refiring which does not change grain size does not affect strength. For the range of surface preparation techniques applied (all good surfaces), little effect on strength was detected. Environmental conditioning of specimens is required to assure that extremes of humidity do not affect strength results. It should be possible to conduct an effective analysis of test methods using the XAD997A alumina; however, some additional work is required to perfect the material and processing parameters.		

DD FORM 1 NOV 65 1473

UNCLASSIFIED

Security Classification

UNCLASSIFIED

Security Classification

14	KEY WORDS	LINK A		LINK B		LINK C	
		ROLE	WT	ROLE	WT	ROLE	WT
	Brittle Materials						
	Alumina						
	Test Methods						
	Fractography						
	Weibull Statistics						
	Fracture Source						
	Surface Finish						
	Environmental Effects						
	Strength Correlations						

UNCLASSIFIED

Security Classification

*i. b.*

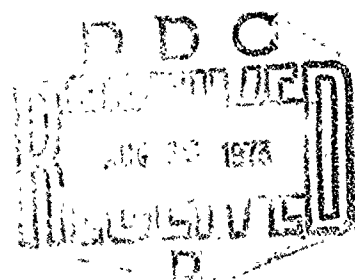
# AN EVALUATION OF MATERIAL FOR INVESTIGATION OF TEST METHODS FOR BRITTLE MATERIALS

J. R. BROWN, JR.  
R. J. BICKELHAUPT  
H. S. STARRETT  
C. D. PEARS

SOUTHERN RESEARCH INSTITUTE

TECHNICAL REPORT NO. AFML-TR-72-219

OCTOBER 1972



Approved for public release; distribution unlimited.

AIR FORCE MATERIALS LABORATORY  
AIR FORCE SYSTEMS COMMAND  
WRIGHT-PATTERSON AIR FORCE BASE, OHIO

is

## FOREWORD

This work was performed by Southern Research Institute under USAF Contract Nos. AF33(615)-3265, and F33615-70-C-1468. This work was initiated under Project No. 7350, "Refractory Inorganic Nonmetallic Materials", Task No. 735003, "Theory and Mechanical Phenomena". This work was administered under the direction of the Air Force Materials Laboratory, Air Force Systems Command, Wright-Patterson Air Force Base, Ohio, with Mr. G. R. Atkins (LLN) acting as project engineer.

The work discussed in this report was conducted from 15 April 1966 to 30 September 1971 by the Mechanical Engineering Division headed by C. D. Pears and others at Southern Research Institute. Specific contributions included H. S. Starrett on the statistics of fracture, D. W. Braswell and J. R. Brown, Jr., on mechanical evaluations, H. G. Sanders on nondestructive testing, and Dr. R. E. Bickelhaupt on structure-characterization.

The manuscript of this report was released by the authors October, 1972, for publication.

This technical report has been reviewed and is approved.



THOMAS D. COOPER  
Chief, NDT & Mechanics Branch  
Metals & Ceramics Division

## ABSTRACT

This report is the final report covering work under Contract Nos. AF33(615)-3265 and F33615-70-C-1468 to perform a quantitative evaluation of test methods for brittle materials. Of primary importance for the completion of this program was the production of parts with a wide range of sizes and shapes which could be made in quantity under production conditions with a minimum of material variability. Work on this program was terminated before complete reproducibility was demonstrated for all blank shapes.

The material used for this investigation was a high purity alumina, XAD997A, produced by Coors Porcelain Company.

Of the 13 blank types investigated, 10 demonstrated the desired uniformity and reproducibility, 1 was slightly deficient, and 2 require additional work. Attempts at demonstrating lot to lot reproducibility were generally unsuccessful.

As measured by macro specimens, the average flexural strength was 48,290 psi, and the average tensile strength was 46,300 psi. The densities of acceptable parts ranged from 3.78 to 3.83 and grain size from 3.0 to 4.1  $\mu$  meters. A regression of strength on grain size and porosity fit the data quite well for a wide range of values of all three variables. Some indications were found that tighter control may be required on green density and firing parameters as well as the end properties of density and grain size to assure parts acceptable for strength.

Studies of fracture source distribution indirectly indicate that surface or near surface damage is not controlling flexural strength. Indications were found that machine shop practices have an effect on strength, but other factors, grain size and porosity, seem to control. Refiring which does not change grain size does not affect strength. For the range of surface preparation techniques applied (all good surfaces), little effect on strength was detected. Environmental conditioning of specimens is required to assure that extremes of humidity do not affect strength results.

It should be possible to conduct an effective analysis of test methods using the XAD997A alumina; however, some additional work is required to perfect the material and processing parameters.

## TABLE OF CONTENTS

	Page
INTRODUCTION .....	1
Status of Project at Termination .....	1
BACKGROUND .....	2
MATERIALS AND SPECIMEN PREPARATION .....	5
Material .....	5
Review of Coors' Reports .....	5
Body Preparation .....	6
Preliminary Kiln Study .....	6
Pressing Study .....	7
Firing Study .....	7
Nomenclature .....	7
Specimen Preparation .....	9
Machining .....	11
APPARATUS AND PROCEDURES .....	11
Flexure .....	11
Tension .....	12
NDT Measurement .....	12
Ultrasonic Velocity .....	12
Bulk Density .....	13
Ultrasonic Pulse-Echo .....	15
Ceramographic Preparation .....	15
Microstructural Features .....	16
Ceramographic Preparation Study .....	17
Later Grain Size Determinations .....	20
RESULTS OF STUDIES ON UNIFORMITY AND REPRODUCIBILITY FOR ALL SHAPES .....	22
Flexural Data on Various Shapes .....	22
Tensile Data on Various Shapes .....	24
Weibull Statistics .....	25
Parametric Correlations - Strength, Density (Green and Fired), Cone Angle, Velocity, Fired Thickness, and Shapes .....	27
Microstructural Characterization .....	29

	Page
Density and Porosity Features .....	30
Uniformity of Grain Size .....	33
Grain Size as a Function of Those Factors	
Contributing to Reproducibility .....	34
Second Phase .....	35
Fracture Mode by Macro and Micro Fractography .....	37
Material Characteristics versus Extreme Differences	
in Strength (Weak/Strong) .....	40
Summary .....	42
Flexural Evaluations on a High-Fired 4All Blank .....	42
NDT Measurements .....	43
Destructive Testing .....	44
PRELIMINARY SURFACE FINISH STUDY .....	46
STUDIES OF SUBSURFACE DAMAGE .....	47
Statistics of Fracture .....	48
Discussion .....	51
Definition of Surface Characteristics by Electron	
Microscopy .....	54
As-Manufactured Surfaces .....	55
Surfaces Cut, Ground, or Lapped after Firing ....	55
Surface Preparation Study .....	57
Machining Study .....	60
Refired Specimens .....	65
ENVIRONMENT STUDY .....	68
LOT TO LOT REPRODUCIBILITY AND UPGRADING STUDY .....	71
REGRESSION ANALYSIS .....	75
CONCLUSIONS .....	78
Material Description and Deviations .....	78
Strength Correlations .....	79
RECOMMENDATIONS .....	80
REFERENCES .....	81
APPENDIX .....	228

# LIST OF ILLUSTRATIONS

Figure		Page
1	Macro Flexural Specimen .....	82
2	Macro Tensile Specimen .....	83
3	Configuration of Specimen Blanks 1A02 as Received from Coors and Cutting Plan for Removing Phase I Tensile and Flexural Specimens .....	84
4	Configuration of Specimen Blanks 2A04 as Received from Coors and Cutting Plan for Removing Phase I Tensile and Flexure Specimens .....	85
5	Configuration of Specimen Blanks 2A05 as Received from Coors and Cutting Plan for Removing Phase I Macro Tensile and Macro Flexural Specimens .....	86
6	Configuration of Specimen Blanks 1A06 as Received from Coors and Cutting Plan for Removing Phase I Macro Tensile and Macro Flexural Specimens .....	87
7	Configuration of Specimen Blanks 2A07 as Received from Coors and Cutting Plan for Removing Phase I Macro Tensile and Macro Flexural Specimens .....	88
8	Configuration of Specimen Blanks 2A08 as Received from Coors and Cutting Plan for Removing Phase I Macro Tensile and Macro Flexural Specimens .....	89
9	Configuration of Specimen Blanks 3A09-083, 3A09-085, and 3A09-086 as Received from Coors and Cutting Plan for Removing Phase I Macro Tensile and Macro Flexural Specimens .....	90
10	Cutting Plan - Specimen Blanks 3A09-081, 3A09-082, and 3A09-084 .....	91
11	Cutting Plan - Specimen Blanks 3A09-120 and 3A09-144 .	92
12	Cutting Plan - Specimen Blanks 3A09-136 and 3A09-137 .	92
13	Configuration of Specimen Blank 3A10-087 as Received from Coors and Cutting Plan for Removing Phase I Macro Tensile and Macro Flexural Specimens .....	94



# LIST OF ILLUSTRATIONS (continued)

Figure	Page
14 Cutting Plan - Scrap from 3A10-087 .....	95
15 Cutting Plan - Specimen Blank 3A10-088 .....	96
16 Configuration of Specimen Blank 4A11-089 as Received from Coors and Cutting Plan for Removing Phase I Macro Tensile and Macro Flexural Flexural Specimens ..	97
17 Cutting Plan - Specimen Blank 4A11-112 .....	98
18 Cutting Plan - Blank 4A11-125 .....	99
19 Configuration of Specimen Blanks 2A12 as Received from Coors and Cutting Plan for Removing Phase I Macro Tensile and Macro Flexural Specimens .....	100
20 Configuration of Specimen Blank 5A13 as Received from Coors and Cutting Plan for Removing Phase I Tensile and Flexural Specimens from Blanks 5A13-101, -102, and -103 .....	101
21 Cutting Plan - Blank 5A13-127 and 5A13-148 .....	102
22 Cutting Plan - Blanks 5A13-149, 5A13-151, 5A13-152, and 5A13-153 .....	103
23 Configuration of Specimen Blanks 6A14 as Received from Coors and Cutting Plan for Removing Phase I Macro Tensile and Macro Flexural Specimens from Blanks 6A14-104 and 6A14-106 .....	104
24 Configuration of Specimen Blanks 6A17 as Received from Coors and Cutting Plan for Removing Phase I Macro Tensile and Macro Flexural Specimens .....	105
25 Configuration of Blank -135 as Received from Coors and Cutting Plan for Macroflexure Specimens .....	106
26 Configuration of Blank -138 as Received from Coors and Cutting Plan for Macroflexure Specimens .....	107
27 Cutting Plan for Ends of Blanks 3A05-024, 3A05-025, 3A05-028, 3A05-031, and 3A05-035 Used for Machining Study .....	108

# LIST OF ILLUSTRATIONS (continued)

Figure		Page
28	Steel Shanks for Providing a Gripping Surface for Precision Tensile Grips .....	109
29	Photograph of Macro Tensile Specimen .....	110
30	Picture of a Tensile Stress-Strain Facility .....	111
31	Schematic of the Gas Bearings and Load Train for the Tensile Apparatus .....	112
32	Precision Collet Grip for Tensile Specimens 2:1 Scale	113
33	Schematic of Miniature Flexural Load Train .....	114
34	Schematic of L-33 Kiln Car Loading Layout .....	115
35	Photomicrographs of the Microstructure Resulting from Each Step of the "Deep Lap" Procedure .....	116
35 (cont)	Photomicrographs of the Microstructure Resulting from Each Step of the "Deep Lap" Procedure .....	117
36	Maximum "Pore Size" Observed after Completion of the "Deep Lap" Procedure .....	118
37	Final Microstructure after Completion of the Conventional Polishing Technique Including the Use of 30- and 15-Micron Diamond Pastes .....	118
38	Microstructure after Progressive Stages of Polishing Using the Procedure with which Specimens Selected for Grain Size Measurements Were Polished .....	119
39	Distribution of the Flexural Strengths of the Macro Specimens .....	120
40	Average Flexural Strengths versus SRI Blank Numbers and Minimum Fired Thickness .....	121
41	Distribution of the Tensile Strengths of the Macro Specimens .....	122
42	Tensile Strength versus SRI Blank Numbers and Minimum Firing Thickness .....	123

# LIST OF ILLUSTRATIONS (continued)

Figure		Page
43	Probability of Fracture versus Fracture Stress for Phase I Tensile and Flexural Data .....	124
44	Average Ultimate Tensile Strength versus Volume, also Showing Standard Deviations, for the Culled Alumina Data from AFML-TR-66-228 and the Phase I Alumina Data on Macro Specimens .....	125
45	Uniformity of Strength in Specimen Blank 3A10-088 as Determined from Flexural Strength Data .....	126
46	Flexural Strength versus Longitudinal Position at Five Transverse Positions for Specimen Blank 3A10-088 .....	127
47	Cross Sectional Variation of Strength for Specimen Blank 3A10-088 .....	128
48	Uniformity of Density in Specimen Blank 3A10-088 as Determined from Macro Flexural Specimens .....	129
49	Density versus Longitudinal Position at Five Transverse Positions for Specimen Blank 3A10-088 .....	130
50	Cross Sectional Variation of Density for Specimen Blank 3A10-088 .....	131
51	Uniformity of Density in Specimen Blank 4A11-089 as Determined from Macro Flexural Specimens .....	132
52	Longitudinal Density Profile for Specimen Blank 4A11-089 .....	133
53	Variation in Average Strengths Among the Several Items of Blank Type A02 .....	134
54	Variation in Average Strengths Among the Several Items of Blank Type A04 .....	135
55	Flexural Specimen 3A09-085-2 Internal Longitudinal Profile, as Polished, 50X .....	136
56	Flexural Specimen 6A14-106-12 Internal Longitudinal Profile, as Polished, 50X .....	137

# LIST OF ILLUSTRATIONS (continued)

Figure		Page
57	Flexural Specimen 6A14-104-7 Internal Longitudinal Profile, as Polished, 50X .....	138
58	Flexural Specimen 5A13-102-6 Internal Longitudinal Profile, as Polished, 50X .....	139
59	Flexural Specimen 2A12-096-11 Internal Longitudinal Profile, as Polished, 50X .....	140
60	Flexural Specimen 3A09-085-1 Internal Longitudinal Profile, as Polished, 50X .....	141
61	Flexural Specimen 4A11-089-1 Internal Longitudinal Profile, as Polished, 50X .....	142
62a	Tensile Specimen 5A13-101-4T Transverse Section at Fracture, as Polished, 50X .....	143
62b	Tensile Specimen 2A12-095-3T Transverse Section at Fracture, as Polished, 50X .....	143
63a	Tensile Specimen 2A05-047-2T Transverse Section at Fracture, as Polished, 50X .....	144
63b	Tensile Specimen 2A05-047-1T Transverse Section at Fracture, as Polished, 50X .....	144
64	Pore Size Distribution for Specific Flexural Macro Specimens of Table 9 .....	145
65a	Flexural Specimen 6A14-106-12 Internal Longitudinal Profile, H <sub>3</sub> PO <sub>4</sub> Etch at 150°C, Position 2, 800X .....	146
65b	Flexural Specimen 6A14-104-7 Internal Longitudinal Profile, H <sub>3</sub> PO <sub>4</sub> Etch at 150°C, Position 2, 800X .....	146
66	Microprobe Stationary Beam Spectral Scan Beam Focused on "Second Phase", Relief Polished .....	147
67	Tensile Specimen 2A05-047-2T Two Stage Replication, Specimen Polished and Etched at 150°C with H <sub>3</sub> PO <sub>4</sub> ....	148
68a	Flexural Specimen 3A09-085-2, 50X External Profile, Compression Region at Top .....	149

# LIST OF ILLUSTRATIONS (continued)

Figure	Page
68b Flexural Specimen 3A09-085-1, 50X External Profile, Compression Region at Top .....	149
69a Flexural Specimen 3A09-085-2, 20X Fracture Face, Compression Region at Top .....	150
69b Flexural Specimen 3A09-085-1, 20X Fracture Face, Compression Region at Top .....	150
70 Electron Fractograph of Flexural Specimen 5A13-102-6 Tension Zone .....	151
71a SEM Photomicrograph of the Fracture Face of a Typical Flexure Specimen at 500X .....	152
71b SEM Photomicrograph of the Fracture Face of a Typical Flexure Specimen at 1000X .....	152
72a SEM Photomicrograph of the Fracture Face of a Typical Flexure Specimen at 10,000X .....	153
72b SEM Photomicrograph of the Fracture Face of a Typical Flexure Specimen at 20,000X .....	153
73 Flexural Specimen 2A05-043-3 External Profile, 50X, Dash Line - Neutral Axis .....	154
74a Density, Blank 4A11-112 Section A .....	155
74b Density, Blank 4A11-112 Section C .....	155
75 Tensile Face of Flexural Specimen 4A11-112-A11 Showing Disparate Void in Fracture, 50X Transmitted Light .....	156
76 Tensile Face of Flexural Specimen 4A11-112-A51 Showing Disparate Void in Fracture, 50X Transmitted Light .....	156
77 Fracture-Source Distribution in Pure Bending for a Rectangular Specimen .....	157
78 Fracture-Source Distribution in Pure Bending (Round Specimen) .....	158

# LIST OF ILLUSTRATIONS (continued)

Figure		Page
79	Fracture-Source Distribution in Pure Tension for a Round Tensile Specimen .....	159
80	Strength Ratio versus Volume in Tension Weibull Predictions .....	160
81	Coefficient of Variation versus Weibull Modulus $m$ for the Weibull Distribution .....	161
82	Probability of Fracture versus Normalized Stress $\beta$ for the Macrotensile Specimens .....	162
83	Probability of Fracture versus Normalized Stress $\beta$ for the Macroflexural Specimens .....	163
84	Probability of Fracture versus Normalized Stress $\beta$ for the Macroflexural Specimens .....	164
85	Family of Weibull Distribution .....	165
86	Electron Photomicrograph - Illustration of Black Line Artifact. Fiducial Bar Equals 0.5 micron .....	166
87	Electron Photomicrograph - As-Received Surface, Pressed and Fired. Fiducial Bar Equals 5.0 microns .	167
88	Electron Photomicrograph - As-Received Surface, Pressed, Green Machined, and Fired. Fiducial Bar Equals 5.0 microns .....	168
89	Electron Photomicrograph - Surface Created by Cutting with a 100-Grit Diamond Wheel. Fiducial Bar Equals 5.0 microns .....	169
90	Electron Photomicrograph - 15-rms Surface Created by Standard Shop Surface Grinding. Fiducial Bar Equals 5.0 microns .....	170
91	Electron Photomicrograph - 15-rms Surface Created by Standard Shop Surface Grinding - Illustration of Surface Crack. Fiducial Bar Equals 0.5 micron .....	171

# LIST OF ILLUSTRATIONS (continued)

Figure		Page
92	Electron Photomicrograph - 5-rms Surface Developed Using Abernathy Lap. Fiducial Bar Equals 5.0 microns .....	172
93	Electron Photomicrograph - <1-rms Surface Developed Using Metallurgical Laboratory Lapping Techniques. Fiducial Bar Equals 5.0 microns .....	173
94	Effects of Thermal Treatment on Strength of Sliced Macroflexure Specimens .....	174
95	Probability of Fracture versus Normalized Stress $\beta$ for the Macroflexure Specimens Machined by Southern Research Institute .....	175
96	Probability of Fracture versus Normalized Stress $\beta$ for the Macroflexure Specimens Machined by Coors Porcelain Company .....	176
97	Probability of Fracture versus Normalized Stress $\beta$ for the Macroflexure Specimens Machined by R and W Products .....	177
98a	Tensile Face of Flexure Specimen 3A09-084-24A, Shop Ground and Metallurgically Lapped, before Refire, Showing 0.0075-inch Void, 50X .....	178
98b	Tensile Face of Flexure Specimen 3A09-084-24A, Shop Ground and Metallurgically Lapped, after Refire, Showing 0.0075-inch Void, 50X .....	178
99	Tensile Face of Flexural Specimen 3A09-084-24A, Shop Ground and Metallurgically Lapped, before Refire and after Refire and Fracture. Arrow on Lower Photomicrograph Points to the 0.002 x 0.004-inch Void. 50X .....	179
100	Tensile Face of Flexural Specimen 3A10-088-C12A, Shop Ground and Metallurgically Lapped, 50X, before and after Fracture. *Artifact-Lint .....	180
101	Fracture Faces of Selected Flexural Specimens from Refiring Study. Lower Edge of Each Fracture Face is the Tension Side. Specimen Numbers and Flexural Strengths are in the Same Order as the Specimens Appear in the Photographs. 7.3X .....	181

# LIST OF ILLUSTRATIONS (continued)

Figure		Page
102	Electron Photomicrograph - Surface of Specimen 3A09-084-13A - Shop Ground. Fiducial Bar Equals 5.0 microns. Arrow Gives Shadowing Direction .....	182
103	Electron Photomicrograph - Surface of Specimen 3A09-084-21A, Shop Ground, Surface Hydrogen Refired to 1550°C. Fiducial Bar Equals 5.0 microns. Arrow Gives Direction of Shadowing .....	183
104	Electron Photomicrograph - Surface of Specimen 3A09-084-24A, Shop Ground, Metallurgically Lapped, and Hydrogen Refired to 1550°C. Fiducial Bar Equals 5.0 microns. Arrow Gives Direction of Shadowing ....	184
105	Electron Photomicrograph - Surface of Specimen 3A09-084-24B, Shop Ground and Air Refired to 1570°C. Fiducial Bar Equals 5.0 microns. Arrow Gives Direction of Shadowing .....	185
106	Flexure Strength versus Average Size of Flaw on Fracture for Environment Study Specimens .....	186
107	Flexure Strength versus Porosity and Grain Size .....	187
108	Porosity versus Normalized Flexure Strength .....	188
109	Grain Size versus Normalized Flexure Strength .....	189
110	Green Density versus Normalized Flexural Strength ...	190



# LIST OF TABLES

Table		Page
I	Firing Analysis Data - Southern Research Institute PO-16-07476 .....	191
II	Results of Flexural Evaluations of Phase I Macro Specimens .....	195
III	Table of Mean Stresses, Standard Deviations, and Coefficients of Variation for Phase I Flexural Data on Macro Specimens .....	199
IV	Results of Tensile Evaluations of Phase I Macro Specimens .....	200
V	Table of Mean Stresses, Standard Deviations, and Coefficients of Variation for Phase I Tensile Data on Macro Specimens .....	203
VI	Summary of Tensile and Flexural Results on Macro Specimens .....	204
VII	Rank Correlation Tests .....	205
VIII	Rank Tests .....	206
IX	Fracture Stress, Density, and Macrostructural Data for Selected Macro Specimens (Weak/Strong Study) .....	207
X	Average Grain Intercept Size for Selected Specimens ..	208
XIa	Specimen Densities, Blank 1831-All-112 Section A .....	209
XIb	Specimen Densities, Blank 1631-All-112 Section C .....	209
XII	Results of Flexural Evaluation of "Improved" All Blank .....	210
XIII	Results of Flexural Evaluations on Macro Specimens from Blank 3A10-088 (Surface Finish) .....	211
XIV	Results of Tensile Evaluations of Polished Macro Specimens Removed from Blank 3A10-088 .....	212
XV	Results of Surface Finish Study on Macro Specimens ...	213

# LIST OF TABLES (continued)

Table		Page
XVI	Flexural Strength of Cambered 3A09 Specimens .....	214
XVII	Results of Various Treatments .....	215
XVIII	Results of Machining Study .....	217
XIX	Results of Refiring Study .....	220
XX	Results of Environment Study .....	221
XXI	Environment Study Statistical Comparisons .....	222
XXII	Firing Analysis Data - Southern Research Institute PO-16-01651 .....	223
XXIII	Flexure Strength of Fired to Size Macro Specimens ....	224
XXIV	Results of Lot-to-Lot Reproducibility and Upgrading Study .....	225
XXV	Average Data for Regression Analysis of Strength versus Porosity, Grain Size, and Green Density .....	227

## AN EVALUATION OF MATERIAL FOR INVESTIGATION OF TEST METHODS FOR BRITTLE MATERIALS

### INTRODUCTION

This is the final report for work done under Contract Nos. AF33(615)-3265 and F33615-70-C-1468 to perform a quantitative evaluation of test methods for brittle materials and an exploration of the relationship between tensile and compressive properties and flexural response. Phase I involved a production control study to demonstrate that a ceramic material as produced for various specimen configurations was uniform and reproducible in strength, microstructure, and density. To this end Southern Research subcontracted with Coors Porcelain Company to perform a production control feasibility study. The primary production parameters included in this study were powder characteristics, forming techniques, green density, and sintering procedures.

Specimen blanks for 13 different specimen configurations were manufactured by Coors during the control and reproducibility studies. These blanks were then evaluated to determine the uniformity and reproducibility of the material with respect to strength and structure.

Phase II as originally defined involved the purchase of a sufficient number of specimens to conduct the comparison of test methods, and the actual comparison of the methods.

#### Status of Project at Termination

The work was completed on evaluating specimen blanks obtained from the production control and reproducibility studies and on establishing the general ranges and correlations for strength, grain size, and density with some degree of confidence. Complete reproducibility was not demonstrated for all of the shapes.

### BACKGROUND

Many, if not most, brittle materials exhibit a somewhat different response to tensile, flexural, and compressive loads as well as when loaded as a disc (Brazil test), a thick ring or a thin ring. For example, the tensile and compressive fracture strengths often differ by a factor of 2 and can differ by a factor of 10 or more. Modulus of rupture values of  $1\frac{1}{2}$  to 3 times the measured tensile strengths are frequently reported in the

literature. It is possible to conceive physical models to explain the difference in response of a material to tensile and compressive loads; however, it is more difficult to conceive a model that will explain any gross departure of MOR values from ultimate tensile strength. Generally, brittle materials are characterized as being governed by a weakest link fracture mechanism such that cracks initiate and/or propagate to fracture as soon as the stress in any localized region of the stressed material reaches the ultimate value. Evidence thus far obtained indicates that brittle materials are weakest in tension; consequently, one would expect flexural specimens to fracture when the extreme outer fibers reached the ultimate in tension.

For quite some time Southern Research Institute has been interested in determining the causes for the discrepancies in reported strengths. We have felt that at least a portion of the discrepancy is due to experimental error caused by the inability of the standard tensile facility to apply truly uniaxial tensile loading. The presence of bending moments during a test will result in a lower "apparent" tensile strength. Interestingly enough, most cases where gross discrepancies in MOR and tensile values are reported, the tensile values are the lower of the two. Also data obtained in Southern's gas-bearing tensile facility indicate that good agreement between tensile and flexural strengths can be obtained on most materials.

Thus while it appears that nonuniform loading of tensile specimens is a major factor in the reported discrepancies, present indications are that other parameters are also exerting influences. For example, tensile values for some materials differ significantly from MOR values even when truly uniaxial loads are applied. In addition, even where good agreement between tensile and MOR values have been obtained, there appears to be a tendency for the MOR to show slight increase in strength with temperature after the tensile strength begins decreasing. Part of this effect at elevated temperature may be caused by plastic deformation and subsequent stress relief at the outer fibers of flexural specimens; however, plastic deformation is hardly the mechanism causing discrepancies observed at room temperature.

One explanation is that errors result from calculating MOR values from classical beam equations. One assumption in the derivation of these equations is that the tensile and compressive moduli are equal, until fracture; hence, the neutral axis coincides with the centroidal axis. According to an analysis developed by

Simon<sup>1</sup> if a material has a higher compressive modulus than tensile modulus the neutral axis will shift to the compressive side of the beam and reduce the peak tensile stress. For a material that fails in tension, the calculated MOR values would give "apparent" tensile ultimates higher than can be observed in a uniaxial tensile test.

Other conditions which could cause the difference between tensile and flexural strengths include surface condition and the volume under stress. Unfortunately, the nature of the effects of these conditions would be different for tensile and flexural evaluations. Surface finish would be very active in setting the strength of a flexural specimen since the peak stress occurs only at the surface, whereas in a tensile specimen the entire volume of the gage section is subjected to the same stress as the surface.

The strength of brittle materials depends on the volume under stress. This has been demonstrated effectively with tensile specimens; however, the effect is not easily defined when using flexural specimens chiefly because of the stress gradient.

We have mentioned some of the difficulties encountered in relating tensile and flexural results. Similar difficulties occur when one considers test methods besides these two, particularly the indirect tensile tests such as the Brazil Test and others.

Having mentioned some of the difficulties in testing brittle materials, consider the plight of the designer. He needs information that will permit him to proceed from specimen data to the proper design of a structure. This information includes the effects of (1) surface finish, (2) stress concentrations, (3) volume, (4) skin discontinuities, (5) Weibull coefficients, (6) biaxial stress, and other physical behavior such as those already mentioned. Before the designer can make this step, the various mechanisms and behaviors must be understood with reference to the test methods.

The solution to the problem is the ordered study of these natural phenomena. However, before this type of study can proceed, a uniform and reproducible material which can be manufactured in large quantities must be found. Otherwise, the effects being

---

1. Superscripts refer to references listed at the end of the text.

investigated may be masked by anomalous material behavior. For instance in a recent program<sup>2</sup> in which volume effects were studied, some of the material was found to have anomalously large grains and areas of incomplete sintering which yielded low strength specimens. If all small volume specimens had been manufactured from this material and all large volume specimens had been made from better material, in all likelihood the volume effect would have been missed. Fortunately, the specimens were located randomly in the several tiles so that the volume effect was not masked. This is merely one example of why a uniform material is needed.

The original scope of this program included obtaining a uniform and reproducible material and then conducting a quantitative comparison of several test methods. The study was primarily phenomenological and analytical in scope, concentrating on the effects of size, surface finish variations, stress-strain response under different types of loadings, and applying the proper analysis to the specimen. These would, in turn, be treated in terms of statistical fracture criteria. The program was terminated before reproducibility was demonstrated for all shapes.

The original criteria for the material was established as "the material is acceptable if it is statistically describable in terms of certain properties between the different blanks even though there may be some differences in structure". Thus, reproducibility (piece to piece) in key properties was the vital point. Uniformity (within a piece) was necessary to good reproducibility since it is doubtful a material can be reproducibly nonuniform. Then, with an adequate material, one would be able to control the range of certain variables and compare different tests by (1) volume normalizing, (2) control of test conditions, and (3) proper analysis.

## MATERIALS AND SPECIMEN PREPARATION

### Material

The material for this program was a high purity alumina manufactured by Coors Porcelain Company of Golden, Colorado. The material and its production were developmental as opposed to the state-of-the-art, but all parts were manufactured on a production basis rather than using research facilities. The emphasis was on the optimization of the material from the standpoint of uniformity and reproducibility with respect to strength. Coors designation for the material originally shipped was XAD997A. Later efforts at demonstrating reproducibility involved materials designated XAD997B and XAD997C. All materials used identical powders but differed from one another in the binders or mixtures used to produce the green shapes.

The material was manufactured in 13 different blank shapes, each representing a particular specimen configuration. The number of blanks of each type was based on the number of macro specimens deemed necessary for the study of uniformity and reproducibility. Blanks received are listed in Tables I and XXII. The number of macro specimens (tensile and flexural) removed from each blank is also listed in columns seven and eight of the table. Note that all parts were not used and this must be kept in mind in reviewing the results; however, representative samples were taken in all cases. There were several Type 4A11 blanks shipped which are not listed in the table. These blanks were sent by Coors for experimental machining purposes and were not considered to be representative of the production material for the study.

### Review of Coors' Reports

The success to be obtained in the subject program was very much related to the quality of the brittle body used. The Coors Porcelain Company was selected to produce an alumina body which would meet the major requirements of uniformity and reproducibility. Although the specific data which define this character were of interest, the main concern was centered on the degree with which properties of interest could be repeatedly produced.

The goal was to have available for study a body demonstrating minimal variation in character within a given object (uniformity) and a minimal variation in character among objects of both similar and dissimilar geometry (reproducibility). Since

some of the required parts were large and the nature of the program would necessitate production over an extended time period, it was desired to have the material produced using a well-documented production procedure. To do this mechanics study with a material which might be defined later as a "laboratory curiosity" was to be strictly avoided.

The specific character of the body was only loosely specified with regard to density and grain size. Although the body selected to be used in the program was not a standard production item, it was one which Coors believed could be made in quantity over a period of time with suitable uniformity and reproducibility. No preconceived limits of homogeneity existed. As is obvious from this report, it was hoped to be able to readily discern deviations from uniformity or reproducibility by review of physical measurements, microstructure, fractography, and mechanical data acquired from specimens taken from larger shapes.

To secure the desired uniformity and reproducibility, Coors spent considerable effort in establishing and documenting the processing parameters. Likewise, the parts produced for Phase I of this program were closely observed during processing and their features were documented. The Coors' reports related this information in an informal manner on a monthly basis. No attempt will be made to discuss these data. This review merely describes the areas of processing which were investigated and controlled during production. Those persons interested in the specific details of the processing are referred to the sponsor of this work for a copy of the original information.

The following outline will describe the various steps taken by the manufacturer to establish the process.

Body Preparation - Since the body used was one which had been previously designed by Coors, this portion of the work was largely concerned with the documentation of initial particle size, specific surface, body chemistry, and spray-dry pellet size distribution.

Preliminary Kiln Study - This study was made to select a production kiln in which to fire the parts for this program. Longitudinal, transverse, and vertical thermal profiles were established using traveling thermocouples and pyrometric cones. The kiln performance was evaluated based on these measurements and a study of kiln losses (camber and cracking) versus position in the kiln.



Pressing Study - The parts used in this program were isostatically pressed (some parts had restraint on one axis) and optimum conditions regarding fill control, rate of pressure rise, ultimate pressure, dwell time, and rate of pressure fall were investigated. Conditions yielding maximum green density with minimal variation were established.

Firing Study - The objective of the firing study was to determine the correct firing parameters to obtain a density of 96.5 percent  $\pm 1.5$  percent of the theoretical at a maximum grain size of less than 25 microns for all six geometries produced. The factors considered in this study included: kiln temperature, car schedule, car load, preheat, soak and cooling profile, cone deformation, etc. Optimization of these factors was established by repeated firings utilizing density and grain size measurements for judgment.

After establishing the production procedures, the parts for Phase I of the program were produced. Green density and fired density were recorded for each part. Cone deformation and grain size determinations were recorded for representative part geometries and kiln positions.

### Nomenclature

Due to large number of specimens and types of specimens involved in this work, it will be convenient to clearly define the nomenclature early in the report.

The material initially was pressed isostatically into basic shapes using different tool sets. There were six basic shapes (or tool sets) for this program. These basic shapes were then green machined into parts which were fired. These parts (or near-shapes) were machined oversize as tensile, compressive, flexural, diametral compression, brittle ring, and pressurized ring specimens and remained about 0.020 to 0.050 inch oversize after firing. They are referred to as specimen blanks. When these specimen blanks are machined to final dimensions, they then will be called specimens.

In order to evaluate the material to determine whether or not it was uniform with respect to strength, it was necessary to examine the material taken from the gage sections of the specimen blanks. To do this it was mandatory to adopt a test method, or methods, that was common to all specimen blanks. For our purposes the tensile and flexural evaluations were used. Thus, small tensile and flexural specimens were removed from the potential

gage sections of the specimen blanks. These small specimens have been called macro specimens.

To summarize thus far, we have mentioned the following categories of parts:

1. basic shapes
2. specimen blanks
3. specimens
4. macro specimens

In the work included in this report, we were concerned primarily with macro specimens.

For each specimen type (large tensile, small flexure, etc.), several specimen blanks were manufactured. Each piece was assigned a specimen number by Coors. This number is referred to as the Coors specimen number. As Coors completed various stages of production control study and as the parts were manufactured, firing data were kept for each part. These data for the production control study are presented in a Firing Analysis Data Table (Table 1). Firing Analysis Data for all later supplied blanks are shown in Table 22. In these tables the specimens were also assigned an Item Number. The item numbers are in ascending order and give easy access to the firing data.

From the above discussion we see that with each macro specimen we can associate the following information.

1. Tensile or Flexural strength
2. The particular specimen blank from which the macro specimen was removed
3. The type of specimen blank from which the macro specimen was removed
4. The basic shape (tool set) from which the specimen blank was derived.

In order to convey all of this information and to provide easy access to the firing data, a numbering system as follows was used. Consider the macro specimen number

1	A02	-	023	-	01	T
---	-----	---	-----	---	----	---

- 1 designates the basic shape number. This number ranges from 1 to 6.

- A02 signifies the type of specimen blank. A02 is a small tensile specimen blank.
- 023 is the Coors item number. This identifies a particular blank and lets one look up the firing data in Table I.
- 01 is the macro specimen number. In most cases more than one macro specimen was removed from each specimen blank.
- T tension. Identifies the macro specimen as to whether it was a tensile or flexural specimen. No letter signifies flexure.

There were 13 different types of specimen blanks manufactured by Coors for evaluation. These are listed below with their identifying number.

- A02 Small Tensile Specimen
- A04 Intermediate Tensile Specimen
- A05 Large Tensile Specimen
- A06 Small Compressive Specimen
- A07 Intermediate Compressive Specimen
- A08 Large Compressive Specimen
- A09 Small Flexural Specimen
- A10 Intermediate Flexural Specimen
- A11 Large Flexural Specimen
- A12 Intermediate Diametral Compressive Specimen
- A13 Large Diametral Compressive Specimen
- A14 Pressurized Ring Specimen
- A17 Brittle Ring Specimen

#### Specimen Preparation

The mechanical evaluations for Phase I of the program were preceded by an inspection of the alumina parts received from Coors Porcelain Company. The parts were inspected for cracks and other anomalies which would affect the testing program.

The testing for the production control study included 20 flexural tests and 8 tensile tests on material from each type of specimen blank as received from Coors to determine material uniformity and reproducibility. All later studies used various numbers of flexural specimens to measure material properties. Because of the limited amount of material available in the gage sections, it was necessary to develop the testing around minia-

ture test configurations (macro specimens). These were taken to be of such size that the required number could be removed from the gage sections of the specimen blanks where practical. The flexural macro specimen selected had dimensions of 0.100 inch x 0.200 inch x 2.0 inches as shown in Figure 1. The tensile macro specimen selected was 0.125 inch in diameter x 2.0 inches long with a gage section of 0.094 inch diameter x 0.188 inch long as shown in Figure 2. These were removed from the blanks according to the cutting plans shown in Figures 3 through 27. The distribution of the macro specimens is shown in columns 7 and 8 of the Firing Analysis Data (Table 1). The distribution was established by distributing the required number of test specimens from each blank configuration in such a manner that the test specimens would be from along both sides and across a section of the kiln car. This distribution is shown in Figure 34. Note that an even distribution according to kiln car location was not attained.

Because of the small size of the macro tensile specimens, adequate gripping area for tensile testing was not available. This was overcome by gluing steel shanks to both ends of the specimens. The steel shanks are shown in Figure 28. Three grooves three mils wide were ground on each end of the cylindrical macro tensile blanks for the purpose of providing a better gripping area for the glue. The blanks were then glued into the shanks with an epoxy glue consisting of a 10:1 mixture by weight of Shell Epon Resin 815 and Triethylene Tetramine hardener. The resin-hardener combination was mixed 4:1 by volume with a 1:1 mixture of alumina powder and Cabosil for reinforcement. The shank-blank combinations were placed in vee-blocks and cured in an oven at about 170°F for two hours. The composite macro specimen blanks were then ground to final size and shape. Grinding the gripping surfaces and gage sections about the same center line insured good alignment which is critical in the tensile testing of brittle materials. A completed macro tensile specimen is shown in Figure 29.

Note that no macro tensile specimens could be removed from specimen blanks 1A06 because the reduced length did not provide adequate surface area for gluing the steel shanks due to the limited shear strength of the epoxy cement. This length limitation of SRI part 1A06 also required that the macro flexural specimens be shorter than the usual two inches. This necessitated relocation of the load points in the flexural apparatus for these specimens.

Machining - The cutting and grinding operations were performed with diamond wheels of No. 100 grit. These proved to be efficient, and they produced a surface finish of from 14 to 18 RMS. The cooling fluid used was a water soluble cutting oil. Preliminary experiments showed that Stuart 4567 water soluble oil mixed about 25 to 1 was a good compromise between wheel wear and labor costs.

The final grinding operation on the macro tensile specimens required the use of steady-rests to insure against accidental breakage of the delicate gage sections. Even with the precautions taken, several were broken in machining and handling and are noted in the data tables. Gage sections were checked with a 20 to 1 optical comparitor for accuracy of shape.

As standard procedure the sharp corners on the tensile side of all flexural specimens were removed for the purpose of eliminating nicks and small cracks which might initiate a premature failure. This procedure was used on the macro flexural specimens by grinding off a few mils at 45° to the faces.

## APPARATUS AND PROCEDURES

Use of the macro specimens for the material evaluations required that special techniques be employed for loading the specimens to provide the correct failure mode with minimum parasitic stress.

### Flexure

For the flexural evaluations of the macro specimens, a precision miniature flexural apparatus was developed which employed rollers for load points and was constructed so that parasitic stresses were minimized. Figure 33 is a schematic of the apparatus.

There are certain practical limitations to the flexural tests. Chiefly, these are wedging, frictional forces at the load points, superimposed torsion, and inaccurate placement of the load points. The miniature flexural apparatus used for these evaluations was designed to overcome these limitations insofar as was possible.

Note in Figure 33 that two rods provide alignment and support for the loading pins. The shallow vee grooves in these rods give the proper spacing and assure that the loading pins

are normal to the length of the specimen. In operation the two rods and the specimen are guided by alignment fixtures until a small preload is applied. The alignment fixtures are then backed away leaving the load train free standing and unaffected by external forces. Load is monitored by an internal load cell in the testing machine and displayed as a load-time trace on an X-Y recorder and on the testing machine dial. Specimen dimensions are measured for each specimen near the fracture and these dimensions were used in stress calculations.

### Tension

The tensile specimens were loaded in tensile frames equipped with gas bearings in the load train to permit procedures that eliminate bending stresses. A typical tensile facility is shown in the photograph in Figure 30 and in the schematic in Figure 31. The primary components are the gas bearings, the load frame, the mechanical drive system and associated instrumentation for measurement of load. The load capacity is 15,000 pounds. This system is described in the literature.

The configuration of the tensile specimen has been shown in Figure 28. This specimen provides a relatively large L/D ratio in the gripping area to ensure good alignment. All surfaces in the gripping area are cylindrical in order to make precision machining easier and repeatable from specimen to specimen.

A schematic of the precision tensile grip is shown in Figure 32. The design is much like the jaws of a lathe head or the chuck of a drill motor made with precision. Observe from the figure the long surface contact of the mating parts and the close fits to establish precise alignment with the specimen. As the load is applied, the wedges maintain alignment to fracture. With this system, the parasitic stresses are less than one percent.

### NDT Measurements

Ultrasonic Velocity measurements were made on most of the macro specimens. This was accomplished by introducing a burst of high frequency energy from the pulse unit of Sperry UM 721 Reflectoscope into one end of the specimen and timing the wave propagation to the opposite end by means of a Tektronix oscilloscope which has a time-base precision of one percent. The sending and pickup units were ten megacycle transducers.

Bulk Density measurements were made on all of the macro specimens. Dimensions were measured with micrometers, and weights were measured with an analytical balance which has a sensitivity of 0.0001 gram. Density measurements for the flexural specimens were made on the final specimens. Density measurements for the tensile macro specimens were made on square blanks prior to grinding them to cylindrical form. These densities are referred to as those of the Mechanics Section. There are also those of the Inorganic Materials Section and those from Coors. There were systematic differences in the measurements from the different sources.

There were some problems associated with the mechanical density measurements which need to be clarified. It will be noted in the tables later that there were some differences between the densities determined on the macro tensile and flexural specimens. These differences do not appear to be systematic, but are believed to be associated with the accuracy of the measurement. For instance on the small flexural specimen, if the measurement is in error by 0.0005 inch on the nominal dimension of 0.100, then the density value can be off by as much as 0.02 gm/cm<sup>3</sup>. This is most apparent for the Al3 macro flexural specimens where the density of the macro flexural specimens from one cutting averaged 3.78 gm/cm<sup>3</sup> and from the second cutting averaged 3.81 gm/cm<sup>3</sup>. More accurate measurements on macro specimens were made in later evaluations with much less scatter in the data.

Bulk density values were determined for some of the flexural specimens from small pieces adjacent to the fracture using a liquid displacement technique. Pieces approximately 0.1 inch x 0.2 inch x 0.2 inch including the fracture face were used. Specimens were placed in a desiccator and covered with distilled water. The desiccator was then connected to a vacuum pump and evacuated. Bubbling subsided after 10 to 20 minutes and the pieces were allowed to remain in the water 24 hours. No absorption could be detected. Dry and saturated weights in duplicate never varied more than 0.2 mg. Suspended weights varied from 0.4 to 1.3 mg between successive measurements on the same piece. Since the specimens were very small, about 0.25 gm, this variation in suspended weight data caused differences of as much as 0.05 gm/cc in bulk density. Thus the results reported are averages of two determinations which individually may have differed by as much as 0.05 gm/cc. Insufficient data are available to present a statistical description of the information. These data are self-criticized on two counts: the specimen weight was too small

for the variations accompanying suspended weight measurements and the technique excludes the surface porosity from the volume of the specimen.

Bulk density values were determined for one group of macro flexure specimens using a slightly different liquid displacement technique. Since whole macro specimens were used, ~2.5 gm, these determinations did not suffer to the same extent as the small pieces. Macro specimens to be tested were dried in a vacuum at 50 microns Hg overnight. After removal from the desiccator, they were immediately weighed for dry weight. Then each dried specimen was placed in a small beaker. The end of the beaker was closed off with gauze. The small beakers were then placed on their side in the bottom of the desiccator with their open ends aligned toward the center. The desiccator was closed off and evacuated to about 50 microns of Hg. After holding this vacuum for about two hours, the desiccator was purged with distilled water. After about 15 minutes, water was introduced more rapidly until the beakers were covered. Then the desiccator was vented, and the samples allowed to soak for 20 minutes to allow any vapor inside the samples to condense. Upon completion of impregnation the samples were weighed (immersed in water and in air). When specimens were removed from the water, they were carefully wiped to remove any excess liquid from the surface and weighed immediately.

From the measurements taken (dry weight and suspended weight), the percent water absorption, open porosity, closed porosity, bulk density and apparent density were determined. These values were calculated as follows:

$$W_a = \left( \frac{W_{sa} - W_d}{W_d} \right) \times 100 \text{ percent}$$

$$P_o = \left( \frac{W_{sa} - W_d}{W_{sa} - W_{su}} \right) \times 100 \text{ percent}$$

$$\rho_b = \left( \frac{W_d}{W_{sa} - W_{su}} \right) \times \rho_w$$

$$\rho_a = \left( \frac{W_d}{W_d - W_{su}} \right) \times \rho_w$$



where

- $W_a$  = water absorption
- $W_{sa}$  = weight of sample when saturated with water
- $W_d$  = dry weight of sample
- $W_{su}$  = weight of sample when suspended in water
- $\rho_w$  = density of liquid water
- $\rho_b$  = bulk density of sample
- $\rho_a$  = apparent density of sample
- $P_o$  = open porosity

The liquid displacement density determinations on whole specimens showed a consistent  $0.030 \text{ gm/cm}^3$  higher bulk density, than did the determinations by dry weight and micrometer measurements. The fact that micrometer measurements were across predominant peaks on the rough (not smooth) surfaces and not across the mean surface could account for the majority of this difference.

A number of other NDT testing techniques were also employed. Cracks and porous regions found visually were enhanced by dye penetrants. Most of the fracture faces of the flexural specimens were scanned with ultraviolet light. Minute fluorescent spots were observed occasionally, but no correlations were noted. The cause of the fluorescence is not known.

Ultrasonic Pulse-Echo examinations were also made on the macro specimens. The porous area mentioned above was initially found by pulse echo indication; however, most of the specimens gave indications of being "clear".

#### Ceramographic Preparation

Specimens for study of porosity features and grain size determinations from the production control study were prepared in the following manner. Specimens from the flexural tests were prepared using those pieces used in the density determination of small pieces adjacent to the fracture. The specimen was diamond sawed to expose a longitudinal section at the centerline with the cut perpendicular to the compression and tension sur-

faces of the mechanical test piece. The specimens were mounted in blue bakelite with the diamond sawed surface exposed. Polishing was done using successively 30-, 15-, 6-, 3-, and 1-micron diamond on nylon cloth at slow-to-moderate wheel speeds.

The tensile specimens were handled in much the same way, except the section represents a plane perpendicular to the longitudinal direction of the mechanical test piece immediately below the fracture surface. Since the relatively rough fracture face was removed, the polishing procedure included the use of silicon carbide papers from 240 to 600 grit before final polishing with diamond as above.

When some structural detail was desired without the influence of etchants, a relief polish was used. This was done using 0.1-micron alumina on a high nap cloth at high wheel speeds. This technique revealed portions of the structure useful in the microprobe analysis.

To reveal the alumina grain boundaries, the specimens were etched in 85 percent  $H_3PO_4$  at 240-250°C for 5 minutes. This procedure at 140-150°C was suitable for revealing a phase other than alumina without having much effect on the alumina boundaries.

#### Microstructural Features

The size of the various microconstituents was measured by a linear intercept method as discussed by Underwood *et al.*<sup>3</sup> Area determinations to obtain volume fractions were made by visually counting grid openings overlying photomicrographs.

For flexural specimens, three photomicrographs were taken at the following positions: along the mid-point between the compression and tension surfaces 1.3 mm (Position 1), 2.5 mm (Position 2), and 3.8 mm (Position 3) from the fracture face. These positions were located within about 0.1 mm using a mechanical stage. To avoid bias, the location was not altered after microscopic focusing. With respect to grain size and the features of the second phase, no difference could be detected among the three photomicrographs. Therefore, the Position 2 photomicrograph was arbitrarily selected. These photomicrographs were made at 800X after etching at 140°C (second phase) and then after etching at 240°C (alumina boundaries). The total intercept length for grain size was 471  $\mu$  and for second phase it was 902  $\mu$ . With respect to the area of second phase, this was done as stated above using the same photomicrograph as was used for the intercept count. The total area surveyed was  $16 \times 10^3$  square microns.

Photomicrographs for the determination of porosity features were taken at 500X in the as-polished condition. Since in some cases the photomicrographs differed visually among the three positions, that position which represented an average of the three was used. If all three were similar, Position 2 was used. Total intercept length used was 902  $\mu$ . Total area examined to determine porosity area fraction was about  $40 \times 10^3$  square microns.

Grain size measurements for tensile specimens were made using single 800X photomicrographs taken at the center of the polished section.

#### Ceramographic Preparation Study

In addition to the previously described procedure, a continued ceramographic preparation procedure study was pursued. It was desired to establish a procedure for polished sections in which confidence could be placed in the structure being relatively free of artifacts. Also, the study was to yield information on a lapping technique for mechanical specimens that would remove, as a goal, 5 mils of presumably damaged material and leave a surface damaged no more than a few grains deep.

Prior to this study Coors' personnel suggested two techniques be tried. In an effort to eliminate subsurface cracks which could possibly be present as a result of the normal grinding procedure used for mechanical specimens, a "deep lap" technique was recommended. The suggested technique consisted of the following steps:

1. Cut specimen with 180-to 240-grit diamond wheel
2. Remove 5 mils by surface grinding with a 240-grit diamond wheel
3. Remove 2 mils using a 400-grit diamond lap
4. Remove 1 mil using a 600-grit diamond lap
5. Remove 1 mil by lapping with 15-micron diamond paste
6. Remove 1 mil total by lapping with 6-, 3-, and 1-micron diamond paste

It was believed that this lapping procedure, in which several mils of stock were to be removed, would eliminate damage incurred during grinding.

Coors also suggested a more conventional procedure for preparing alumina polished sections. The following steps were included:

1. Cut specimen with a diamond wheel
2. Face off with a 400-grit diamond lap
3. Lap using the following steps employing diamond paste on a pelon covered bronze lap

<u>Diamond Size</u>	<u>Wheel Speed</u>	<u>Relative Pressure</u>	<u>Time</u>
6 micron	400 rpm	Heavy	1 minute
6 micron	1200 rpm	Medium	2 minutes
3 micron	400 rpm	Heavy	1 minute
3 micron	1200 rpm	Medium	2 minutes
1 micron	1200 rpm	Light-Medium	1-2 minutes

In attempting the "deep lap" procedure, certain modifications were dictated by the equipment and supplies available. The specimen was cut using a 100-grit diamond wheel. Surface grinding was done with a resinoid bonded - 180 grit - 100-concentration diamond wheel. Grinding conditions were:  $\frac{1}{4}$ -mil depth of cut, 500 inches/minute feed, 6500 SFM and water soluble oil coolant. Diamond pastes of 45- and 30-micron size were substituted for 400- and 600-grit diamond laps, respectively. Nylon cloth was substituted for pellaon. For lapping with the smaller sizes of diamond paste, the wheel speeds and relative pressures suggested for the more conventional procedure were used.

It was learned that one could not comply with the suggested amounts of material removal when diamond sizes of 15 microns and smaller were used. Using heavy pressure and a wheel speed of 400 rpm, four minutes were required to remove 2 mils with 45-micron diamond, and 13 minutes were required to remove 1 mil with 30-micron diamond. Using 15-micron diamond, the removal of material was negligible for micrometer measurements across a mounted specimen even after 30 minutes to an hour of polishing.

The results for the "deep lap" procedure are shown in Figure 35, a through g. This series of photomicrographs shows the microstructure at 500X after each step of the preparation. The final structure is quite similar to those developed by the earlier method. Maximum "Pore size", whether an inherent micro-constituent or an artifact created during polishing, was 1 to 2 mils as shown in Figure 36, a and b. From earlier work, this maximum "Pore size" would be considered normal for this specimen, 3A10-088-C12B. That the microstructure resulting from the "deep

lap" procedure is similar to that from earlier work is not unexpected. The major differences between the "deep lap" and the procedure heretofore used were: (1) the original procedure involved no surface grinding and (2) the lapping time using 30 micron diamond paste was less than 13 minutes.

The "deep lap" procedure with the modifications declared above was used to produce the lapped 0.1 inch x 0.2 inch x 1.65 inch flexural specimens used in the refiring studies. Attempting to lap the rather large tensile face area of a flexural specimen by hand on laboratory equipment was a difficult task. It was apparent that these lapped surfaces were not of polished section quality over their entire area.

The conventional polishing technique suggested by Coors was attempted with poor results. This was probably due to this laboratory's unfortunate choice of 45-micron paste as a substitute for a 400-grit diamond lap. Obviously, it would not be expected that the after-6-micron structure could be obtained from the after-45-micron structure with no intermediate steps (see Figures 35, b and 3).

The conventional technique was repeated with 30 and 15 micron steps inserted. The resultant structure was identical to that produced using the "deep lap" procedure, see Figure 37 and compare with Figure 35g. The conventional technique also produced areas similar to Figure 36, a and b.

The results using the conventional polishing technique would indicate that to attain representative microstructure, one need not remove material by surface grinding or by excessive lapping. In this laboratory, it was found that the rough polishing technique using 30-micron diamond was critical. Using 45-micron diamond, the removal of surface material was readily accomplished and a rather featureless appearance was obtained. During the 30-micron polishing step, the microstructure started to develop. If the basic features of the microstructure are not developed at this point, the remaining rough and fine polishing steps are incapable of producing a suitable end product. The optimum polishing time using 30-micron diamond has not been established.

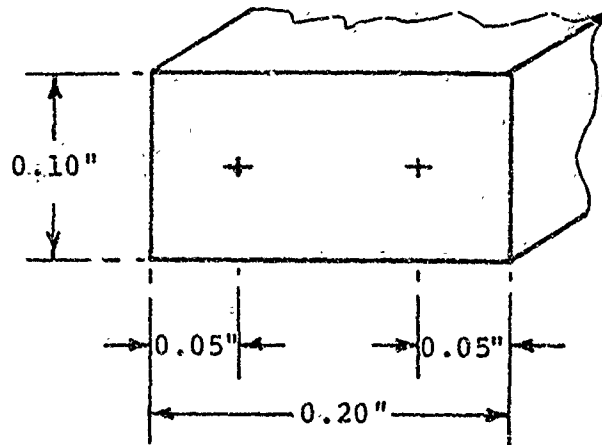
The procedure selected with which the specimens were polished for the later grain size determinations was a compromise between the "deep lap" and more conventional techniques. Regions to be examined were exposed by cutting with a 100-grit diamond wheel. The polishing procedure is tabulated below.

<u>Diamond Paste Size in Microns</u>	<u>Wheel Speed in RPM</u>	<u>Hand Pressure</u>	<u>Polishing Time in Minutes</u>
45	400	Heavy	4
30	400	Heavy	12
15	400	Heavy	2
15	1200	Moderate	2
6	400	Heavy	2
6	1200	Moderate	2
3	400	Heavy	1
3	1200	Moderate	2
1	1200	Moderate	2

In the course of establishing this procedure, a specific area was photographed after each polishing step. These are shown in Figure 38, a through e. By detailed comparison of each pair of contiguous polishing steps, it can be seen that certain pores are reduced in size, while others are enlarged or new ones appear. Even though an extremely small amount of surface material is removed during polishing with diamond pastes of 15 micron size and less, the enlarged or new areas may be either inherent structure or destruction of the surface by the polishing action.

#### Later Grain Size Determinations

Specimens for the later grain size analyses were ceramographically prepared according to the final procedure outlined above. In each case the polished section was a 0.1 inch x 0.2 inch transverse section of a previously tested flexural specimen. The polished sections were etched in orthophosphoric acid at 240-250°C for 5 to 10 minutes. This procedure adequately revealed the alumina grain boundaries but completely dissolved a second phase. Second phase regions delineated by straight lines on one or more sides were treated as existing grains when grain boundary-fiducial line intercepts were counted. (It should be noted that an alternate etchant, H<sub>2</sub>SO<sub>4</sub> at 200°C, was tried with the same end result. When the alumina boundaries were distinct, the second phase had been removed.) After vacuum depositing a thin layer of platinum-carbon, two photomicrographs were taken of each specimen at 800X. The two positions at which the photomicrographs were taken for each specimen are indicated below. These arbitrary positions were located using a mechanical stage.



One photomicrograph was selected for measurement. This selection was based on photographic quality and freedom of microstructural artifacts.

The average grain intercept was measured by counting the number of interceptions between grain boundaries and a fiducial straight line 10 centimeters long dropped randomly on the 800X photomicrograph. For each calculation of average grain intercept, 10 such drops were made. The average grain size interpreted in this matter is calculated from:

$$\text{A.G.I.} = \frac{L}{N \times M}$$

where:

$L$  = length of fiducial line ( $10^5$  microns)

$M$  = magnification (800X)

$N$  = average number of interceptions for ten drops

It is believed that the values obtained in this manner are within three percent of the correct mean value for the specific photomicrograph. The number of drops to be used for each measurement (10) was determined in the following manner. One photomicrograph was used, and interceptions were counted for 100 individual drops of the 10 centimeter fiducial line. Using a table of random numbers, the 100 elements of data were placed in groups of 3, 5, 10, and 20. In each case 100 data elements were

used, e.g., 20 groups of 5 elements each. Using this technique, it was found that one could expect the following maximum deviations from the true mean grain intercept value:

<u>Number of Drops of the 10 Centimeter Fiducial Line</u>	<u>Maximum Deviation from Mean in Percent</u>
1	±30
3	±15
5	±10
10	±3
20	±2.7

From these data it was decided to use ten random drops of the fiducial line for subsequent data acquisition.

#### RESULTS OF STUDIES ON UNIFORMITY AND REPRODUCIBILITY FOR ALL SHAPES

##### Flexural Data on Various Shapes

The flexural data for the production control study are presented in Table II. The SRI run number shown in column 1 indicates the order in which the specimens were evaluated.

There were a total of 314 flexural evaluations excluding those used for the brief surface finished study. Of these 314, fourteen were from specimen blanks 1A06 which were shorter and were evaluated using a slightly different loading setup. Thus, there were 300 flexural evaluations under the same conditions with respect to the loading fixture and setup. Five of the 300 specimens failed outside of the gage section. Several of the specimens fractured in two places, and it was not possible to determine which fracture occurred first. In those cases where two fractures occurred, the data were included for only those specimens where both fractures were located equidistance from the midpoint.



The distribution of fractures along the gage section was as follows:

<u>Distance from Midspan-inch</u>	<u>No. of Fracture</u>
0-0.025	25
0.025-0.125	74
0.125-0.225	74
0.225-0.325	64
0.325-0.375	<u>51</u>
	288
Fractured out of the gage section	5
Fractured in two places	<u>7</u>
	300

The observed distribution agrees rather closely with the uniform distribution and indicates there was no prejudice or systematic bias in the flexural loadings.

Although five of the specimens fractured out of the gage section, this does not create any conflicts when one considers the Weibull Volume Theory. Recall that the risk of rupture includes the stress level and volume and does not depend only on the maximum or minimum stress developed in a part.

Figure 39 is a frequency plot for the flexural strengths. All data except those few specimens used for the surface finish studies have been included in this plot. The average flexural strength (MOR) was 48,290 psi with a standard deviation of 4610 psi and a coefficient of variation of 9.5 percent. The maximum and minimum values reported were 58,950 psi and 29,810 psi. The histogram is slightly skewed by several low values. Fifteen out of 314 values or 5 percent fell outside of the  $2\sigma$  limits. Fourteen of the fifteen were on the low side.

Also shown plotted on the figure is the probability density function for the normal distribution. It appears to fit the data rather well.

The Weibull parameters, calculated using a modification of an iterative graphical technique were:

$$m = 12.4 \text{ and } \sigma_u = 0 \text{ psi.}$$

Table III is a summary of the flexural results by specimen blank type. Included in this table are the number of specimens, average MOR, standard deviation, and coefficient of variation. Blanks of the type 4A11 and 5A13 gave the lowest average strengths and the 1A02 and 1A06's exhibited the highest values. The average strengths were plotted versus specimen blank numbers and minimum fired thickness in Figure 40. A slight negative correlation with fired thickness is apparent. Note that except for the ring configuration, the strength decreased for each type configuration as the size of the fired piece increased. The two weakest sets of flexural specimens are seen to be from Blanks 9A11 and 5A13.

#### Tensile Data on Various Shapes

The tensile data for the production control study are presented in Table IV.

Because of the configuration of the tensile specimen, it was very difficult to locate the exact location of the fracture. However, by using a 20:1 optical comparator, we were able to determine whether or not the specimen failed within the uniform diameter gage section. This is noted in Table IV by a "G" for gage section or an "R" for radius. Where a break occurred in a radius, the diameter of the fracture surface has also been noted. Twenty-five out of 141 specimens or about 17 percent fractured outside of the gage. The strength values noted in the tables are based on the minimum cross-sectional dimensions. The stress concentration associated with the breakdown radius is something less than 1.1. The value of 17 percent for out of gage breaks is slightly higher than has been observed in the past, but fracture in the radius is not inconsistent with the Weibull theory, since it also is part of the stressed volume.

Strength distribution for the tensile data is shown in Figure 41. The mean values of fracture stress, standard deviations of fracture stress and coefficients and scatter ranges are plotted versus SRI blank numbers and minimum fired thickness in Figure 42. Three blanks showed low average strengths, namely, 2A05, 4A11, and 5A13. A closer examination of the data discloses that one extremely weak specimen (22,800 psi) from 2A05 greatly affects the average value. This particular specimen, 2A05-047-01T, came from a blank which had been fired to a higher than normal temperature. If the extreme value is discarded, the 2A05 average becomes 44,860 psi and again, as was found in the case of flexure, the 4A11 and 5A13 blanks were the low strength pieces.

The average value of strength for the entire population of tensile specimens was found to be 45,180 psi as opposed to 48,290 psi for the total population of flexural specimens. The fact that the flexural test yields slightly higher values is probably attributable, as discussed later, to the stress gradient of the flexural specimen.

It is interesting to note that if the single extremely weak tensile specimen is ignored, the standard deviation for tension for the entire population was 4500 psi which compares quite closely with the value of 4610 psi for the flexural specimen population. The coefficients of variation compare favorably with the values of 0.098 and 0.095 for tension and flexure, respectively.

Table VI is a summary table of the tensile and flexural results. Average strength values are shown here for the various types of blanks along with the densities, velocities, number of specimens, and extreme values.

#### Weibull Statistics

The tensile and flexural data were subjected to analysis by way of the Weibull distribution function. A computer program assembled for computing the Weibull distribution was a slight modification of the program written by L. A. Jacobson.<sup>9</sup> The essential steps executed in the program are the same in that it is designed to converge on the most likely value of  $\sigma_u$  which will produce the best straight line fit, by the method of least squares, of  $\log \log [(N + 1)/(N + 1 - n)]$  versus  $\log (\sigma - \sigma_u)$  where  $\sigma_u$  is the strength below which the probability of fracture is zero. Because a negative value of  $\sigma_u$  would have no physical interpretation, the program restricts the value of  $\sigma_u$  to be not less than zero. In the case where the theoretical value of  $\sigma_u$  is less than zero, this restriction will result in some error in the fitting of the computed probability curve to the experimental values depending on how much less the theoretical value is than zero. Some indication of the magnitude of the error can be obtained from the magnitude of the sum of the squares of the deviations used in the method of least squares. For the tensile and flexural data under consideration here, the values of  $\sigma_u$  were essentially zero.

The Weibull distribution is very sensitive to extreme values. The tensile data were run with the computer program two

times; once with the entire population and once with the extremely low value deleted. The resulting curves are presented in Figure 43 along with the curve for the flexural data. The effect of the single extreme value is quite apparent. Note that the curve for the truncated tensile population has nearly the same character as the flexural curve with nearly identical Weibull parameters. The primary difference in the two curves is that the tensile curve is displaced about 2000 psi to the left or toward lower strengths.

During the course of the work, the Air Force brought Professor W. Weibull to Southern Research Institute for discussions of various aspects of his statistical distribution theory as applied to this program. Professor Weibull's intuitive remarks regarding the application of his theory to real materials were interesting. He stated that the distribution for the Coors alumina for the various SRI parts with respect to the computed probability curve is what one might expect. He explained that a similar distribution might be expected of a similar group of subsets of numbers taken from a population of random numbers.

Another interesting point discussed by Professor Weibull was that of truncation of extreme data points, such as the one extremely low value encountered in the alumina tensile data. Truncation is a legitimate operation if there is some physical basis for it, such as flaws in the material. He mentioned that there are various statistical methods for justifying truncation in some cases. As an extreme example of truncation, it may be proper to treat specimens in a bimodal distribution as two separate groups, particularly if differences in failure mode or criteria were suspected.

Test methods were also discussed, including pressurized rings, Brazil, thick rings, flexural and tensile tests. The point was made that the various indirect tests have the inherent disadvantages of nonuniform and, for many geometries in current use, inadequately defined stress fields.

Certain other aspects of Professor Weibull's Theory of Rupture were discussed, including the interaction of volume and  $\sigma_0$ , the uniqueness of the parameters  $m$  and  $\sigma_0$  and stress gradients.  $\sigma_0$  is a normalizing factor which adjusts with volume changes. Stress gradients such as those present in flexural tests and other indirect techniques were discussed in light of their effect upon the theory. It was brought out that according to the theory the stress gradient has no effect except as it affects the volume of material under consideration.

The influence of other factors encountered in the mechanical evaluation of real materials was discussed. These included the influence of surface finish, crack blunting, the interaction of voids, sample size, and others. The main conclusion seemed to be that these influences might change the shape of the distribution curve but that the results still could be defined statistically if the sample were representative.

A major conclusion of the total conversation was that judgments remain important in the statistical treatment of data. This seems to conflict with some views seen in past work and reported in the literature in this area where the material aspects were ignored and obvious differences in a parameter still grouped.

Figure 44 shows a comparison of the production control study flexural and tensile macro specimen data with the alumina data from Technical Reports Nos. AFML-TR-66-228 and AFML-TR-62-254. The original data shown here were obtained on a high purity, hot pressed alumina body. Note the macro tensile data fall fairly well in line with the past tensile results. The flexural data were pretty much off the curve. This behavior will be discussed later as part of the Statistics of Fracture.

#### Parametric Correlations - Strength, Density (Green and Fired), Cone Angle, Velocity, Fired Thickness, and Shapes

For the purpose of studying uniformity within specimen blanks, it was decided to choose some of the larger parts and remove specimens from a sufficient number of locations to allow profiling of properties. One specific part chosen for the study was Blank 3A10-088, the intermediate size flexural configuration. The cutting plan and data have been shown previously (Figure 15 and Table II, respectively). Figure 45 shows the longitudinal, transverse, and cross-sectional variations of strength for the piece. These are displayed graphically in Figures 46 and 47. In Figure 46, it is seen that uniformity was relatively good except at Section C where the top two layers of specimens were weaker. Figure 47 which shows the strengths at Section B, illustrates the trend towards lower strength at interior positions and higher strengths near the surfaces. Figure 48 depicts the longitudinal, transverse, and cross-sectional variations in density for Blank 3A10-088. These are displayed graphically in Figures 49 and 50. The density values were somewhat scattered longitudinally. Cross-sectionally, the variation was considerably more uniform except at Section B.

Figures 51 and 52 show density profiles for Blank 4A11-089 (large flexural blank). The values are fairly scattered and there are no definite trends shown. Two longitudinal strips show lower than average densities but their relative positions are not indicative of any particular trends.

Reproducibility or piece to piece variation in strength is another important factor which must be considered. Figures 53 and 54 show average flexural strengths versus item numbers for 10 different 1A02 tensile specimen blanks and 7 different 2A04 tensile specimen blanks. The maximum deviation from the total mean strength was 11 percent for the 1A02 blanks and 8 percent for the 2A04 blanks. For the 1A02 blanks (Figure 53) it is seen that except for Items 7 and 16 there was only a 3000 psi spread in the average flexural strengths.

Computer programs for nonparametric statistics were assembled to perform Kendall rank correlation tests, Kruskal-Wallis and Wilcoxon rank tests.

The more obvious rank tests and rank correlation tests were run for the data generated for the production control specimens. The results from these tests are shown in Tables VII and VIII.

Observations based on the results were as follows:

From Table VII:

1. There were mixed indications concerning a relationship between strength and green density. There were strong indications of a positive correlation for data from all blanks and from Blank Types 4A11, 2A12, and 5A13. No correlation was indicated when data from Blanks 4A11, 2A12, and 5A13 were excluded.

2. There were mixed indications of a positive correlation between strength and fired density. Tensile data gave an indication only if data from Blanks 4A11, 2A12, and 5A13 are included. Flexural data gave indications both with and without data from Blanks 4A11, 2A12, and 5A13.

3. There was a strong indication of a negative correlation between strength and cone angle.

4. There was a strong indication of a negative correlation between strength and minimum fired thickness.

5. Sonic velocity did not appear to correlate with strength

6. There was a weak indication of negative correlation between green density and fired density.

7. There was a mixed indication of a positive correlation between cone angle and fired density. Flexural data gave a very strong indication and tensile data gave essentially no indication.

From Table VIII:

1. There was a strong indication that different tool sets yield different green densities.

2. Reproducibility of tensile and flexural strengths between blank types for a given tool set gave mixed indications. Tool Set 6 gave an indication that tensile strengths differ. Tool Set 2 gave a fairly strong indication that flexural strengths differ. All other tool sets gave no significant indications.

3. There was a good indication that strength varies from blank type to blank type.

4. There was a strong indication that fired density varies from blank type to blank type.

5. Reproducibility of strength for different items within a blank type gave mixed indications. There was a good indication that flexural strength varied from item to item for 3Al0, 5Al3, and 6Al4 type blanks. Flexural data from the remaining blanks did not give significant indications.

6. There was a weak indication that the strengths for the center of 3Al0-088 were different from the strengths for the ends.

#### Microstructural Characterization

A study was made to record the general microstructural characteristics relating to the uniformity within a given blank and of reproducibility between blanks made from the same tool set and among all blanks.

The characterization was based on the following determinations. Bulk density was determined on whole mechanical macro specimens and on small pieces from locations near the area of fracture. Microstructural detail, including pore characteristics, grain size and shape, and the identification of microconstituents, was obtained by metallographic and microprobe analyses. Fracture mode was examined by macro and microfractography. Surface conditions were recorded using electron photomicrographs.

Density and Porosity Features - The greatest manifestation of deviation from uniformity and/or reproducibility can be seen from the data for density and porosity. Four sets of information are available with which to judge the degree of variation. The Mechanics Section of the Institute obtained bulk density values for all macro specimens. The weight and physical dimensions of the entire macro specimen were used in this determination. The Inorganic Materials Section of the Institute determined bulk density of small fractions of specific flexural specimens by liquid displacement method and also obtained porosity data from photomicrographs. Coors' reports furnished bulk density values determined by liquid displacement. The Coors' data were obtained from end pieces of blanks from which the mechanical specimens were obtained. If no data were available for the specific blank in question, then data for a blank fired in a nearby or equivalent kiln position were used.

Considering the differences in measurement procedures, the amount of material examined and the variety of techniques used, one would not expect absolute agreement between all the values. Indeed, when one examines these data, the values are found to differ depending on the source of data. If one converts the density data to porosity data for the 15 individual specimens of Table IX, a comparison of the ranges of porosity becomes apparent depending on the measuring technique:

<u>Data Source</u>	<u>Porosity Range</u>
Coors' Data	3-5 percent
SRI Inorganic Materials Section	3-5 percent
SRI Mechanics Section	3-7.5 percent
From Photomicrographs	5-10.6 percent

Two important points should be noted: (a) the relative agreement of data is good, that is, the specimens with lowest or highest porosity occupied that position regardless of data source, and (b) the principal concern in this program involved material uniformity and reproducibility, not the specific level of any given property or characteristic. It is believed that a significant difference in material and porosity existed which was relateable to the average fracture stress.

The data of Table IX show that the density was lower and porosity higher for the 4A11, 2A12, and 5A13 specimens than for the specimens of the other groups. The data for flexural specimens 4A11-089-1 are quite obvious in this respect, regardless of



the source of information used. The photomicrographs of Figures 55 through 63 illustrate the nonuniformity of pore volume among the 15 specimens examined. Figures 55 through 61 show longitudinal sections of the flexural specimens starting at the fracture face and continuing into the specimen for a depth of about 0.2 of an inch. The top of each picture represents the compressive surface and the bottom is the tensile surface. Figures 62 and 63 reveal the cross-sectional view of the tensile specimens near the plane of fracture. It is believed that these low power photomicrographs generate an impression of the relative magnitude of porosity which is in agreement with the data displayed in Table 9. From these photomicrographs, it can be seen that the pore volume was greater for the 4A11 (Figure 61), 2A12 (Figures 59 and 62b), and 5A13 (Figures 58, 62a) specimens.

When the data of Table IX and the remaining density information acquired by the Mechanics Section are considered together, the lack of reproducibility with respect to density or porosity over the entire collection of blanks produced is seemingly related to the size of the part fabricated. Items made from Tool Sets 4(A11) and 5(A13) had the highest porosity. Items made from Tool Sets 1(A02 and A06), 3(A09 and A10), and 6(A14 and A17) had the lowest porosity. Those items (A04, A05, A07, A08, A12) made from Tool Set 2 are somewhat ill-defined with respect to porosity. It is difficult to present data on this point since five different sizes of parts were cut from a rather large master form. For example referring to Table IX, the 2A12 blanks would indicate the lower limit of density while the 2A05 blanks would indicate high density. Although the specific tensile specimen listed for 2A05 was fired at a higher than normal temperature, the group average density was greater than 2A12.

It is believed that the higher porosity of the 4A11 and 5A13 parts is associated with a greater frequency of pores of all sizes and that the maximum pore size was greater. Figure 64 illustrates this point. These data were obtained from pore size frequency counts, using the low magnification photomicrographs of Figures 55, 58, 60, and 61. The smallest pore area that could be conveniently measured was 1 square mil. Therefore, this figure only compares the pore size-frequency distribution at the large pore end of the spectrum. Figure 64 shows that the increased frequency of occurrence of large size pores for specimens of higher total porosity was uniform with respect to pore size. Furthermore, using the density values acquired by the Mechanics Section, it can be shown that the porosity represented by these distributions represents about 30 percent of the total

porosity for each pair of specimens. Therefore, it is apparent that the higher total porosity did not come exclusively from pores of large size.

The specimens used to develop the information shown in Figure 64 illustrate a second point. On the basis of weak/strong studies of the individual mechanical specimens where one makes a direct comparison of the structures of a weak and a strong specimen, the amount of total porosity (within the range of porosity of the specific material used in this study) and the frequency of the larger pores did not apparently affect the strength. The effect of porosity on strength is only correlatable when average fracture stress for groups of mechanical specimens is considered.

In theoretical sintering studies using specimens of equal green consolidation, one expects total porosity to decrease and the frequency of large pores to increase with increased thermal input. However, in the present study involving the data for Figure 64, there is no evidence of advanced sintering (advanced grain growth) and the specimens of greatest porosity contained the larger pores; therefore, one concludes that items such as 5A13 and 4A11 were not consolidated in the green state to the same extent as the other parts. This is suggested also by an inspection of the green densities in Table I.

The porosity features listed in the last four columns of Table IX were obtained from 500X photomicrographs. These photomicrographs were taken at one of three positions along the centerline of these specimens. The percentage porosity by area values are not in very good agreement with density values on an absolute basis, but are in agreement on a relative basis. (It is believed that the porosity value for flexural specimen 2A12-096-11 is too low.) The area count method in general yields high porosity values because of grain pullout, rounding and enlarging of the pores during polishing, and an apparent tendency to trace the pore to larger-than-true size on the light table. There seems to be little difference in average pore size. The percentage porosity and average pore size were determined from the photomicrograph which appeared to be an average of the three taken. The maximum pore size was taken from the largest pore shown on the three 500X photomicrographs. It is questionable as to the definitive value of this maximum size data. Another set of photomicrographs would probably give an entirely different set of data. The information in Figure 64 and the 50X pictures in Figures 55 through 63 give a better picture of maximum pore size.

To summarize the above observations, it would seem that there were at least two levels of porosity existing. The denser parts had a porosity of approximately 3-4 percent with a maximum size of 50 microns, while the less dense parts had about 4-7 percent and a maximum size of 125 microns. Parts from Tool Sets 4 and 5 seem to be different with respect to porosity features from those parts made with Tool Sets 1, 3, and 6.

Within the limited examination described above, no indication on nonuniformity within a given blank or nonreproducibility within a group of identical blanks was found.

The less dense blanks, 4A11 and 5A13, possess a lower average fracture stress, but 1:1 correlation between fracture stress and density for individual mechanical specimens was not detected in the weak/strong studies.

Uniformity of Grain Size - One item, 3A10-088, which had been previously cut into macro specimens for evaluation of the uniformity with respect to strength and density was used in this study. The cutting plan is shown as Figure 15. Fourteen specimens were selected from this cutting plan. The polished sections were made from areas near the center of each macro specimen. The following data were acquired:

<u>Specimen</u>	<u>Average Grain Intercept Size in Microns</u>
3A10-088-A1	3.9
3A10-088-A3	3.5
3A10-088-A5	3.6
3A10-088-B3	3.9
3A10-088-B6	3.5
3A10-088-B8	3.7
3A10-088-B10	3.5
3A10-088-B13	3.6
3A10-088-C6	3.4
3A10-088-C8	3.8
3A10-088-C10	4.0
3A10-088-D6	3.6
3A10-088-D8	3.7
3A10-088-D10	3.6

The average of these data is 3.7 microns with a low-high of 3.4 to 4.0. Maximum grain size for all specimens was about 20 microns. One would conclude from these data that the uniformity of Item 088 was excellent with respect to average grain size.

Grain Size as a Function of Those Factors Contributing to Reproducibility - The factors contributing to reproducibility which were considered in the selection of specimens to be examined include: tool set, green density, minimum fired section dimension and thermal input. Even though 23 specimens were evaluated, this represents a rather cursory examination when one considers the total number of specimens available. An attempt was made to choose specimens with widely differing thermal inputs and green densities for a given tool set or minimum fired section size. These data are presented in Table X along with other information pertaining to the specific specimens.

Before attempting to state observations from the above data, it may be well to note the rather narrow range of average grain intercept size that this material possessed. The following data illustrate this point.

<u>Measurements Made</u>	<u>Average Grain Intercept Size in Microns</u>	<u>Range Microns</u>
1. Ten sets of measurements from one photomicrograph	3.7	3.6-3.8
2. Fourteen sets of measurements from fourteen specimens from one item	3.7	3.4-4.0
3. Twenty-three sets of measurements from twenty-three specimens from nineteen items selected for widely differing processing factors	3.6	2.9-4.2

From these data it is apparent that the average grain intercept size is 3.6 microns. When one considers the data spread allowed by the precision of measurement ( $\pm 3\%$ ) and the spread which would surely be introduced by the examination of many photomicrographs for each specimen, the range of average grain intercept size would probably be less than 1 micron. As shown above with no allowances, the range is only slightly greater than 1 micron even though the method of specimen selection should yield the widest possible

range. Therefore, in consideration of this narrow range in average size, opinions formed with respect to the grain size-processing factor relationship based on the data in Table X should be developed with some degree of reservation.

Additional reasons contribute to the difficulty of forming concrete opinions. For each correlation one attempts to make between grain size and the factors under consideration, at least one direct contradiction is found. Also in most cases the processing factors are combined in a manner so as to have a compensating or leveling effect on end point characteristics. Therefore, one does not find extreme values very helpful in the formulation of conclusions. It is not believed that this is a fortuitous occurrence. It is likely a manifestation of the efforts of a skillful manufacturer striving for uniformity and reproducibility.

In general the grain size increased with thermal input as measured by the degree of cone deformation. Also, it would seem that with thermal input (cone deformation) constant, grain size increased with decreasing minimum fired section dimension. The lack of suitable data precludes comment on the effects volume pressed (tool set) and green density have on grain size. If a range in average grain size of one micron is acceptable and the variations in the factors included in Table 10 are typical of the processing, one would conclude that reproducibility with respect to grain size was good.

The comments made in this section are based on the visual inspection of the data in Table X.

Second Phase - In the course of this characterization, an unknown microconstituent was detected. It differs from  $\alpha$  alumina with respect to polishing, chemical etching, morphology, and chemical constitution. If relief polishing is used to reveal microstructure, this material appears readily, while the alumina grain boundaries do not. In this study, 85 percent  $H_3PO_4$  acid was used as an etchant. This reagent at  $150^\circ C$  brings out the detail of the "second phase" without extensively developing the appearance of the alumina grain boundaries. At  $250^\circ C$ , this etchant reveals alumina grain boundaries and takes the unknown phase into solution. The photomicrographs of Figure 65 show the grain shape to be prismatic rather than the more-or-less equiaxed structure expected of alumina. Since the volume present and size of these grains varied little among the specimens examined, only two photomicrographs are presented. These two specimens

were from the same type of blank and exhibited high and low strength.

Qualitative chemical constitution concerning the second phase was examined using normal microprobe techniques. The specimens were in a relief-polished condition and had been lightly coated with carbon. A Materials Analysis Company Model 400 microprobe was used.

When compared with adjacent alumina grains, the unknown phase indicates the presence of magnesium, calcium, sodium, and silicon, in addition to aluminum. This was shown by stationary beam-spectral scanning and by line traverses for the specific elements which had been qualitatively identified. Scanning-beam technique searching for magnesium also revealed these areas of unknown material, both on polished and fracture faces. Figure 66 shows one piece of microprobe evidence. This is a reproduction of a stripchart from a spectral scan using a beam sufficiently small so that the X-ray output was coming exclusively from the unknown phase. Peaks associated with sodium, magnesium, aluminum, and silicon are visible. Other scans were made which more prominently displayed the silicon peak and showed the presence of calcium. Similar scans on areas immediately adjacent to the unknown phase, revealed only aluminum.

One unsuccessful attempt was made to identify the material by X-ray diffraction. Only the pattern for  $\alpha$  alumina appeared. Although only the alumina pattern was present, the "d" spacings calculated were not in as good agreement with ASTM values as one might expect.

One can only speculate regarding the identity of the micro-constituent. It could be suggested that the questionable phase was an impure spinel or an aluminosilicate. The microprobe analysis indicated about the correct amount of aluminum in the unknown for it to be a spinel. However, the raw count data were not corrected so the other elements of lesser concentration are quantitatively in doubt. If this questionable phase were spinel, it should be noted that only about 1 percent RO would be sufficient to create the quantity seen. Since the measured volume percentage present may be in error to the high side and the density of the unknown lower than alumina, a weight percentage too low for detection by diffraction may be present. On the other hand, one might suggest that the area represents an alumina solid solution which has had its lattice spacing altered by the foreign ions and its crystal morphology modified due to the initial

reaction state which may have been a spinel formation. Finally, existence of an amorphous phase.

Whether the cations other than aluminum which have been qualitatively identified occur as inherent impurities or intentional additions, their presence was noted only in isolated positions (the unknown phase). These elements were not detected within alumina grains. No specific effort was made to examine alumina grain boundaries. The line traverses made with the probe adjusted to detect magnesium did not delineate alumina grain boundaries but showed dramatic response when the beam crossed the unknown phase. Obviously, grain boundary impurity may have been overlooked using a rather rapid line traverse.

In any event, the amount and size of this phase seems to be equal in all specimens examined. For the seven flexural specimens examined, Table 9 shows that the volume percentage present varied from 5.1 to 7.7, and the average size varied from 1.7 to 2.4 microns. As in the case of the data on porosity, the volume percent may be a little high, and the largest crystal dimension is considerably greater than the average size.

An electron photomicrograph is shown in Figure 67 to indicate more clearly the morphology of the grains and their size. Tensile specimen 2A05-047-2T was used for this photomicrograph. The surface was polished and etched at 150°C with  $H_3PO_4$  before replication. No evidence was obtained that microcracks developed at the interface between the unknown phase and the alumina matrix.

It would be impossible to say that this unknown microconstituent contributed in any way either to failure at stress levels well below the expected average value or to the primary failure criterion. Its potential role in the mode of fracture will be mentioned in the section on fractography.

#### Fracture Mode by Macro and Micro Fractography

All flexural and tensile specimens examined were photographed at 20X or 50X magnification using oblique lighting. The magnification used was subject to the size of the object. Views of the fracture face and the region of fracture in profile were used.

A correlation seems to exist between the appearance of macrofractographs and the stress required for fracture. Specimens

which required a higher stress to fracture developed a rough undulating fracture face, while those fracturing at a lower stress revealed an almost planar fracture face. Although it was most obvious for flexural specimens, this was also true for tensile specimens. The macrofractographs of Figures 68 and 69 illustrate this observation. These figures show a comparison of flexural specimens 3A09-085-2 and 3A09-085-1 high and low (weak/strong) strength mechanical specimen from the same blank. Figure 68 compares the fracture paths for the two mechanical specimens viewed in profile, with the top of the picture representing the region of compression. Note the irregular fracture path of the stronger specimen and the rather classic relation to the stress fields on the tensile and compressive sides. A comparison of the fracture faces of these two specimens at low magnification is shown in Figure 69. It is apparent that the stronger specimen possesses a rougher, more undulating fracture face.

That the stronger specimen reveals the creation of more new surface in fracture than the weaker one is a rational observation. However, it does not offer direct evidence of explanation for the weaker or stronger blanks or for the weaker or stronger specimens from a given blank. From the observations above, it was assumed that electron fractography would reveal a difference in fracture mode between weak and strong specimens.

Fracture and external surfaces were examined by light and electron microscopy. Suitable specimens for examination were prepared by a two-stage replication technique. The electron microscopy was done on a Siemens Elmiskop 1A microscope.

Fractography studies made in later work of this program utilized a direct replication technique which eliminated certain structural ambiguities and reduced the number of artifacts. The direct replication technique used is described by Gutshall and Shaw.<sup>4</sup> Artifacts which appear in the earlier electron photomicrographs of this report include tears in the replica, undissolved plastic, round black particles at grain boundaries and other discontinuities, and black bands between specific grains. The black particles were not identified. They may be due to poor conditions of evaporation or atmosphere pollution during preparation. The black bands are believed caused by replica collapse at points of sharp surface discontinuity.

Fracture surfaces were examined by electron microscopy for the same two specimens as above, 3A09-085-1 (35,000 psi) and 3A09-085-2 (52,000 psi). From examining many photomicrographs of these specimens, it was found that the primary fracture mode



was intergranular. Less than 10 to 20 percent of the fracture surface was intragranular and that between the upper and lower limits of strength for a group of specimens, the stronger specimens showed more intragranular fracture. Both the stronger and weaker specimens displayed what has been tentatively termed "a second phase" or intergranular impurity. Almost all fractographs contained this structure. Little porosity can be seen in the fracture surface.

Two additional specimens were examined which also showed divergent strength values and similar densities. However, these two specimens had a lower density than the specimens mentioned above. A typical microfractograph from the tensile region of specimen 5Al3-102-6 is shown in Figure 70. From examining many such microfractographs, the primary fracture mode for these specimens also was intergranular. Less than 10-20 percent of the fracture surface was intragranular. The amount of intragranular fracture was greater for the stronger specimen. The amount of intragranular fracture was less in the compression region for both the stronger and the weaker specimens. Both specimens had an intragranular phase and little detectable porosity within the fracture face.

SEM photomicrographs at different magnification are shown in Figures 71 and 72 and are included to enhance the general appreciation of the fracture morphology for a typical flexural specimen. They primarily confirm the results based on other techniques of characterization. These photomicrographs indicate that the principal fracture mode was intergranular and that microporosity was present in the grain boundaries. A few areas resembling curved depressions can be interpreted as pores similar in size to alumina grains. For this particular specimen, no microstructural feature could be identified as second phase and no area resembled a macropore.

In this limited fractography study, weak and stronger specimens at two porosity levels were examined. A correlation seemed to exist. For each porosity level, the stronger specimen revealed more transgranular fracture and a more tortuous fracture path. The stronger of the less dense specimens fractured in about the same manner as did the stronger of the more dense specimens. The fractography study did not suggest any nonuniformity or nonreproducibility which might contribute to the presence of more transgranular fracture in certain specimens. Within a given strength and density range, a small difference in fracture topography has been noted but no explanation is available.

### Material Characteristics versus Extreme Differences in Strength (Weak/Strong)

In the foregoing sections the characterization was largely concerned with material uniformity or reproducibility and a search for evidence which might explain the variation in strength within a range of values adhering to statistical description. The study also attempted to learn why certain specific specimens failed at a much lower-than-expected stress. This is the weak/strong study. This problem has been referred to in some of the information above, but a concentrated effort was made on this point using tensile Specimens 2A05-047-2T and 2A05-047-1T. These specimens came from the only A05 blank tested which was intentionally fired to a higher temperature than normal. From the gage section of this blank, four specimens were cut: two flexural and two tensile. The two flexural specimens had strengths of 45,140 psi and 45,420 psi, compared with an average strength of 49,050 psi for all A05 specimens tested in flexure. Tensile Specimens 2A05-097-2T and 2A05-047-1T had strengths of 46,540 psi and 22,800 psi, respectively, compared with an average of 45,000 psi for all A05 specimens tested in tension with the exception of the 22,800 psi value. Since these two tensile specimens came from essentially adjacent volumes of material and had such different strengths, it would seem they were excellent candidates for the investigation.

Probably the most obvious difference in these two specimens was recorded in the low magnification inspection of the fracture. The stronger specimen developed a classic fracture plane normal to the outer surface where it then became inclined to the longitudinal specimen axis, while the fracture path of the weaker one was normal to this axis. The fracture surface of the stronger specimen was rougher than that of the weaker one. These observations parallel those previously cited for the flexural specimens.

The size, amount, and distribution of pores and second phase were similar for the two specimens. The porosity shown in photomicrographs may be slightly greater than the 3 percent indicated by density measurements and this is attributed to a certain amount of pullout. A value of 6.9 microns was determined for the average grain size of both specimens.

Replicas were prepared from the fracture faces of the remaining halves of tensile Specimens 2A05-097-2T and 2A05-047-1T. The fractographic examination revealed information similar to that previously stated for the flexural specimens. That is, the

primary mode of fracture was intergranular for both specimens, with the stronger one displaying more intragranular fracture.

Within the limits of this study, it was impossible to determine the reason for the unusually low strength displayed by specific specimens. Prior to this examination, it was believed that a disparate flaw contributed to the very low strength. This type of flaw may include any structural detail that is abnormal to the general microstructure; for example, a heterogeneous distribution of porosity, a pre-existing large crack, a large void, etc. Such dispartates critically located in the specimen should produce low strength.

Evidence of disparate flaws was not found during the fractographic examination. However, it is quite possible that: the descriptive detail was overlooked, the evidence is not sufficiently different from the other fractographic structure, or the definitive structure is destroyed during fracture.

On several occasions, cracks were found in noncritical positions away from the fracture zone. These cracks usually entered the specimen at a rather shallow angle and it would seem that a chipped surface would result if the crack were propagated. Such a crack could develop during processing or during grinding as a result of relieved residual stress or due to grinding abuse. Since a meticulous microscopic inspection of specimen surfaces prior to testing was not part of the procedure, no conclusion is available. However, if this type of flaw critically positioned served as a source of fracture, there is reasonable doubt that one could detect it during post-test fractography. Another disparate that was observed during post-test examination was a very large void probably associated with the bridging of powders during compaction. This void is shown in Figure 73, and in this view the cross section of the void is about 5 x 30 mils. It occurred within the gage length of flexural specimen 2A05-043-3, which had a strength of 54,000 psi. It was located on the side of the specimen and in the tension region near the neutral axis. It is difficult to imagine that a disparate of this magnitude would not play a role in low stress fracture had the volume of material been extracted from the blank in a manner which would have placed the flaw in a critical position. Having examined replications of as-fired surfaces, one would say that evidence of this void within a fracture surface could be overlooked in electron fractography.

Summary - Within a given blank and among identical blanks, uniformity, with respect to microstructural features, was good. One must include specific features, such as the maximum grain size or maximum pore size as shown by a single photomicrograph to demonstrate differences.

Within the limits of present knowledge, one can also say that reproducibility was good for all blanks produced by a given tool set. For example, the blanks making up Groups A09 and A10 produced from Tool Set 3 were quite similar. This point is somewhat difficult to judge for Tool Set 2 since five different blank shapes of great size difference were made from this tool set.

When all the blanks produced are considered, a detectable degree of nonreproducibility is apparent. The Groups A11 and A13 were similar in characteristics to each other, but differ from the other groups. This difference is manifested by lower average fracture stress, lower density, greater total porosity, and larger maximum pore size for those specimens from Groups A11 and A13.

Efforts were not conclusive to relate specific microstructural detail to failure at lower-than-average stress (weak/strong studies) for specific specimens within a group. Only fracture mode correlated with fracture stress for this part of the study. Low stress fracture resulted in a more or less planar fracture surface, while fractures at high stress developed an irregular surface. Although it was not quantitatively established, microfractography indicated more intragranular fracture for the high fracture stress parts. Within the effort used, these features could not be related back to the source of fracture.

#### Flexural Evaluations on a High-Fired 4A11 Blank

After discussions with Coors and the Air Force, it was decided to evaluate one of the later 4A11's that had been fired at a higher temperature to determine whether it would more nearly "fit" into the general population. Blank 4A11-112 was selected for these additional evaluations. The cutting plan, shown in Figure 7, was designed to (1) test an "improved" type 4A11 blank, (2) give more information for analysis of property variations versus location within a blank and (3) check for skin effects.

In addition, more extensive nondestructive testing, a limited postfracture examination, and a limited number of statistical calculations were performed.

NDT Measurements - Nondestructive testing preceded the destructive testing of the fifty 4A11-112 flexural specimens. These included density determinations by liquid displacement and mechanical methods, sonic velocity, X-ray, black light and white light inspections. Dye penetrants were used on the total surface of the specimens to enhance cracks and defects prior to the white light inspection.

The results of density determinations for the 4A11-112 blank are shown in Tables XIa and XIb. Position on these tables represent the relative positions of the specimens on the cross section of the original blank. Shown in Figures 74a and 74b are density contour maps derived from the data from Tables 11a and 11b.

The terms "wet" density and "dry" density refer to data obtained by water immersion and mechanical techniques described earlier. Both densities are for vacuum dried specimens.

The mean "dry" density from the 4A11-112 blank was 3.829 gm/cm<sup>3</sup> with a standard deviation 0.026 gm/cm<sup>3</sup>. Individual "wet" density values were consistently higher than "dry" densities by about 0.030 gm/cm<sup>3</sup> and, as expected, mean density was also higher by this amount; standard deviations were essentially equal. At least 60 percent of the difference between "wet" and "dry" densities can be explained by surface roughness. The remainder of the difference must be due to surface porosity.

The mean density of the flexural specimens from the 4A11-089 blank was 3.775 gm/cm<sup>3</sup> with a standard deviation of 0.019 gm/cm<sup>3</sup>. The difference in mean densities between Blanks 4A11-089 and 4A11-112 was significant at the 99 percent confidence level. The increase in mean density was expected since the 4A11-112 blank was fired at an 80°C higher temperature. The increase in standard deviation of the density between the 4A11-089 and 4A11-112 blanks was not necessarily expected. A portion of this increase in standard deviation can be explained by the removal of specimens from material much closer to the surface of the 4A11-112 blank. The density contour maps of Figures 74a and 74b show that position alone does not fully explain this difference.

The results of the sonic velocity measurements are shown in Table XII. The mean velocity was 0.4016 inch/μ sec with a standard deviation of 0.0035 inch/μ sec. Comparisons with the 4A11-089 blank were not possible since velocity measurements were not taken for that blank.

Destructive Testing - The specimens were evaluated in flexure using the apparatus described earlier. The specimens were loaded in random order. Specimen orientation in the original blank was identified by a corner cut. Specimens were loaded in the flexural apparatus with the orientation mark randomly located left and right. The tensile faces of all specimens from Section A were uppermost for the blank orientation shown in Figure 7. The tensile faces of all Section C specimens were the lower faces. Three specimens were strain gaged for determination of flexural modulus prior to their destructive testing.

The results of the flexural evaluations are shown in Table XII. The average flexural strength (MOR) was 40,920 psi with a standard deviation of 4,550 psi and a coefficient of variation of 11.11 percent. The figures from previous flexural testing of Blank 4All-089 were 44,320 psi, 4,790 psi, and 10.8 percent, respectively. The difference in the average strengths was statistically significant at the 99 percent confidence level. A slight difference existed between the average strengths for Sections A and C but this difference was not significant.

Prior to testing to failure, Specimens All-112-C11, C25, and C32 were used for the determination of flexural moduli. They were strain gaged and incrementally loaded to 25 pounds load (~15,000 psi or 40 percent of the mean fracture stress). These flexural moduli and their corresponding sonic moduli are shown below.

Modulus Values

Specimen	Modulus from Strain Measurements psi	Sonic Modulus psi	Average Sonic Modulus (previous)
C11	$51.8 \times 10^6$	$53.9 \times 10^6$	$53.6 \times 10^6$
C25	$49.3 \times 10^6$	$52.3 \times 10^6$	
C32	$51.4 \times 10^6$	$50.2 \times 10^6$	

During the flexural evaluations, four specimens fractured in two places, and, of these, one had a fracture outside the region of maximum moment. For this work, fractures in two places or fracture outside the region of maximum moment were not considered sufficient grounds to exclude data for these specimens from statistical calculations.

As a check on the apparatus, specimens were loaded with the specimen orientation mark randomly placed left and right. No significant difference was detected between the mean fracture locations of the left and right oriented specimens. This result indicates that the rig was applying an essentially uniform moment.

The higher firing temperature (+80°C) for this blank gave larger grain size. The average grain size for specimens from the center of Sections A and C was 6.7 microns and the maximum grain size was approximately 35 microns. The average grain size at the corner of the blank was 7.7 microns but this was not considered particularly significant.

An examination was made of the data for possible correlations. The following comments are the more obvious ones.

1. A positive correlation seems to exist between strength and density of individual specimens, but it is not a strong one. The major exceptions to this are the four corner specimens from Section A which have higher densities but lower strengths than the neighboring specimens. Larger grain size due to increased thermal input helps explain this anomaly.

2. From 10X to 20X observation of the specimens, the impression is that this material had many voids in the range of 1 to 5 mils maximum dimension. This is in marked contrast to the specimens for which pore counts were run previously, but this was probably due to the greater surface surveyed.

3. Shown in the remarks column of Table XII are the disparate flaws or voids which coincided with fracture location. The three largest disparate flaws found during the prefracture visual inspection caused fracture at their location—Specimens 4A11-112-A11, A51, and C53. Photomicrographs of two of these dispartes are shown as Figures 83 and 84. Less severe dispartes did not exert such a marked influence apparently due to their smaller size. The major exception to the influence of large dispartes on the location of fracture was a 6 x 1-mil void 0.060 inch outside the area of maximum moment on Specimen 4A11-112-C42.

The column of Table XII labeled Strength Rank shows that in general the specimens which exhibited dispartes in their fracture face are contained in the group with lower strengths. In particular, Specimen 4A11-112-C53 had the lowest strength.

## PRELIMINARY SURFACE FINISH STUDY

The nominal surface finish on all the specimens discussed to this point was approximately 15 rms. A brief study was undertaken to investigate the effect of surface finish on strength. Flexural specimens from Blank 3A10-087 were considered along with those from Blank 3A10-088 for the as-ground examples. Specimens 3A10-088C-11, -12, and -13 were cut into two pieces of approximately one inch in length, designated A and B. The three pieces designated A were polished and lapped with  $\frac{1}{2}$ -micron diamond compound. Both one-inch pieces from each specimen were loaded in flexure. The data are presented in Table 13.

Specimens 3A10-088-A4, -B5, -C1, -C2, -C3, -D1, -D2, and -D3 were polished to a surface finish of 3 to 4 rms. The data for these specimens are shown in Table 13. Tensile specimens 3A10-088-C4T, -C5T, -C14T, -C15T, -D4T, and -D5T were also polished to a finish of 3 to 4 rms, and their strength values are presented in Table 14.

The polishing procedure employed was as follows:

1. Initial grinding with Norton D100-R50B56-3/32 diamond wheel
2. Lap out grinding scratches with 15-micron diamond compound on wooden paddle
3. Lap with 5-micron diamond compound
4. Lap with 1-micron diamond compound on wooden lapping disk
5. Final lapping with  $\frac{1}{2}$ -micron diamond compound

It was also deemed desirable to consider the influence of an as-pressed-and-fired surface and a green-machined-fired surface of a macro specimen. These surfaces were positioned as the tensile surfaces when the specimens were loaded. Data are presented in Table XV. The results of the cursory surface finish investigation are briefly summarized in Table XV. These results show that, except for the as-fired surface, and the green-machined surface, the surface finish did not have an appreciable effect on the strength of the specimens. The ground surfaces, polished surfaces (by machine shop), and metallurgically lapped surfaces all gave essentially the same strength values in both flexure and tension. The nominal flexural strength was about 49,000 psi. The pressed and fired surface gave about a 15 percent lower strength value of 40,820 psi.



## STUDIES OF SUBSURFACE DAMAGE

The lack of clear-cut differences in strengths of different specimens with differing surface finishes (all good) and preparation technique during earlier phases on this program raised questions concerning specimen preparation, surface finish, and subsurface damage. Some such questions are:

1. Is there a surface finish optimum such that a better finish does not enhance strength simply because internal flaws are continuously exposed with progressive polishing?
2. Are the strength data being normalized by slicing-grinding damage which precedes the finer finishing steps without large material removal by gentle polishing?
3. Are fractures initiating internally; away from the effects of polished surfaces?
4. Are cracks, flaws, and voids distributed throughout the material of sufficient size to cause crack propagation at the stress levels of these evaluations?

Five separate efforts were followed to help clarify some of these questions. The first effort was an analytical study of the statistics of fracture.

The second effort was concerned with the examination of surface structure by electron microscope to build a background of surface description and then to search for indications of surface or subsurface damage which may be responsible for fracture initiation. Some evidence was found which strongly suggested intergranular cracks on a ground surface of a specimen, Figure 91. The evidence, however, was not conclusive.

The third effort was an attempt to see if significant changes in strength could be detected for any of a large number of surface preparation techniques. The fourth effort was to determine whether specimens produced using Southern Research machine shop practices gave significantly different strengths than specimens produced using different machine shop practices. The last effort was a study to determine the effects of refiring on strength.

## Statistics of Fracture

As reported elsewhere, some limited work was conducted on surface finish effects, but the results were inconclusive. Generally, improving the surface from an as-ground to metallurgically lapped surface had little effect on the flexural strength of the material.

To investigate the idea of surface and/or subsurface damage and what effect it might have on the flexural strength, the distribution of the fracture-source location is needed. There is inherent in the Weibull model a statistical description of the fracture location. The following is a brief outline of this analytical study. A complete derivation is included in the Appendix.

Beginning with the Weibull Distribution in the following form:

$$S = \exp \left[ - \int_V \left( \frac{\sigma}{\sigma_0} \right)^m dV \right]$$

this can be altered by choosing normalized variables describing the stress distribution and the volume.

$$\begin{aligned} \sigma &= \sigma_T \cdot f(\xi) \\ dV &= C V_T d\xi \end{aligned}$$

where

- $\sigma_T$  = reference stress, usually maximum tension
- $V_T$  = volume in tension
- $C$  = constant
- $\xi$  = normalized position variable

For a rectangular flexural specimen, the dimensionless functions are

$$\sigma = \sigma_T \xi, f(\xi) = \xi$$

where  $\xi$  is the dimensionless transverse distance from the neutral plane and the volume under tension is

$$dV = V_T d\xi$$

Now the probability of fracture initiating between the neutral axis and the fraction  $\xi$  of the beam half-height is (see Appendix).

$$F = \frac{G_S}{G_T} = \frac{\xi^{m+1}}{m+1} \cdot \frac{m+1}{1} = \xi^{m+1}$$

Figure 77 shows the fracture source distribution in a rectangular bar under pure bending for various values of  $m$ . Figure 78 shows the same curves for a round flexural specimen.

For a specimen subjected to uniform tension

$$\sigma = \sigma_T, f(\xi) = 1$$

$$dV = 2V_T \xi d\xi$$

The probability of fracture is given by

$$F = \frac{G_S}{G_T} = \xi^2$$

which is independent of  $m$ . Figure 79 shows the curve for a uniform tensile specimen.

For a group of specimens with a particular form of stress distribution, the Weibull Distribution function reduces to

$$S = \exp \left[ - \left( \frac{\sigma_T}{\sigma_0} \right)^m V_{EQ_T} \right]$$

where

- $S$  = specimen survival probability
- $\sigma_T$  = a convenient reference stress, such as the maximum stress in the specimen
- $\sigma_0$  = constant
- $V_{EQ_T}$  = equivalent volume in tension
- $m$  = Weibull modulus

The mean failing stress can be shown to be

$$\bar{\sigma}_T = \sigma_o \left( V_{EQ_T} \right)^{-1/m} \Gamma(1+1/m)$$

Substitution into the reduced form of the Weibull Distribution function yields

$$S = \exp \left[ \beta^m \Gamma^m \right]$$

where

$$\beta = \text{normalized stress} = \frac{\sigma_T}{\sigma_T}$$

$$\Gamma = \Gamma(1+1/m)$$

Comparing two different volumes in uniform tension having the same form of the distribution function gives

$$\frac{\sigma_{T_1}}{\sigma_{T_2}} = \left( \frac{V_{T_2}}{V_{T_1}} \right)^{1/m}$$

Comparing a volume in uniform tension and a volume of a rectangular beam in pure bending gives

$$\frac{\sigma_T}{\sigma_F} = \left[ \frac{V_F}{V_T} \cdot \frac{1}{m+1} \right]^{1/m}$$

These last two equations were used to plot the curves shown in Figure 80. The average strength and volume of the macrotensile specimens are used as the base for these plots. Also plotted are the average results of evaluations of macroflexure specimens and some full size A09 flexure bars. (The results from these latter evaluations are shown in Table XVI. They were not a direct part of this program at this time, but did provide useful information). Note that all three of the measured responses fit the predicted response curve very well.

Before proceeding to a discussion of the curves, consider the techniques used to determine the Weibull Modulus  $m$ . Several estimators may be used. The more familiar of these estimators are: (1) the least value, (2) the greatest value, (3) the standard deviation, (4) the maximum likelihood, and (5) the log-log slope estimator. The last three of these have been used in the past. In the most recent work, the standard deviation and maximum likelihood estimators have been used. For the current data, the standard deviation appears to give the best estimate; however, a detailed analysis has not been run.

The standard deviation (Coefficient of Variation) is related to the Weibull Modulus by the following equation:

$$COV = \left[ \frac{\Gamma \left(1 + \frac{2}{m}\right)}{\Gamma^2 \left(1 + \frac{1}{m}\right)} - 1 \right]^{1/2}$$

Figure 81 is a plot of COV versus  $m$  from this equation. This relation was used in a computer program to obtain values for  $m$  for the standard deviation.

Figures 82, 83, and 84 show plots of the macrotensile and macroflexural data using the equation

$$S = 1 - \exp \left[ -(\Gamma\beta)^m \right]$$

where  $S$  is the probability of fracture. This is the same data as shown in Figure 43 except it has been replotted using the dimensionless parameter, beta. Note that the values of  $m$  (standard deviation estimate) for the tensile and flexural data are in good agreement, 12.5 and 12.9. The curves appear to fit the data quite well, but no quantitative estimate has been made. Figure 84 shows that the maximum likelihood estimate for  $m$  was 14.7 for the flexural data; the curve for this value does not seem to fit as well as did the curve for  $m = 12.9$ .

Discussion - From Figures 82 and 83  $m \sim 12.5$  for the material we are considering. With this value for  $m$  and Figure 77, a statistical look at the fracture source distribution can be obtained. Note in Figure 77 that 50 percent of the time fracture in the rectangular flexural bar should initiate within 0.003 inch of the surface; 80 percent of the time within 0.005 inch of the surface and 95 percent of the time within 0.010 inch of the

surface. Thus, any subsurface damage which penetrated deeper than about 0.0005 inch would have considerable effect on the results (10 percent of the fractures should initiate in the first 0.0005 inch).

For a uniform tensile specimen, the fracture-source distribution is independent of  $m$  and depends only on the area (volume) ratios. The distribution (see Figure 79) shows that 50 percent of the time fractures should initiate within 0.013 inch of the surface and that only 20 percent initiate within the first 0.005 inch.

The above figures show that the flexural results would depend much more heavily on the condition of the material close to the surface. The good predictions of flexural response from tensile results shown in Figure 80 may be taken as indirect evidence that the flexural specimens are not responding to "damage" near the surface. Probably, it would still be wrong to conclude that the same mechanisms were operating in the tensile and flexural specimens. It may be possible to make this conclusion if the material could be affected in some known way and thereby change  $m$ . If so, one would conclude that the surface 5 mils of material as it now exists is like the internal material and that "damage" is not created by grinding, but simply "exposed".

Recall earlier the equation

$$S = \exp \left[ - \int_V \left( \frac{\sigma}{\sigma_0} \right)^m dV \right]$$

was transformed into the equation

$$S = \exp \left[ - \frac{m}{\beta} \frac{m}{\Gamma} \right]$$

The equation

$$S = \exp \left[ - \int_A \left( \frac{\sigma}{\sigma_0} \right)^m dA \right]$$

could just as easily been transformed where  $\int_A dA$  is an area integral in place of a volume integral. The distribution

$$S = \exp \left[ - \frac{m}{\beta} \frac{m}{\Gamma} \right]$$

is very general. Some of its redeeming virtues, as noted by Robinson<sup>5</sup> are:

- a. Data from a variety of studies may be pooled to yield large samples, since normalization eliminates the stress distribution integral.
- b. A single chart may be made to depict uniquely the family of Weibull Distribution (see Figure 85).
- c. It is a convenient analytical form to use in extreme-value computations or other computations.
- d. The constant  $\sigma_0$  has been replaced by a more convenient parameter, the mean value.
- e. If the sample average is accepted, this form shows that there is only one parameter,  $m$ , left to define the distribution.
- f. The  $k^{\text{th}}$  moment of the distribution is given by

$$\mu_k = \frac{\Gamma \left( 1 + \frac{k}{m} \right)}{\left[ \Gamma \left( 1 + \frac{1}{m} \right) \right]^k}$$

Unfortunately, because the distribution is general, it cannot be used to give specific conclusions directly. There are no clues from one set of data as to whether the value of  $m$  is generated by volume effects or surface effects (or both). If  $m$  depends on volume only, it should not change regardless of the specimen configuration. If  $m$  depends on surface only, it probably should change with surface preparation. The machining studies and the surface preparation studies hold the key here. If  $m$  could be effected by grinding, lapping, refiring, etc., then it might be

possible to determine whether there is subsurface damage and what its effect might be.

#### Definition of Surface Characteristics by Electron Microscopy

The purpose of this phase of the investigation was to familiarize the investigators with the minute detail of surface structure resulting from: the manufacturing process, conventional grinding, metallurgical laboratory lapping, commercial lapping, and post grinding thermal effects. It was hoped that this work might lead to a better understanding of surface effects as applied to the fracture of the material of interest.

The photomicrographs described below were made by transmission electron microscopy. A single stage replication technique was used for most of the specimens. Shadowing was done at 35° with carbon-platinum pellets. Carbon applied at normal incidence formed the replica. This technique eliminates most of the artifacts associated with two-stage replication and provides a more easily interpreted shadowing effect. Two specimens, because of severe surface discontinuities, required the use of a two-stage technique. These will be identified below. The fiducial bar on the photomicrographs represents a measure of magnification and the nearby arrow shows the direction of shadowing. Reverse printing was not employed. Therefore, the shadows appear light in the figures.

An artifact common to all of these photomicrographs is a black line delineating a grain periphery on the side of the grain opposite that from which the shadowing material was directed. An example of this is identified by an arrow in Figure 88.

Since one may attempt to reason that this is evidence of a surface crack, an explanation is in order. This is primarily a result of a collapsed replication of a rather large, steep incline. At these points, the electron beam is more efficiently scattered due to the disproportionate replica thickness. Factors which contribute to this in a secondary manner are: replica thickness and migration of shadowing material. This type of artifact has been observed on replicas of such widely different subjects as: minute particulate matter lying on a glass slide and cross sections of blood vessels. When replica density permits the observation of the fine structure of one of these black lines, it appears as a wrinkled or folded film. These regions may be clearly observed in Figure 86.



As-Manufactured Surfaces - Figures 87 and 88 show, respectively, as-manufactured surfaces which have been pressed-fired (3A10-088-A7) and pressed-green machined-fired (a radius, 2A04-026). Figure 87 is from a two-stage replica. The pressed and fired surface consists of many large mounds protruding from the surface, each consisting of many individual grains. Some of these mounds are visible to the naked eye. In this photomicrograph, a region of finely structured debris marks a valley between two mounds. When machining is employed before the final firing, Figure 88, the mounds are eliminated and a surface develops which is somewhat similar to that obtained in refiring. Thermal faceting is more pronounced in Figure 88; however, this feature may be obscured in Figure 87 because of the poorer replication using the two-stage technique. It is also noted from Figure 88 that grain intersections which are relatively free of shadowing effect show no indication of intergranular separation.

Surfaces Cut, Ground, or Lapped after Firing - Figure 89 is taken from a two-stage replication of a surface exposed by slicing the material with a 100-grit diamond wheel. The cutting action is obviously one of fracture with the proportion of intergranular and transgranular fracture being similar to that of a fracture surface created during mechanical testing. Certain regions strongly suggest intergranular cracks in this surface. The white areas of granular shape are probably positions where a grain not securely anchored was removed during replication to be subsequently lost along with its contiguous replica.

Figure 90 represents a standard 15-rms ground surface (3A10-088-C13B) prepared by the Institute's shop. Grinding was done with a 100-grit diamond wheel. The improved clarity of this photomicrograph over the preceding one is a result of the single-stage technique being used. The comments extended for the sliced surface also apply to this ground surface. Regions which suggested surface cracks on the replicas for Figures 89 and 90 were examined in detail at high magnification. Very few areas could be interpreted as cracks. An example of what may be assumed to be a crack is shown in Figure 91. In this photomicrograph, the shadowing direction was from the upper-left corner to the lower-right corner. The crack is indicated by the shadow region (light area) appearing on the side of the black line toward the shadowing direction. If this were a projecting ridge, the light area would appear on the opposite side of the black line. All other regions in this photomicrograph are virtually at the same elevation. It seems that this crack is the result of chippage at a grain boundary which intersected the surface at a shallow angle.

With regard to improved finishing, lapping was considered. Looking ahead to the possible request for many specimens to be prepared by lapping, the effect of a commercial lapping tool was examined. An Abernathy lap was tried. This lapping tool consists of an anodized aluminum plate which has had its surface previously impregnated with diamonds of desired grit size. The specimen used in this trial was one which had been ground to 15 rms in the Institute's shop. Using several grit size laps and finishing with 1800 grit, 3 mils of material were removed. The surface finish improved to 5 rms. The resultant surface structure is shown in Figure 92, a two-stage replication. Obviously, some flat or smooth areas have been developed; however, it is doubtful that this would represent a true surface improvement. Between the flat areas, the structure is similar to that of the original 15-rms ground surface.

Figure 93 shows the surface of Specimen 3A10-088-C13A which was metallurgically lapped in this laboratory. The surface finish measured less than 1 rms. Scratches remaining after final polishing are obvious. The smaller, 1 to 2 microns, surface discontinuities may be exposed pores. The larger depressions are probably areas damaged in grinding which have not been lapped out or are the result of grain pullout during lapping. The black silhouettes are alumina grains which have been extracted from the lapped surface by the replica. They have remained intact with the replica and are opaque to the beam. This would suggest that even if no other type of flaw existed and reasonably good grinding and lapping techniques were employed, flaws in the form of intergranular cracks may be present to a depth equal to some percentage of the maximum grain size. The larger surface discontinuities (pullout or porosity) that are usually seen in optical photomicrographs are absent on these replicas. It is believed these positions are associated with mutilated sections of replica destroyed when the delicate film is removed from the rough surface area.

After viewing this photomicrograph, Figure 93, it is not surprising that the metallurgically lapped specimens did not yield greater-than-normal strength values. A large selection of fracture criteria is still available including (1) exposed pores, (2) the interface between the alumina matrix and the second phase, alumina grain boundaries (not visible), (3) fracture surface developed during grinding which was not completely removed by lapping, and (4) possibly microcracks.

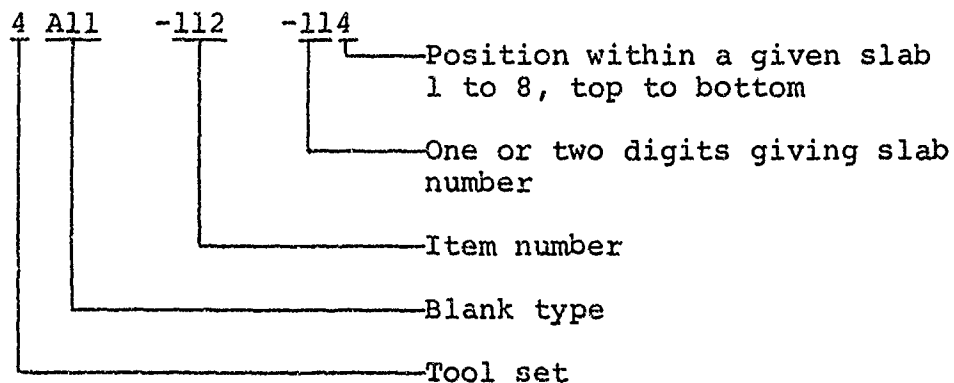
It is obvious that none of the secondary finishing operations completely eliminate the features developed during the initial grinding step, even though from the standpoint of profilometry,

the surface was greatly improved. Since the strength was not increased with improved surface finish, one must question the advisability of using conventional surface finish measurements to relate finish to strength for this material. It would seem that the question of the effect that surface finish or damage due to grinding has on strength cannot be answered until only the inherent material characteristics are present on the surface. At the present time, it is not known whether fracture was associated with damage induced during grinding or was initiated by some inherent external or internal structural characteristic.

### Surface Preparation Study

As a second look at the effects various surface finishing techniques might have on this material, a large number of techniques were applied to small numbers of specimens. The specimens were then evaluated in flexure to measure the effects.

Little of the high quality material was available for this study and that which was available was in the form of small blanks and scrap. Since this study would consume a fairly large volume of material and to eliminate the confounding factors which would be introduced by use of many different pieces with differing properties, one of the larger pieces of scrap of lower quality was chosen. This piece of scrap was from one of the higher fired All blanks, 4All-112. Specimens were sliced to size using a 100-grit diamond cutoff wheel. Nominal specimen dimensions were 0.100 inch x 0.200 inch x 2.00 inches. A cutting plan is not shown for these specimens. Specimen numbers are descriptive of specimen location within the piece of material. The specimen identification is as follows:



The results of the various treatments tried are shown in Table XVII. A baseline strength was established for the sliced specimens and the results of most surface preparation treatments, heat treatments, etc., were measured against this. The average strength of the 4Allsliced specimens was 37,125 psi which was significantly below the average strength of 40,920 psi for ground specimens from this blank. A deep lap, slow machining rate, intermediate machining rate, sandblast machining, and specimens sliced with the predominant wheel marks normal to the specimen length all gave average strengths which could not be shown to differ from the as-sliced specimens.

The sliced specimens and sliced with predominant wheel marks normal to the specimen length were repeated using a scrap of "good" material from Blank 3Al0-088. The sliced specimens from the "good" material were weaker than the ground specimens from this material by about the same amount as those from Blank 4All-112. The sliced-normal specimens were much weaker than the other sliced specimens from this "good" material, however.

Chemical machining was tried using hydrofluoric acid. The gross cross section did not change perceptibly for the specimens exposed to hydrofluoric acid. Chemical attack was evidenced by an obvious increase in porosity. Specimens were exposed to the hydrofluoric acid for 10 and 60 minutes. Those specimens exposed for 10 minutes showed a depth of attack of ~0.005 inch while those exposed for 60 minutes showed a depth of attack of ~0.010 inch. If it is assumed that a macroflexure specimen, 0.100 inch x 0.200 inch x 2.00 inches, was completely undamaged material and 0.005 inch (or 0.010 inch) of material was removed from the surface, its fracture load in flexure would be reduced 22 percent (42 percent). Fracture stress calculations based on gross cross section would show similar decreases in apparent strength. The actual decrease in strength was 6.5 percent (30 percent). The difference between the predicted and actual decrease in strength can be interpreted as indirect evidence that surface material is indeed damaged and that the depth of damage is of the order of 0.004 inch. Applying the above analysis to the specimens exposed to hydrofluoric acid required the assumption that the material in the attacked region has zero or very low strength. The very obvious increase in porosity in this region would seem to justify this assumption.

As an extension of the above experiment, a group of specimens was exposed to hydrofluoric acid for 10 minutes (attack depth ~0.005 inch) and then ground on all surfaces to a depth of 0.004 inch. The porous (attacked) material should require less

energy to remove than solid (unattacked) material and therefore reduce grinding damage. The results were not conclusive. The average strength of these specimens was 39,803 psi which was significantly stronger than the as-sliced specimens. A better comparison would be the ground specimens from Blank 4A11-112. From this comparison, it could not be concluded that the strengths of the etched and machined specimens and the ground specimens were different.

Chemical machining using molten borax was tried on sliced specimens from Blank 4A11-112 and on ground specimens from 3A10-087. The sliced, borax-machined specimens had an average strength of 39,750 psi which was significantly stronger than the as-sliced specimens from this same blank. The ground, borax-machined specimens had an average strength of 45,300 psi which was weaker (but not significantly weaker) than the strength of ground specimens from this blank.

Thermal treating of sliced specimens using an oxy-acetylene torch was tried. Specimens heated momentarily to 2000°F had an average strength of 38,740 psi which could not be shown to be different from the as-sliced specimens. Specimens heated to 2900°F tended to develop thermal cracks on cooling and these data though weaker are not considered significant.

Thermal treating of sliced specimens for various lengths of time from 5 minutes to 168 hours in a furnace was tried with inconclusive results. In addition to the tabulated results in Table XVII, the results are also presented in Figure 94. The following comparisons are all against the as-sliced specimens. The 5-minute and one-hour thermal treatments indicated increases in average strength. The 1/2-hour and 3-hour thermal treatments indicated reductions in strength. The 12-hour and 168-hour thermal treatments indicated no change in average strength. A relation between strength and length of thermal treatment can be imagined if the data from the 5-minute and 1-hour thermal treatments are ignored. Since there are no justifications for ignoring these data, the only conclusion possible is that the thermal treatments tried had no consistent effects.

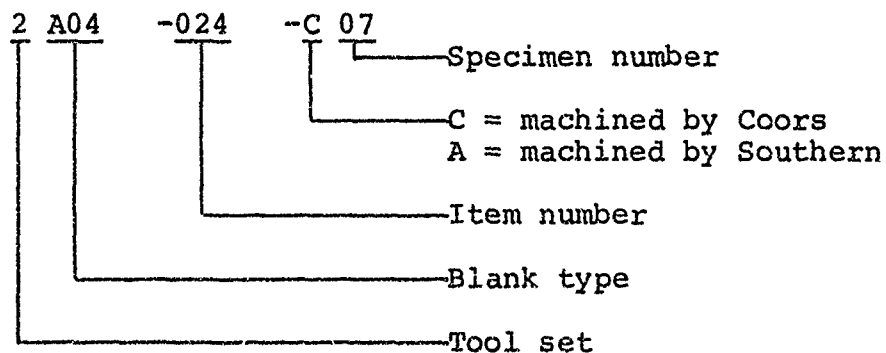
Thermal treatment in conjunction with vacuum during thermal treatment, after thermal treatment, or both before and after thermal treatment was tried on sliced specimens. The only one of these treatments which gave a strength which differed from that of the sliced specimens was a single specimen heated to 660°F for 2 hours in a vacuum and fractured in the vacuum environment at room temperature. This single specimen had a strength of 46,435

psi. This large increase in strength probably was due to the thorough removal of moisture. With the exception of fracturing in the vacuum environment, this experiment was repeated on 20 ground specimens from "good" material which appears elsewhere in this report under "Environemnt Study".

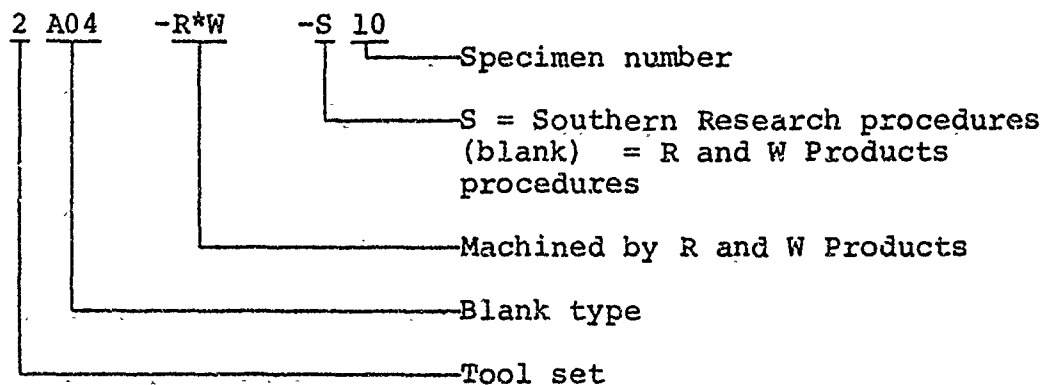
#### Machining Study

The lack of clear-cut differences in strength of specimens with different surface preparation techniques raised the question of whether machine shop practices at Southern Research might be causing damage which was not completely removed by the polishing, lapping, etc. If specimens produced by other machine shops using other practices have different strengths, it could be concluded that indeed machine shop practices had an effect.

For this study, the large ends from 2A04 blanks were chosen. The machine shop of Coors Porcelain Company of Golden, Colorado, and R and W Products of Redwood City, California, agreed to machine specimens. Both Coors and R and W were sent one end each (randomly selected) from Blanks 2A04-24, 2A04-25, and 2A04-28. For comparison, Southern Research machined 28 macroflexure specimens from one end each of Blanks 2A04-31 and 2A04-35. All used the same cutting plan which is shown in Figure 27. Coors and Southern specimens were identified as follows:



Due to a misunderstanding, specimen identification was not maintained by R and W Products and an arbitrary specimen identification system was used as follows:



The procedures followed by the Southern machine shop were:

Machine: Do All Surface Grinder

Coolant: Flooded with water soluble oil (25:1 mix)

Wheel speed: 6,500 surface feet per minute

Table speed: 400 inches per minute

1. Slice specimens using 100-grit diamond cutoff wheel (7-inch diameter x 1/32 inch). Downfeed  $\leq 0.002$  inch per pass.
2. Using suitable precautions to assure flatness, grind specimens to size using 100-grit diamond wheel (7-inch diameter x 1/4 inch). Downfeed  $\leq 0.00025$  inch. Finishing cuts 0.0001 inch. Crossfeed  $\leq 0.125$  inch per pass.

Coors machine shop used identical methods and wheels on twenty-one macroflexure specimens (numbered 01 through 07) machined using Southern Research procedures. The other twenty specimens (numbered 08 through 14) were machined using the procedure in ACMA Test No. 2 standard with the exception that a 220-mesh diamond surface grinding wheel was used. These procedures can be summarized as follows:

Wheel-specimen relative speed  $\leq 6000$  feet per minute

Downfeed  $\leq 0.001$  inch

Crossfeed  $\leq 0.010$  inch per pass } Down to final 0.001 inch

Downfeed  $\leq 0.0002$  inch

Crossfeed  $\leq 0.005$  inch per pass } Final 0.001 inch

All grinding parallel to length of bar

R and W Products used Southern Research procedures on twenty macroflexure specimens except that a 320-grit diamond surface grinding wheel was used. The remaining twenty specimens were machined using unspecified procedures and also using the 320-grit diamond surface grinding wheel.

The specimens were subjected to nondestructive testing consisting of bulk density, sonic velocity, and visual inspection (10X-20X) in white light. The results of these evaluations are shown in Table XVIII. The materials appeared similar from the standpoint of density. The average density of the specimens machined by all three machine shops was  $3.809 \text{ gm/cm}^3$ . The sonic velocity measurements were not comparable since specimens machined by Coors and R and W had not been machined flat on the ends of the specimens. The specimens machined by Coors and R and W also did not have the chamfers along the edges of the tensile face of the macroflexure specimens. The chamfers were machined by Southern Research using half the normal downfeed for this operation. The specimens machined by Coors had had a few small chips along the edges of the tensile face and these all cleaned up. The specimens machined by R and W had had several long shallow chips along the edges of the tensile face but not all of these cleaned up. Those chips which did not clean up did not affect fracture initiation, however, as in every case, fracture occurred at a position away from these remaining chips.

Surface finish was measured using a profilometer on two specimens chosen at random from each group of specimens. The specimens machined by Southern Research had a surface finish of 20-26 microinch rms. Those machined by Coors had a surface finish of 23-28 microinch rms using Southern Research procedures and 22-30 microinch rms for those using ACMA Test No. 2 Standard. The specimens machined by R and W using Southern Research procedures and their own procedures had surface finish of 9-12 microinch rms and 11-15 microinch rms, respectively. It was felt significant that the use of a 220-mesh wheel by Coors did not result in a finer surface finish than that given by a 100-grit wheel. The 320-grit wheel used by R and W gave a much finer surface finish than that obtained by either Coors or Southern Research.

The results of flexure evaluations are also shown in Table XVIII. The specimens machined by Southern Research had an average strength of 47,768 psi. One specimen, 2A04-031-A-1, had a particularly low strength. Examination of the fracture faces of this specimen revealed debris and a significant deviation of the crack at the site of fracture initiation but no identifiable



flaw was found. The result from this specimen was included in the statistics. Various voids were found on other specimens, but they seemed to have little effect on strength. The largest of these voids, 0.004-inch round, occurred on a specimen, 2A04-035-A02, which had a strength of 53,300 psi. Average data from Blanks 2A04-031 and 2A04-035 were compared. Average strengths were almost identical, 47,802 psi and 47,737 psi, even though density and sonic velocity were somewhat different.

The average strength of the specimens machined by Coors using Southern Research procedures was 48,435 psi. The average strength of specimens produced using ACMA Test No. 2 Machining procedures was 47,615 psi. One specimen, 2A04-024-C04, had a strength of 35,510 psi and a 0.003 x 0.004-inch void in the fracture face which had been found in pre-evaluation inspection. The strength of this specimen was excluded from all strength statistics. Comparison of the average strengths of specimens machined by Coors using Southern Research procedures and using ACMA Test No. 2 machining procedures yields the inference that it cannot be concluded that they differ. Comparisons among the average strengths of specimens from each of the blanks ignoring the differences in machining procedures lead to the results that none can be concluded to differ from the others. Comparing the average strength of all specimens machined by Coors against that of the specimens machined by Southern Research yields the inference that it cannot be concluded that they are different. The average density of specimens from Blank 2A04-028 was the lowest of the three blanks and the average strength was the highest.

The specimens machined by R and W using Southern Research procedures and using their own procedures had average strengths of 45,431 psi and 44,864 psi, respectively. One specimen from each group had a low strength and a severe void. Specimen 2A04-R\*W-S13 had a strength of 30,860 psi and a large irregular void with a major dimension of 0.028 inch. Specimen 2A04-R\*W-19 had a strength of 39,900 psi and a void that appeared on the surface to have dimensions 0.005 x 0.008 inch at the chamfer. After fracture, the void was revealed to continue at a low angle to the surface and had a major dimension of 0.012 inch. The strength of neither specimen was included in the strength statistics. Specimen 2A04-R\*W-14 had a strength of 37,800 psi. Examination of the fracture faces revealed debris and a significant deviation of the crack at the site of fracture initiation but no flaw could be identified. The strength of this specimen was included in strength statistics. Other specimens contained voids on their fracture faces which were much less severe than those mentioned above. It might be argued that Specimens 2A04-R\*W-S06 and 2A04-R\*W-18 should

be excluded from strength statistics because of the voids on their fracture faces. Their strengths, however, are close to the average strength and their exclusion would have little effect on the results.

Comparison of average strengths of specimens machined by R and W using Southern Research procedures and using their own procedures shows that they cannot be concluded to differ. Comparing the average strength of all specimens machined by R and W to that of all specimens machined by Coors yields the conclusion that they are different. Comparison of the average strengths of all specimens machined by R and W and those machined by Southern Research leads to the conclusion that at a 90-percent confidence level it can be stated that the strengths are different. This latter result is not considered as significant as the conclusion that R and W and Coors specimen strengths are different. This one is more significant because the same fired blanks provided material for both machine shops. Perhaps the use of downfeed and crossfeed rates similar to those used by Southern Research with the 100-grit diamond wheel are not suitable for use with the 320-grit diamond wheel used by R and W. Comparison of the variances of the strengths of all specimens machined by each of the three machine shops leads to the conclusion that the variance for specimens machined by R and W is significantly smaller also.

Plots of probability of fracture for the specimens machined by each of the machine shops are shown in Figures 95, 96, and 97. The curves were fitted to the data using the COV estimator. This is another way of displaying the material variability. The Weibull modulus,  $m$ , for the specimens machined by Southern Research, Coors, and R and W were 14.269, 15.227, and 19.625 compared to 12.923 for the earlier macroflexure specimens.

There seemed to be a slight difference between the strengths of materials from the center section and the ends of the 2A04 blanks. Specimens from the center section of Blanks 2A04-024, -025, and -028 had an average strength of 49,050 psi. Specimens from the ends of the same blanks machined by Coors had an average strength of 48,025 psi. Specimens from the center section and ends of Blanks 2A04-031 and -035 had average strengths of 50,045 psi and 47,740 psi, respectively. These differences were about as expected from the strength-fired thickness relation of Figure 40.

The major result of this study is the conclusion that machine shop procedures do make a significant difference in strength results. The lower strength together with the lower variance of specimens machined by R and W are a strong indication that

either the material they machined was different or some factor in their machining practice masked both the inherent strength and variability. The former seems unlikely since pieces from the same blanks were also used by Coors. This is not to argue that machining by Coors and Southern Research was not masking the "true" strength and variability nor that their procedures were the best that can be used. For this study, on this material, less effect of "damage" (as measured by strength) was detected for specimens machined by Coors and Southern Research.

### Refired Specimens

Refiring has been proposed as a method of improving the surface and near surface material which is very likely to be damaged during specimen preparation. To study the effects of refiring, macroflexure specimens were prepared from three 3A09 type blanks from the stock of "good" materials. These blanks were 3A09-081, 3A09-082, and 3A09-084. The cutting plan for these blanks is shown as Figure 10. The specimens were subjected to nondestructive testing consisting of bulk density, sonic velocity, X-ray, and 50X white light visual inspection. Of the 72 specimens prepared, 50 were chosen as representative and shipped to Coors for refiring according to the schedule shown in Figure 10. Specimen groupings were randomly selected.

The specimens were refired by Coors under the following conditions:

Hydrogen refire            1550°C for 1 hour and 20 minutes

Oxygen (air) refire    1570°C for 1 hour and 10 minutes

Specimens were reinspected following the refire and the only obvious changes were to the specimens refired in a hydrogen atmosphere. All these specimens were gray (as opposed to creamy white for materials refired in oxygen or not refired). The gray coloration was generally uniform over the entire cross section on fracture faces. The gray coloration was mottled in places on the surface with lighter coloring and marked by small infrequent dark spots. The dark spots were not associated with surface voids nor were they later associated with fractures. Neither mottling nor dark spots correlated with weak or strong specimens.

The results of the destructive flexural evaluations on the refired specimens are shown in Table IXX. Control specimens which were not refired were also evaluated and results are also in Table IXX.

Several of the specimens had unusually low strengths. The fracture faces of each of the low strength specimens were inspected at 10X to 20X in white light. Only two specimens, 3A09-081-24A and 3A09-082-24A, showed significant flaws and were excluded from strength statistics. One specimen, 3A09-084-24A, was mapped prior to refiring to see if the fracture path ran through or avoided surface flaws. This specimen had a significant disparate, a 7.5-mil void (Figure 98), just outside the region of high stress, but fractured at a 2 x 4-mil void (Figure 99). Before and after fracture photomicrographs in Figure 100 of Specimen 3A10-088-C12A, which had been evaluated in the preliminary surface finish study, show that for this specimen the fracture path did not include any of the surface discontinuities.

Comparisons were made of the average strength of each of the refired specimen groups with the average strength of the control specimens. The control specimens had an average flexural strength of 47,712 psi. The average flexural strengths of the lapped-hydrogen refired specimens, the hydrogen refired specimens, and the oxygen refired specimens were 44,558 psi, 45,823 psi, and 44,452 psi, respectively. Only the strength of the oxygen refired specimens was significantly different from that of the control specimens. The actual decrease in average strength for each of the refiring treatments and the fact that the only statistically significant effect, the change in strength of the oxygen refired specimens, was negative leads to the conclusion that refiring, while not strongly detrimental, was definitely not beneficial. It was decided that the specimens to be lapped after refiring would offer little additional information and they were not evaluated.

Average flexural strengths were also compared among the three different blanks ignoring possible refiring effects. These comparisons gave mixed results. Only the comparison between Blanks 3A-9-082 and 3A09-084 showed significantly differing strengths.

Figure 101 is a group photograph at 7.3X of fracture faces of half of the specimens in each treatment group evaluated. The specimens are arranged in descending order of strength in each group. The lower edge of each fracture face is the tension side of the specimen. Note the extensive crack branching apparent in the stronger specimens, especially in the hydrogen refired specimens. Crack branching left large chips and wedges which appear much lighter colored where they reduce to very thin sections. Note also the contrast between the rough, undulating surface of the strong specimens and the flat, smooth surface of the weak

specimens. The lapped-hydrogen refired specimens, however, are smoother than the hydrogen refired specimens even though the strength range is about the same. This was probably due to the thinner cross section of these specimens. The thinner cross section of the lapped-hydrogen refired specimens results in a lower failing load at a given stress level and therefore a lower strain energy available to propagate a crack. A lower strain energy is also associated with the weaker specimens within a given group.

Average grain size was determined for one specimen from Blank 3A09-084 from each of the refired groups. The average grain sizes were 3.9  $\mu\text{m}$ , 3.8  $\mu\text{m}$ , 3.9  $\mu\text{m}$ , and 3.8  $\mu\text{m}$  for no treatment, the lapped-hydrogen refired, hydrogen refired, and the oxygen refired specimens, respectively. These values of average grain size also agree with the overall average grain size, 3.7  $\mu\text{m}$ , from good blanks previously evaluated. The lack of a change in grain size from no treatment to refired and the good agreement with previous data indicate that the Coors refiring had no detectable effect on grain size.

In addition to grain size determinations, the refired surfaces of the same specimens as above were examined by electron microscopy using single stage replicas. The ground surface of the specimen with no treatment, Figure 102, was very similar to ground surfaces examined in prior work, Figure 90. Material removal occurred primarily by intergranular fracture. Few areas showed transgranular fracture or true cutting action. There was considerable evidence of insecurely held grains at the ground surface. These grains were pulled out by replica removal and appeared as black grain-shaped areas in the photomicrograph. Microstructure which may be interpreted as surface cracks also appeared. Had the refiring made a significant improvement in the bonds around a number of these loose grains and "surface cracks", a significant improvement in strength should have been detected.

The specimens refired by Coors showed no change in grain structure with respect to grain size and distribution—compare Figure 102 with Figures 103, 104, and 105. The structure consisted of larger grains (10-20  $\mu\text{m}$ ) in a matrix of smaller grains (1-3  $\mu\text{m}$ ). As expected, considerable thermal faceting took place. Little material was transported thermally and this was predominantly at grain intersections. This material transport at grain intersections appeared as a good thermal etch. No evidence of surface cracks could be found on the refired surfaces. The thermal etch may have masked such cracks.

## ENVIRONMENT STUDY

The strength of alumina has been shown to be affected by the presence of water.<sup>6</sup> An environment study was run to gain some insight into the extent of changes in average strength which could be attributed to differences in relative humidity at different laboratories which might evaluate this particular alumina. The remaining portions of Blank 2AlO-087 were utilized for this study. Twenty-six macroflexure specimens had been previously evaluated from this blank. Eighty macroflexure specimens were machined from the remaining portions of this blank as shown in the cutting plan, Figure 14. The macroflexure specimen is shown in Figure 1. The specimens were evaluated nondestructively prior to environmental treatments and destructive evaluations. The nondestructive evaluations consisted of bulk density and sonic velocity. Three different treatments were to be applied before destructive flexure evaluations. A random order computer program was used to select twenty specimens each for the three different treatments. Sixty of the eighty specimens were evaluated.

All sixty specimens were dried at 1800°F at a pressure of 2.1  $\mu$ m of mercury for two hours in a graphite resistance furnace. The furnace had been baked out at 2700°F for 1-1/2 hours to remove volatiles prior to the vacuum drying cycle. All sixty of the specimens exhibited a dark gray coloration on removal from the vacuum furnace. This was surprising since other alumina specimens had also been vacuum dried in this same furnace without any visible changes. It was decided at this time to split the twenty specimens originally scheduled to be held at room conditions into two groups of ten each. The first ten were ultrasonically cleaned and then oven dried. The second ten were held as originally planned. The treatments for the remaining 40 specimens were carried out as planned and described below.

The ten specimens ultrasonically cleaned showed a decrease in the gray coloring, but did not return to the original creamy white appearance. Subsequent examination of fracture faces of broken specimen showed the coloring extended beyond the surface in only a few isolated places on each specimen. The places where the color extended below the surface could be interpreted as either porous areas or voids. This interpretation made the search of fracture faces for flaws much easier than searches on non-colored specimens had been. It was feared that the discoloration, or its cause, would have a negative effect on strength. This occurrence was common to all specimens and should not invalidate

comparisons among the specimen treatments. Descriptions of the four treatments after the vacuum drying cycle follow in the paragraphs below.

After vacuum drying, the first group (twenty specimens) was stored in a dry desiccator for two weeks before flexure evaluations. A dish of phosphorus pentoxide was used as a desiccant. Specimens were stored in individual glass beakers and physically separated from the dessicant by a ceramic rack. As a worst case, the relative humidity inside the desiccator should have been no higher than 0.2 percent. All specimens were removed from the desiccator and sealed in a plastic bubble enclosure which contained the flexure apparatus and loading mechanism. The enclosure was purged with dry nitrogen gas and a small positive pressure was maintained throughout the evaluations to prevent infiltration of moist atmospheric air. The specimens were loaded into the flexure apparatus using gloves built into the wall of the enclosure.

After vacuum drying, the second group (twenty specimens) was stored for two weeks in a desiccator at room temperature and 100 percent relative humidity. The specimens were in individual glass beakers and physically separated from the water and wicking. No attempt was made to prevent or cause moisture to condense on the specimens. No visible moisture was found on the specimens or beakers during the flexure evaluations. The specimens were removed from the desiccator one at a time and evaluated in the flexure apparatus.

After vacuum drying, the third group (ten specimens) was cleaned in an ultrasonic cleaner and oven dried at 235°F overnight before flexure evaluation. Cleaning and oven drying is the procedure which has been used on all other specimens evaluated at Southern Research.

The fourth group (ten specimens) after vacuum drying was stored at room conditions for two weeks. During this interval, the relative humidity in the laboratory remained fairly constant at about 60 percent. The specimens were then destructively evaluated in flexure.

The results of the flexure evaluations are shown in Table XX and statistical comparisons are shown in Table XXI. Previous evaluations on specimens from this blank, 3Al0-087, gave an average strength of 47,890 psi. The average strengths for this study were 50,798 psi, 46,230 psi, 44,359 psi, and 45,074 psi for

the specimens evaluated dry, stored at 100 percent relative humidity, ultrasonically cleaned, and stored at room conditions, respectively.

Statistically, no differences were detected among the average strengths of the specimens stored at room conditions, those ultrasonically cleaned and those stored at 100 percent relative humidity even when the first two are lumped together. From these results, one could conclude that the usual laboratory procedure of ultrasonic cleaning followed by oven drying was neither harmful nor beneficial.

Comparing the results of previous evaluations to those for ultrasonically cleaned specimens, room conditioned specimens, and 100 percent relative humidity conditioned specimens gave mixed results. The average strengths of specimens ultrasonically cleaned and those stored at room conditions gave strong indications that they were weaker than those of previous evaluations. The indication for the 100 percent relative humidity conditioned specimens was not quite strong enough for a decision at the 90 percent confidence level. The conclusion is that either the vacuum drying cycle used in this study or the vacuum drying plus subsequent exposure to moisture had a detrimental effect on strength. The mechanism which caused the effect is unknown.

The average strength of the specimens vacuum dried and evaluated dry was significantly higher than those for each of the other treatments run on specimens from Blank 3A10-087. This was true in spite of the apparent detrimental effect that the vacuum drying had on the specimens with other treatments. More work is needed in this area to define the relation between strength and relative humidity conditioning in the range of 60 percent to ~0 percent humidity.

Elimination of laboratory condition effects from results of evaluations from different laboratories and different testing methods could be more reliably handled if all specimens were conditioned in the same manner rather than relying on computed corrections from a regression analysis.

The unexpected discoloration of the specimens during the vacuum drying cycle had one beneficial result. Inspection of fracture faces for flaws, discontinuities, etc., was greatly aided. Areas which were interpreted as porous regions became visible which had been at best only vaguely seen on other specimens. The results of the flaw search are shown in the remarks column of Table 20. A plot of flexure strength versus the average



size of the flaw on the fracture face is shown as Figure 106. Flaws seemed to occur singly, that is, no more than one flaw was found on a given fracture face. Separate regressions were fitted to the data for dry specimens and those exposed to moisture of any extent. Specimens without detectable flaws were plotted at flaw size of zero. Those porous areas too vague to measure were assigned a flaw size of 0.002 inch. Statistical parameters infer that the slopes of both regression lines are significant, that is, the slopes of the "true" relationships are not likely to be zero. No great significance is attached to these findings, however. Each specimen had several flaws on the tensile surface that appeared to be of about equal size and severity as those detected on fracture faces. What was detected was probably the "background" voids and porous areas for this blank. Though an apparent relation exists, present inspection techniques would need to be greatly improved to reliably detect flaws in this size range.

#### LOT TO LOT REPRODUCIBILITY AND UPGRADING STUDY

During the initial phases of this program, Coors produced a number of specimen blanks in a very wide range of sizes and/or shapes. The majority of these specimens had properties measured by small macrotensile and macroflexure specimens which fell within a narrow range and seemed well suited for the intent of the program—to provide quantitative comparisons of test methods. The two blank shapes with the largest cross section seemed to differ most from the majority. Blanks 4A11 had lower strength and lower density than the majority while Blanks 5A13 had lower strength and slightly lower density. Blanks 2A12 with fairly large fired cross section had slightly low strength and low density. In a study of porosity features, these three blank types showed higher porosity and larger maximum pore size. It was felt, however, that it should be well within the capability of a joint effort of Coors and Southern Research to upgrade these three blank types to the properties demonstrated by the other ten blank types.

As an effort to demonstrate the upgrading of the three somewhat deficient blanks, two each of Blanks 4A11 and 5A13 were to be produced by Coors. These two, if successful, should be adequate proof that the less deficient 2A12 blank could be upgraded also. To demonstrate lot to lot reproducibility, at least five 2A7 blanks and two 3A09 blanks were to be produced. To provide in one piece of uniform material an adequate source of specimens for studies of secondary finishing techniques and

requirements, one 3A10 blank was to be produced. As an exercise to see if near-shapes for macro specimens could be developed, sixty specimens fired to near size and shape of the MOR macro specimens. The reasoning for this final exercise was that machining in the green state is much easier than machining in the fired state. If the extra handling required of the larger number of green pieces were cheaper than the extra cost of machining fired pieces, a net saving would result.

Firing analysis data for alumina blanks from the reproducibility and upgrading study are shown in Table XXII. These blanks were fired by Coors at intervals from October 16, 1970, to May 1, 1971.

It became obvious quite early that the MOR bars would be difficult to produce. The first bars produced had cambers of up to 0.022 inch with an average of about 0.002 inch. A second firing on grooved refractories to minimize the distortion resulted in a maximum camber of 0.004 inch and an average camber of less than 0.002 inch. A total of eighty of these MOR bars were received at Southern Research. Thirty-five of the MOR bars were fired as-pressed. The remaining forty-five MOR bars had 0.002 inch of material removed from all surfaces prior to firing. Two or three specimens were selected from each group of (1) as-pressed surface, first firing, (2) green machined, first firing, (3) as-pressed, second firing, and (4) green machined, second firing. The results from flexural evaluations on these specimens are shown in Table XXIII. These specimens had the very disappointing strengths of 31,084 psi, 39,299 psi, 32,608 psi, and 40,870 psi in the same order as the groups listed above. Note that green machining seemed to raise the strength in both cases when compared to firing a piece that had not been green machined. An additional ten specimens were evaluated later from which a minimum of 0.005 inch was removed from all surfaces after firing. The results from flexural evaluations on these specimens are also shown in Table 23. The average strengths of these specimens were dramatically greater than those with as-fired surfaces above. The average strengths were 49,925 psi, 48,490 psi, 45,216 psi, and 46,816 psi for the as-pressed first firing, green machined first firing, as-pressed second firing, and green machined second firing specimens, respectively. Thus, machining after firing wiped out the effect of machining in the green state, but allowed the effect of different firings to be seen. These last two strengths are significantly lower than the average strength of "good" specimens machined from the earlier pieces made in the production control study of this program. Specimen MOR-129-88, from the second firing of specimens with as-pressed surface, had an average grain

size of 5.2  $\mu\text{m}$ ; specimen MOR-132-61, an as-pressed specimen from the first firing, which had had the as-fired surface machined away, also had an average grain size of 5.2  $\mu\text{m}$ . The extra handling required to manufacture these specimens, the fact that their properties were not yet representative of "good" material, and the fact that the slicing operation in machining macro specimens from larger pieces was not the largest expense of providing macro specimens all combined to make the further pursuit of this experiment perhaps unattractive.

The materials for the lot to lot reproducibility and upgrading demonstration were received at Southern Research in December of 1970. The parts received and firing analysis data are shown in Table XXII. Four macroflexure specimens were extracted from Blank 2A07-117. Five specimens each were taken from Blanks 3A09-120, 4A11-125, and 5A13-127. Cutting plans for these blanks are shown as Figures 7, 11, 18, and 21. The average strengths, shown in Table XXIV, were 42,176 psi, 44,974 psi, 42,006 psi, and 40,944 psi for the 2A07, 3A09, 4A11, and 5A13 blanks, respectively. These contrasted with the overall average of 48,290 psi and blank type averages of 49,010 psi, 48,283 psi, 44,320 psi, and 44,650 psi for the same type blanks, evaluated earlier in this program. Thus, all blanks made in the effort to raise their strength or demonstrate lot to lot reproducibility were weaker.

Early in the program, tentative specifications were suggested for density and average grain size which should hold average strength to certain limits. The suggested density limits were 3.80 to 3.84  $\text{gm/cm}^3$  and average grain size limits were 2 to 5  $\mu\text{m}$ . It was thought that the limitations on density and grain size, together with certain controls on fired thickness, other firing parameters, and the production figure of merit (a qualitative variable concerned with the ratio of pressing area to pressing volume) should limit average strength to the range of 46,000 psi to 51,000 psi. Table 22 shows that the later 2A07 blank had a density of 3.801  $\text{gm/cm}^3$  and an average grain size of 4.2  $\mu\text{m}$ , which were within the tentative specifications, but still did not come within the desired strength range. The 3A09 blank had an average grain size of 5.5  $\mu\text{m}$  and a density of 3.810  $\text{gm/cm}^3$ . This density was within the tentative specification, but grain size was large. The density of the 4A11 blank was 3.735  $\text{gm/cm}^3$  with an average grain size of 3.7  $\mu\text{m}$ . This density was low and the grain size was within the tentative specification. The 5A13 blank had a density of 3.766  $\text{gm/cm}^3$ , which was below the tentative specification, and an average grain size of 4.7  $\mu\text{m}$ , which was within but on the high side of the tentative specification. With the exception of the 2A07 blank, the above data

indicate that there were explanations for most of the strength data being low.

A significant difference in appearance was visible from the core material to the outer 0.10 inch of material on the 4A11 blank. The one macro specimen from this outer material also had a significantly higher density than the other macro specimens.

In addition to the above, Table XXII also shows that the blanks evaluated had low green densities compared to the acceptable parts produced earlier in the program. For instance, the 2A07 blanks produced earlier in the program had a green density of 2.59 to 2.61 gm/cm<sup>3</sup> while the 2A07 blank evaluated from the December, 1970, shipment had a green density of 2.51 gm/cm<sup>3</sup>. The firing parameters indicate that the December, 1970, 3A09 and 5A13 blanks were fired to greater cone deformations than the earlier blanks. The higher firing and lower green density should have had offsetting effects on fired density and this was borne out by the fired density data. However, the average grain size was greater than for earlier 3A09 and 5A13 blanks. The 2A07 blanks from the December, 1970, shipment were fired slightly higher than earlier 2A07 blanks, but this was not sufficient to offset the lower green density. The net results were lower fired density and greater average grain size. Firing data were not available for the earlier 4A11 blanks, therefore, no comparisons can be made for the 4A11 blanks from the December, 1970, shipment.

Since lower green density seemed to be contributing to the problems encountered, Coors then attacked this problem. All parts had been pressed to the same pressure, 30,000 psi, but still gave lower green densities. Tooling, pressure, and the alumina body (XAD997A) were all identical to those used earlier. The one possibility of a change was that the binder used in the alumina body had aged in the three years since the earlier blanks were produced. In an effort to improve the flow properties, moisture content control, heating, or both were tried with only modest success. One effort which seemed to work was mixing two parts of another body, PS-144-1, with three parts of the original body, XAD997A. The PS-144-1 alumina body was made from identical powder but used a different binder. Blanks 2A07 and 3A09, produced from this mixture, XAD997B, and received in March, 1971, were within the density, grain size, and strength limits.

The average strength of the March 2A07 blanks, 2A07-140, -141, and -142, was 48,188 psi, Table 24. The average density and grain size were 3.802 gm/cm<sup>3</sup> and 3.5  $\mu$ m, respectively. The surprising fact was that they were fired to only Cone 31 at 1:00 to

6:00. The March 3A09 (3A09-144) blank had an average strength of 48,572 psi. Its average grain size and density were 3.7  $\mu\text{m}$  and 3.832  $\text{gm/cm}^3$ , respectively. This piece was fired to Cone 31 at 5:30. These pieces provided promise that modifying the powder mix would solve the problem by permitting improved green densities.

Coors continued efforts in the same direction, producing in April and May, 1971, additional Al3 blanks from mixtures of bodies of XAD997A, PS-144-1, and PS-176-5 in various proportions. Those blanks evaluated (5Al3-149, 5Al3-151, 5Al3-152, and 5Al3-153) all fell outside the specification limits. The average strengths of these blanks were 42,301 psi, 46,321 psi, 42,491 psi, and 40,288 psi in the same order as above. Blank 5Al3-151 had an acceptable strength, but was unlike other blanks in that its fired density was 3.885  $\text{gm/cm}^3$ . Thus, this last effort did not provide reproducibility for the larger of the blanks, nor did they match the population of the other shapes.

#### REGRESSION ANALYSIS

The data from the final shipments of blanks presented a confusing picture. Wide variations in strength, fired density, grain size, green density, firing parameters, etc., were included. Attempts at explaining differences in strength data by use of strength-porosity relations or strength-grain size relations were helpful, but still left questions of interpretation of the plots. Simultaneous regressions of strength on grain size and porosity were more useful.

Data used for this regression analysis are shown in Table XXV. The strength and density are average data for many macro-flexure specimens. Most grain size data were measured on a single macro specimen in a given group and these data are assumed to apply to all in a given group. Where only singleton grain size data were available for several blanks within a blank type, the blank is identified with the blank type without an item number.

Several different equations were tried which related strength to grain size and porosity. The equation form proposed by Passmore, Spriggs, and Vasilos<sup>7</sup>

$$\sigma = Ae^{\frac{BP}{G}C+DP}$$

where

$\sigma$  = flexure strength

P = volume fracture porosity

G = mean grainsize

e = base for natural logarithm

A, B, C, and D - empirical constants

was rejected for the simpler equation form proposed by Knudsen<sup>8</sup>

$$\sigma = Ae^{BP}G^C$$

The additional factor in the first relation does not, for these data, represent an improvement in the goodness of fit.

The first observation about the data is that the blanks 5A13-151, -152, and -153 seem unlike the remainder of the blanks even when they are included in the data used to define the regression. (Data from these blanks were not used in the final regression analysis.) The decision to exclude these points from the regression analysis seems justified on the fact that the aluminabodies from which these blanks were pressed are quite unlike the original alumina body, XAD997A. An argument could also be advanced that all blanks pressed from the alumina body XAD997B should also be excluded since XAD997B was not identical with XAD997A. Similar arguments could be made against the high fired blanks, the double fired blanks, and the MOR bars, but all XAD997B and blanks fired differently were included in the regression analysis. There is no reason to believe that a single universal regression applies to all these data, but the real strength of this analysis is that it seemed to work in spite of the wide variation in processing parameters.

The regression relation which gave the best fit was

$$\sigma = 89026 \cdot \text{Exp} \left[ -8.48264P \right] G^{-0.19282}$$

This regression was derived using all the data from Table xxv with the exception of data from Blanks 5A13-151, -152, and -153. The regression relation is presented in two different forms. The first, Figure 107, is a three dimensional plot of the regression surface and all individual data points including the three which were not used to define the surface. The individual data points

are connected by vertical straight lines to their projections on the regression surface. The lengths of these vertical lines represent the deviations of the individual data points from the regression surface.

The second presentation of the same data is shown in Figures 108 and 109. The first of these figures shows the intersection of the regression surface with the plane  $G = 3.7 \mu\text{m}$ . Individual data points which have been normalized to a common grain size of  $3.7 \mu\text{m}$  are shown about the curve of the intersection. A way of visualizing this plot is as the distribution of data points one would see if he were an observer on the plane  $G = 3.7 \mu\text{m}$  and could look only along curved lines parallel to the regression surface and normal to the  $G = 3.7 \mu\text{m}$  plane. The second figure is the intersection of the regression surface with the plane  $P = 0.0451$  and individual data points normalized to this plane. From this second figure, it is quite apparent that Blanks 5A13-151, -152, and -153 are not from the same population as the remaining blanks.

Some preliminary work by Coors early in this program showed a nonlinear increase in grain size with decreasing green density for a given thermal input. Since fired density is directly related to green density and to thermal input, and grain size is directly related to thermal input, but inversely related to green density, green density offers a tool which may control to some extent the resulting microstructure of parts made from this alumina.

Figure 110 is a plot of strength normalized to common grain size and porosity of  $3.7 \mu\text{m}$  and  $0.0451$ , respectively, plotted against green density. This plot also shows the nonagreement between 5A13-151, -152 and -153, and the remaining data points. This figure demonstrates an apparent residual relation between strength and green density after allowing for grain size and porosity. The word apparent was used above since it is not certain that the strength-green density relation is a direct relation or the result of other parameters or interrelationships not considered in this analysis. Additional study in this area would be necessary to resolve the problem. The relation, if real, would give both another parameter to be controlled and a tool which could allow control of microstructure and therefore strength.

Figure 110 also shows the range of "corrected" strengths for these probably diverse populations. The spread is from 43,203 psi to 51,733 psi, a range of 8,530 psi.

## CONCLUSIONS

### Material Description and Deviations

1. Typical average grain size for this alumina was 3.6 microns with a maximum grain size of 15-25 microns. Specimens intentionally fired to a higher temperature had an average grain size of about 7.0 microns with a maximum grain size of 30-35 microns. Within a given large blank, average grain size was reasonably uniform, typically ranging from 3.4 to 4.0 microns. Among the blanks evaluated, grain size was reasonably reproducible.

2. A second phase other than alumina was observed as discrete grains similar in size to the alumina grains, but was prismatic in shape as opposed to the equiaxed shape expected of alumina. About six volume percent of this phase was present, having an average size of 2 microns. This material was uniformly present in most specimens examined. Only a few of those blanks with nonstandard firing or made from a different alumina body showed a lack of the second phase near the fired surface of the blank.

3. The average pore size was 1.3 microns with a maximum size of 50 microns. The maximum pore size is open to debate. Enlarging of existing voids due to rounding of void edges during polishing is apparent in photomicrographs. The area surveyed was small compared to the surface area of macro specimens. Low power surveys of the tensile faces of macroflexure specimens discovered voids of 50-300 microns maximum dimension.

Typical porosity values based on bulk density ranged from 3.8 to 4.7 percent. Porosities of Blanks 4A11, 2A12, and 5A13 were different from those of other blanks, ranging from 4.8 to 5.4 percent. Reproducibility of porosity between blanks other than 4A11, 2A12, and 5A13 was good.

4. The predominant fracture mode for all specimens examined was intergranular. Up to about 20 percent transgranular fracture was noted. In all cases, the stronger specimens had higher percentages of transgranular fracture regardless of density level.

5. The average tensile strength was 46,300 psi and the average flexure strength was 48,290 psi. Strengths of 4A11 and 5A13 blanks were low compared to the average strengths. Tensile



strengths of 2A05 blanks were low probably due to one very low strength specimen. Flexural results disagreed with tensile results on 2A05 blanks.

6. Regression analyses for grain size and porosity tended to normalize strengths to a tighter range.

7. A much tighter fit to a regression of strength on porosity and grain size would be obtained if the factors green density, cone deformation, fired thickness, etc., were varied in a more controlled manner. Green density could be a major parameter actually related to the structure of the material since the physical events related to compacting the powders could "wipe" the interfaces and influence diffusion processes and impurity location, such as glassy phases in the grain boundaries. Even fired thickness could have a similar affect by influencing internal firing rates and thus diffusion rates and grain boundary composition plus residual stresses.

#### Strength Correlations

8. Porosity and grain size correlate to average strength and seem to control over other parameters.

9. Green density may correlate to strength after allowances for porosity and grain size.

10. Fired thickness seems to correlate to average strength even for areas of different thickness within a given item and when microstructures seem similar.

11. Weibull statistics may be used to quantitatively predict flexural performance from tensile results, but only within perhaps one decade on volume. Weibull does not quantitatively predict strengths over several orders of magnitude on volume. Volume affects seem to predominate over area affects.

12. Small ranges in "good" surface finish generated after firing had little effect on strength. Presumably, rough surfaces would have reduced strength as was the case for "sliced" finishes. As-fired pieces were not stronger and their strength depended on green-state finish.

13. Subsurface damage may normalize strength of specimens. The competing theory is that inherent or volume flaws are exposed by fine polishing and "set" the strength.

14. Environmental conditioning of all specimens is required to assure that extremes of relative humidity do not affect results.

15. Refiring of specimens in a manner which does not increase average grain size had negligible effect on strength.

16. Higher firing temperatures yield higher fired densities, but the increase in strength due to higher density is offset by the decrease in strength due to the accompanying increase in average grain size.

17. Statistically larger disparate pores on the faces of the flexural specimens reduced strength.

#### General

18. Coors can reproduce all blanks other than 4A11, 2A12, and 5A13 provided a fresh batch of the XAD997A alumina body is prepared and used. There are reasons to suspect that 4A11 and 2A12 can be brought into the population.

### RECOMMENDATIONS

The comparison of test methods for brittle materials must be done if brittle materials are to go into widespread use. A material which will behave in a predictable manner from one shape to another and from item to item of the same shape will be an essential part of such a program. This alumina has not yet shown the desired predictability, but offers by far the best hope of meeting that goal. It is felt that part of the problem in obtaining this predictable material was too rigid an adherence to "production procedures" before the properties which must be controlled were properly defined. An example of this is the use of a fixed pressing pressure of 30,000 psi. A better control would probably have been pressing to a certain green density for a particular shape. The green density for each shape would depend on the fired thickness (or area or volume) of this shape and the controls on cone deformation.

It is recommended that:

- (1) this program be resumed
- (2) Coors Porcelain Company and their XAD997A alumina be the producer and material used in this continuation
- (3) some consideration be given to defining the effects of green density and firing parameters on the properties of shapes of differing sizes
- (4) investigation of parameters which would tighten the relation between strength, grain size, porosity, and other factors be included
- (5) an extensive fractology study of the specimens be conducted.

## REFERENCES

1. Simon, A. W., "Theory of Beams Composed of Two Elastic Materials", American Journal of Physics, Vol. 27, 1959, p 500.
2. Pears, C. D., and Starrett, H. Stuart, "An Experimental Study of the Weibull Volume Theory", AFML-TR-66-228.
3. Underwood et al., "Ceramic Microstructures", Part I, Chapter I, John Wiley and Sons, Inc., New York.
4. Gutshall and Shaw in "Proceedings of the Electron Microscopy Society", 25th Annual Meeting, 1967, pp 282 and 283.
5. Robinson, "Some Problems in the Estimation and Application of Weibull Statistics", Technical Report UCRL-70555, September 1, 1967, University of California, Lawrence Radiation Laboratory.
6. Sedlacek, R., "Processing of Ceramics - Surface Finishing Studies", Final Technical Report under Contract No. N00019-67-C-0494, November, 1968, prepared for Naval Systems Command.
7. Passmore, E. M., Spriggs, R. M., and Vasilos, T., "Strength - Grain Size - Porosity Relations in Alumina", Journal of the American Ceramic Society, Vol. 48, No. 1, pp 1-6, 1965.
8. Knudson, F. P., "Dependence of Mechanical Strength of Brittle Polycrystalline Specimens on Porosity and Grain Size", Journal of the American Ceramic Society, Vol. 42, No. 8, pp 376-387, 1959.
9. Jacobson, L. A., "The Weibull Statistical Distribution as Applied to Brittle Fracture", AFML-TR-65-176, August, 1965.

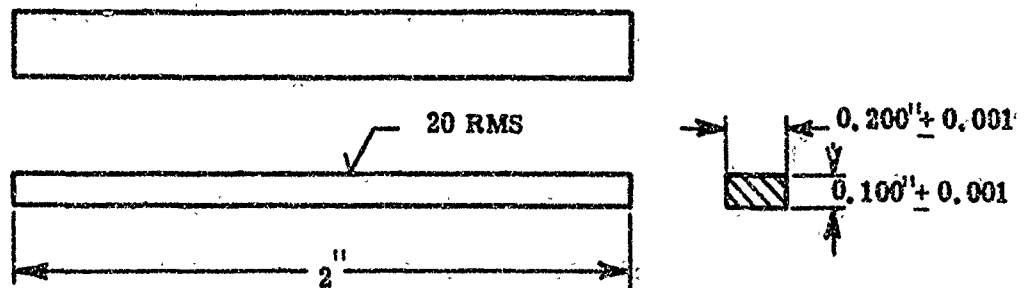
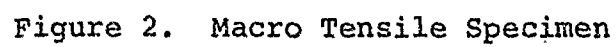


Figure 1. Macro Flexural Specimen



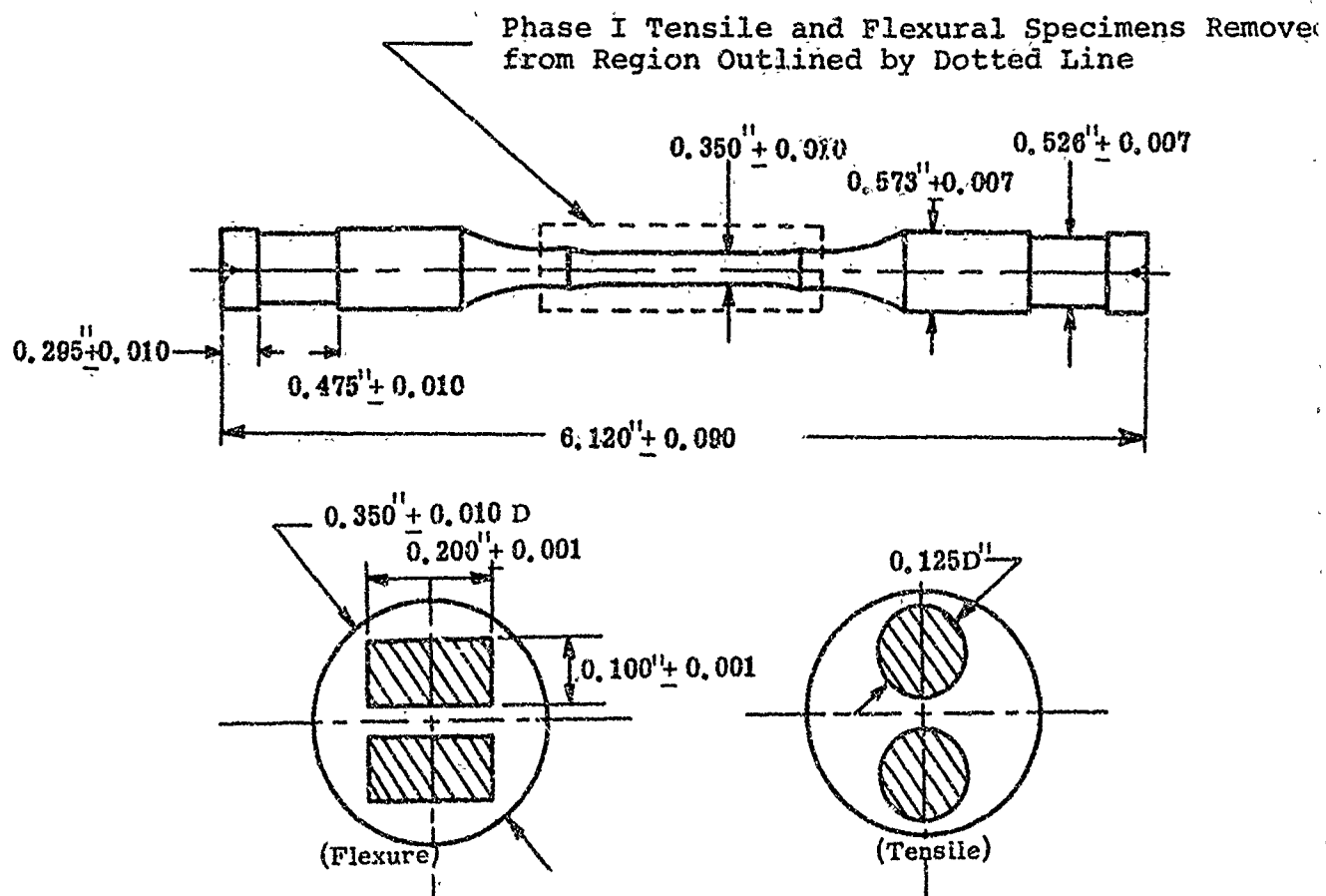


Figure 3. Configuration of Specimen Blanks 1A02 as received from Coors and Cutting Plan for Removing Phase I Tensile and Flexural Specimens

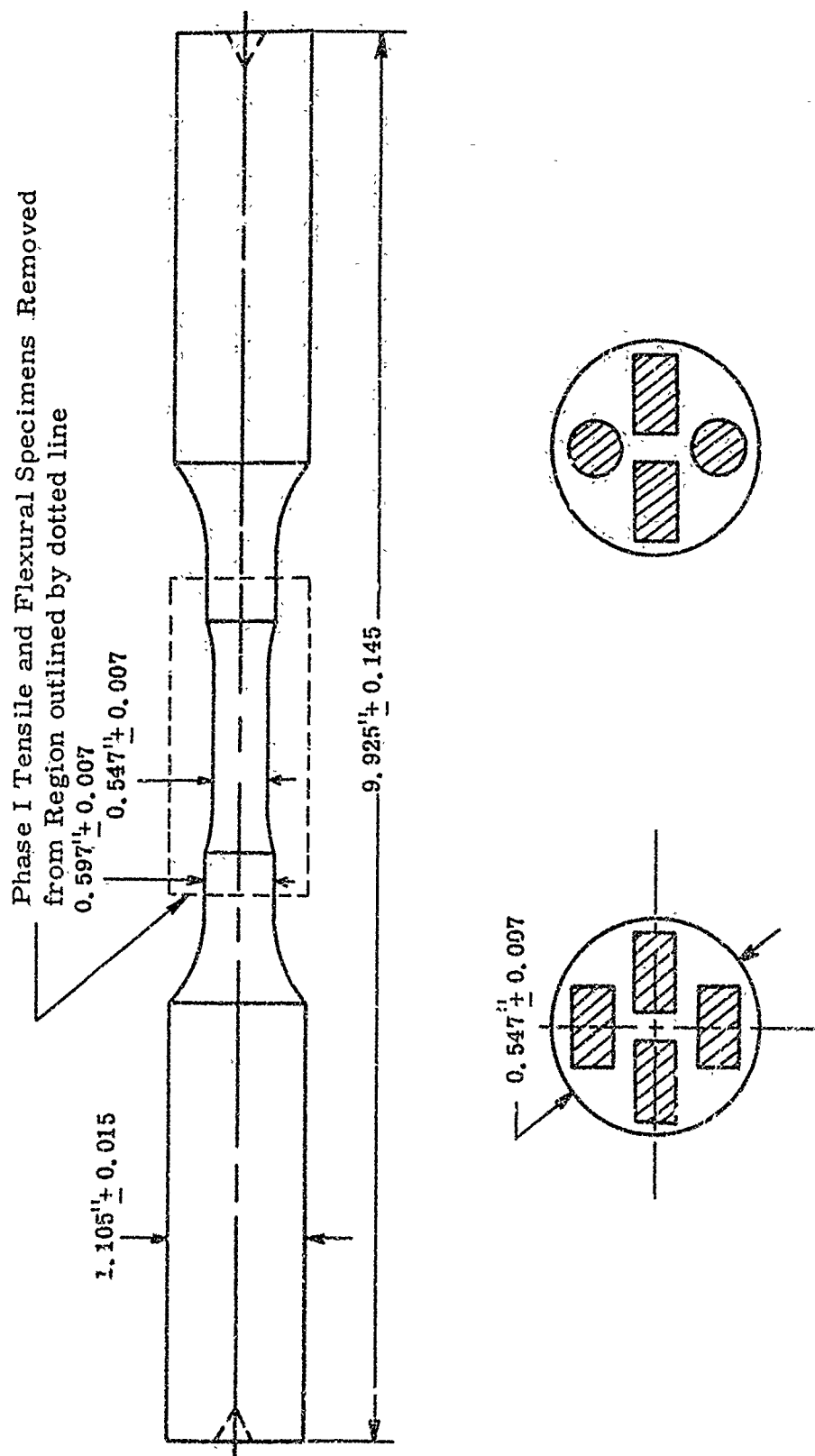


Figure 4. Configuration of Specimen Blanks 2A04 as Received from Coors and Cutting Plan for Removing Phase I Tensile and Flexure Specimens.

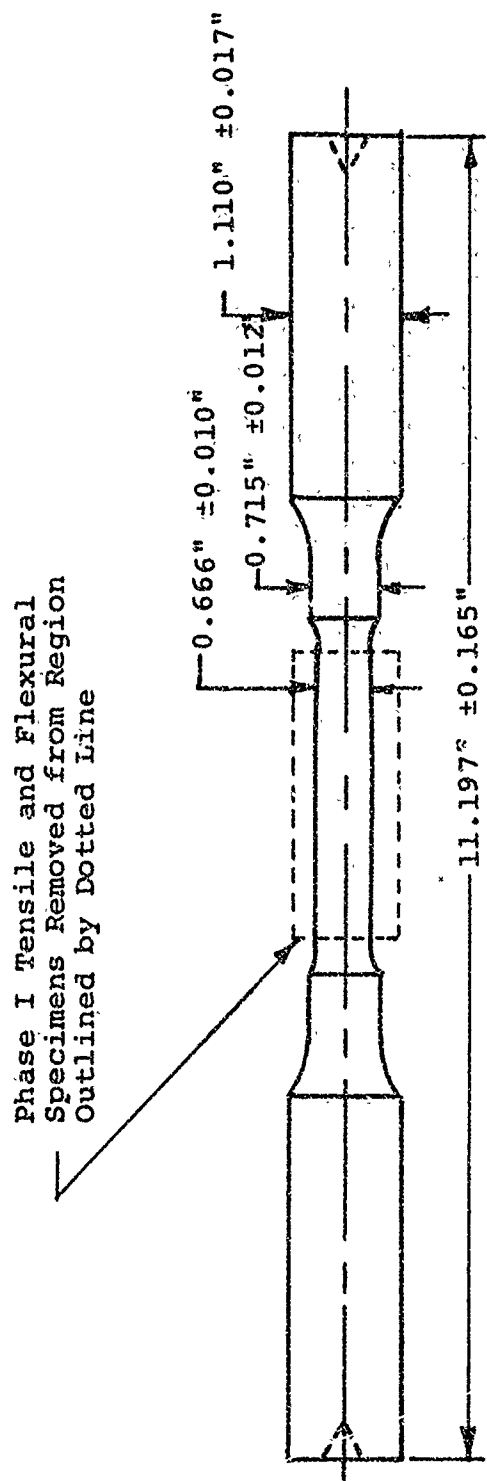


Figure 5. Configuration of Specimen Blanks 2A05 as Received from Coors and Cutting Plan for Removing Phase I Macro Tensile and Macro Flexural Specimens



Phase I Flexural Specimens Removed from Region Outlined by Dotted Line

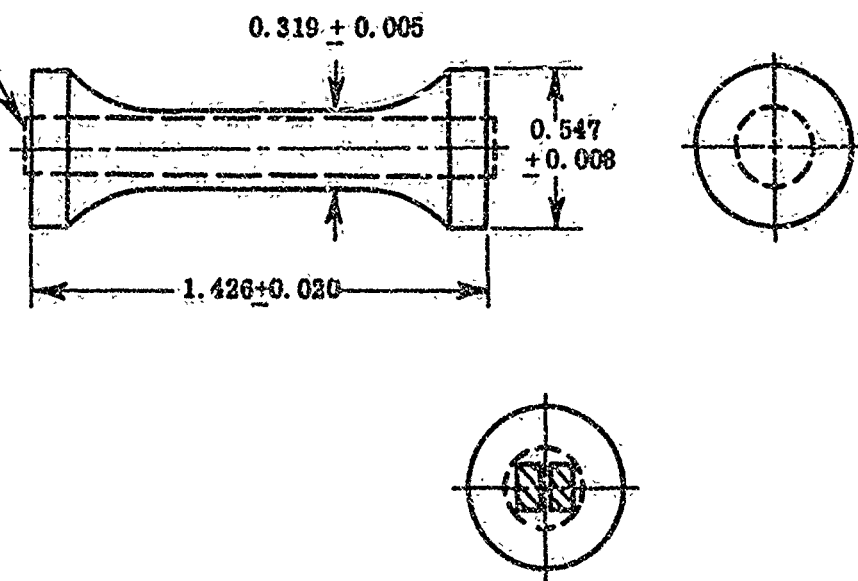


Figure 6. Configuration of Specimen Blanks 1A06 as Received from Coors and Cutting Plan for Removing Phase I Macro Tensile and Macro Flexural Specimens

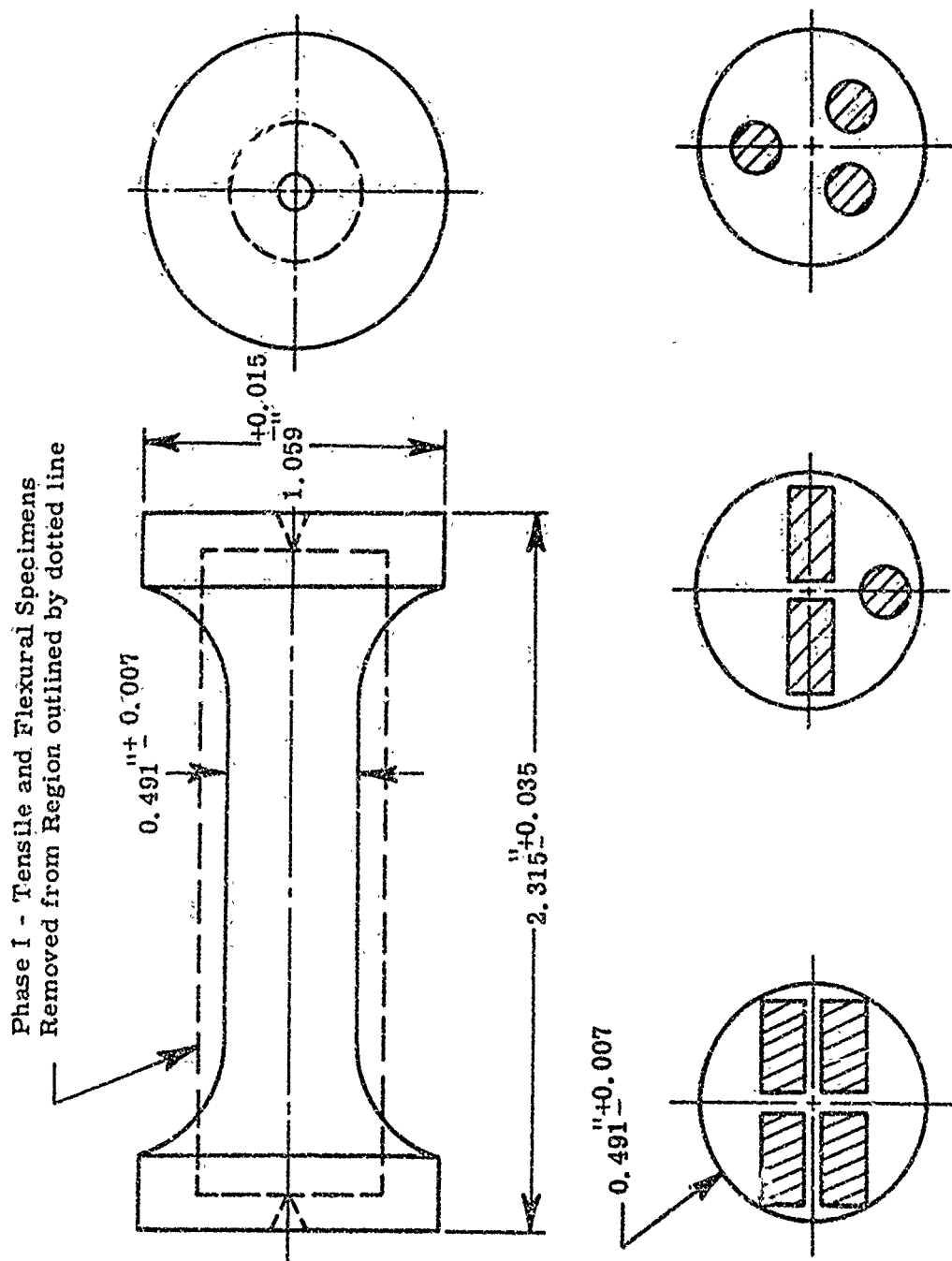


Figure 7. Configuration of Specimen Blanks 2A07 as Received from Coors and Cutting Plan for Removing Phase I Macro Tensile and Macro Flexural Specimens

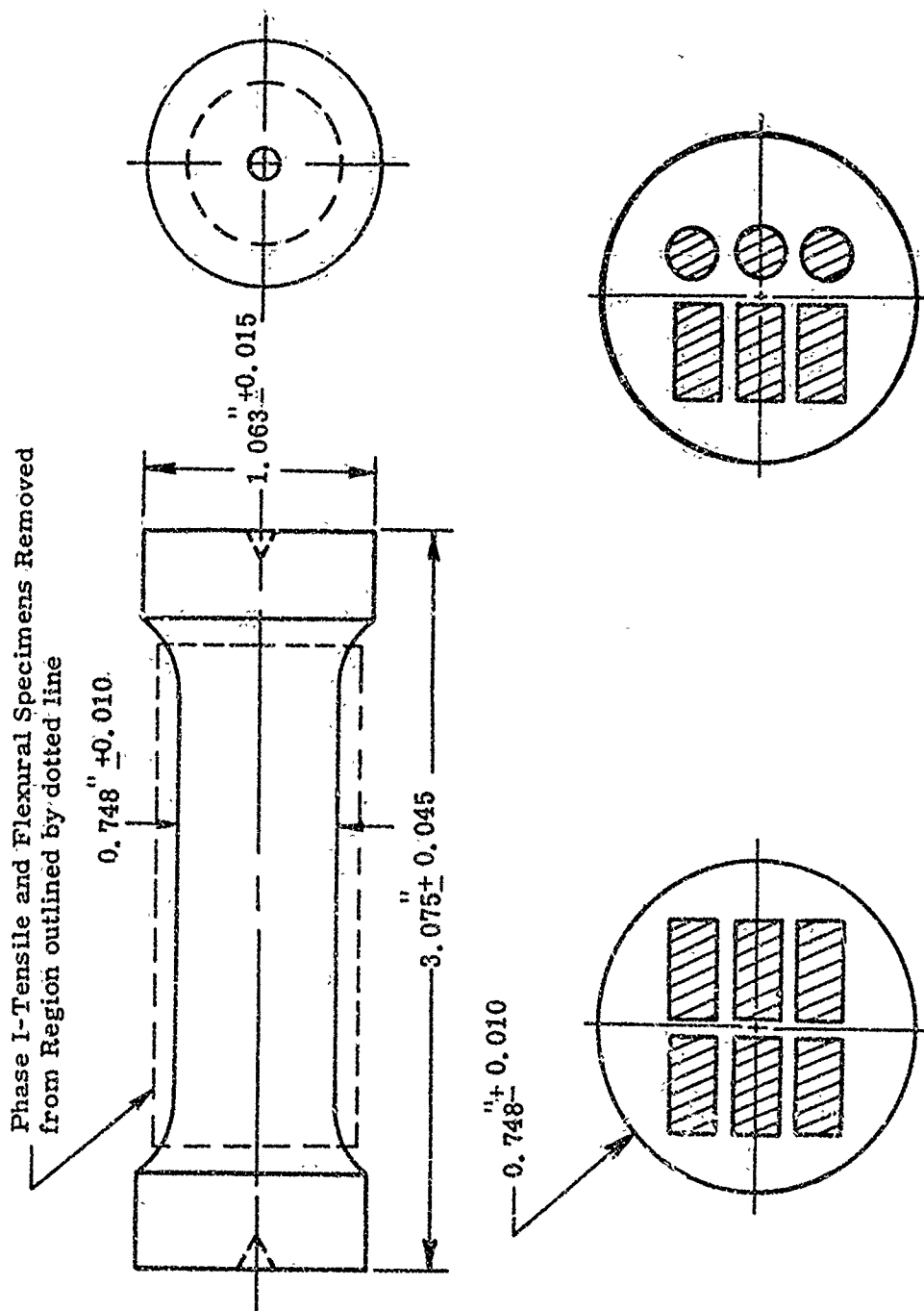


Figure 8. Configuration of Specimen Blanks 2A08 as Received from Coors and Cutting Plan for Removing Phase I Macro Tensile and Macro Flexural Specimens

Phase I Tensile and Flexural Specimens removed from Regions outlined by dotted lines.

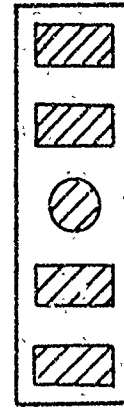
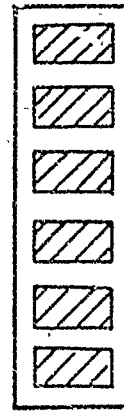
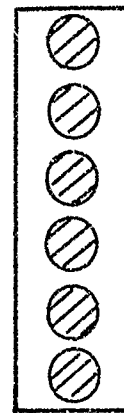
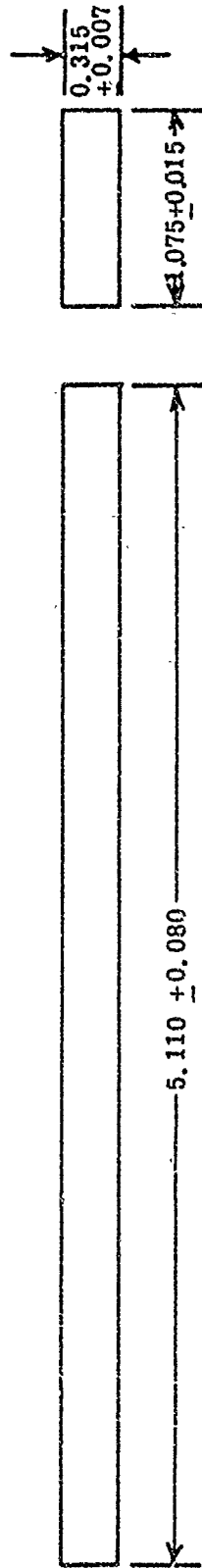
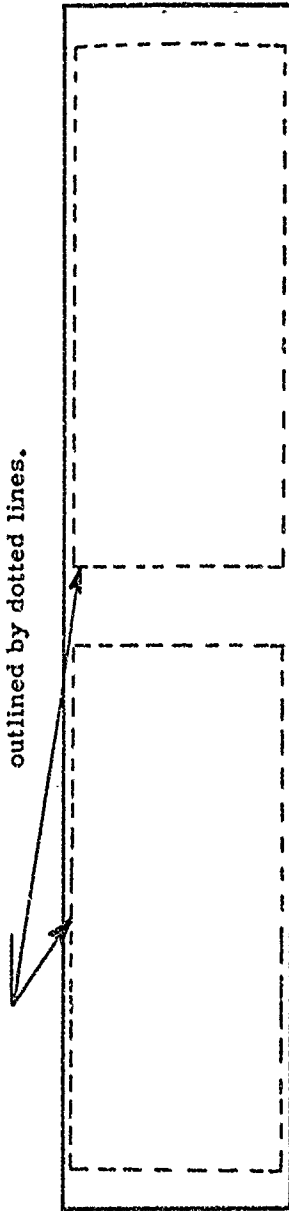
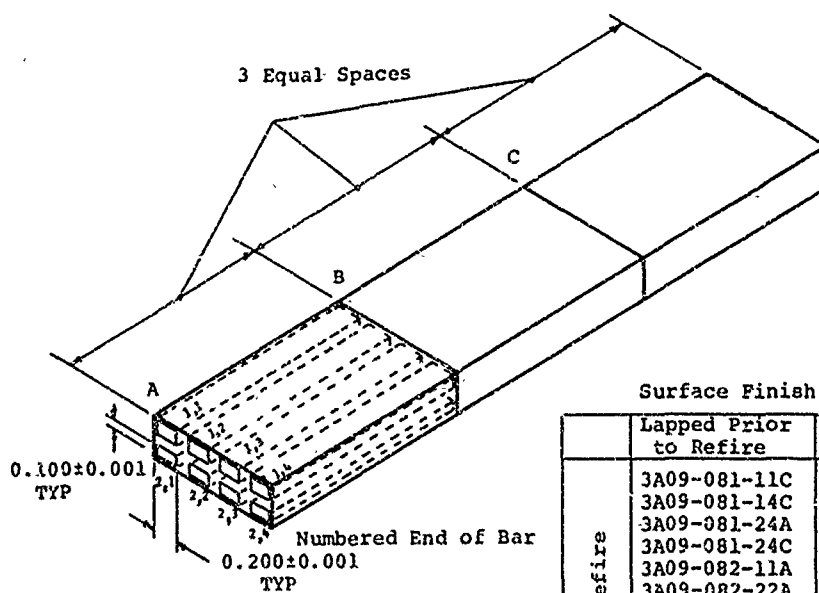


Figure 9. Configuration of Specimen Blanks 3A09-083, 3A09-085, and 3A09-C.5 as Received from Coors and Cutting Plan for Removing Phase I Macro Tensile and Macro Flexural Specimens



Surface Finish Study, Specimen Groupings

	Lapped Prior to Refire	Lapped after Refire	Not Lapped
H <sub>2</sub> Refire	3A09-081-11C	3A09-081-11A	3A09-081-21A
	3A09-081-14C	3A09-081-13A	3A09-081-21C
	3A09-081-24A	3A09-081-13B	3A09-081-23B
	3A09-081-24C	3A09-081-23A	3A09-082-12A
	3A09-082-11A	3A09-082-11C	3A09-082-23A
	3A09-082-22A	3A09-082-13B	3A09-082-23C
	3A09-082-23B	3A09-082-21B	3A09-082-24A
	3A09-084-12A	3A09-084-14C	3A09-084-12C
	3A09-084-21C	3A09-084-22B	3A09-084-21A
	3A09-084-24A	3A09-084-23A	3A09-084-23B
O <sub>2</sub> Refire		3A09-081-21B	3A09-081-11B
		3A09-081-22A	3A09-081-12A
		3A09-081-22C	3A09-081-12B
		3A09-082-13A	3A09-082-11B
		3A09-082-14B	3A09-082-13C
		3A09-082-21A	3A09-082-22C
		3A09-082-24C	3A09-084-13B
		3A09-084-11A	3A09-084-13C
		3A09-084-21B	3A09-084-14B
		3A09-084-22C	3A09-084-24B

Figure 10. Cutting Plan - Specimen Blanks 3A09-081, 3A09-082, and 3A09-084

Macro Flexural  
Specimen Dimensions  
0.100 x 0.200 x 2.000 inches

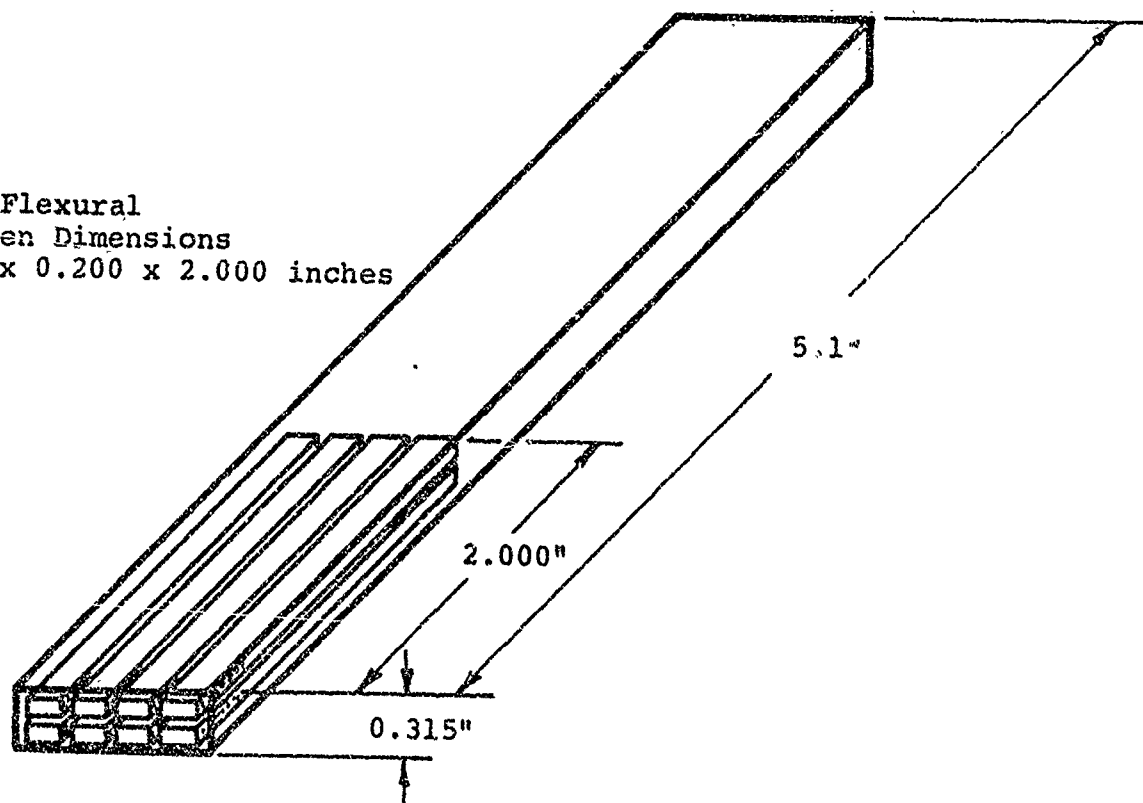


Figure 11. Cutting Plan ~ Specimen Blanks 3A09-120 and 3A09-144

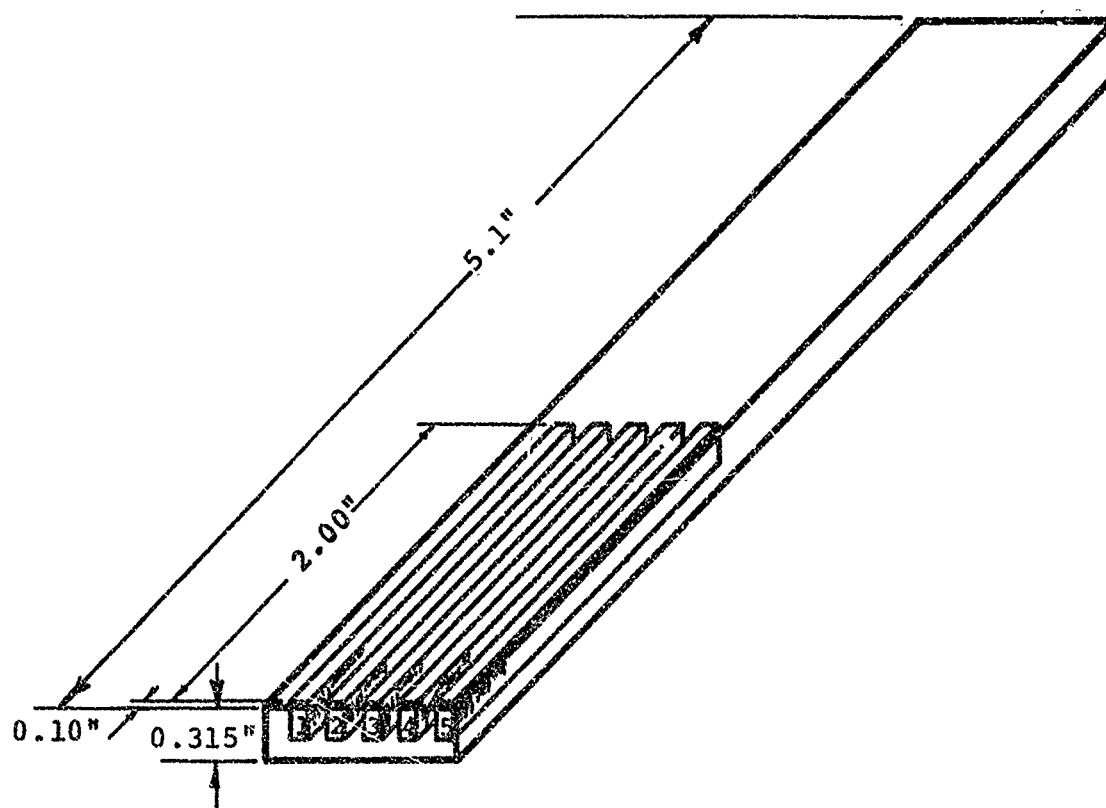


Figure 12. Cutting Plan - Specimen Blanks 3A09-136 and 3A09-137

Phase I Tensile and Flexural Specimens Removed from Regions  
Outlined by Dotted Lines

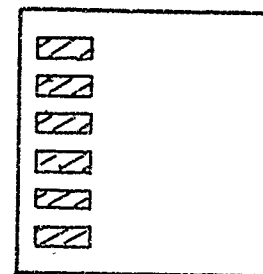
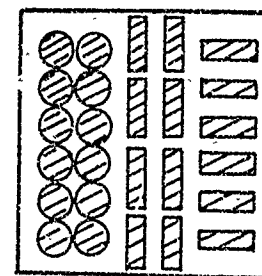
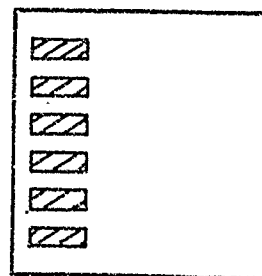
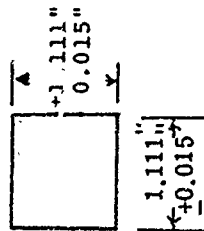
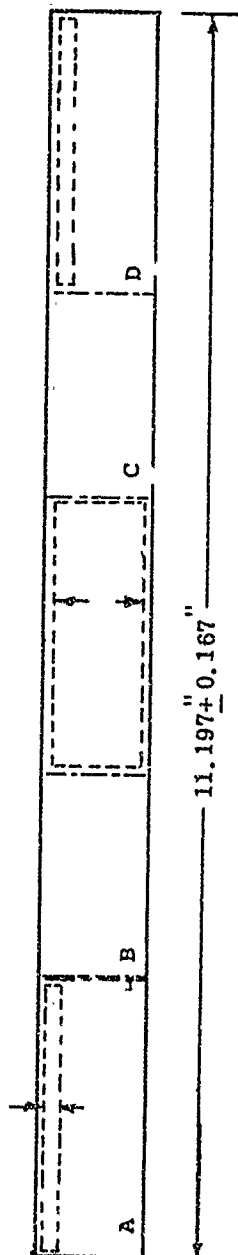


Figure 13. Configuration of Specimen Blank 3A10-087 as Received from Coors and Cutting Plan for Removing Phase I Macro Tensile and Macro Flexural Specimens



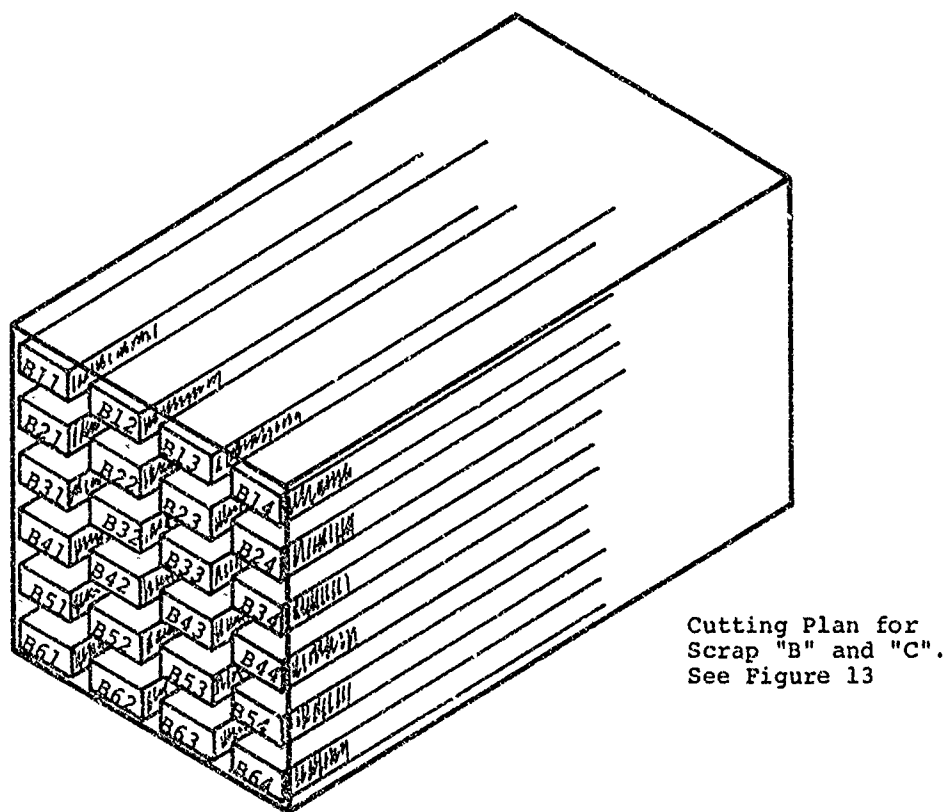
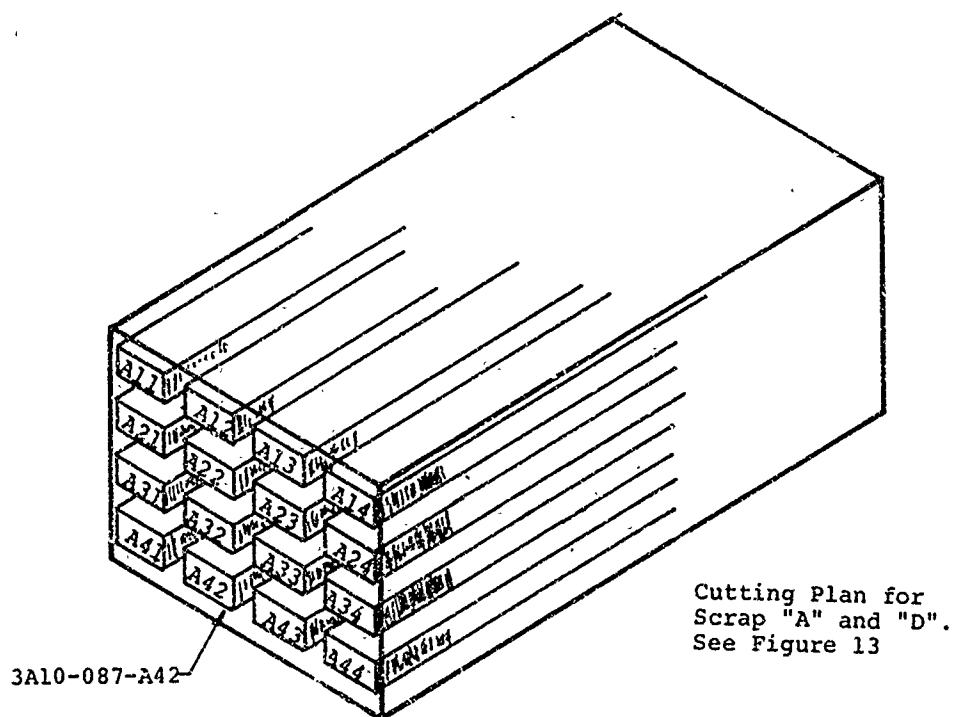
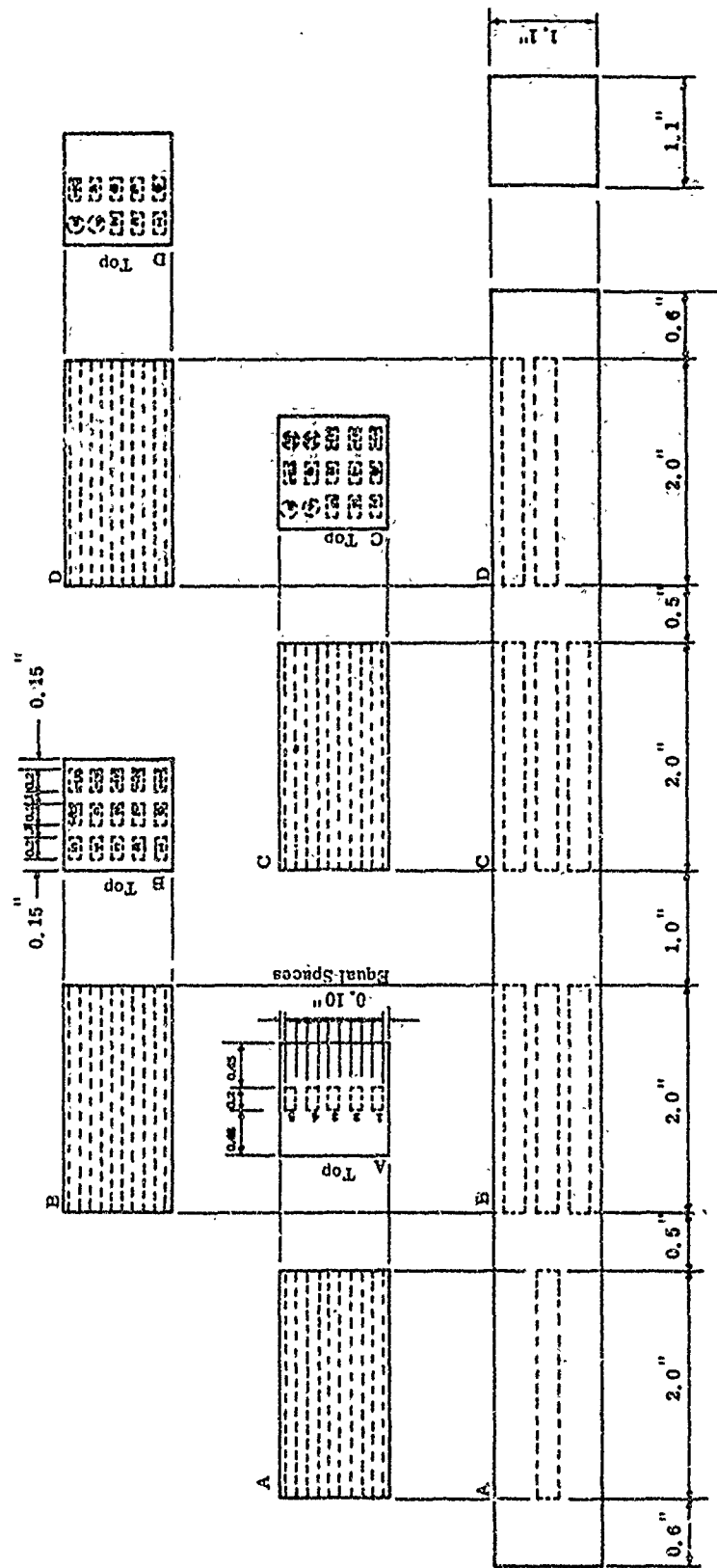


Figure 14. Cutting Plan - Scrap from 3A10-087



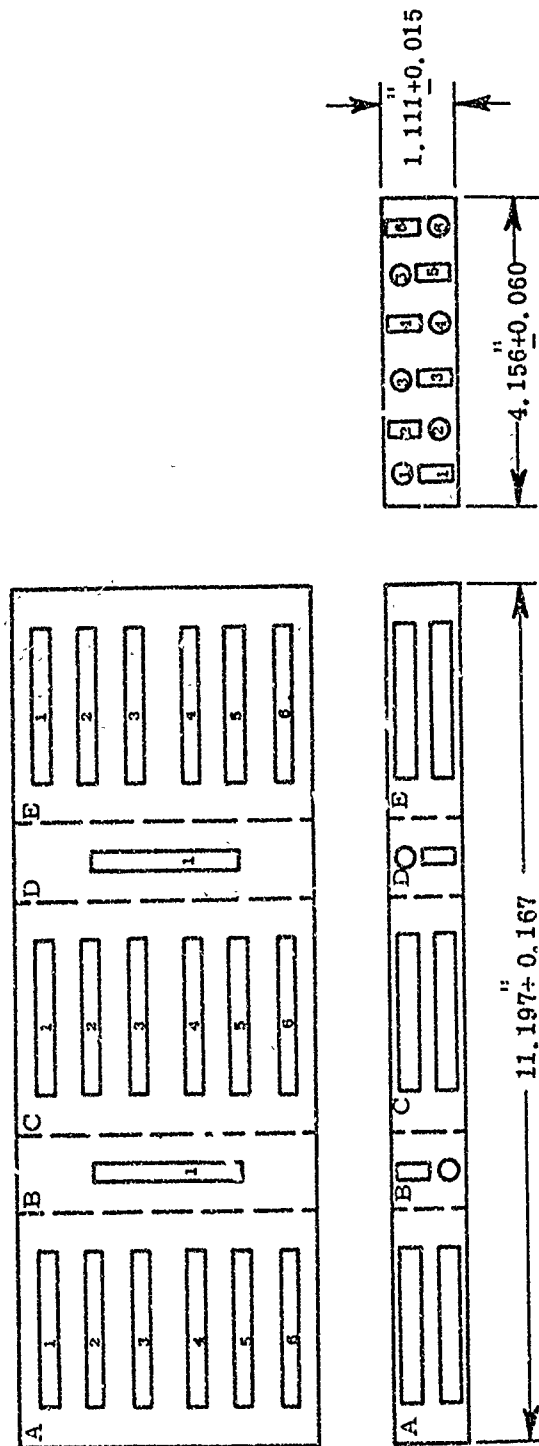


Figure 16. Configuration of Specimen Blank 4All-089 as Received from Coors and Cutting Plan for Removing Phase I Macro Tensile and Macro Flexural Specimens

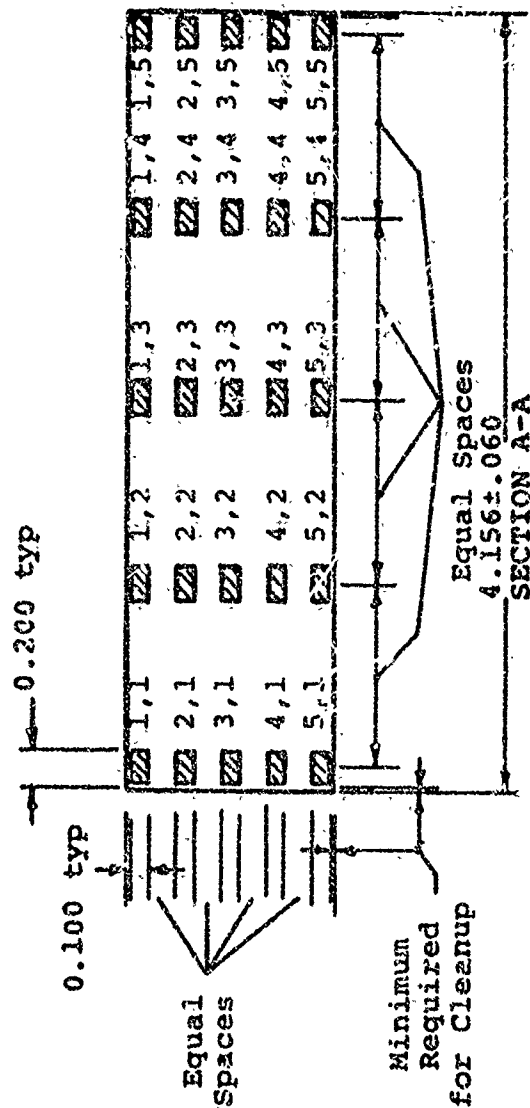
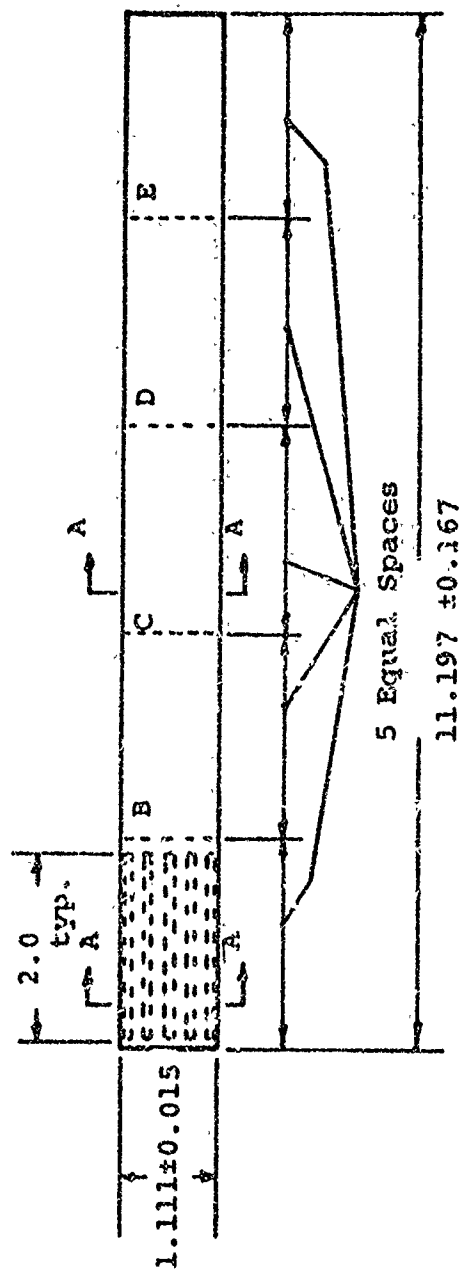


Figure 17. Cutting Plan - Specimen Blank 4A11-112

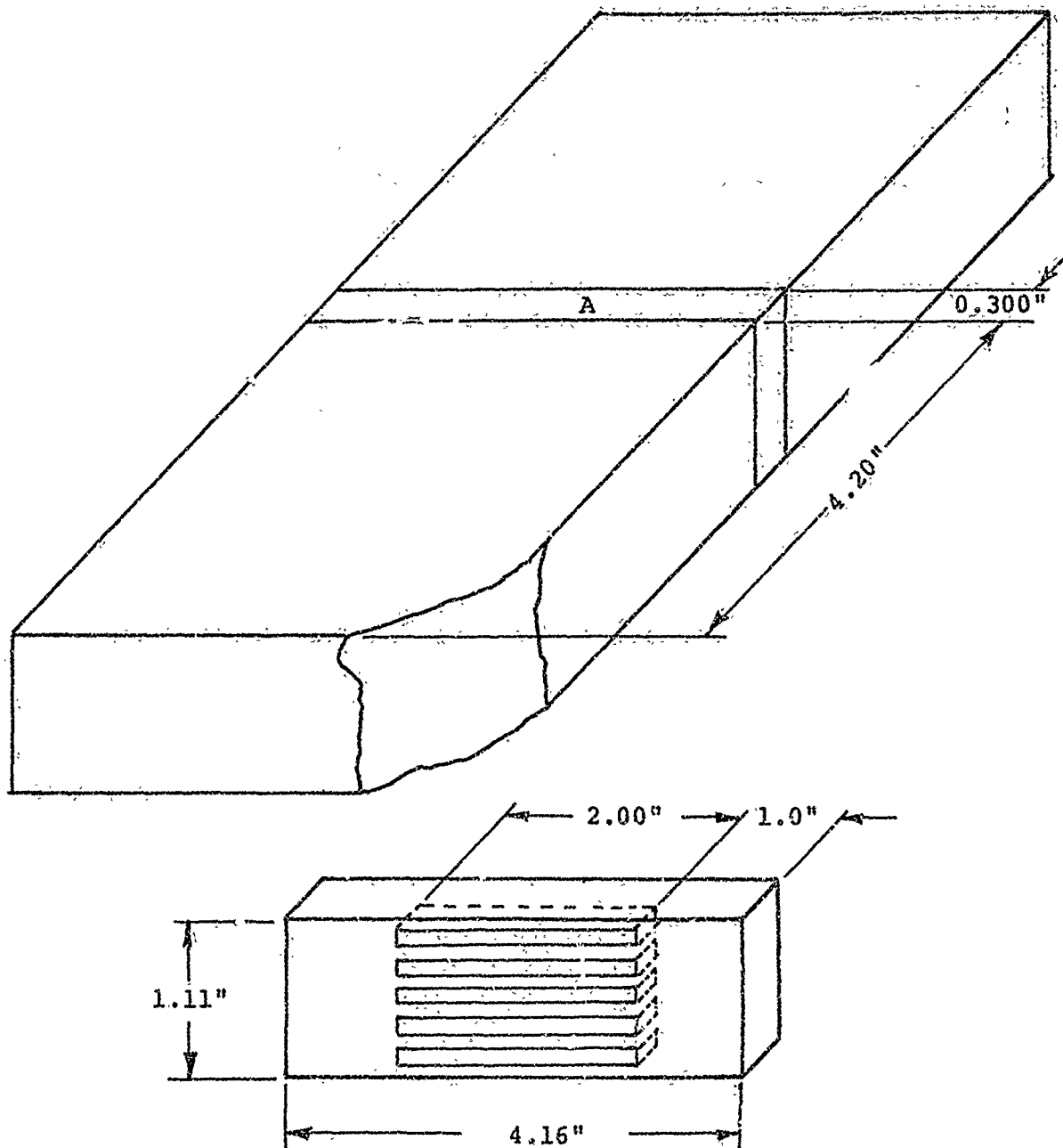


Figure 18. Cutting Plan - Blank 4A11-125

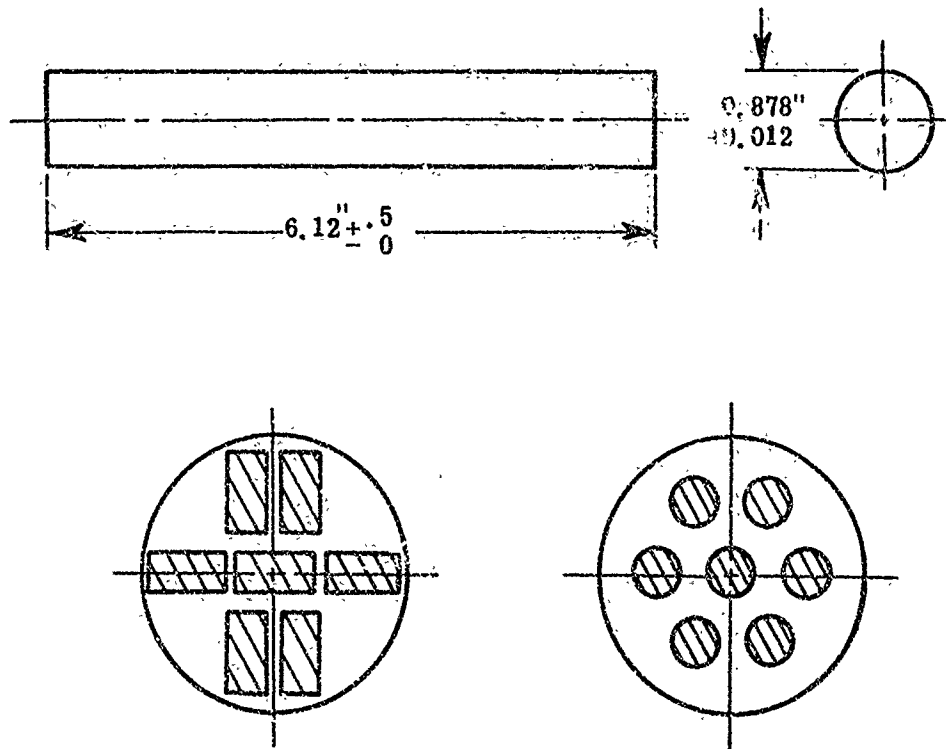


Figure 19. Configuration of Specimen Blanks 2A12 as Received from Coors and Cutting Plan for Removing Phase I Macro Tensile and Macro Flexural Specimens

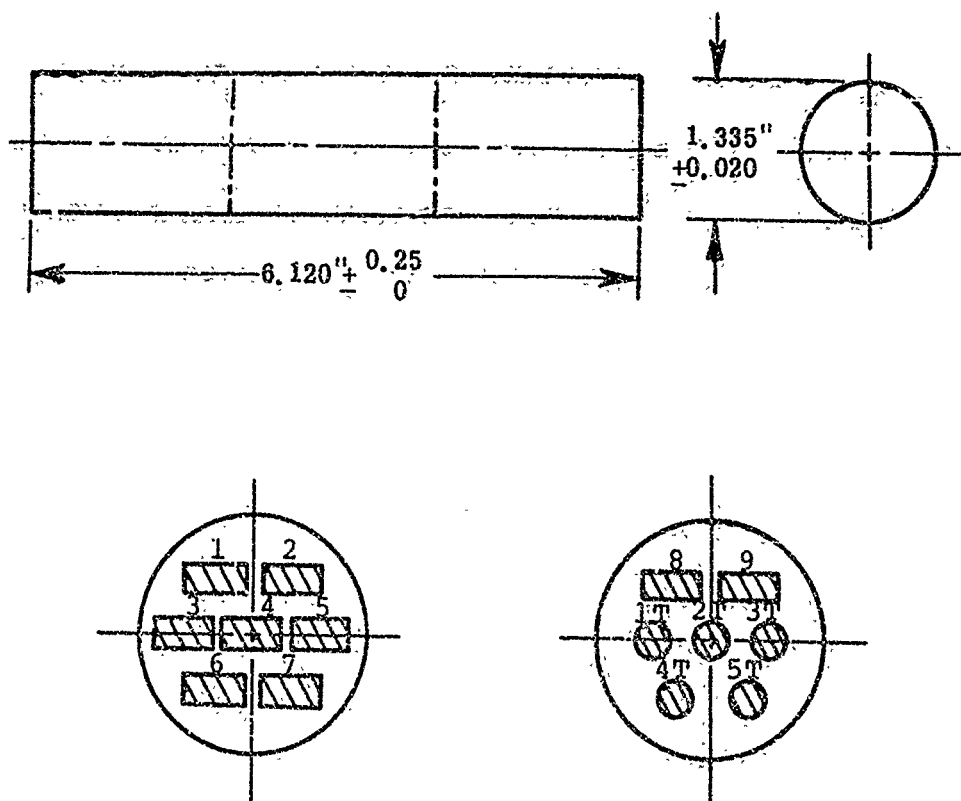


Figure 20. Configuration of Specimen Blank 5A13 as Received from Coors and Cutting Plan for Removing Phase I Tensile and Flexural Specimens from Blanks 5A13-101, -102, and -103

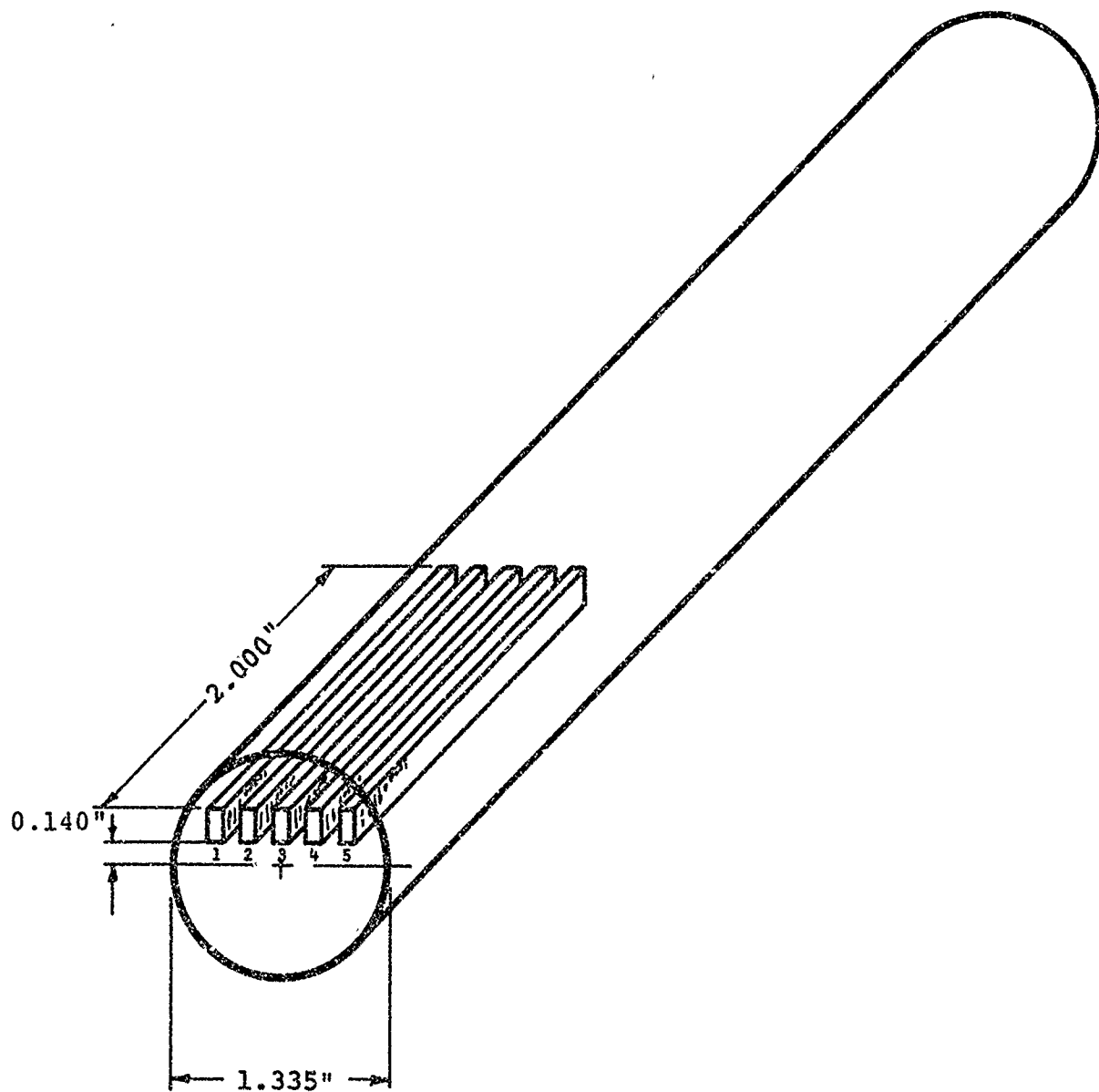
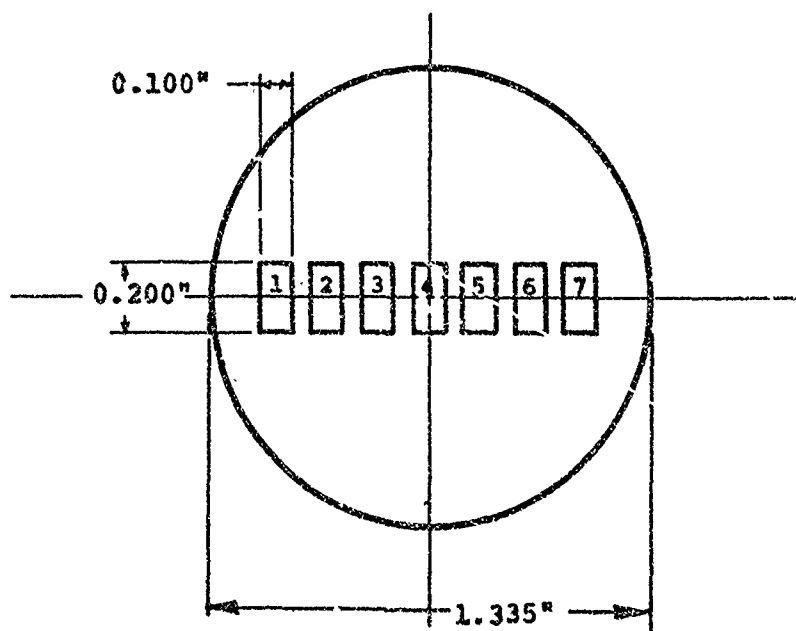
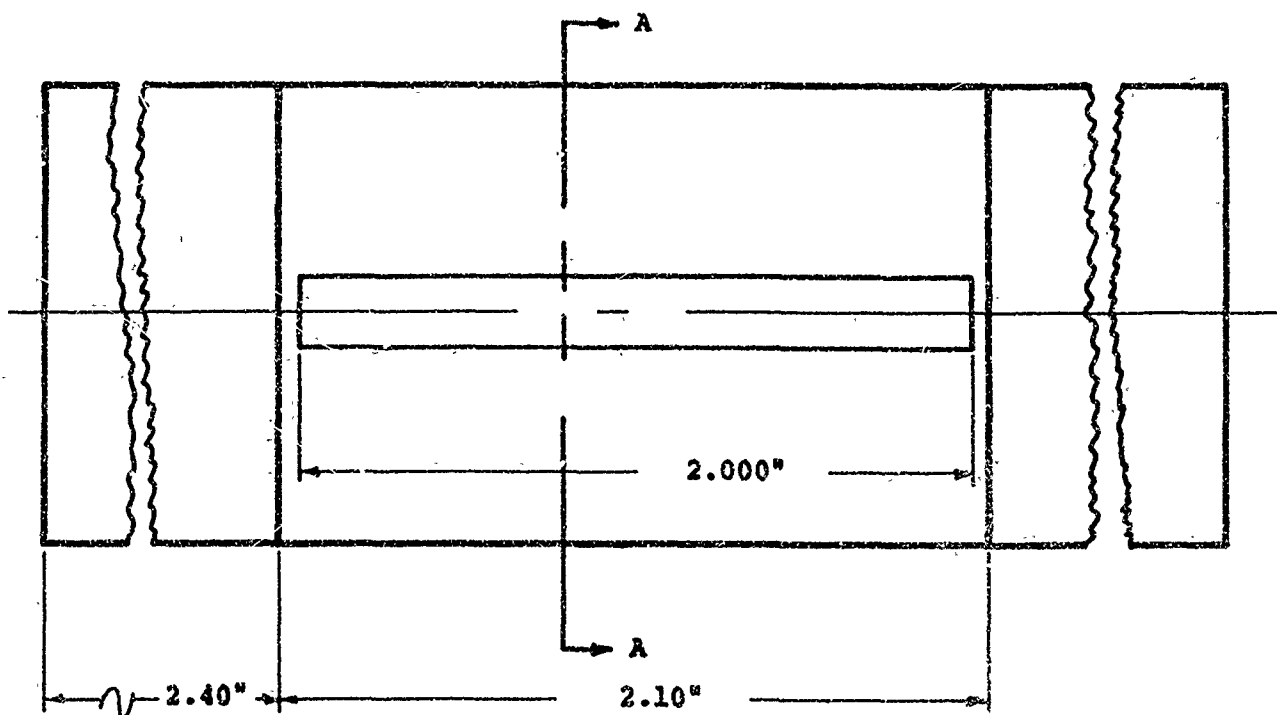


Figure 21. Cutting Plan - Blank 5A13-127 and 5A13-148





Section A-A

Figure 22. Cutting Plan - Blanks 5A13-149, 5A13-151, 5A13-152, and 5A13-153

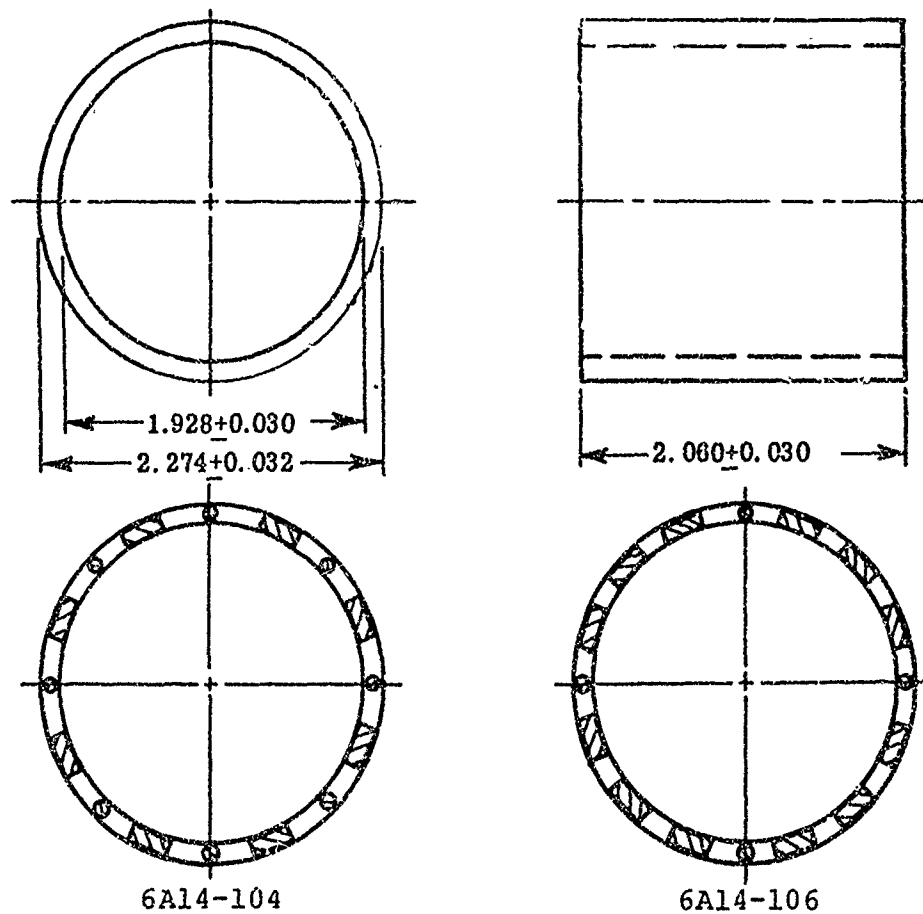


Figure 23. Configuration of Specimen Blanks 6A14 as Received from Coors and Cutting Plan for Removing Phase I Macro Tensile and Macro Flexural Specimens from Blanks 6A14-104 and 6A14-106

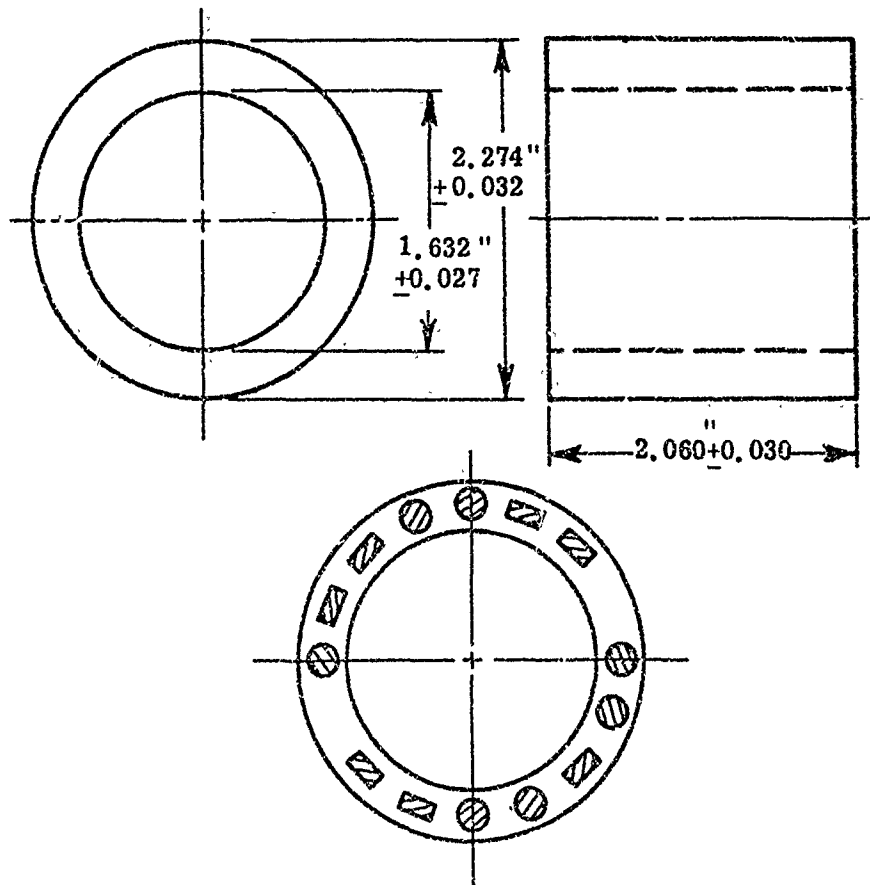


Figure 24. Configuration of Specimen Blar's 6Al7 as Received from Coors and Cutting Plan for Removing Phase I Macro Tensile and Macro Flexural Specimens

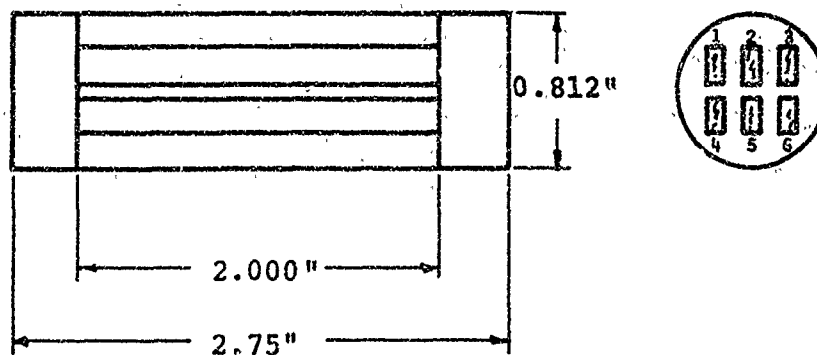


Figure 25. Configuration of Blank -135 as Received from Coors and Cutting Plan for Macroflexure Specimens

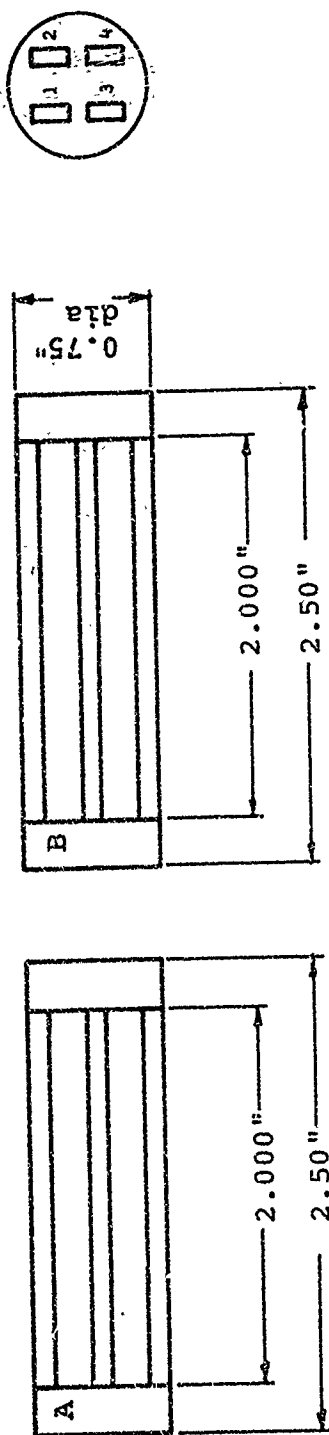


Figure 26. Configuration of Blank -138 as Received from Coors and Cutting Plan for Macroflexure Specimens

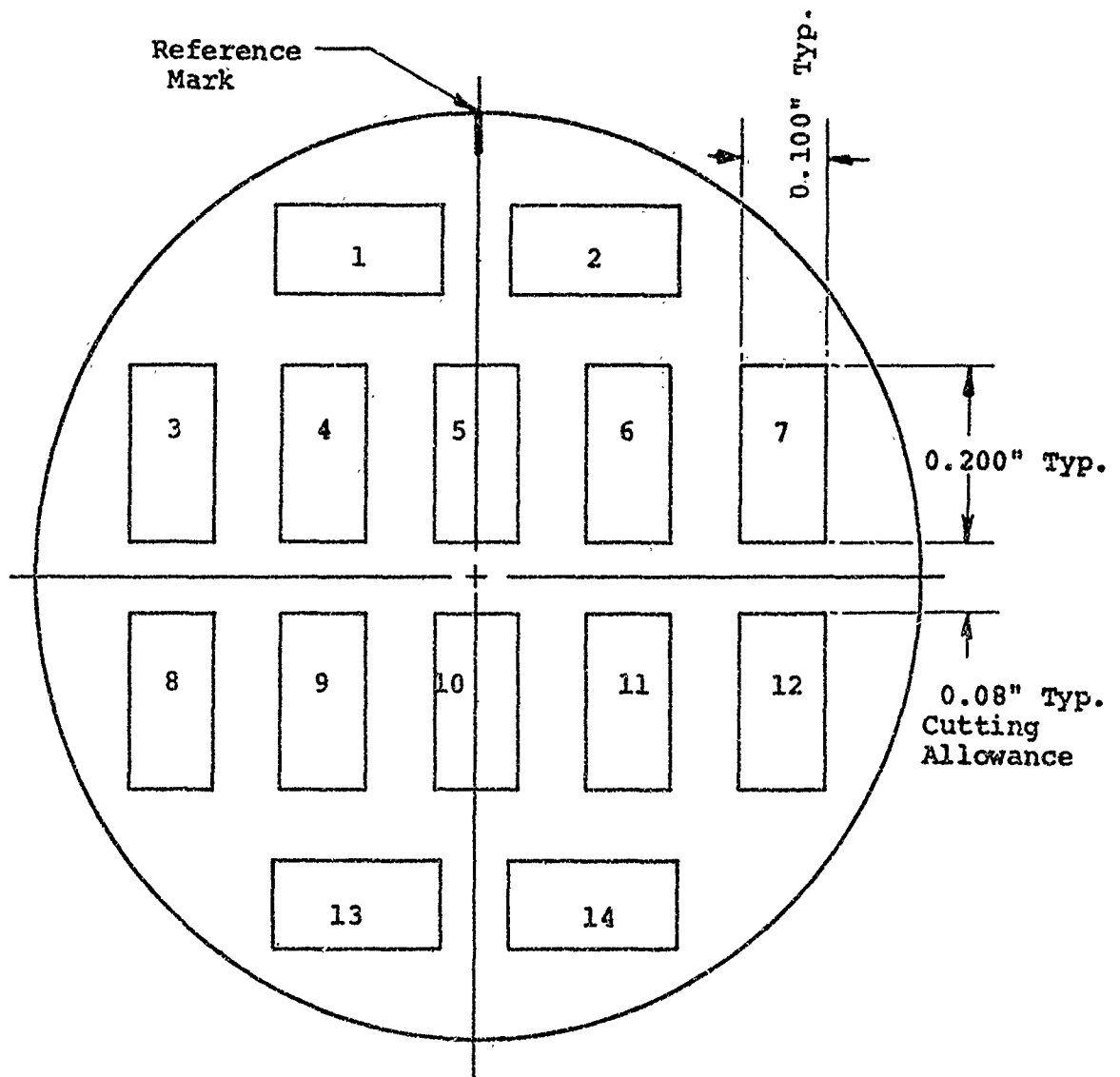
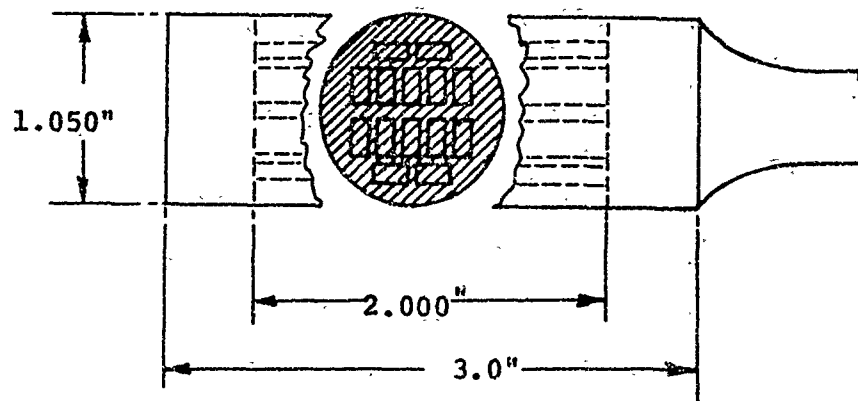


Figure 27. Cutting Plan for Ends of Blanks 3A05-024, 3A05-025, 3A05-028, 3A05-031, and 3A05-035 Used for Machining Study

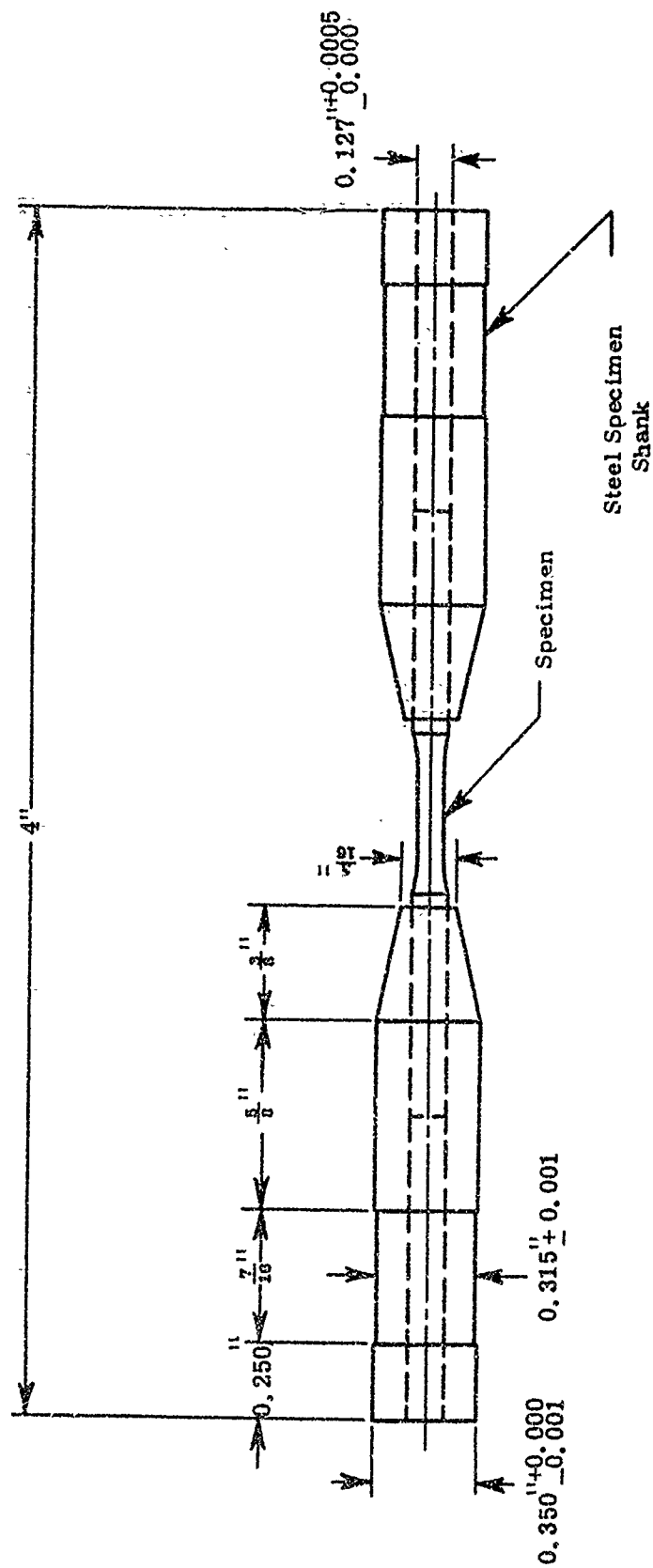


Figure 28. Steel Shanks for Providing a Gripping Surface for Precision Tensile Grips

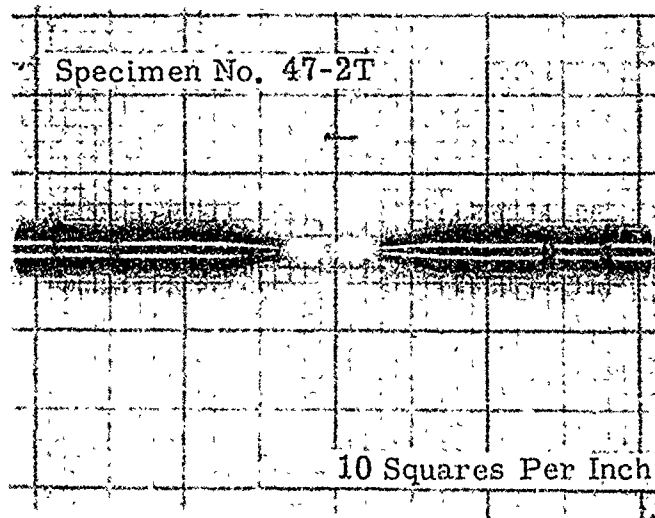


Figure 29. Photograph of Macro Tensile Specimen



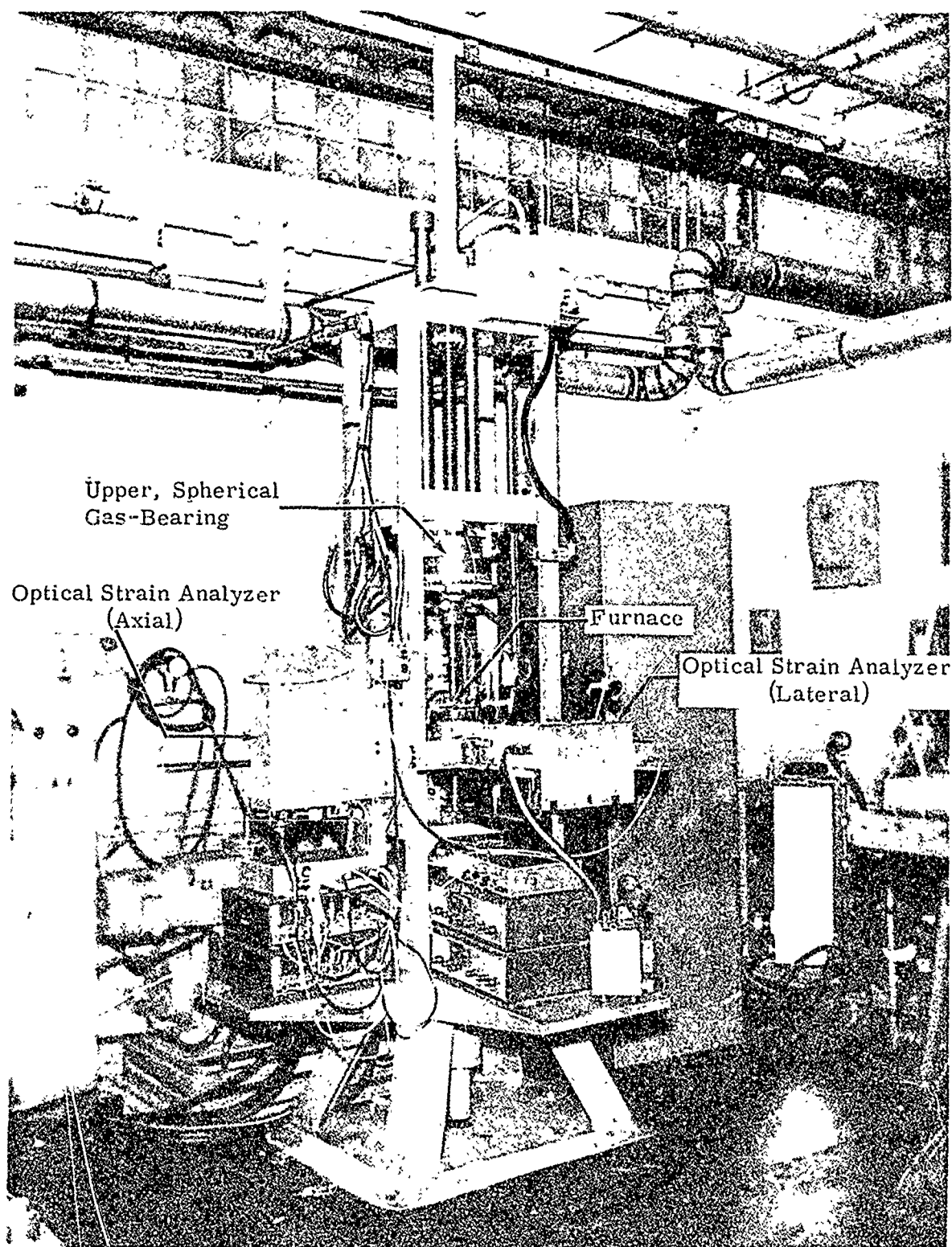


Figure 30. Picture of a Tensile Stress-Strain Facility

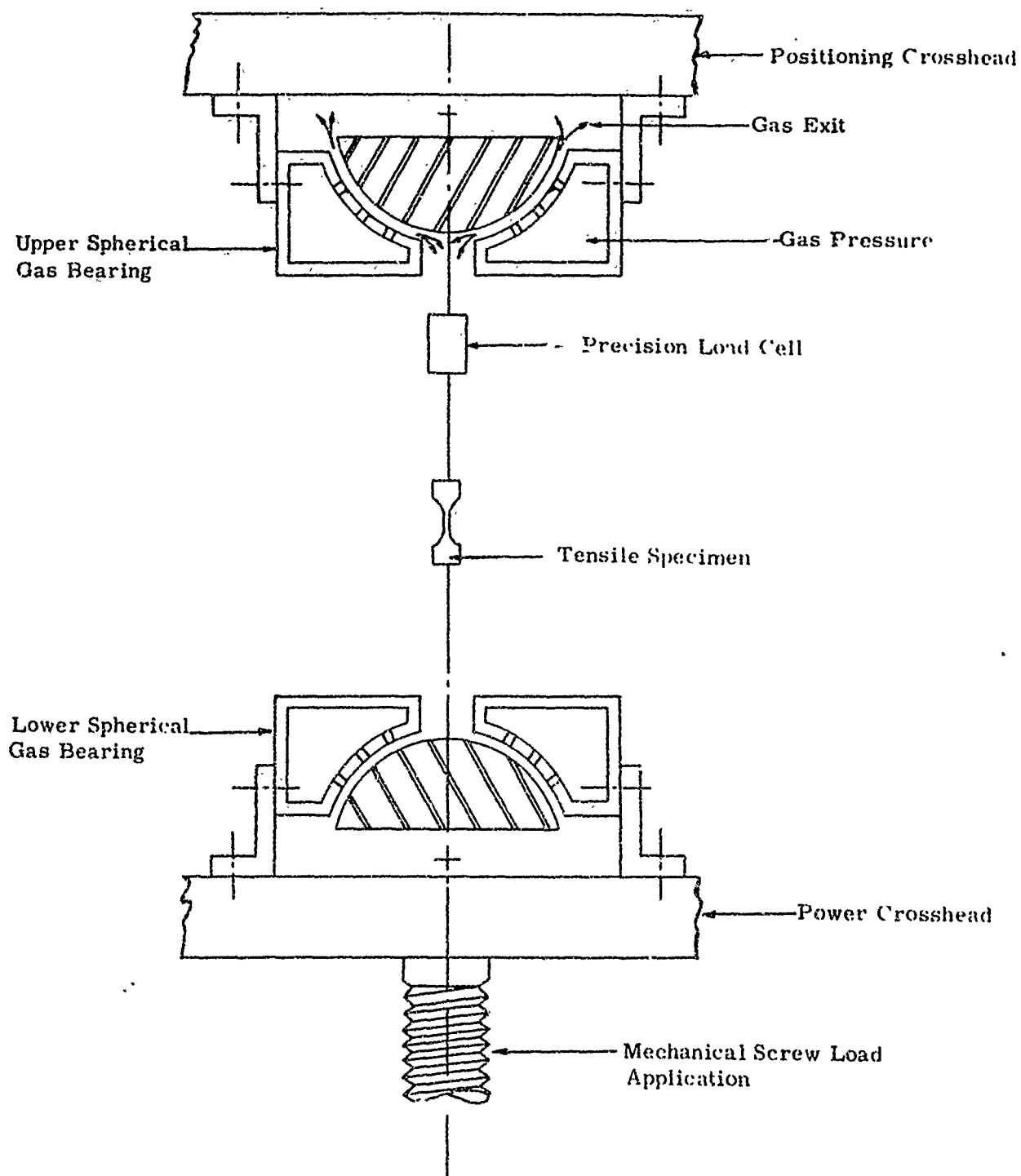


Figure 31. Schematic of the Gas Bearings and Load Train for the Tensile Apparatus

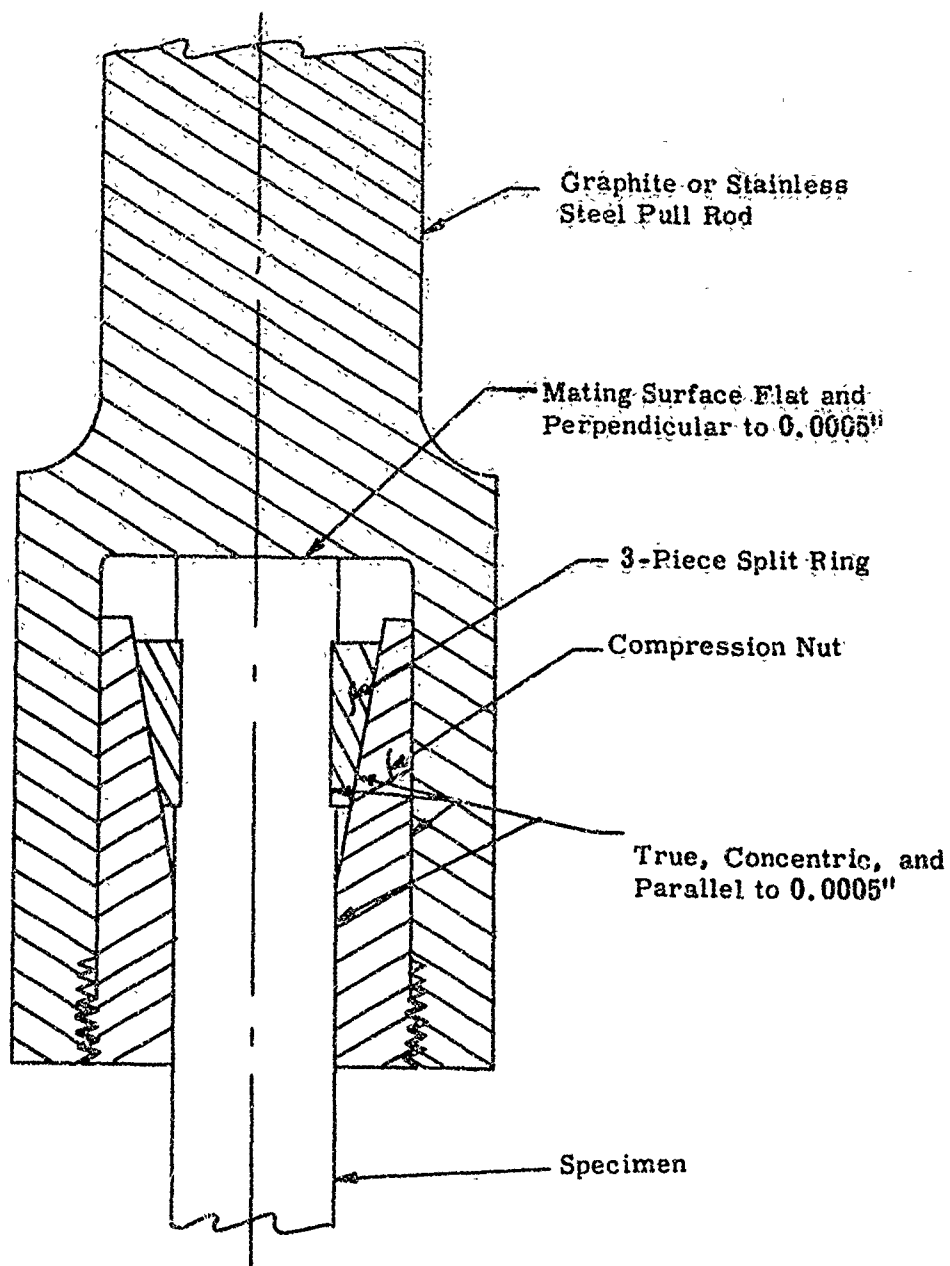


Figure 32. Precision Collet Grip for Tensile Specimens 2:1 Scale

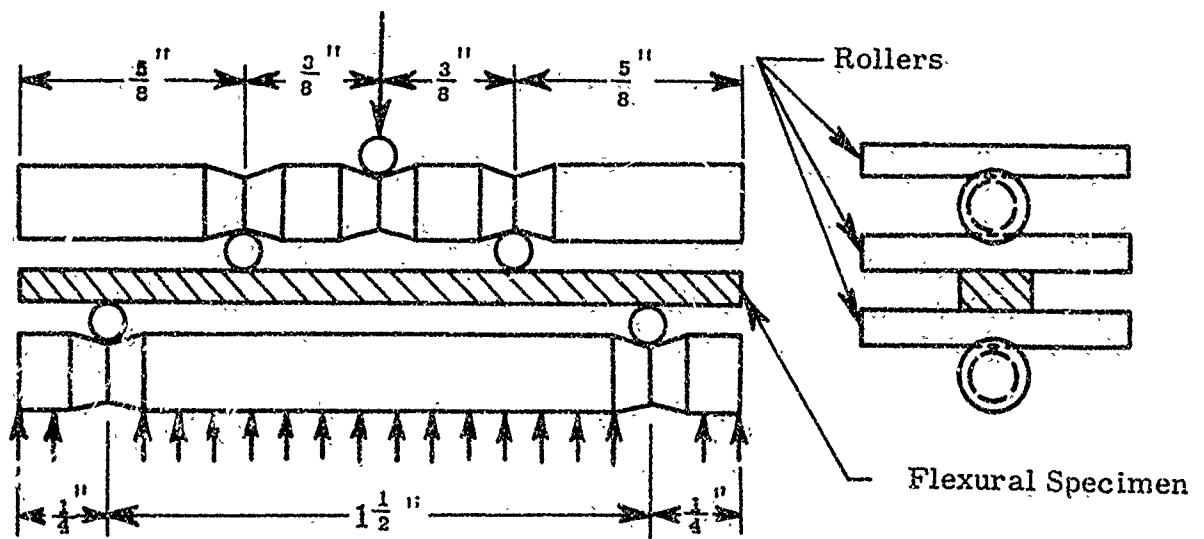
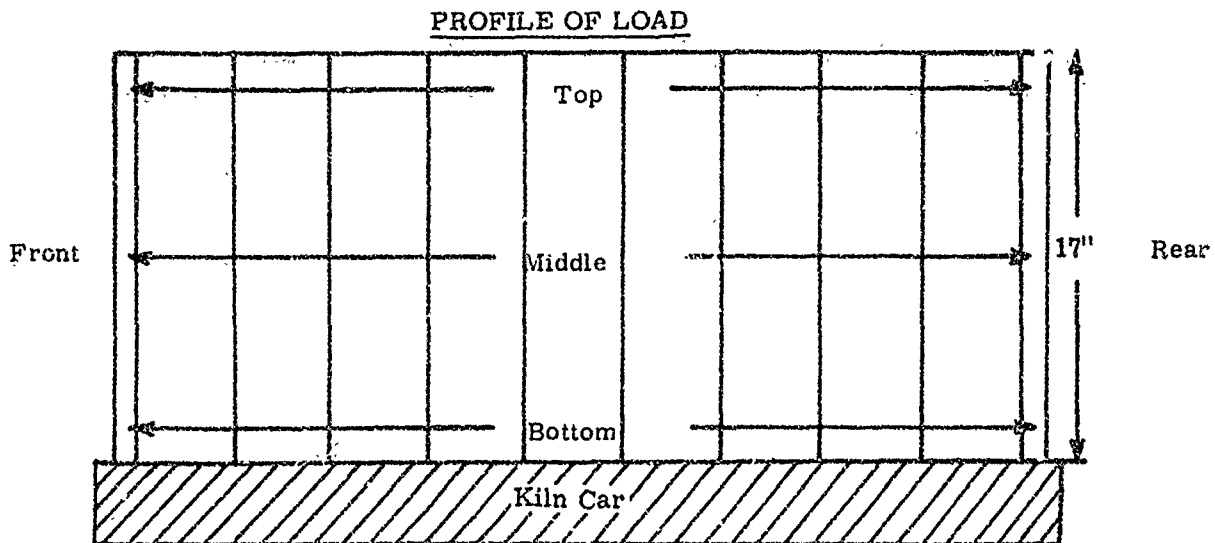
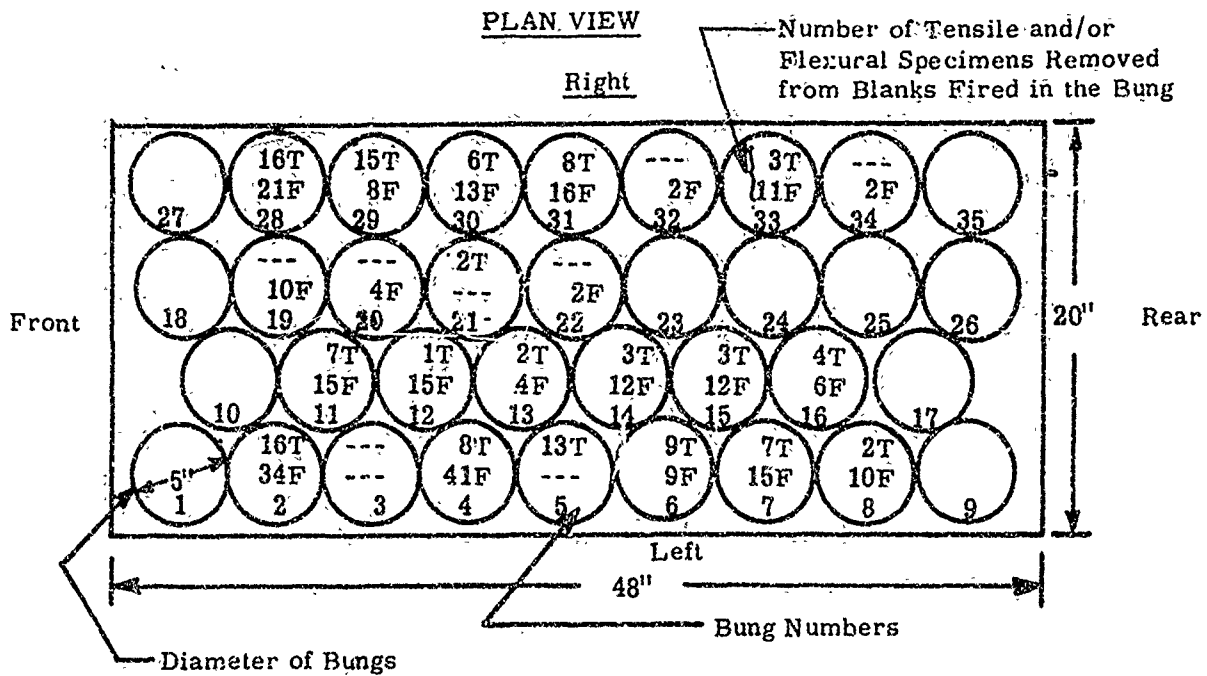


Figure 33. Schematic of Miniature Flexural Load Train

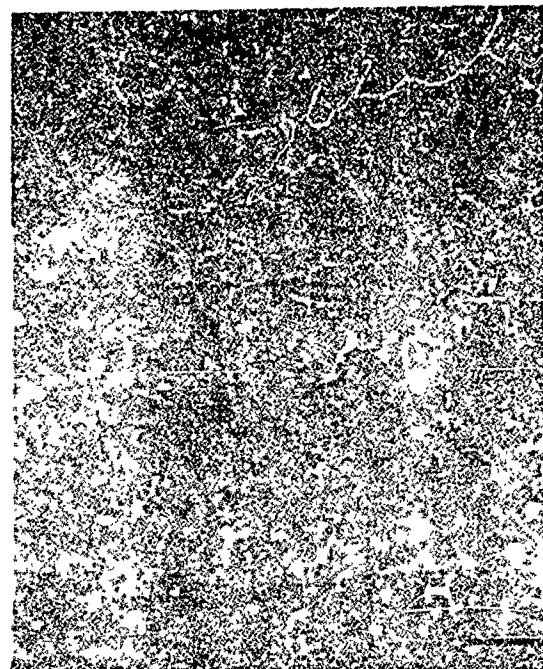


Parts shall be loaded on kiln cars in covered bungs as shown above

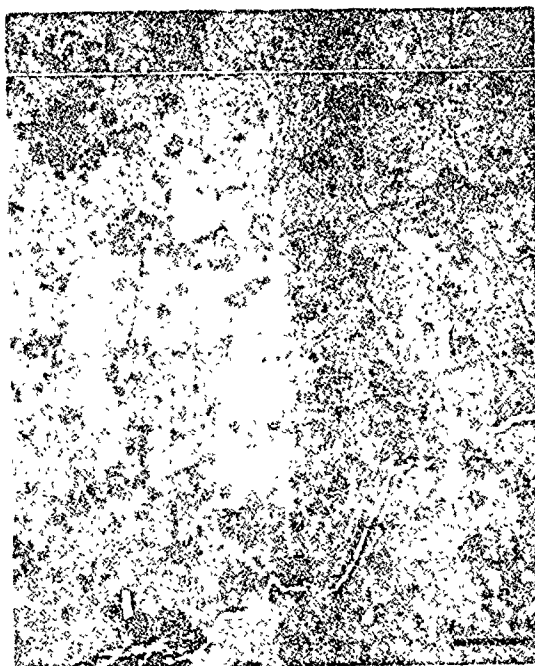
Figure 34. Schematic of L-33 Kiln Car Loading Layout



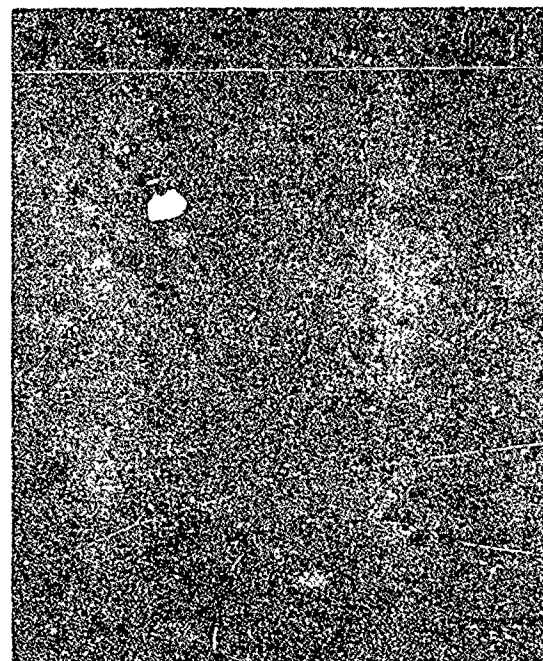
a



b

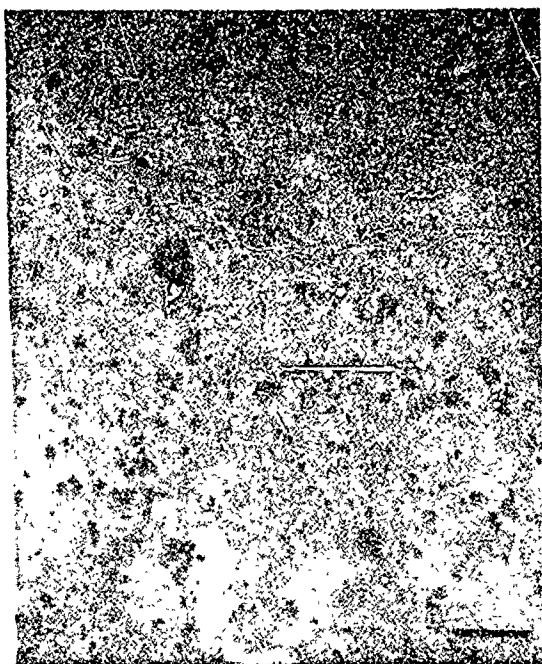


c

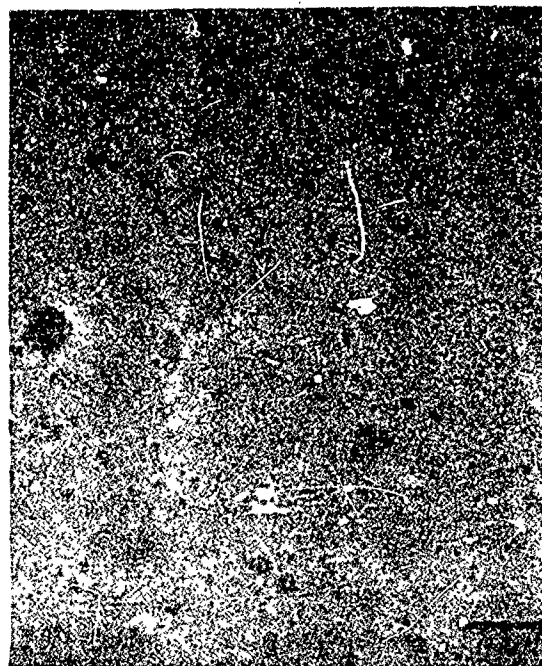


d

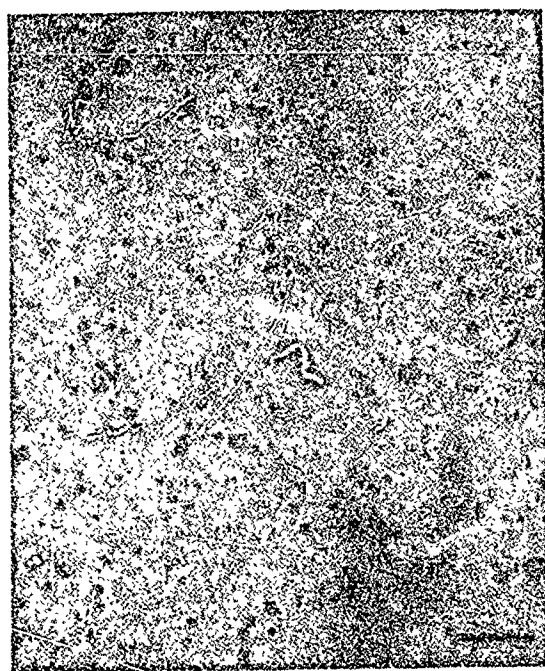
Figure 35. Photomicrographs of the Microstructure Resulting from Each Step of the "Deep Lap" Procedure



e



f



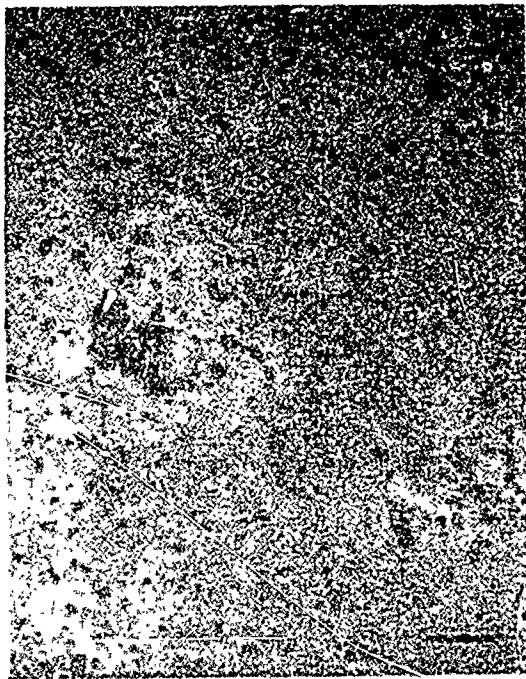
g

\*Fiducial bar equals 20 microns

- a - after surface grinding
- b - after 45 micron lapping
- c - after 30 micron lapping
- d - after 15 micron lapping
- e - after 6 micron lapping
- f - after 3 micron lapping
- g - after 1 micron lapping

Figure 35 (Continued). Photomicrographs of the Microstructure Resulting from Each Step of the "Deep Lap" Procedure





a\*



b

\*Fiducial bar equals 20 microns

Figure 36. Maximum "Pore Size" Observed after Completion of the "Deep Lap" Procedure

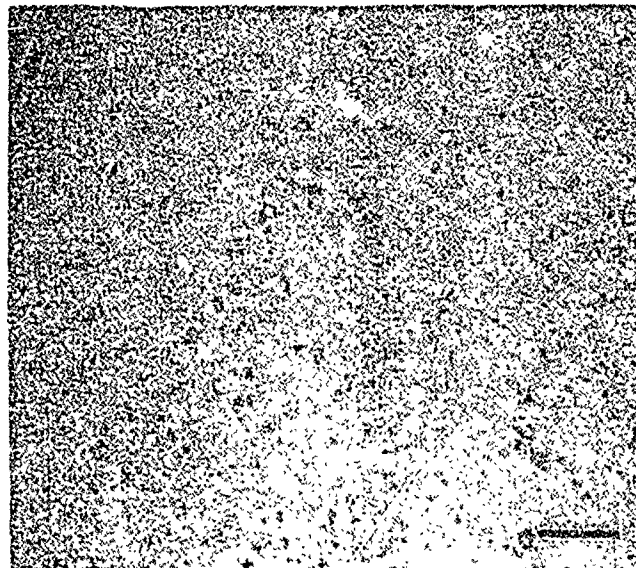
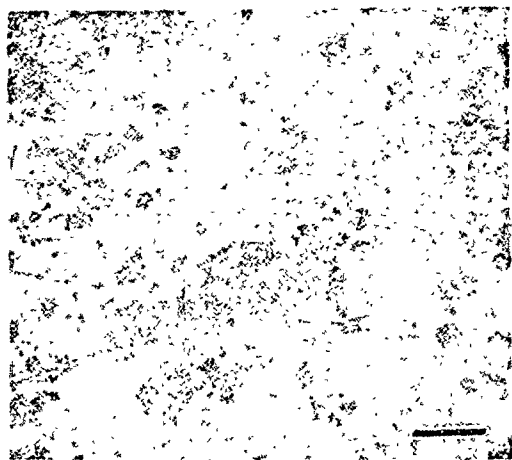


Figure 37. Final Microstructure after Completion of the Conventional Polishing Technique Including the Use of 30-and 15-Micron Diamond Pastes

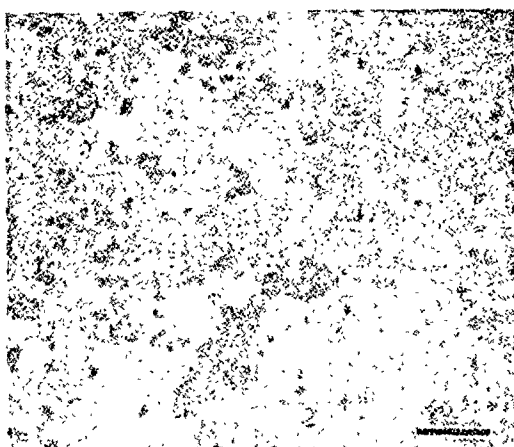




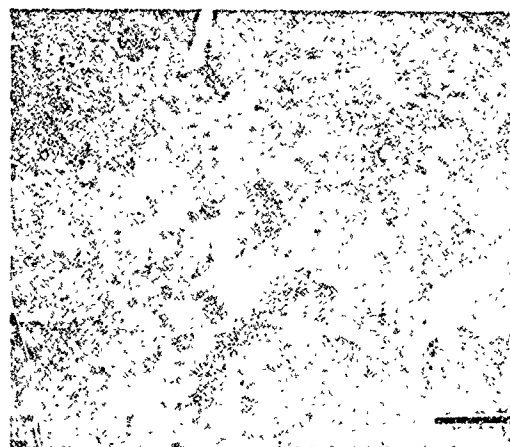
a



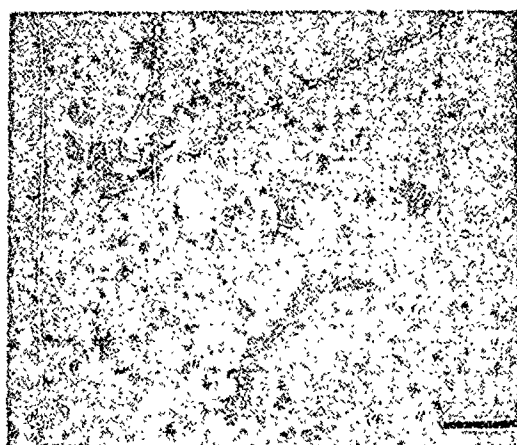
b



c



d



e

\*Fiducial bar equals 20 microns

a - after 30 micron polish

b - after 15 micron polish

c - after 6 micron polish

d - after 3 micron polish

e - after 1 micron polish

Figure 38. Microstructure after Progressive Stages of Polishing Using the Procedure with which Specimens Selected for Grain Size Measurements Were Polished

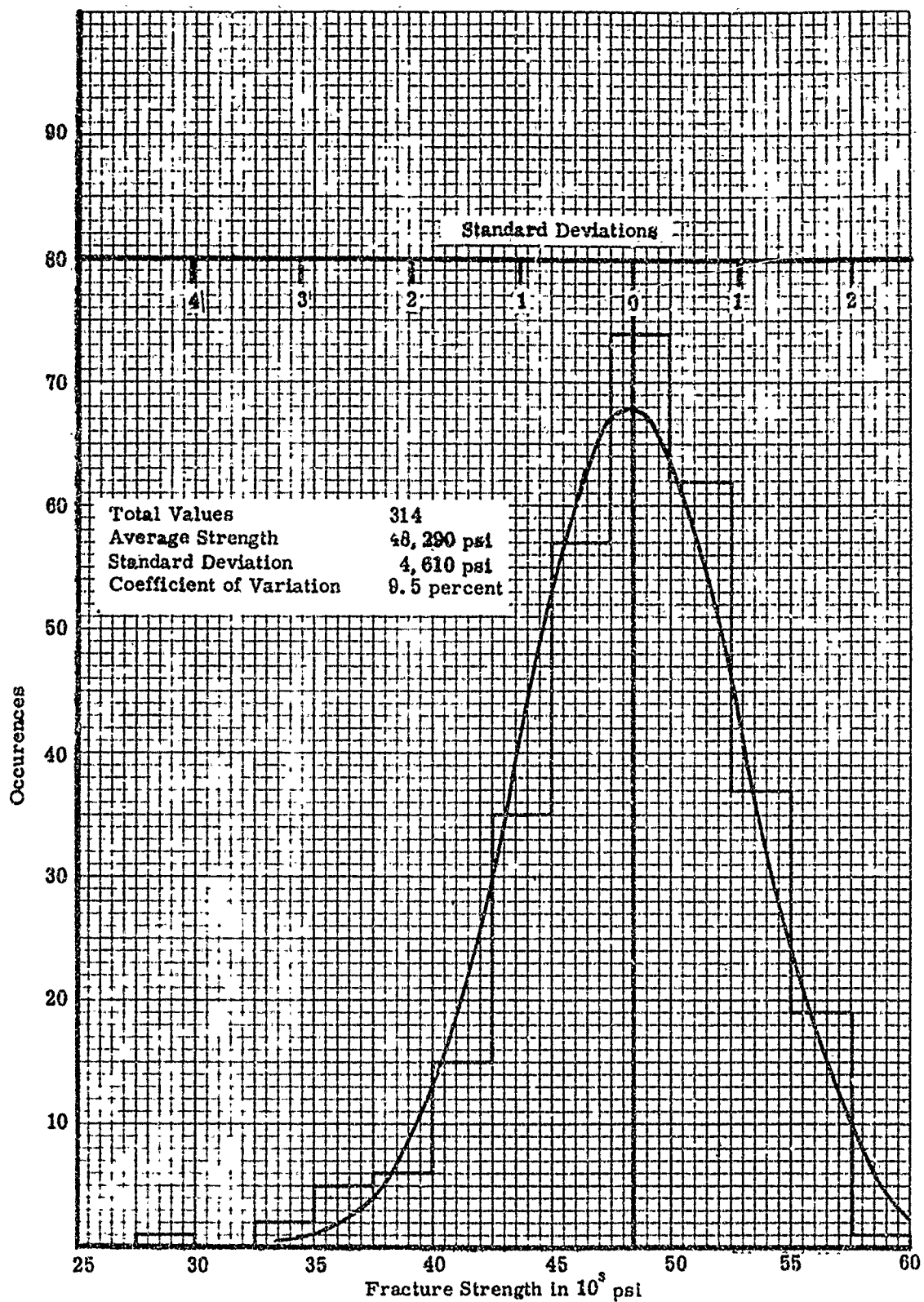


Figure 39. Distribution of the Flexural Strengths of the Macro Specimens

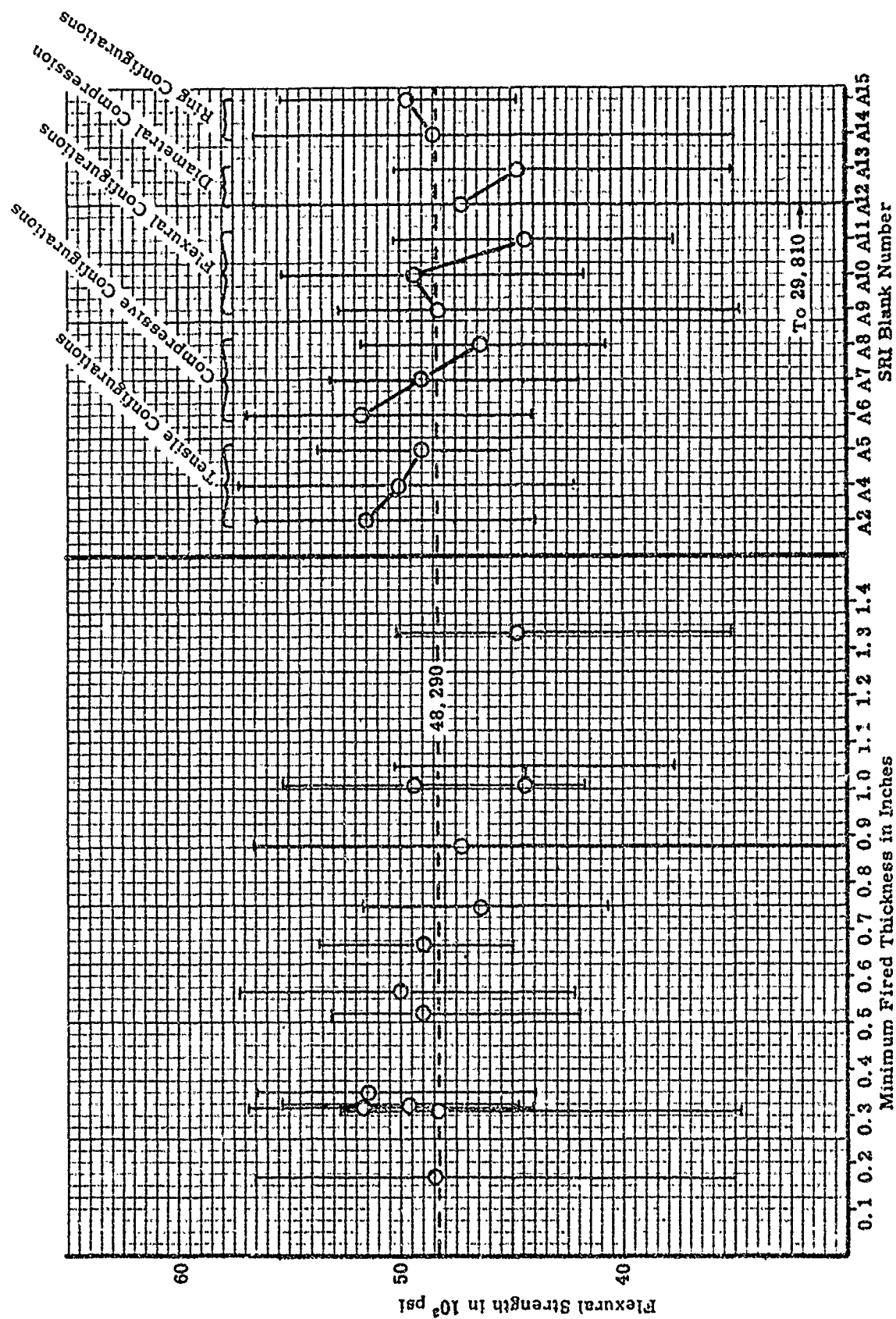


Figure 40. Average Flexural Strengths versus SRI Blank Numbers and Minimum Fired Thickness

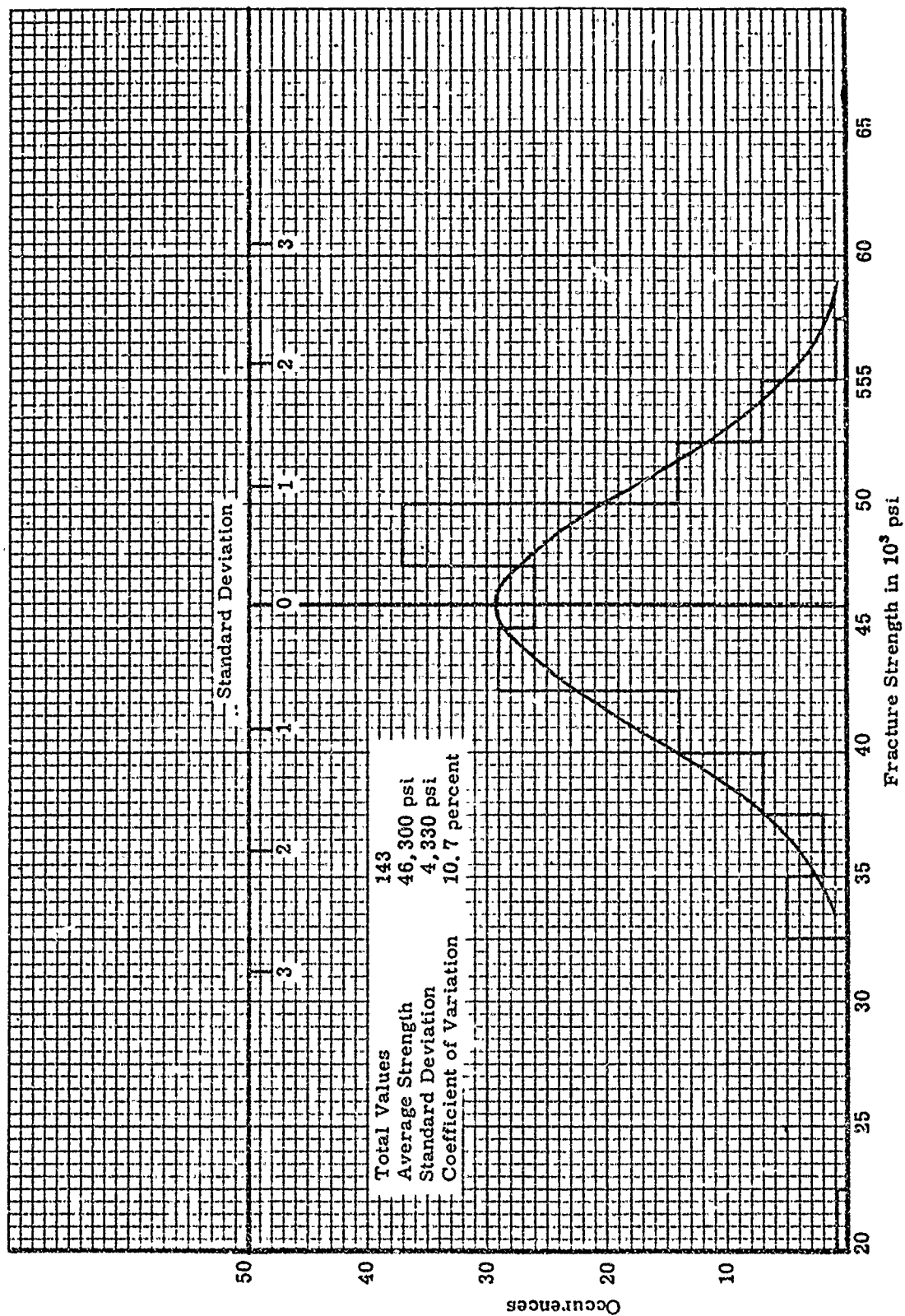


Figure 41. Distribution of the Tensile Strengths of the Macro Specimens

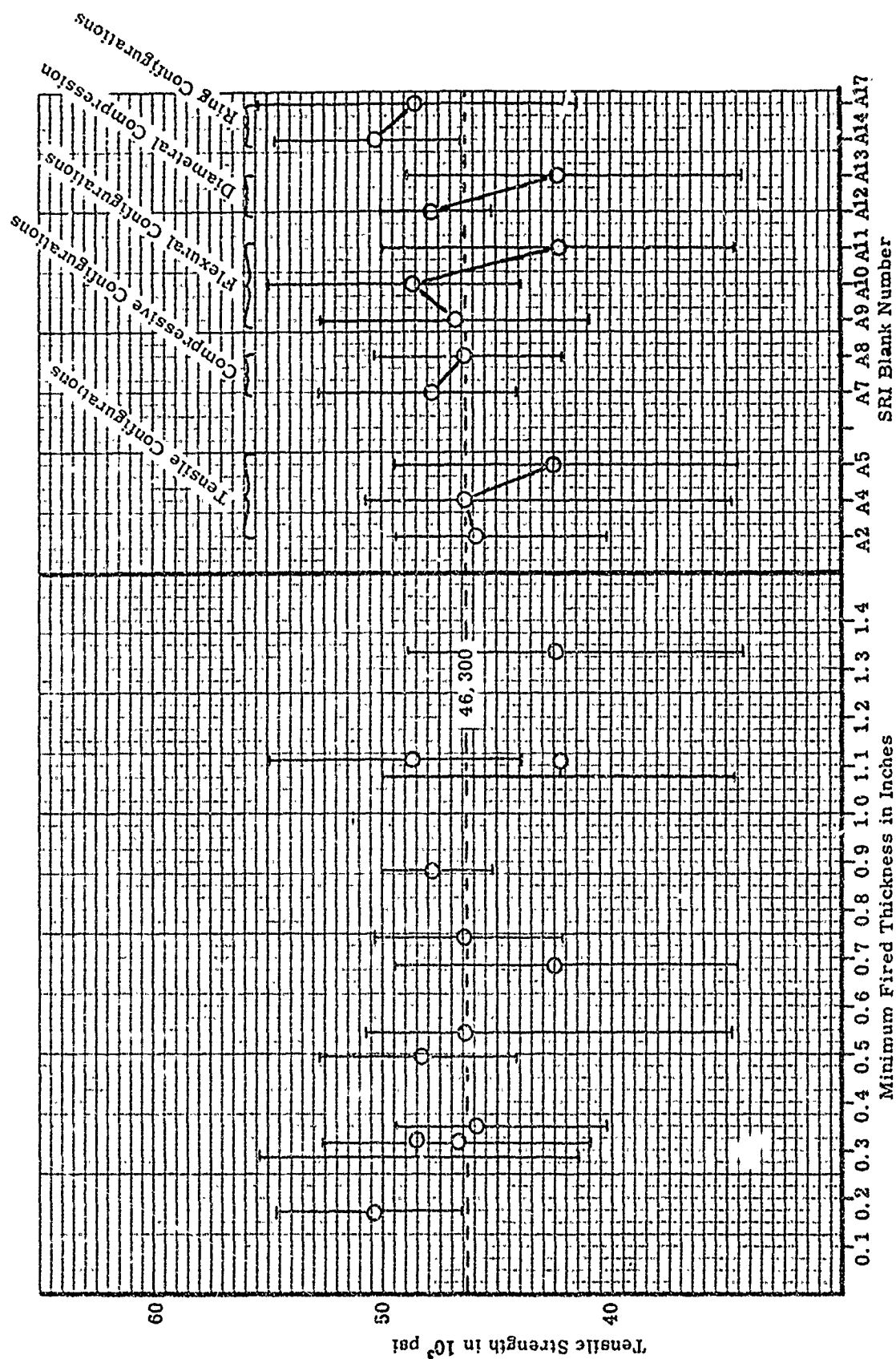


Figure 42. Tensile Strength versus SRI Blank Numbers and Minimum Firing Thickness

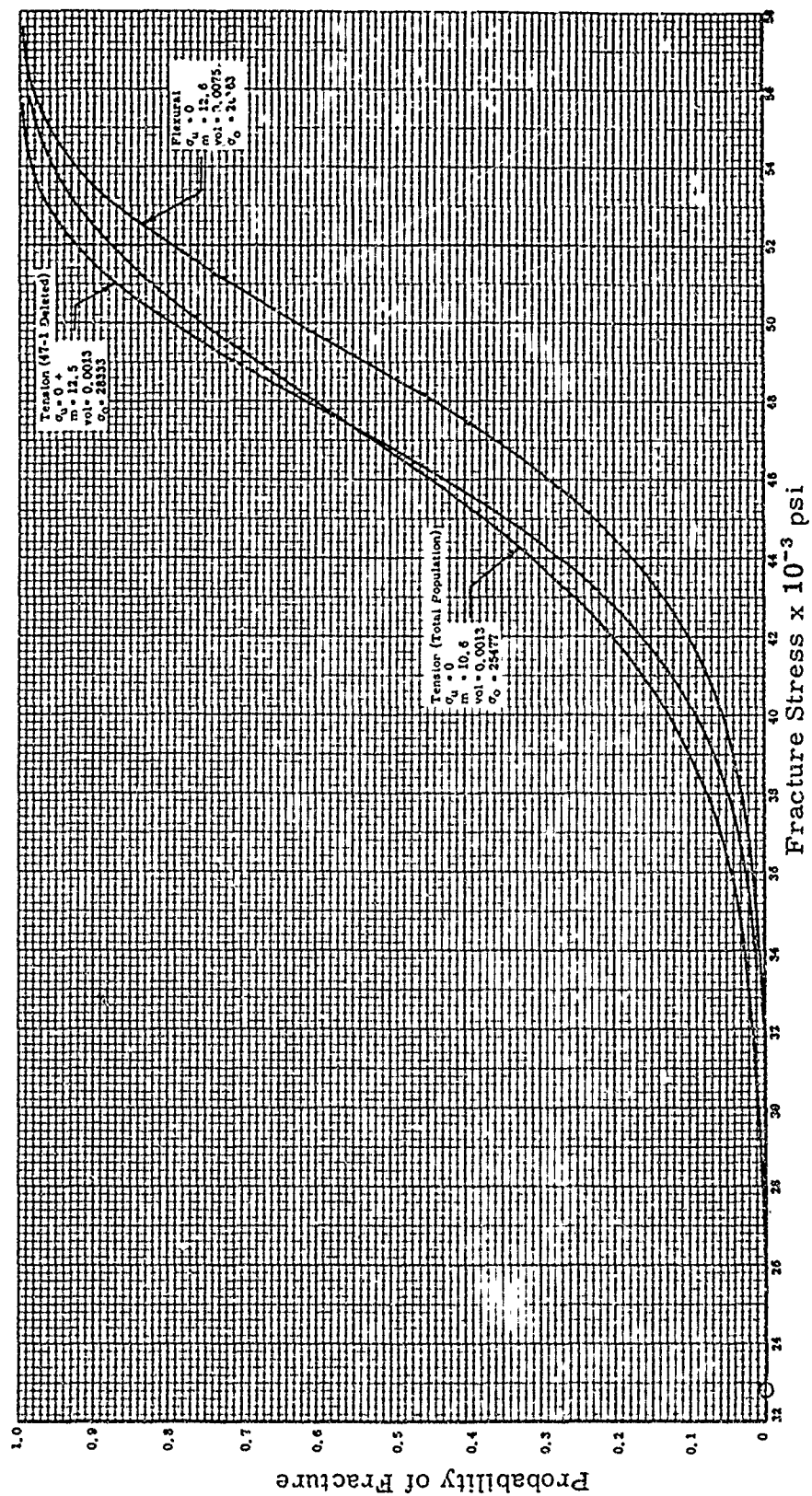


Figure 43. Probability of Fracture versus Fracture Stress for Phase I Tensile and Flexural Data



$$-1 \left[ \begin{matrix} \times (0.0004, 58,500) \\ \times (0.00022, 88,500) \end{matrix} \right]$$

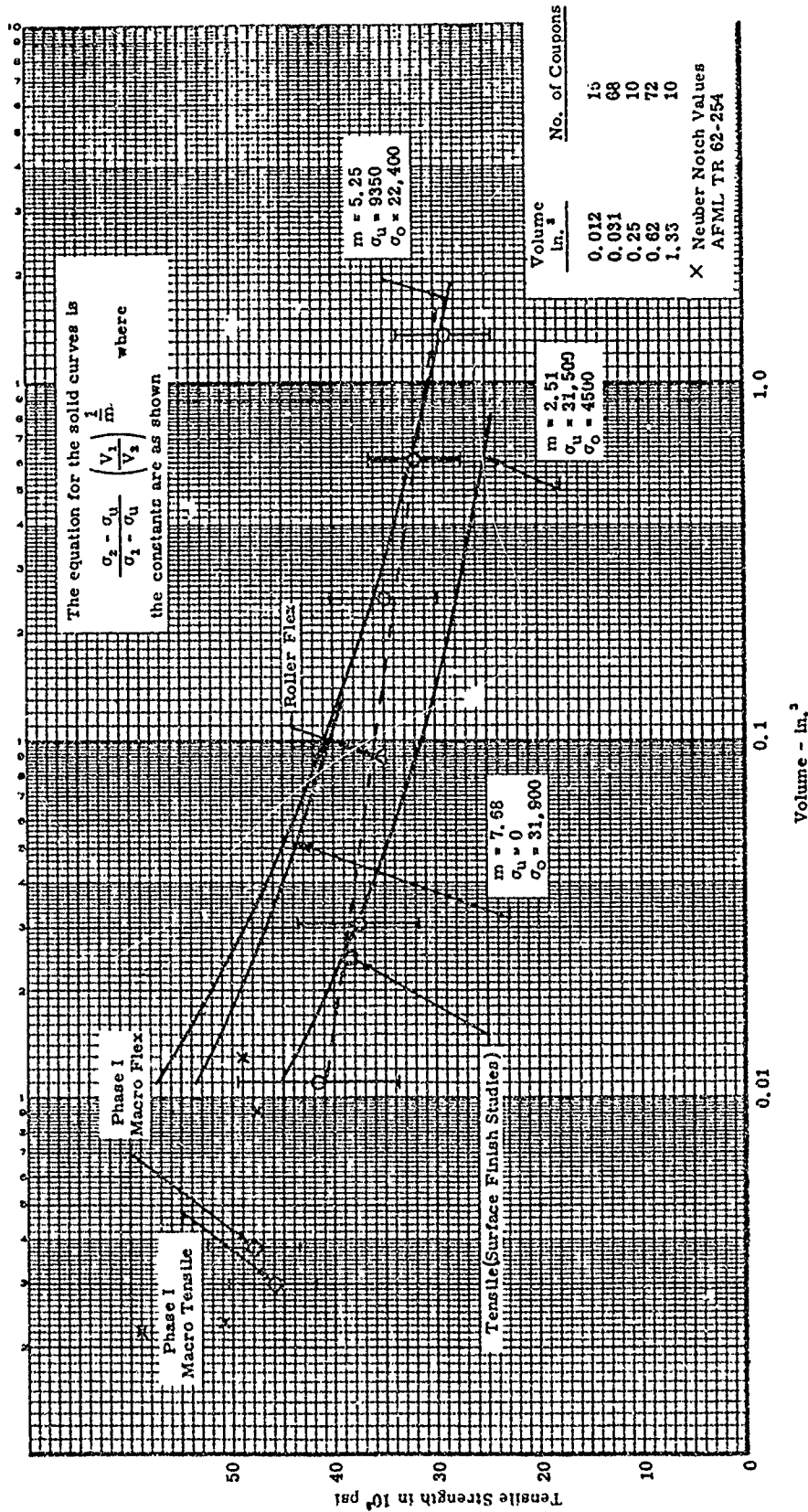
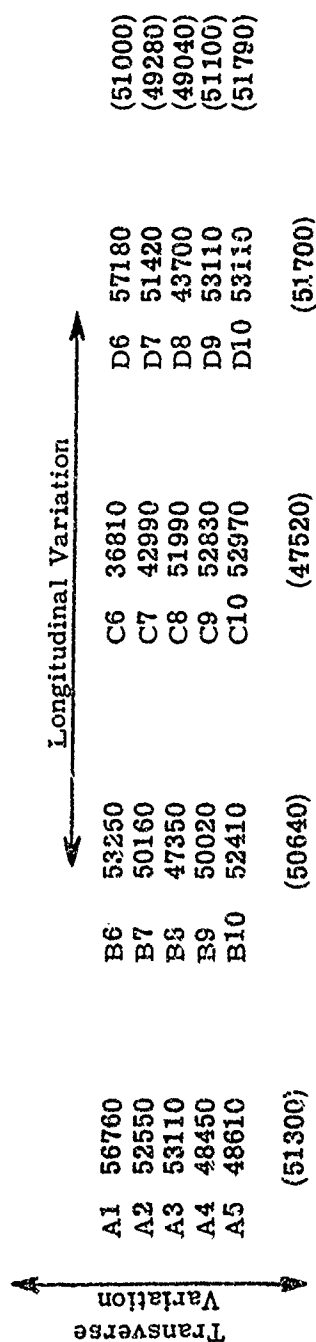


Figure 44. Average Ultimate Tensile Strength versus Volume<sup>2</sup>, also Showing Standard Deviations, for the Cullied Alumina Data from AFML-TR-66-228 and the Phase I Alumina Data on Macro Specimens



### Cross-sectional Variation

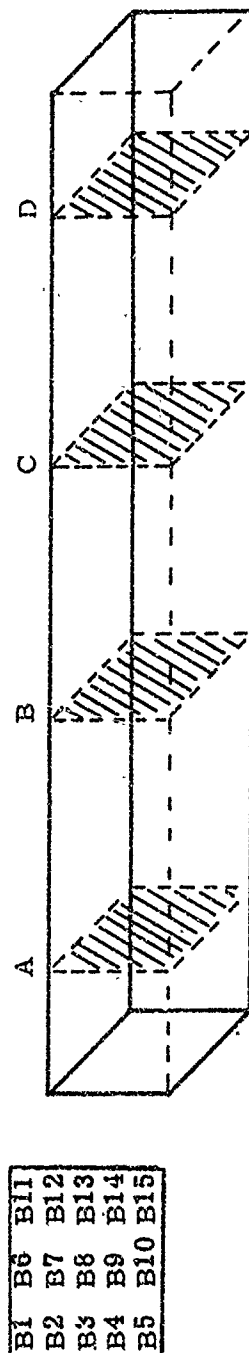
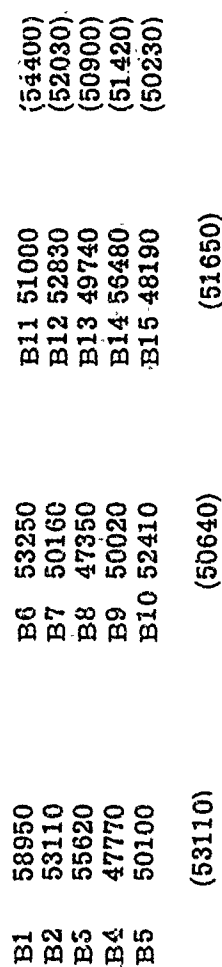


Figure 45. Uniformity of Strength in Specimen Blank 3A10-088 as Determined from Flexural Strength Data



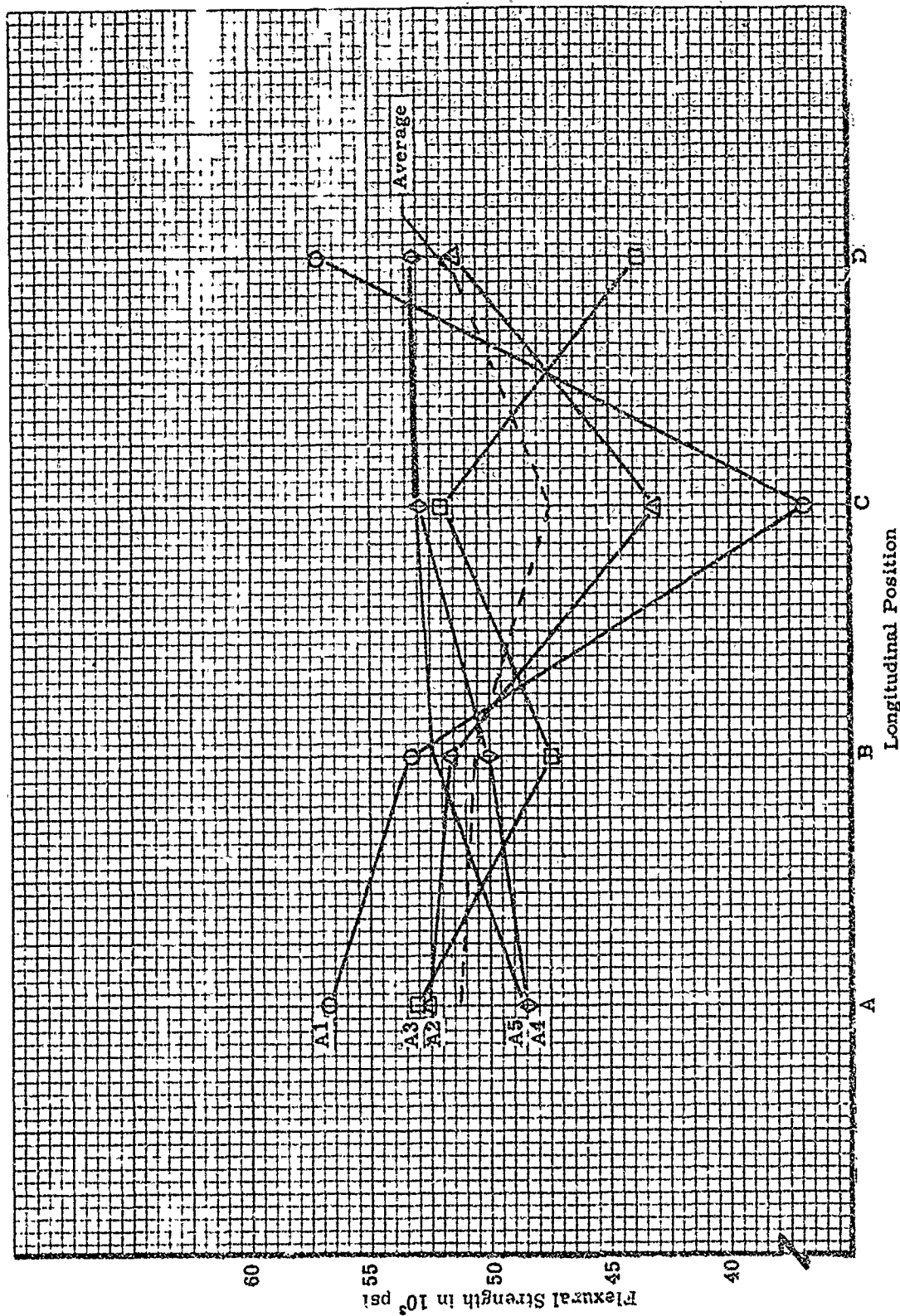


Figure 46. Flexural Strength versus Longitudinal Position at Five Transverse Positions for Specimen Blank 3A10-088

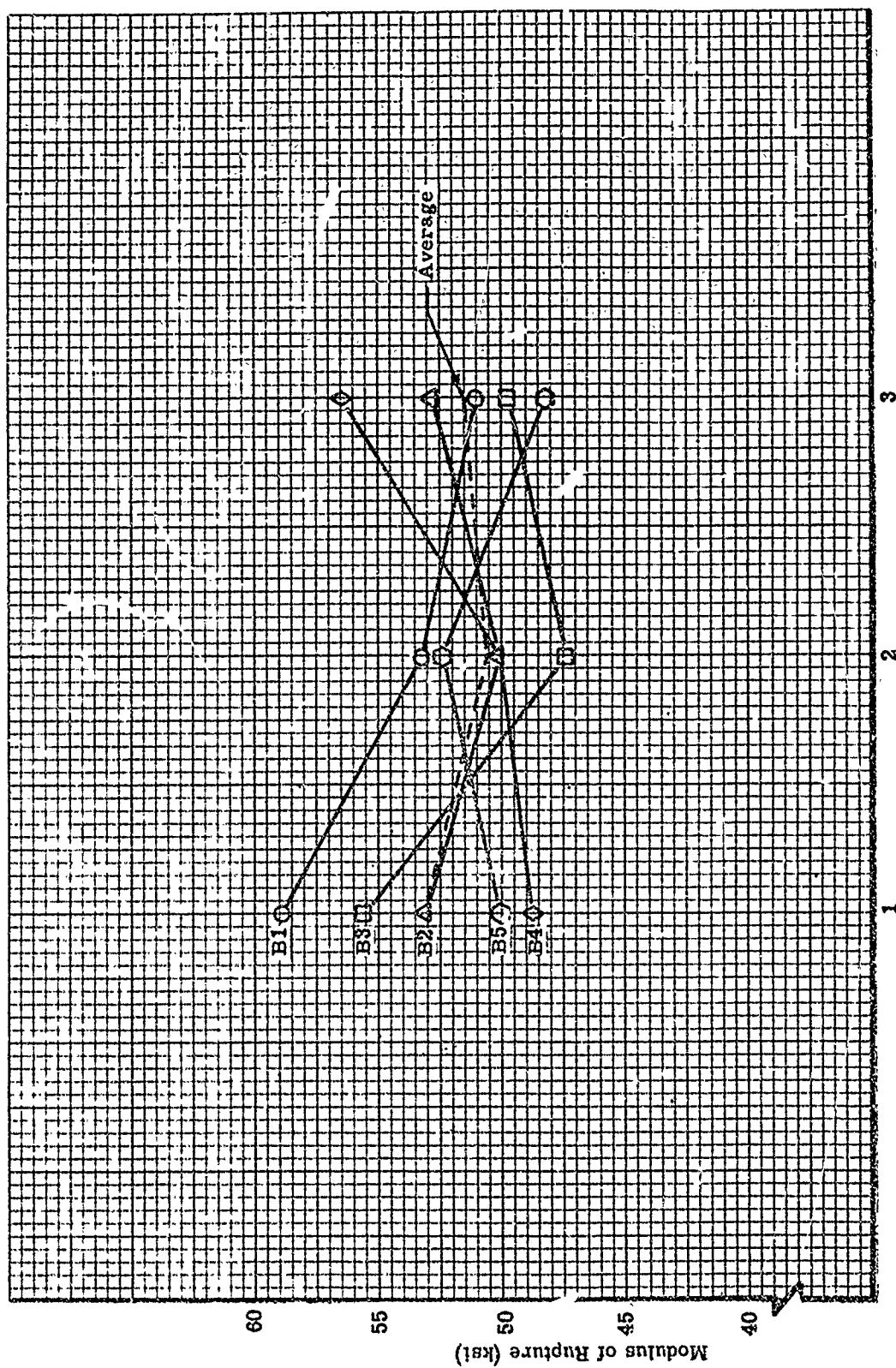


Figure 47. Cross Sectional Variation of Strength for Specimen Blank 3A10-088

Transverse Variation		Longitudinal Variation	
A1	3.814	B6	3.852
A2	3.834	B7	3.838
A3	3.817	B8	3.805
A4	3.855	B9	3.842
A5	3.855	B10	3.841
	(3.832)		(3.836)
		C6	3.850
		C7	3.834
		C8	3.831
		C9	3.831
		C10	3.834
		D6	3.844
		D7	3.835
		D8	3.823
		D9	3.841
		D10	3.821
			(3.838)

# Cross-sectional Variation

B1	3.837	B6	3.852	B11	3.851
B2	3.823	B7	3.838	B12	3.841
B3	3.835	B8	3.805	B13	3.843
B4	3.825	B9	3.842	B14	3.844
B5	3.830	B10	3.841	B15	3.822
	(3.830)		(3.836)		(3.840)

A1
A2
A3
A4
A5

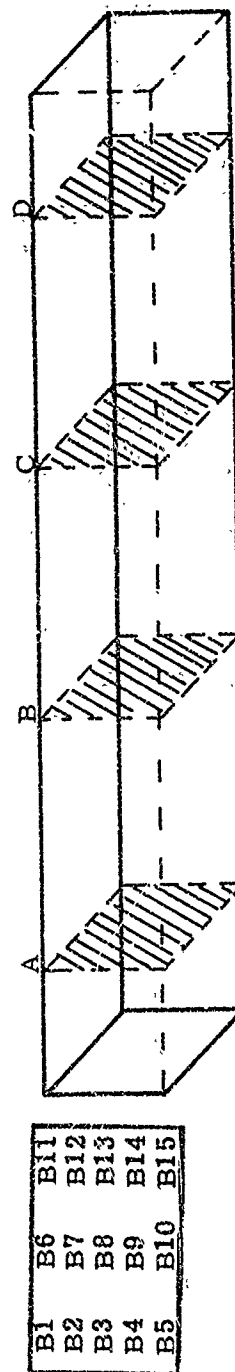


Figure 48. Uniformity of Density in Specimen Blank 3A10-088 as Determined from Macro Flexural Specimens

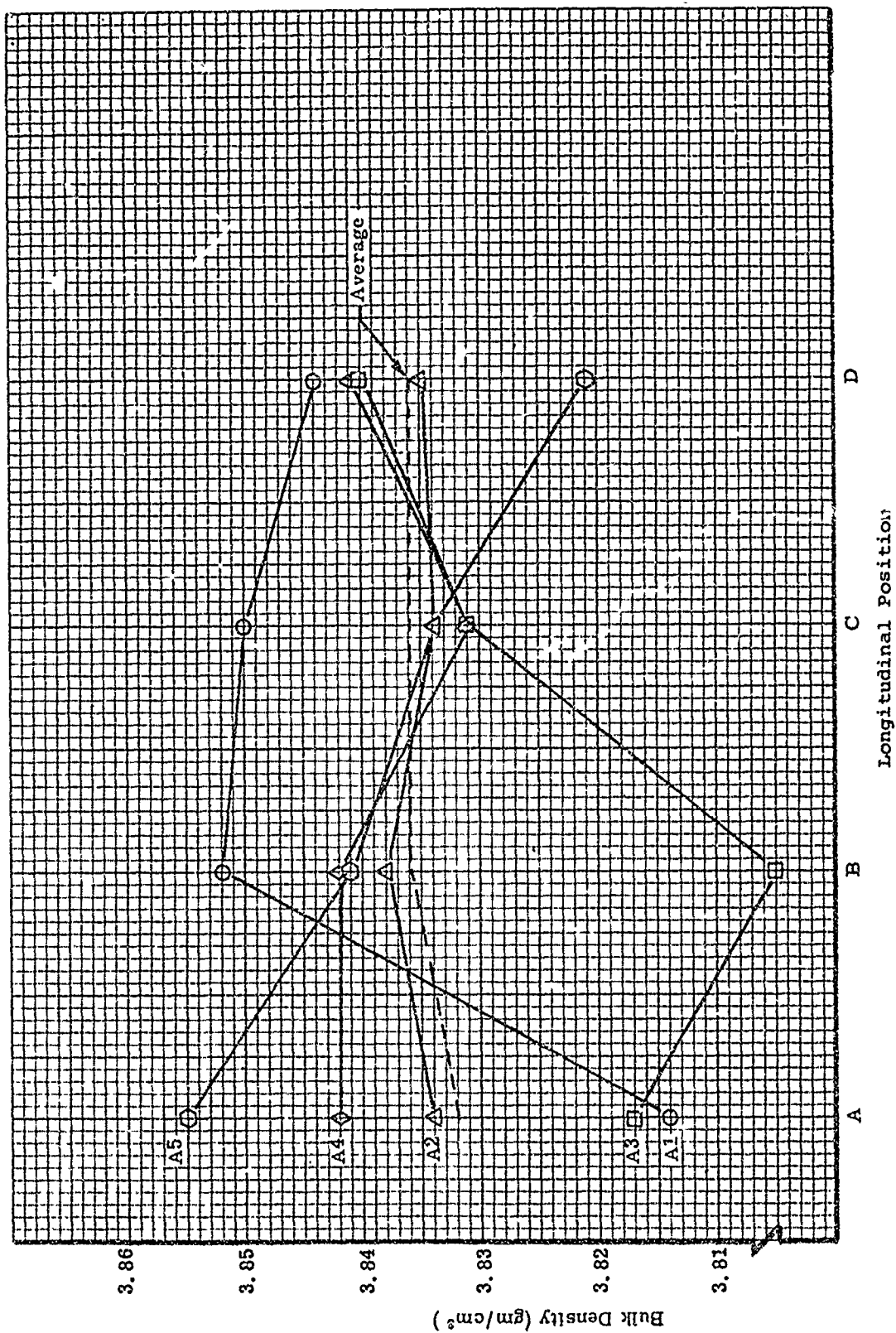
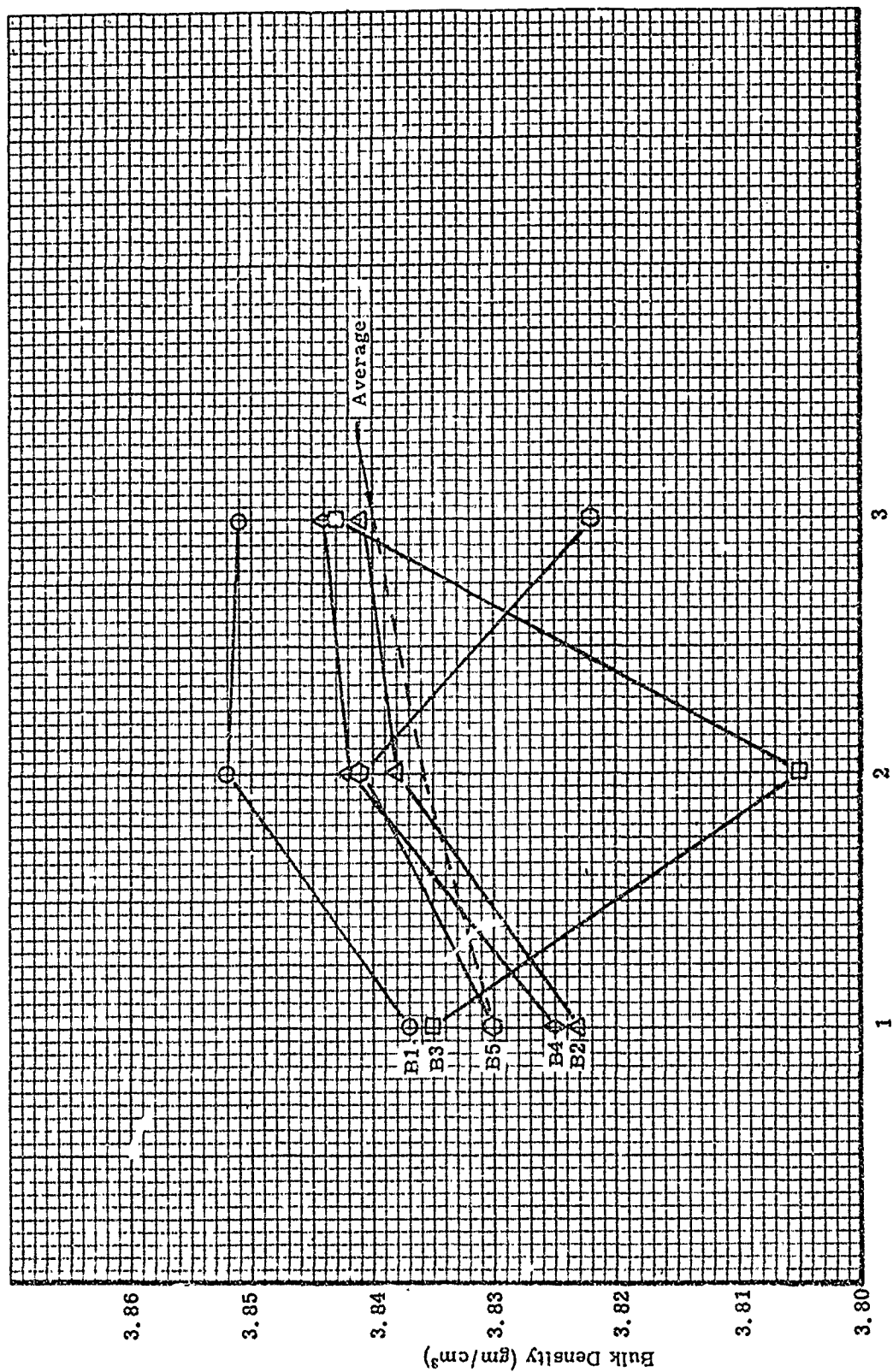


Figure 49. Density versus Longitudinal Position at Five Transverse Positions for Specimen Blank 3A10-088



Lateral Position Across Section B

Figure 50. Cross Sectional Variation of Density for Specimen Blank 3A10-088

Transverse Variation			Longitudinal Variation		
A1	A2	A3	C1	E1	(3.792)
3.782	3.787	3.755	3.802	3.791	(3.782)
3.787	3.755	3.786	3.790	3.768	(3.763)
3.755	3.786	3.756	3.765	3.768	(3.784)
3.786	3.756	3.791	3.776	3.789	(3.768)
3.756	3.791	(3.776)	3.773	3.775	(3.788)
3.791	(3.776)		3.786	3.787	
			(3.782)		(3.780)

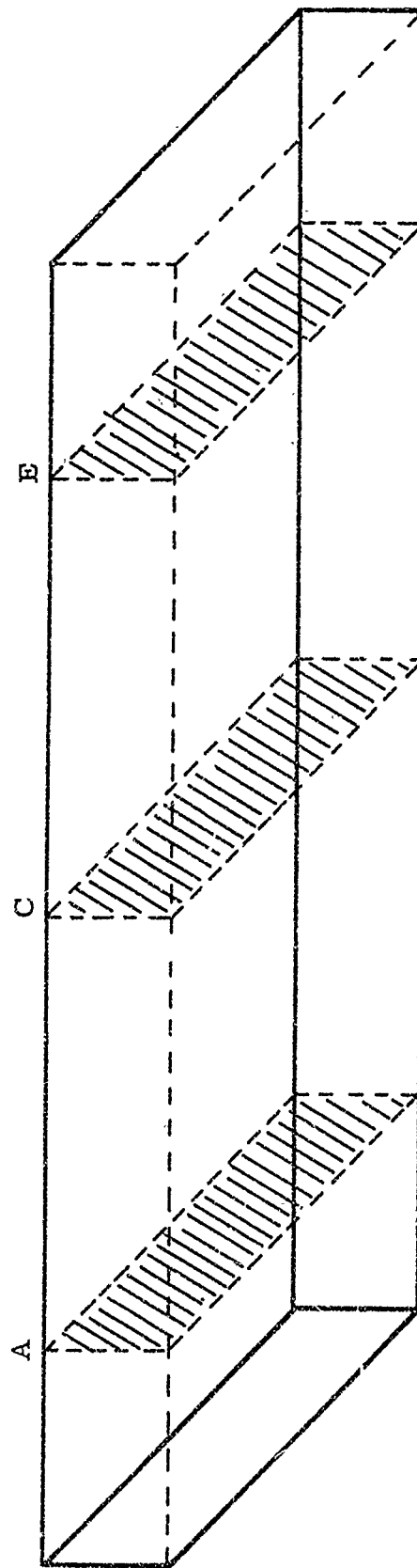


Figure 51. Uniformity of Density in Specimen Blank 4A11-089 as Determined from Macro Flexural Specimens

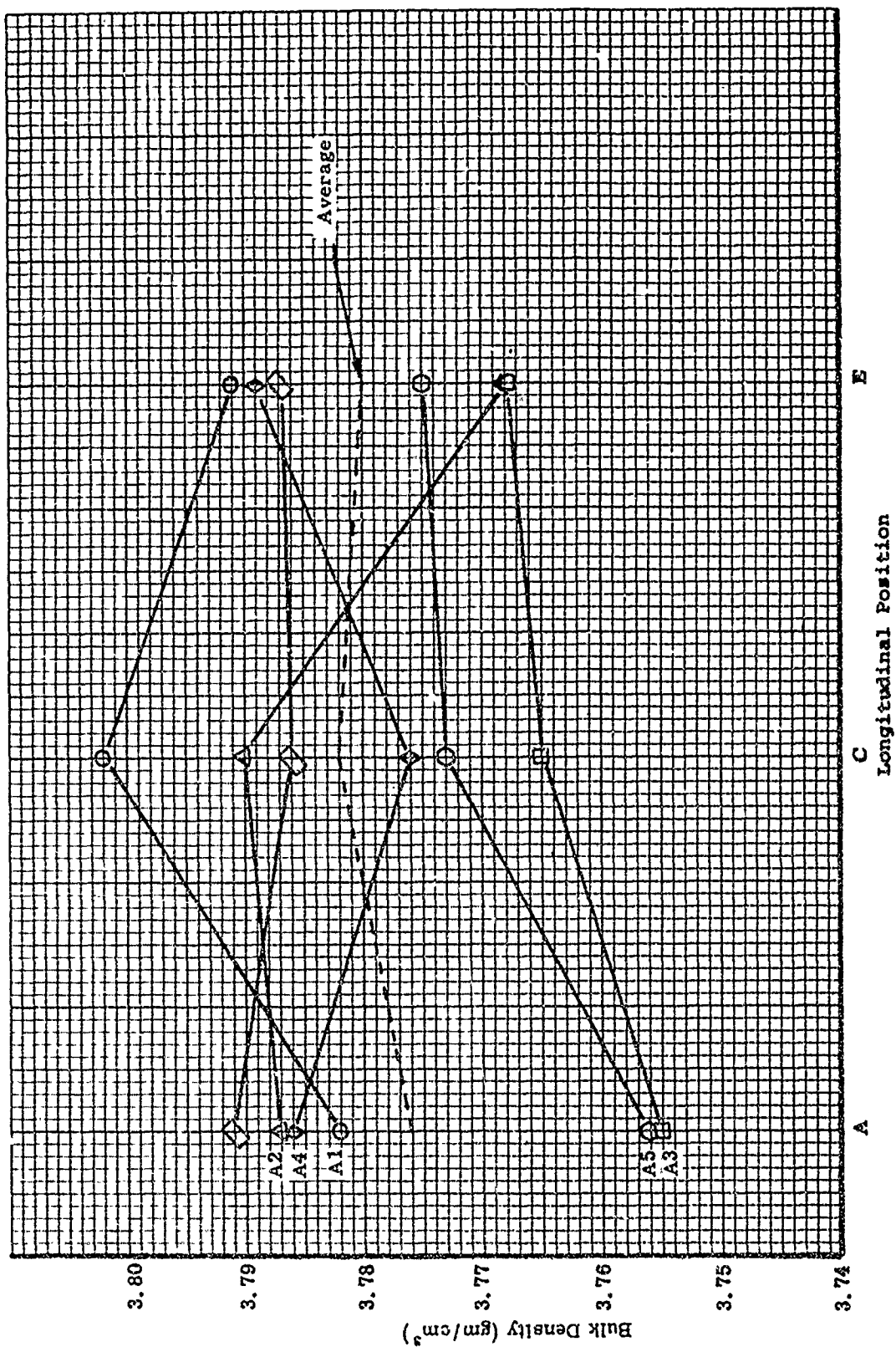


Figure 52. Longitudinal Density Profile for Specimen Blank 4A11-089



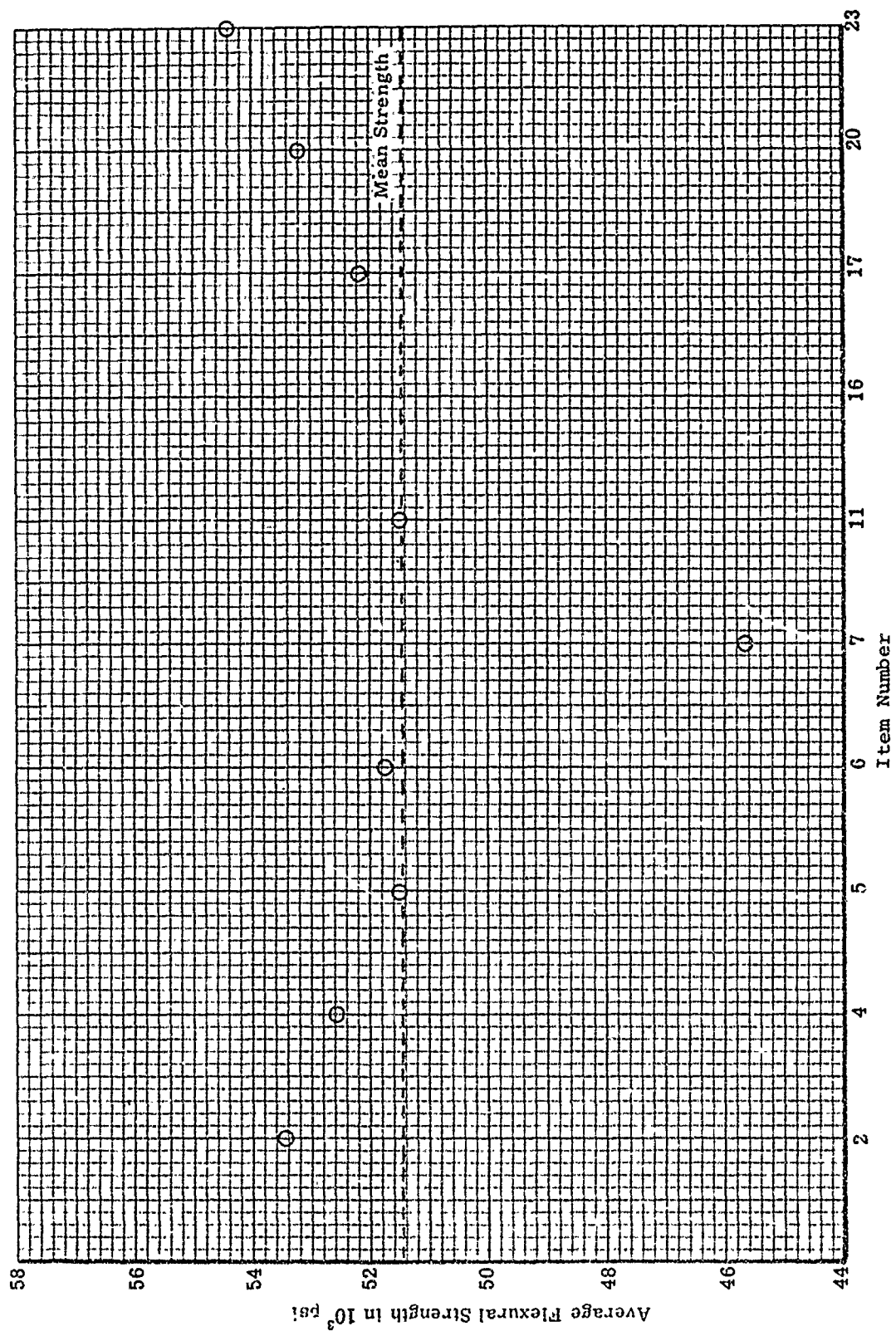


Figure 53. Variation in Average Strengths Among the Several Items of Blank Type A02



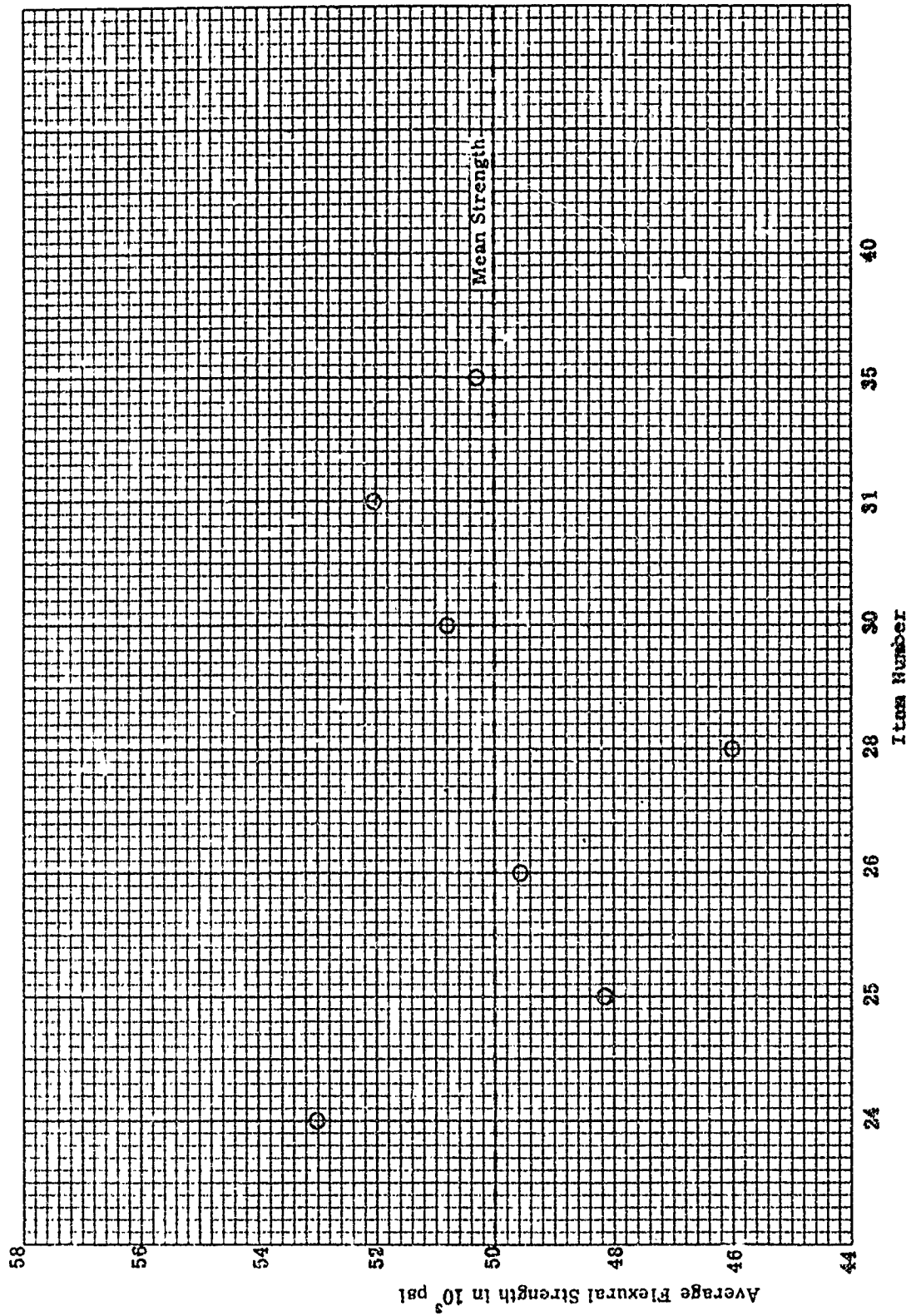


Figure 54. Variation in Average Strengths Among the Several Items of Blank Type A04

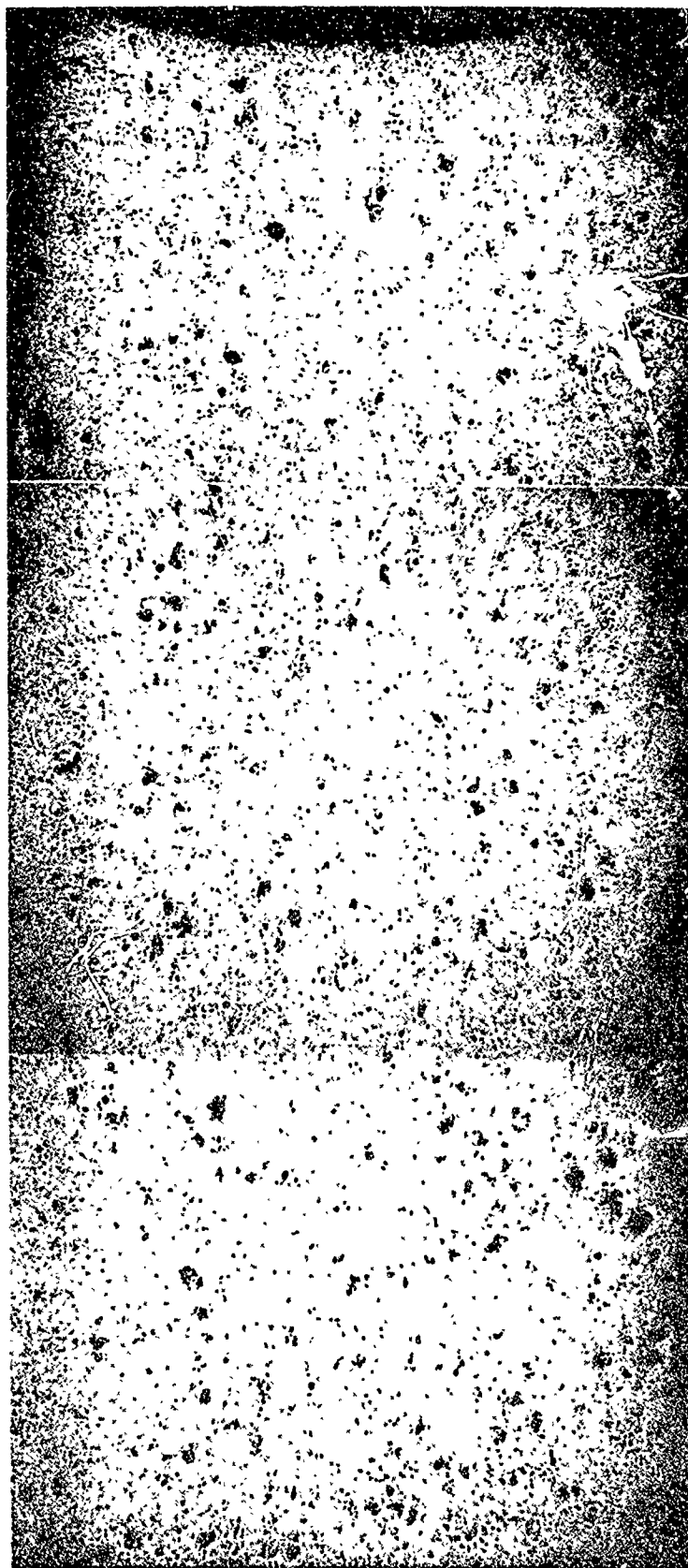


Figure 55. Flexural Specimen 3A09-085-2 Internal Longitudinal Profile, as Polished, 50X

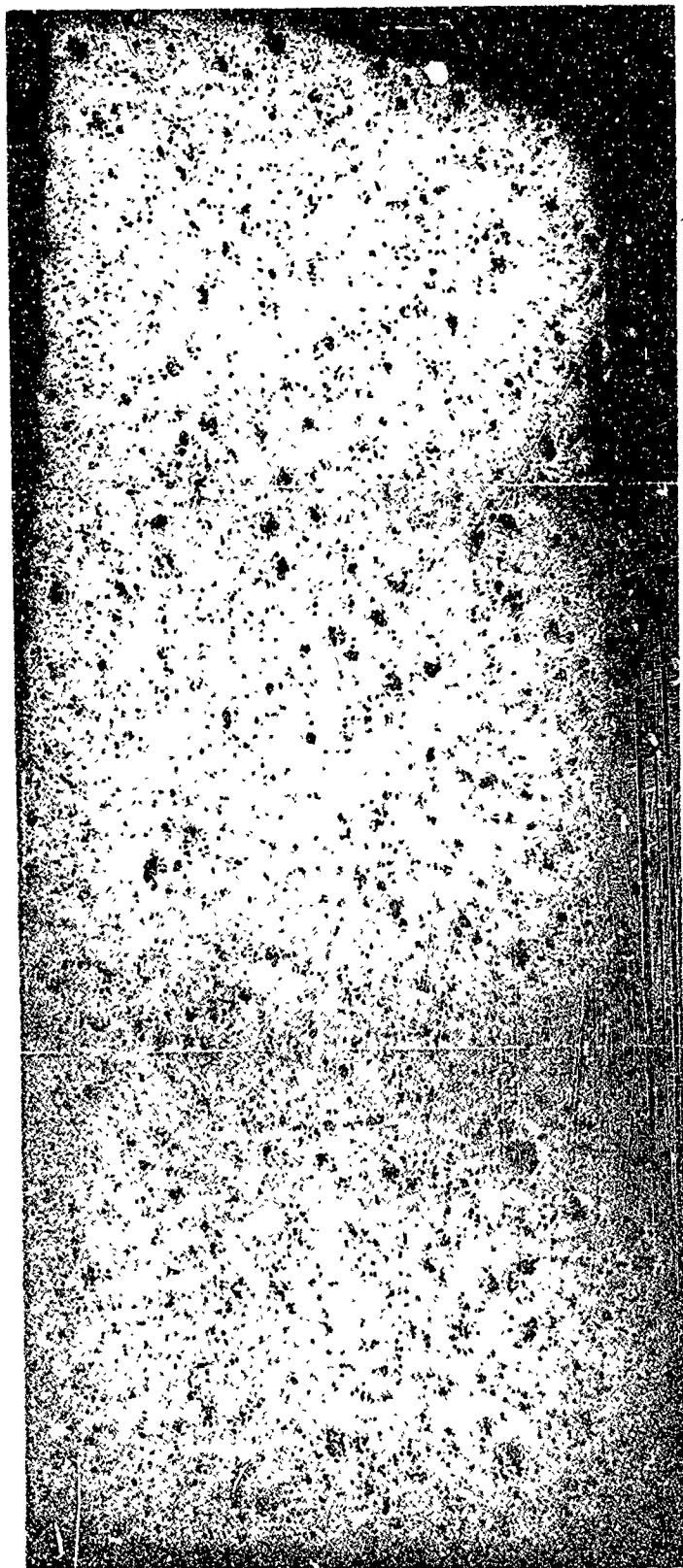


Figure 56. Flexural Specimen 6Al<sub>4</sub>-106-12 Internal Longitudinal Profile, as Polished, 50X

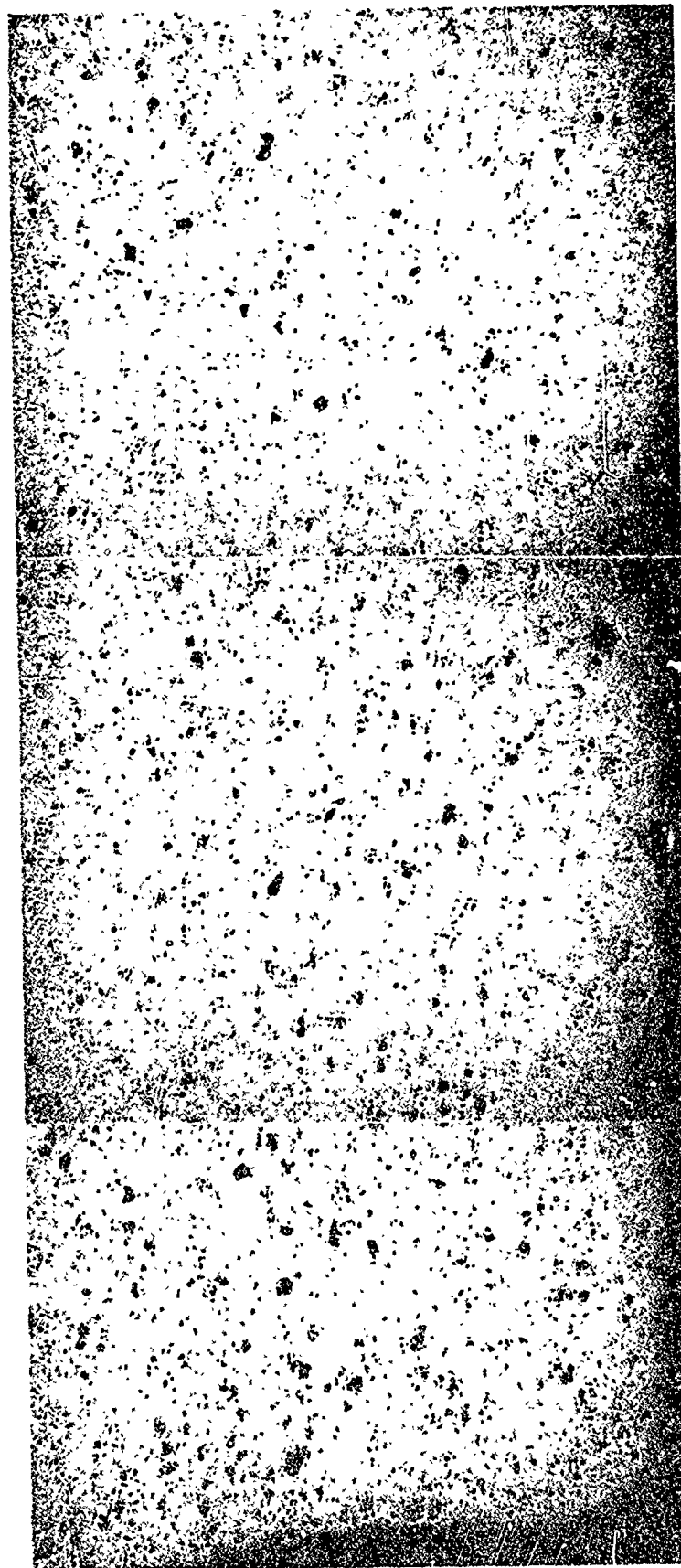


Figure 57. Flexural Specimen 6Al4-104-7 Internal Longitudinal Profile, as Polished, 50X

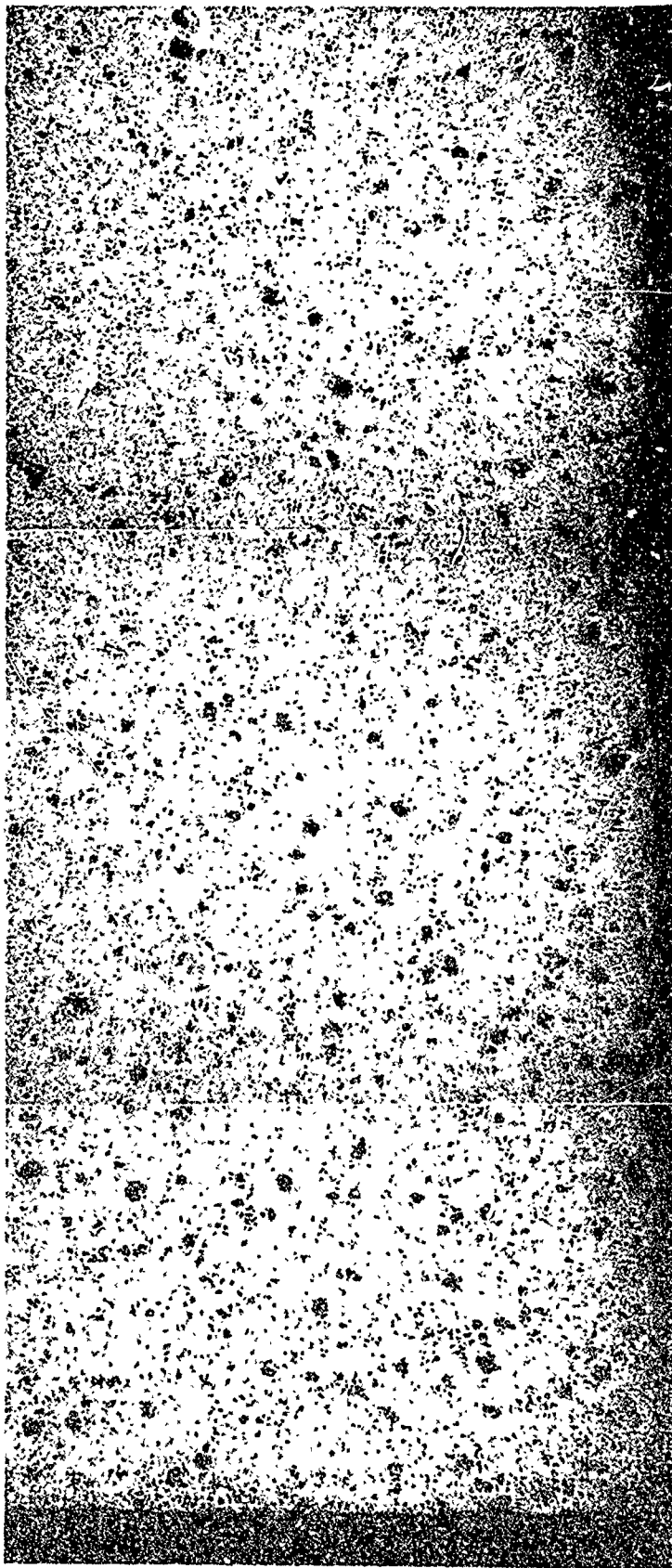


Figure 58. Flexural Specimen 5A13-102-6 Internal Longitudinal Profile, as Polished, 50X

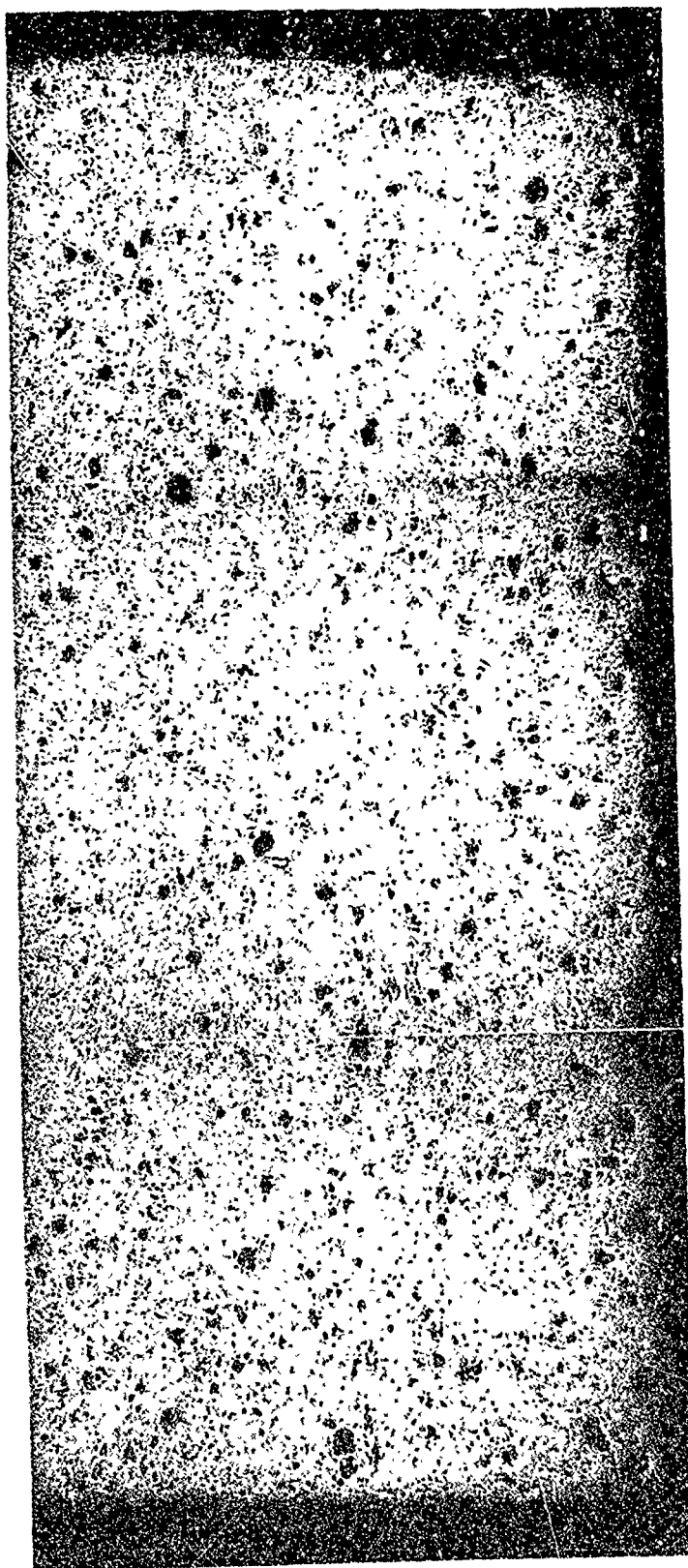


Figure 59. Flexura) Specimen 2A12-096-11 Internal Longitudinal Profile, as Polished, 50X

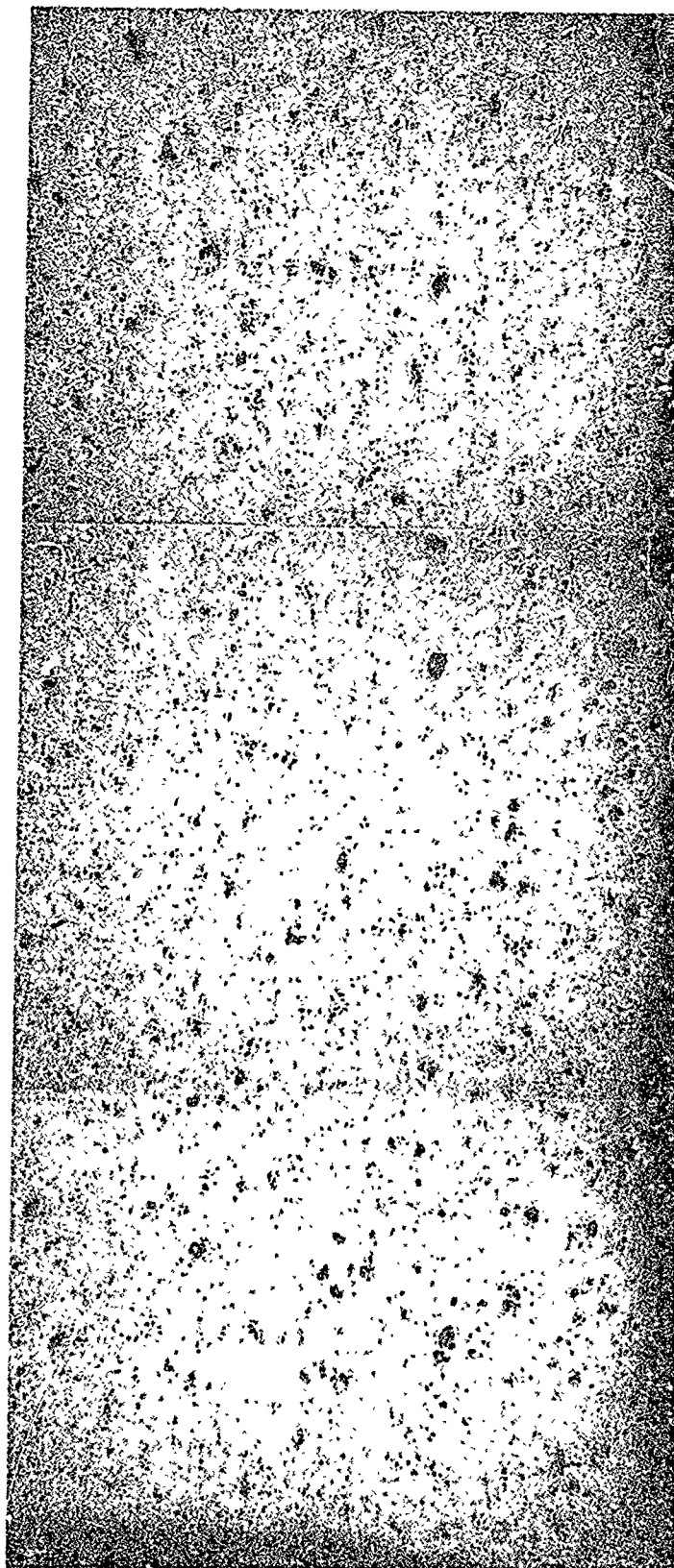


Figure 60. Flexural Specimen 3A09-085-1 Internal Longitudinal Profile, as Polished, 50X



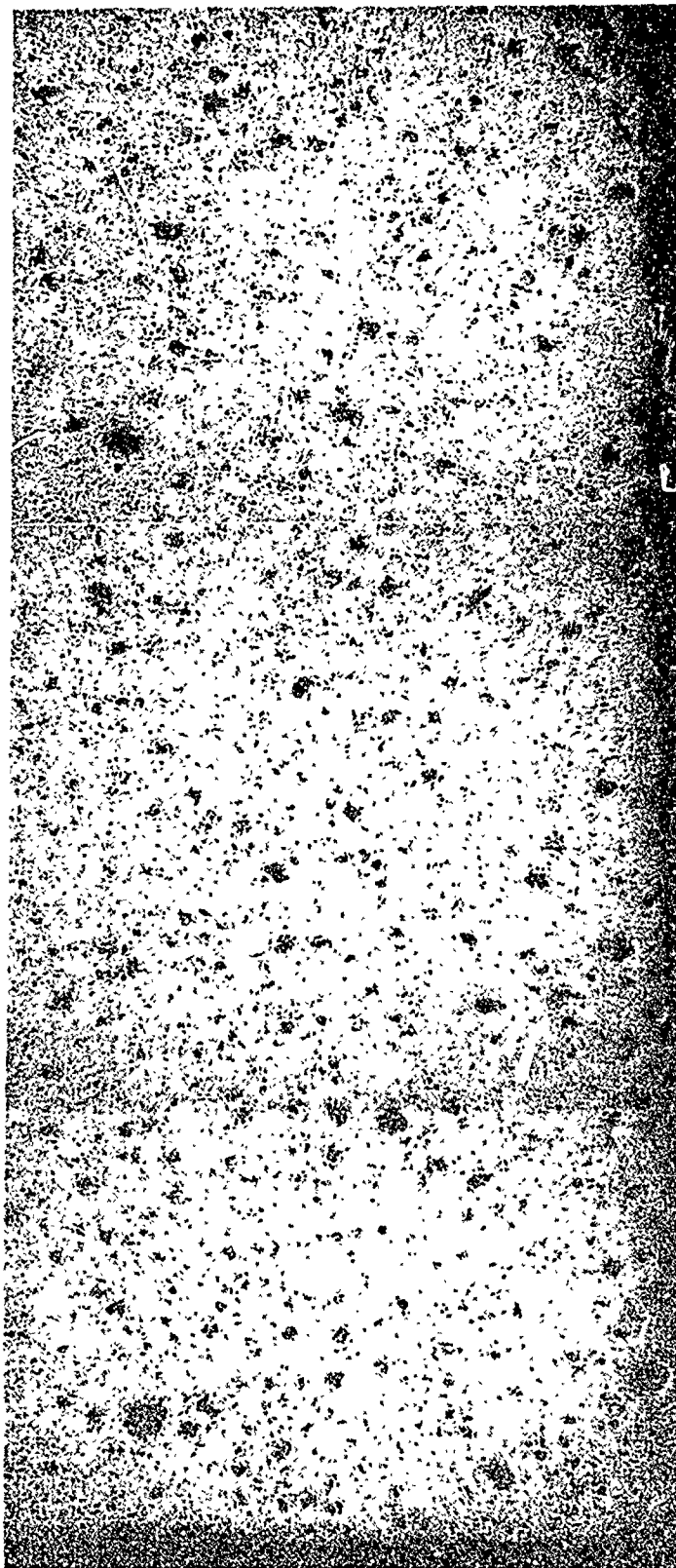


Figure 61. Flexural Specimen 4All-089-1 Internal Longitudinal Profile, as Polished, 50X



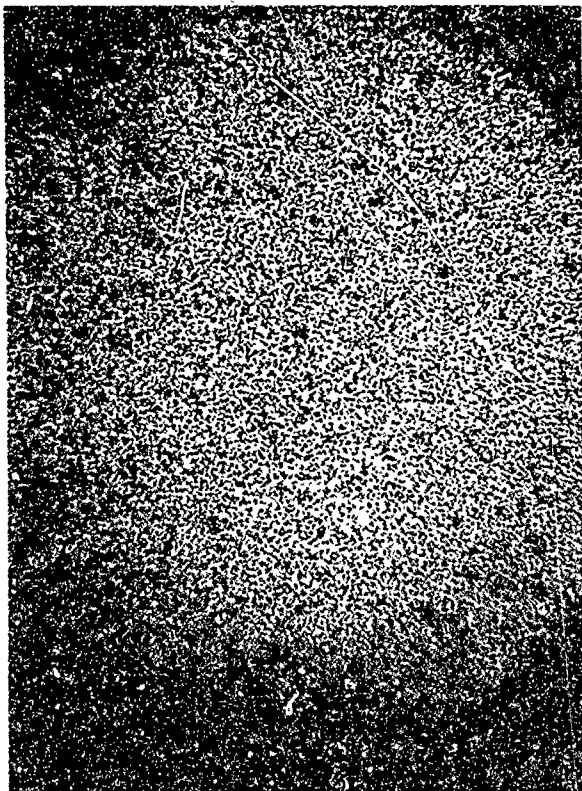


Figure 62a

Tensile Specimen 5A13-101-4T  
Transverse Section at Fracture,  
as Polished, 50X

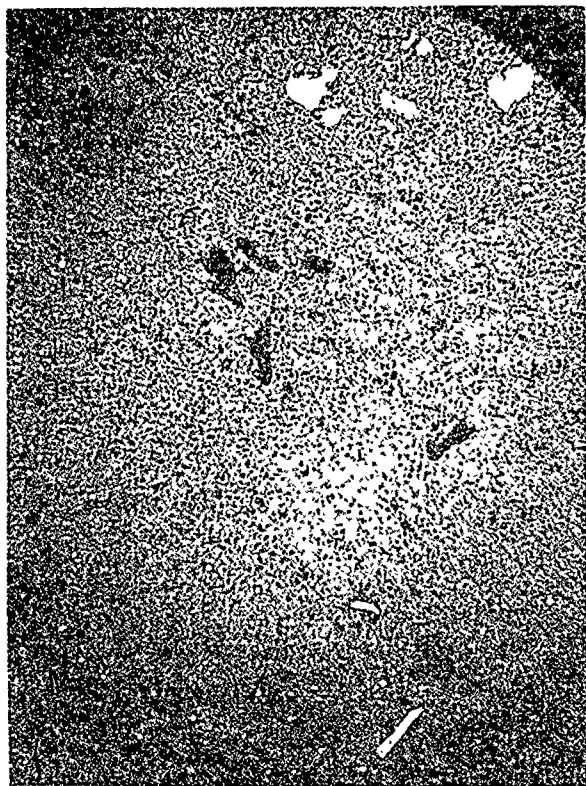


Figure 62b

Tensile Specimen 2A12-095-3T  
Transverse Section at Fracture,  
as Polished, 50X

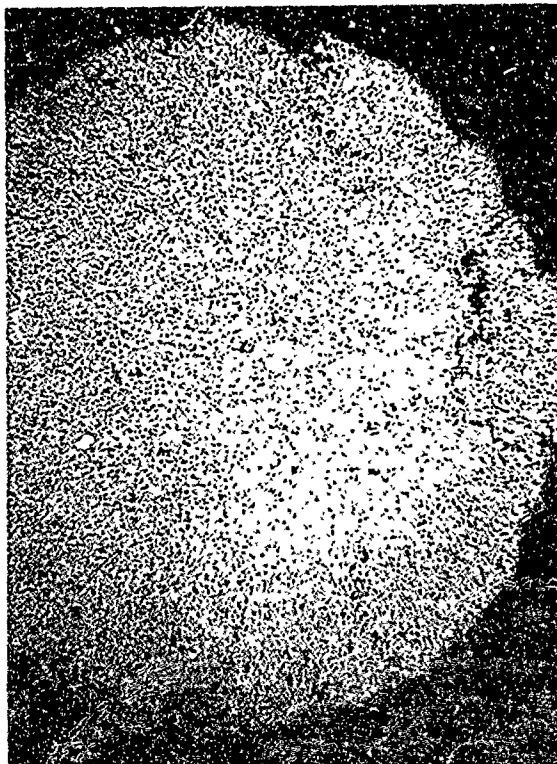


Figure 63a

Tensile Specimen 2A05-047-2T  
Transverse Section at Fracture,  
as Polished, 50X

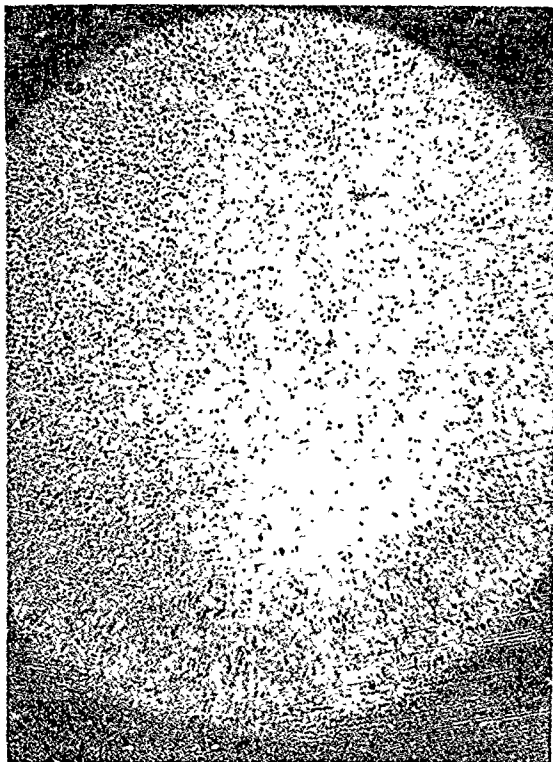


Figure 63b

Tensile Specimen 2A05-047-1T  
Transverse Section at Fracture,  
as Polished, 50X

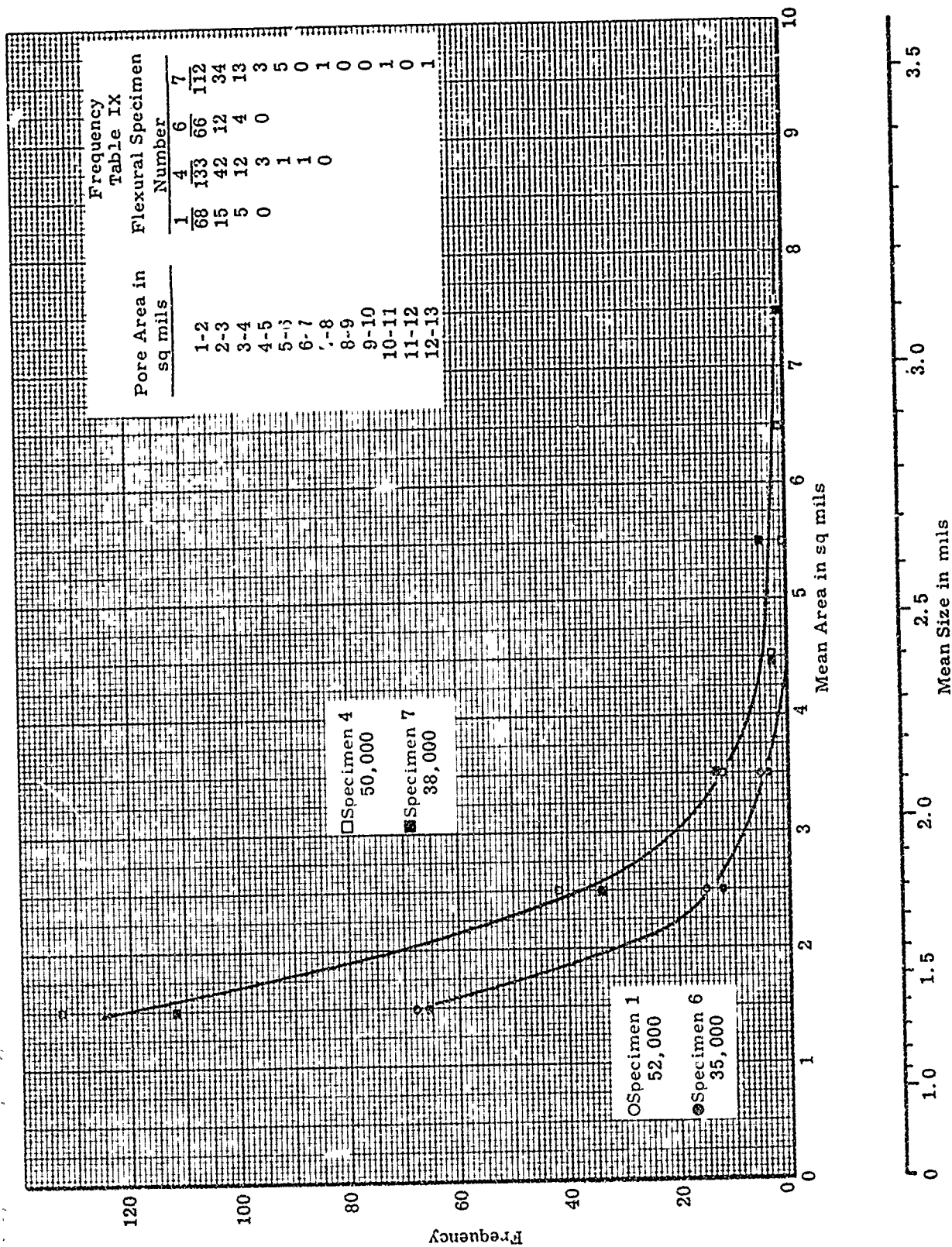


Figure 64. Pore Size Distribution for Specific Flexural Macro Specimens of Table IX



Figure 65a

Flexural Specimen 6Al4-106-12  
Internal Longitudinal Profile,  
 $\text{H}_3\text{PO}_4$  Etch at  $150^\circ\text{C}$ , Position 2,  
800X

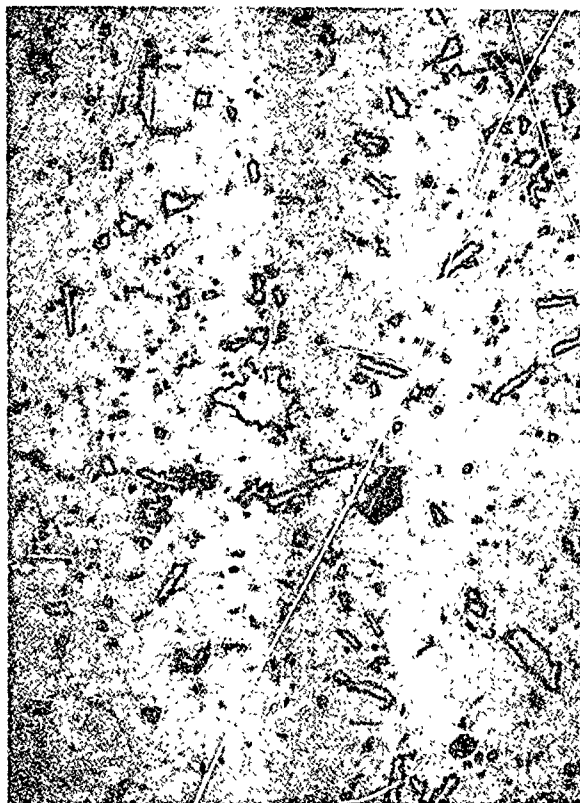


Figure 65b

Flexural Specimen 6Al4-104-7  
Internal Longitudinal Profile,  
 $\text{H}_3\text{PO}_4$  Etch at  $150^\circ\text{C}$ , Position 2,  
800X

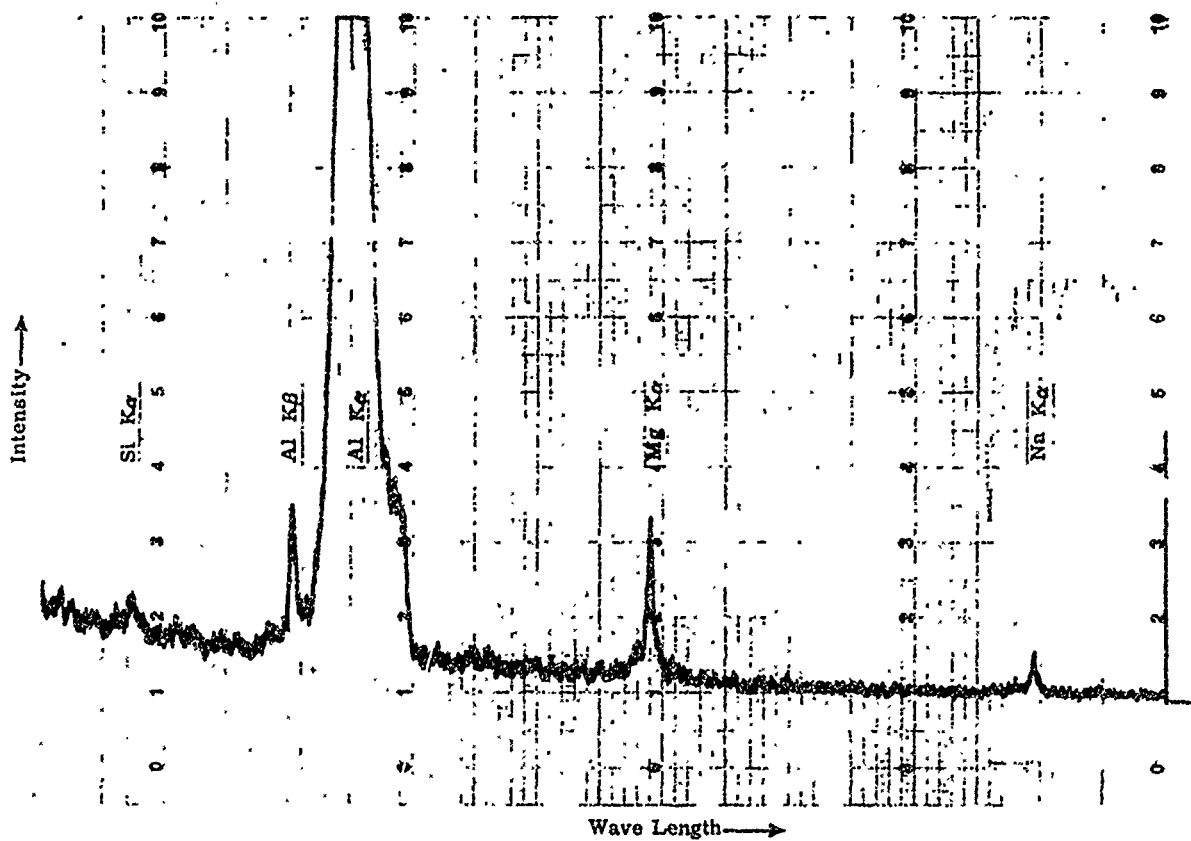


Figure 66. Microprobe Stationary Beam Spectral Scan Beam Focused on "Second Phase", Relief Polished

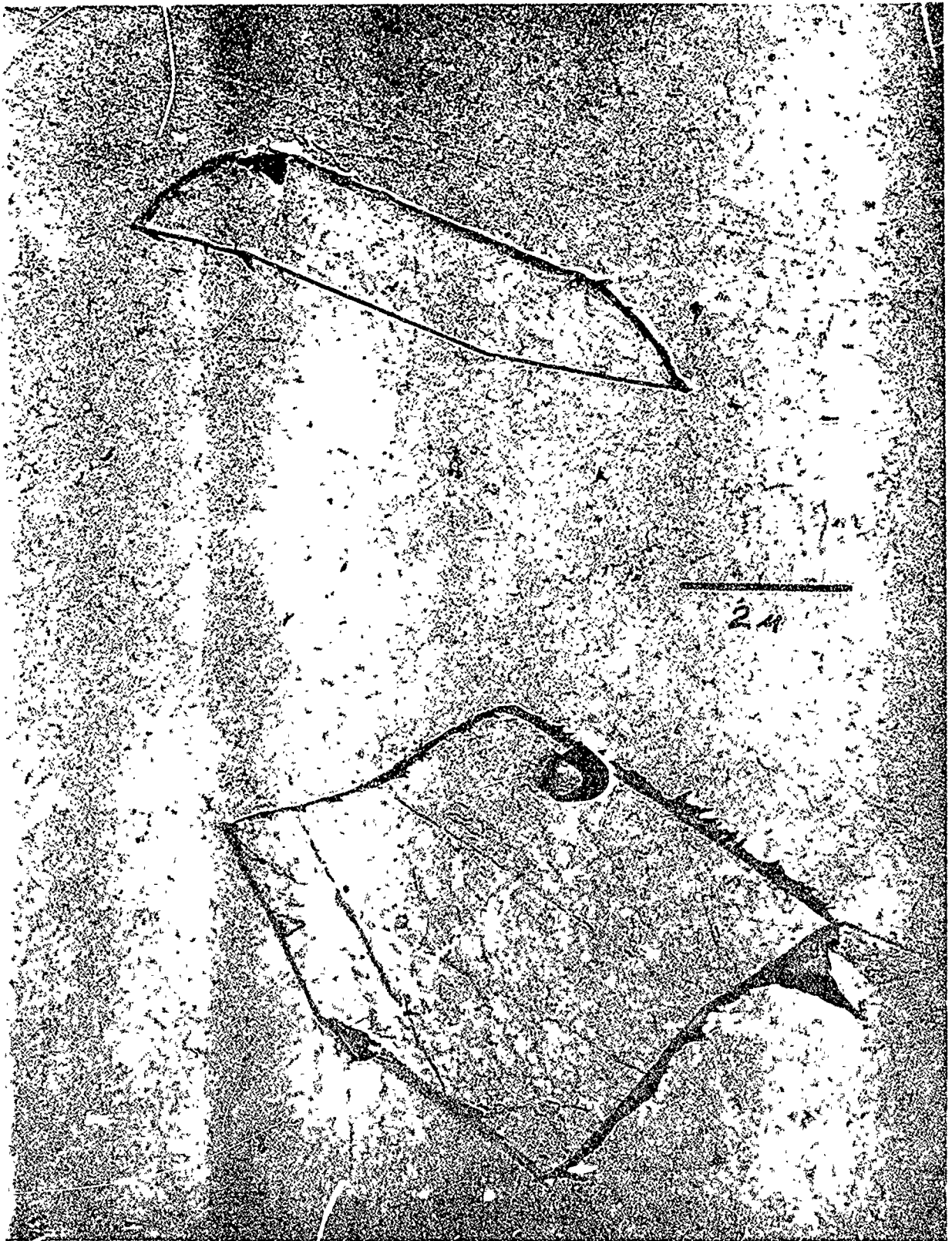


Figure 67. Tensile Specimen 2A05-047-2T Two Stage Replication, Specimen Polished and Etched at 150°C with  $H_3PO_4$ .



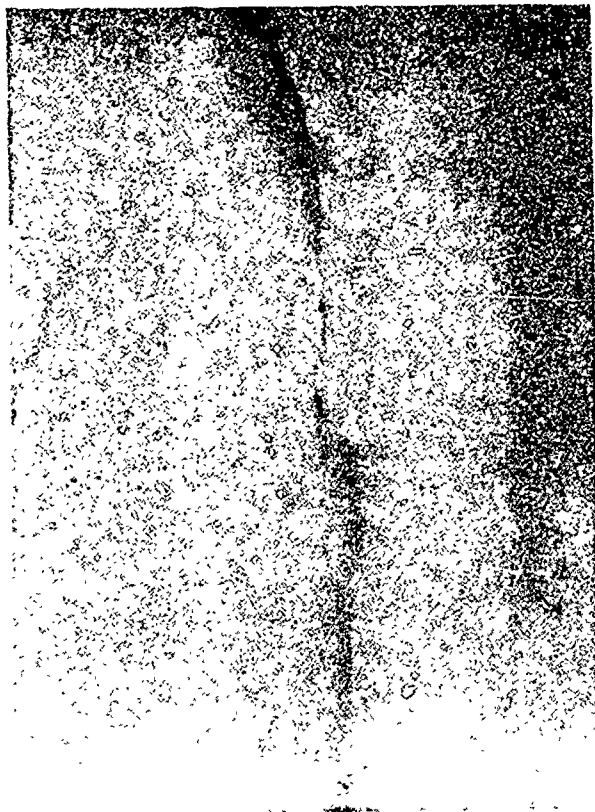


Figure 68a

Flexural Specimen 3A09-085-2,  
50X External Profile,  
Compression Region at Top

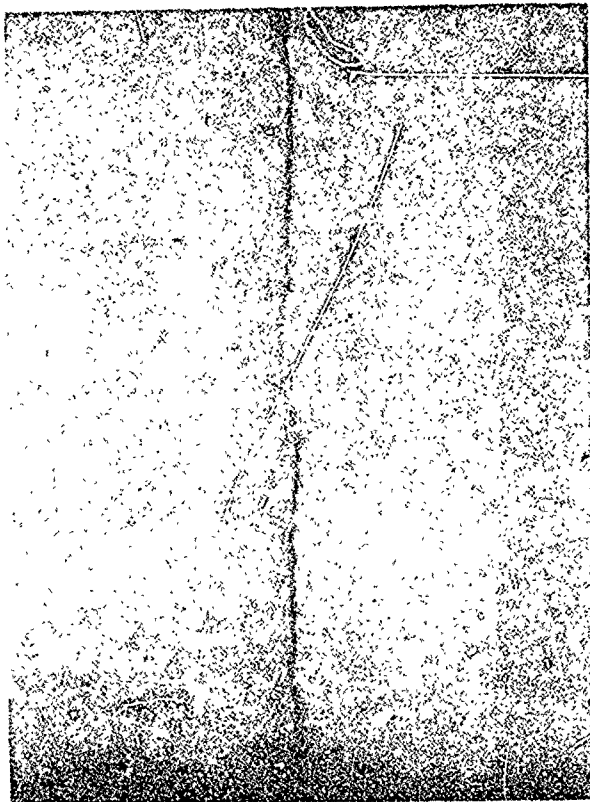


Figure 68b

Flexural Specimen 3A09-085-1,  
50X External Profile,  
Compression Region at Top

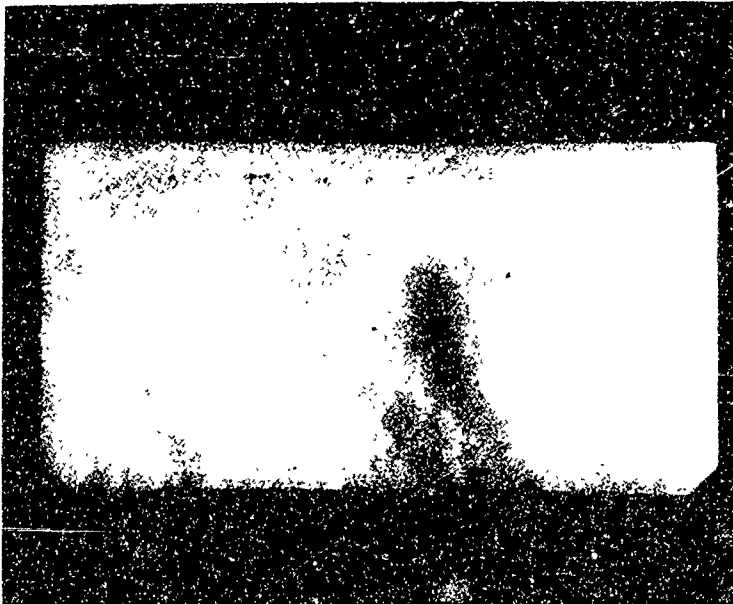


Figure 69a

Flexural Specimen 3A09-085-2,  
20X Fracture Face, Compres-  
sion Region at Top

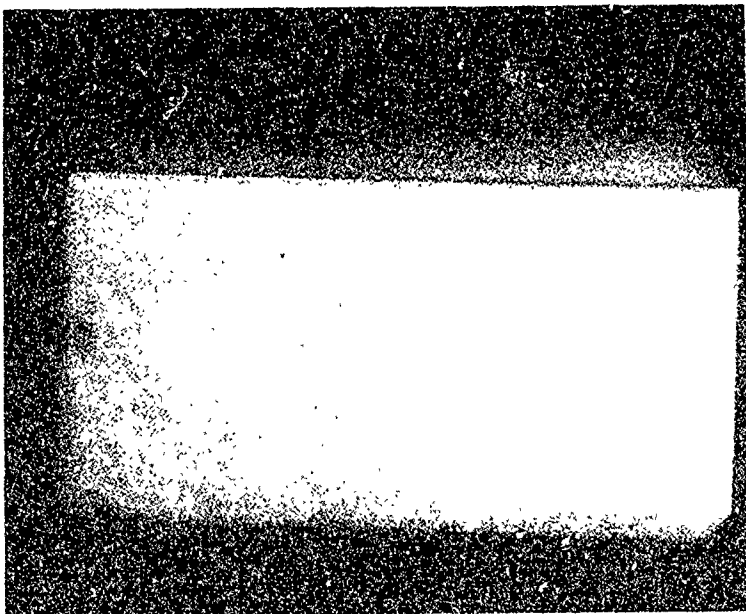


Figure 69b

Flexural Specimen 3A09-085-1,  
20X Fracture Face, Compres-  
sion Region at Top





Figure 70. Electron Fractograph of Flexural Specimen 5A13-102-6  
Tension Zone

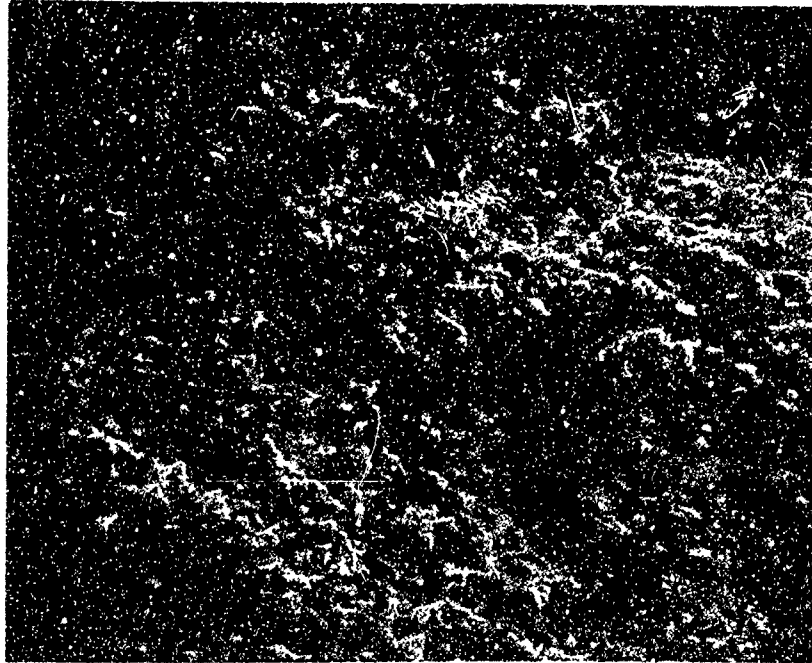


Figure 7la. SEM Photomicrograph of the Fracture Face  
of a Typical Flexure Specimen at 500X

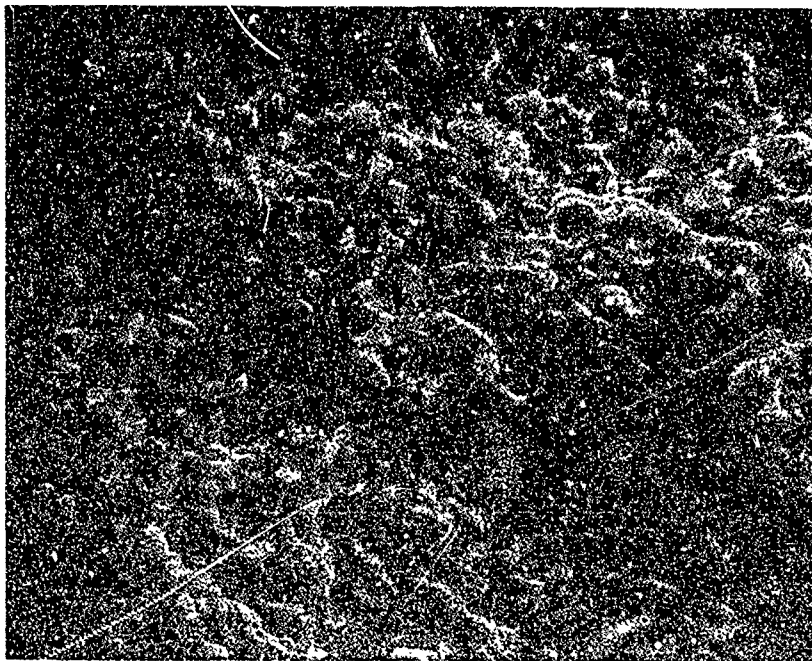


Figure 7lb. SEM Photomicrograph of the Fracture Face  
of a Typical Flexure Specimen at 1000X



Figure 72a. SEM Photomicrograph of the Fracture Face  
of a Typical Flexure Specimen at 10,000X



Figure 72b. SEM Photomicrograph of the Fracture Face  
of a Typical Flexure Specimen at 20,000X

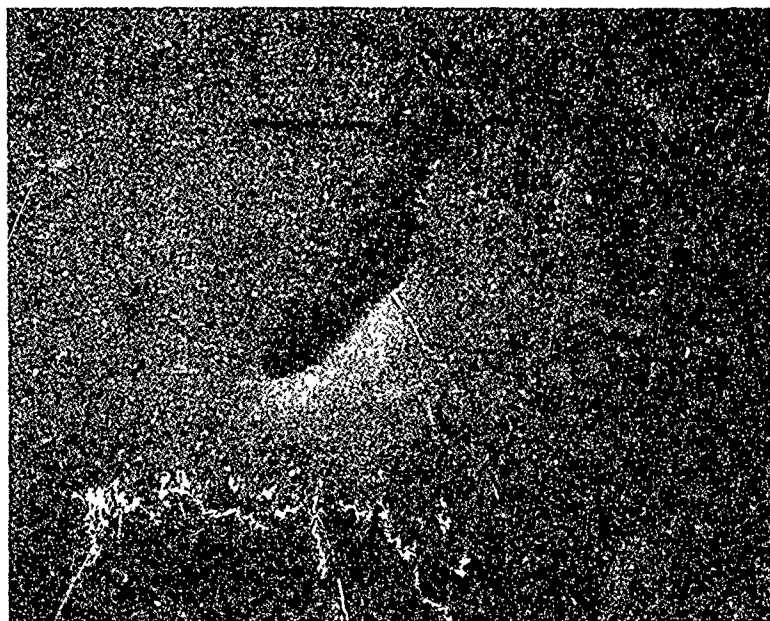
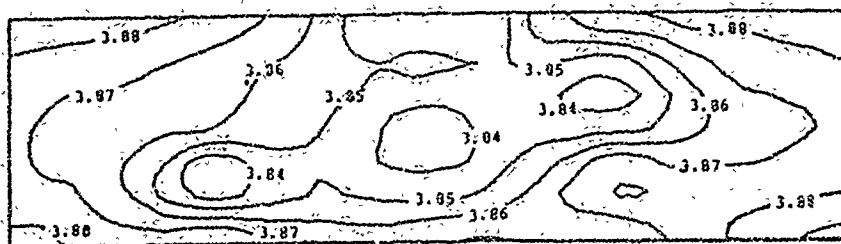


Figure 73. Flexural Specimen 2A05-043-3 External Profile, 50X,  
Dash Line - Neutral Axis

Contour Map  
Section A "Wet" Density



Contour Map  
Section A "Dry" Density

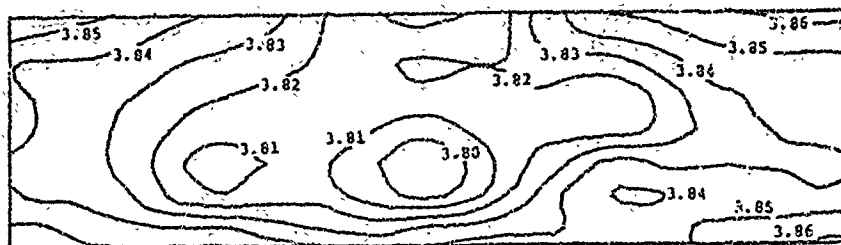
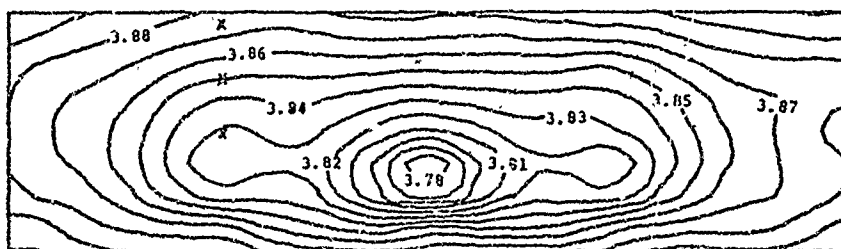


Figure 74a. Density, Blank 4A11-112 Section A

Contour Map  
Section C "Wet" Density



Contour Map  
Section C "Dry" Density

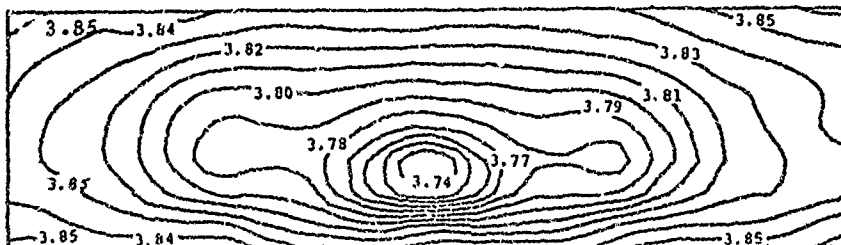


Figure 74b. Density, Blank 4A11-112 Section C

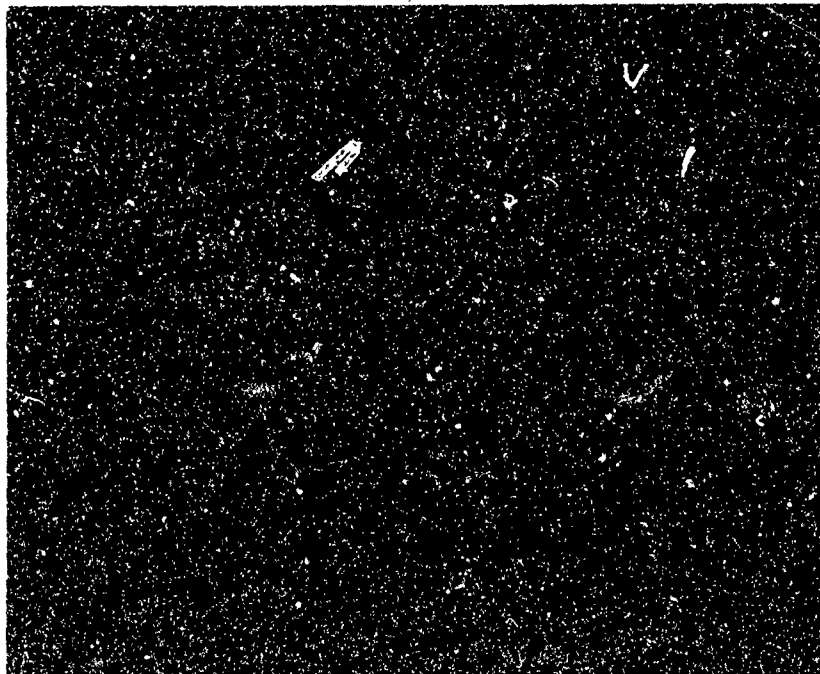


Figure 75. Tensile Face of Flexural Specimen 4A11-112-A11 Showing Disparate Void in Fracture, 50X Transmitted Light

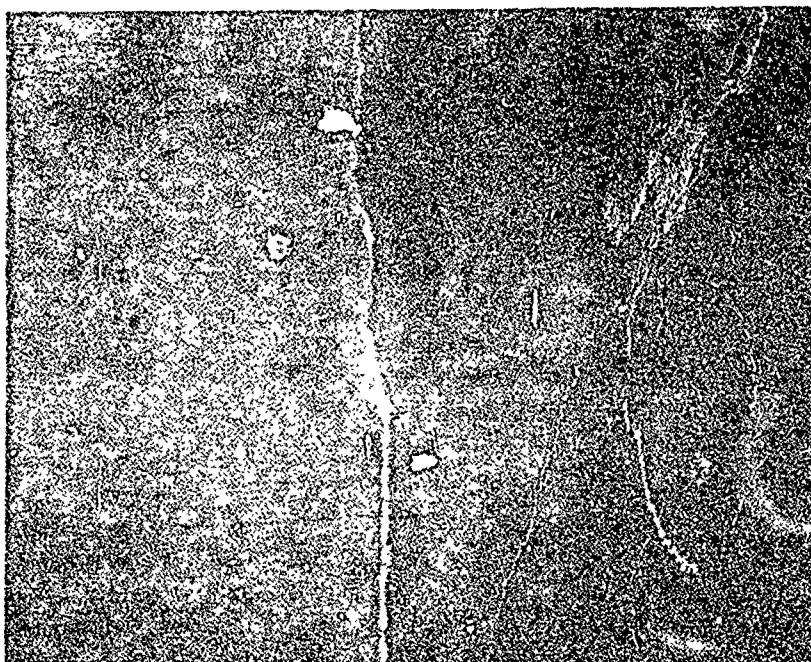


Figure 76. Tensile Face of Flexural Specimen 4A11-112-A51 Showing Disparate Void in Fracture, 50X Transmitted Light

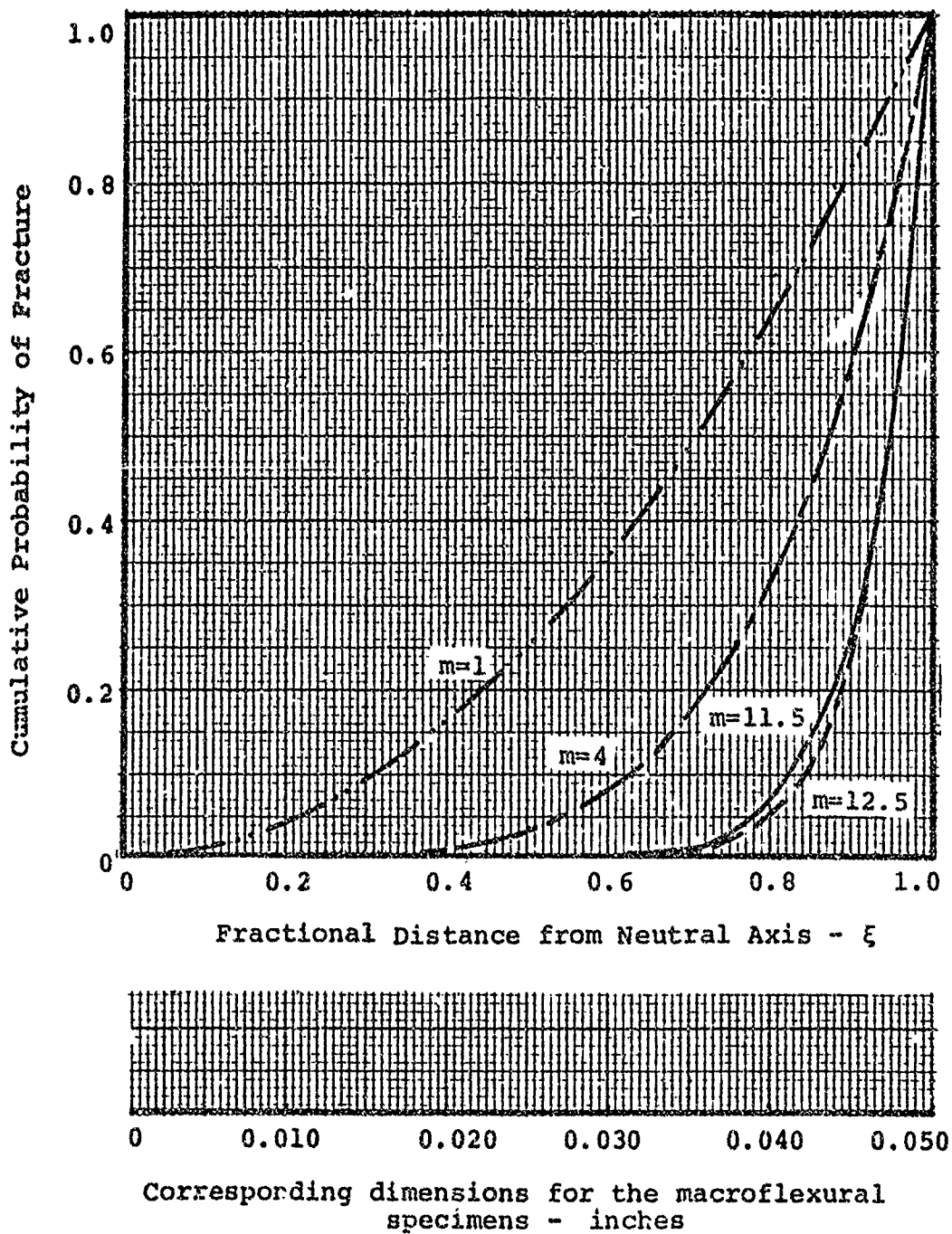


Figure 77. Fracture-Source Distribution in Pure Bending for a Rectangular Specimen



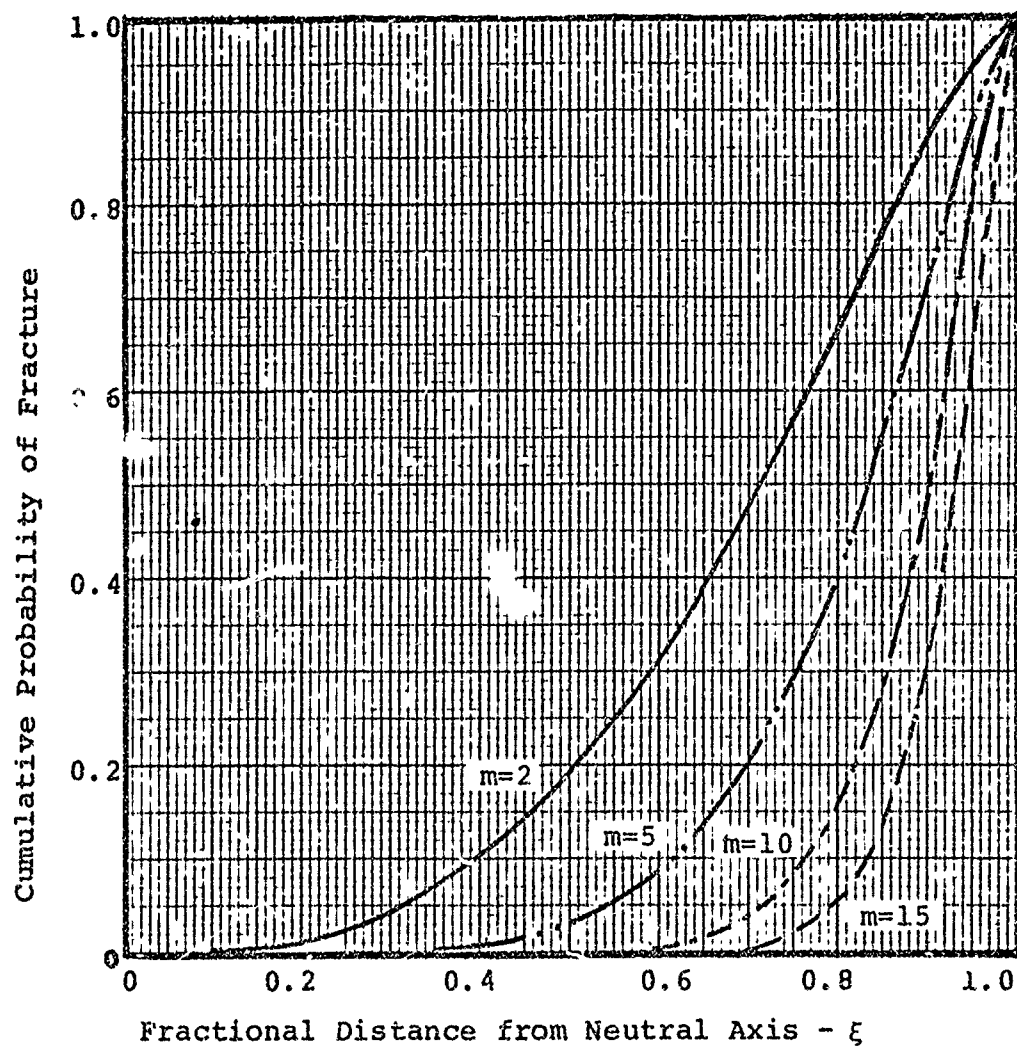


Figure 78. Fracture-Source Distribution in Pure Bending  
(Round Specimen)



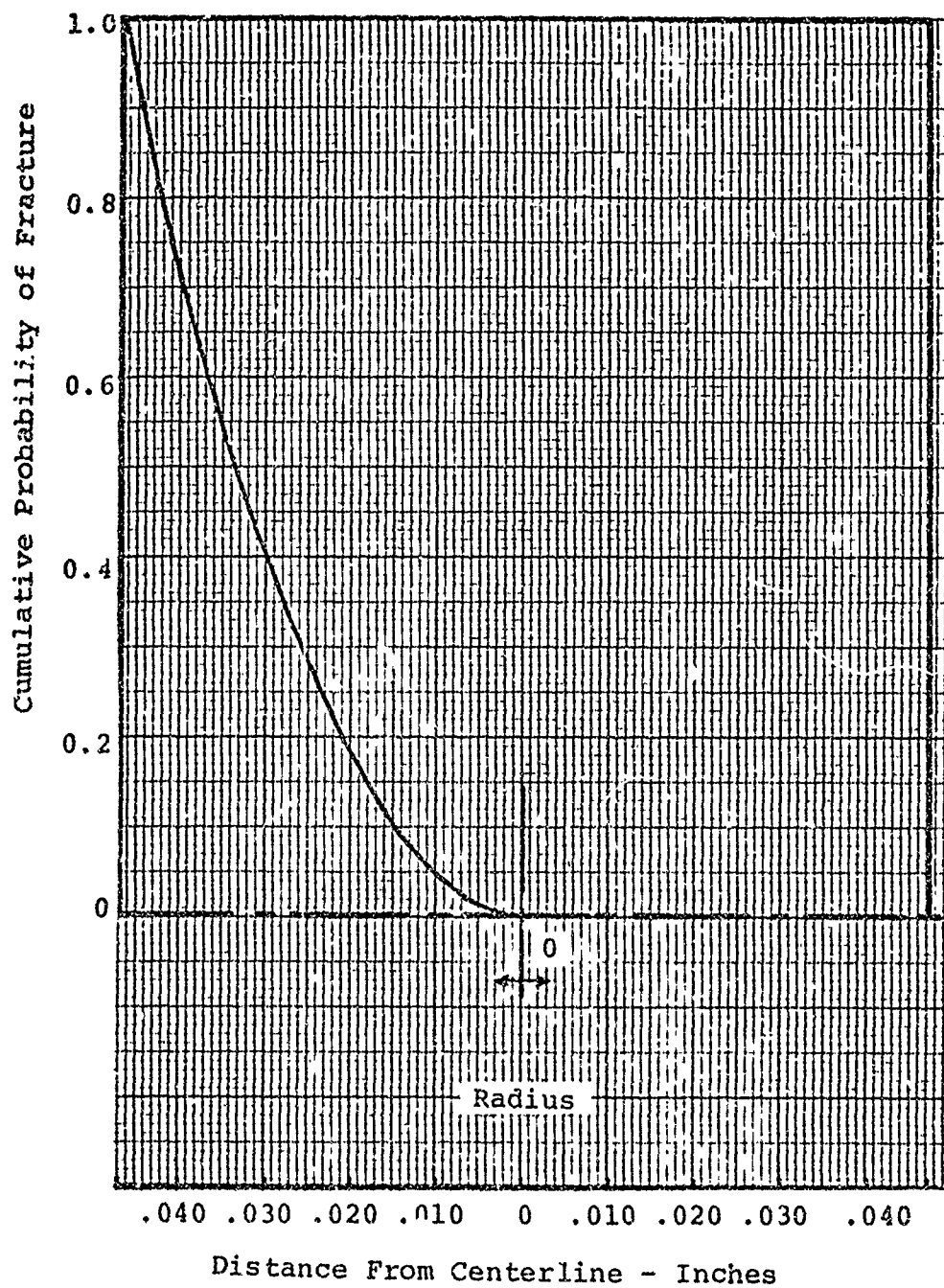


Figure 79. Fracture-Source Distribution in Pure Tension for a Round Tensile Specimen

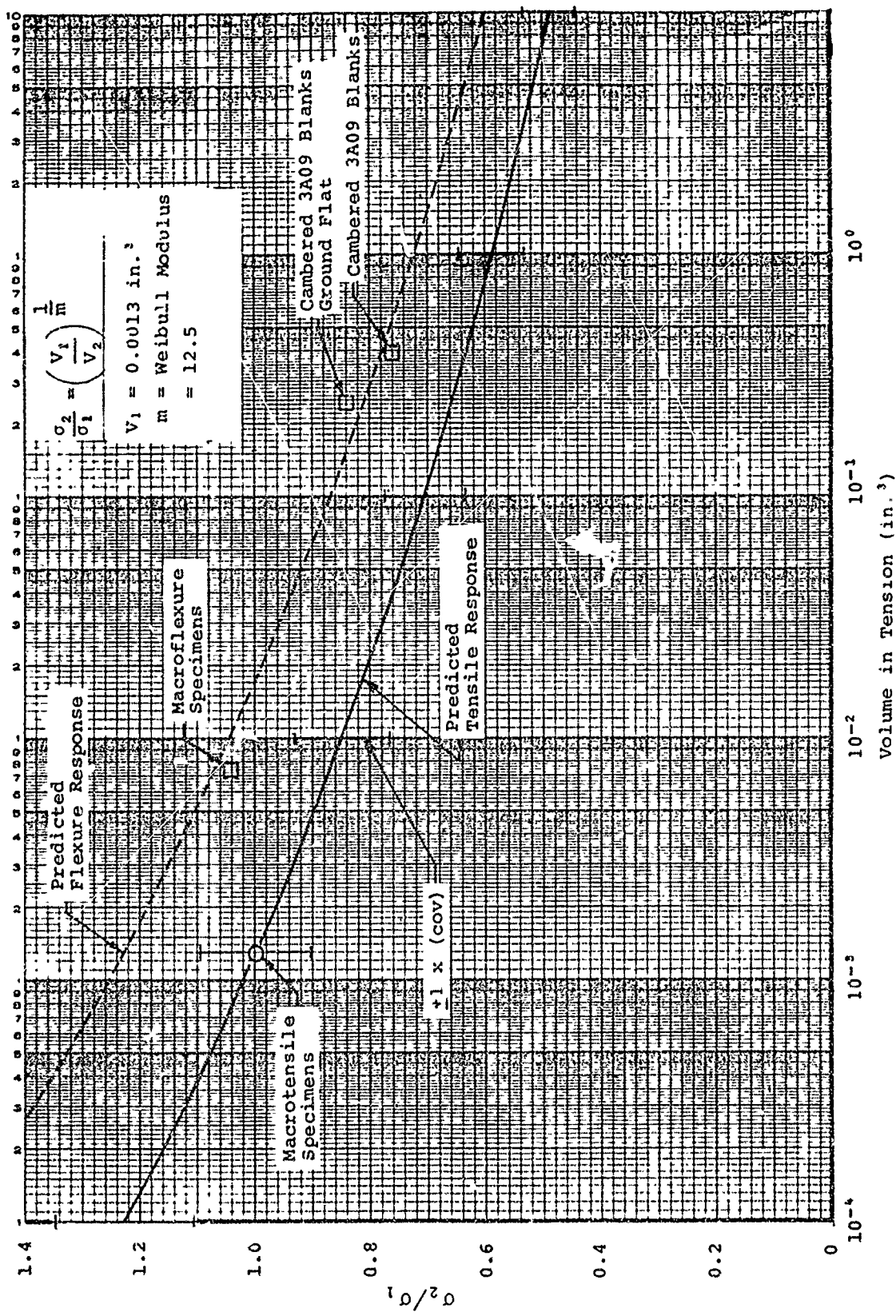


Figure 80. Strength Ratio versus Volume in Tension Weibull Predictions

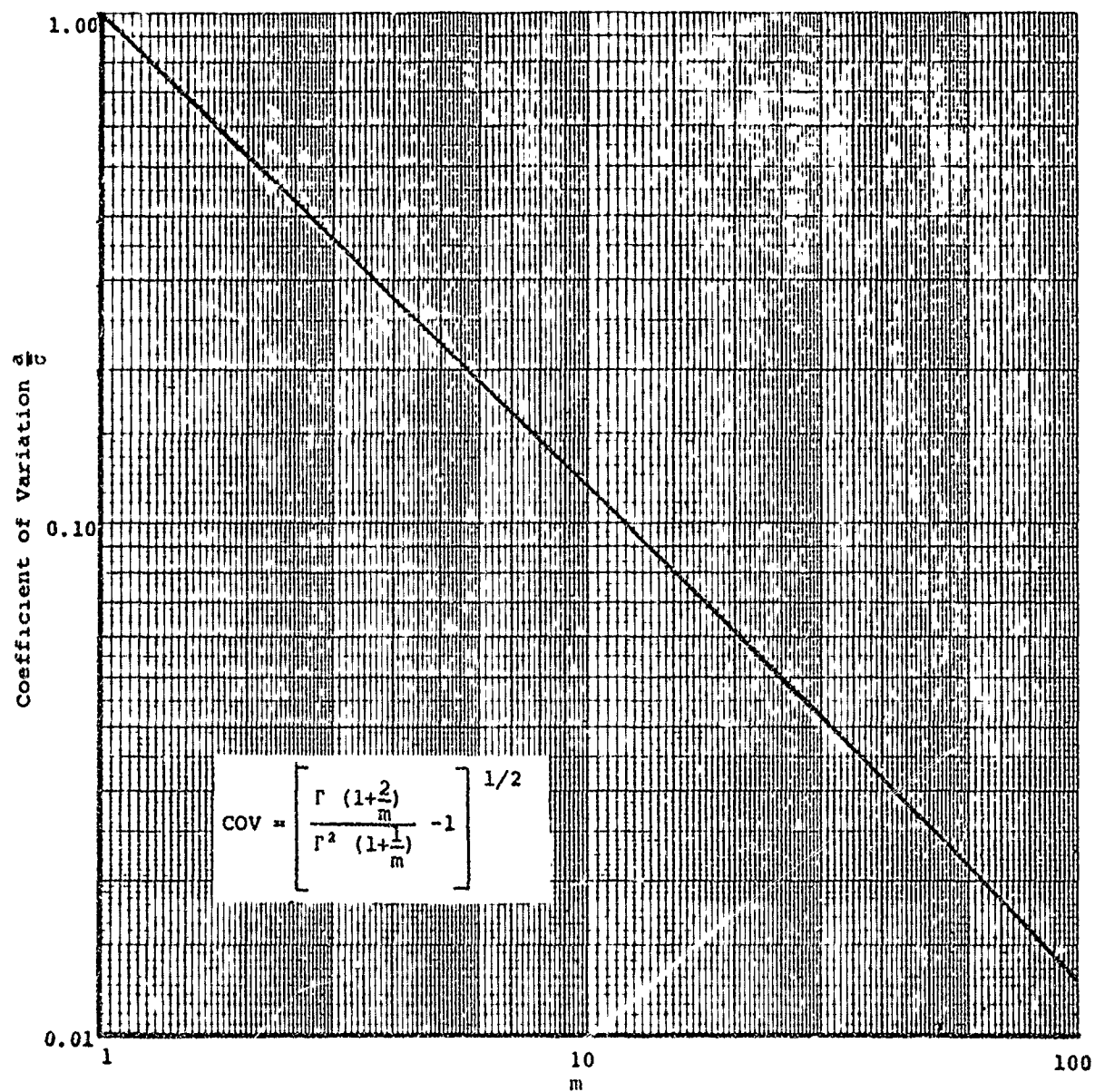


Figure 81. Coefficient of Variation versus Weibull Modulus  $m$  for the Weibull Distribution

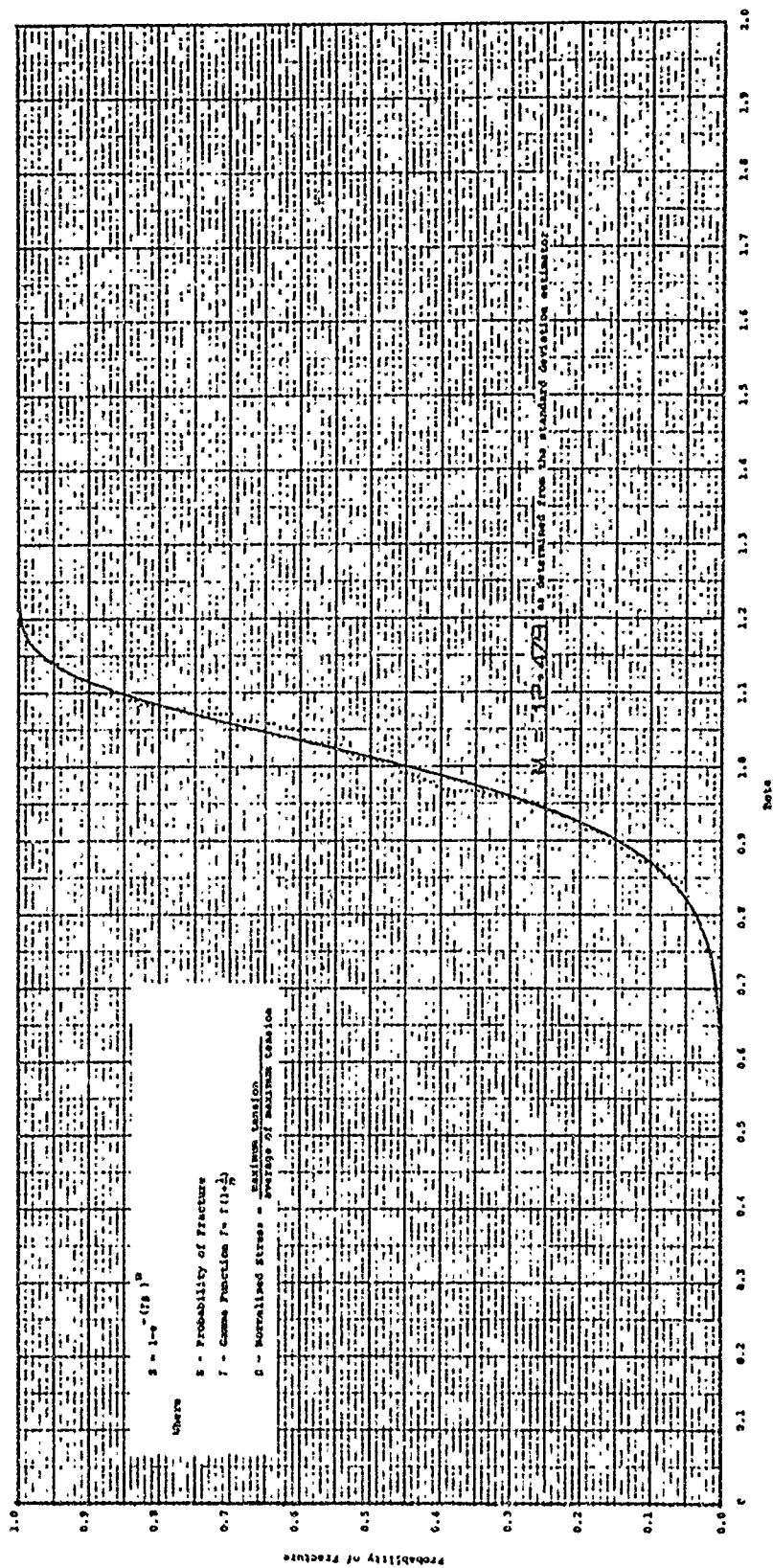


Figure 82. Probability of Fracture versus Normalized Stress  $\beta$  for the Macrotenstile Specimens

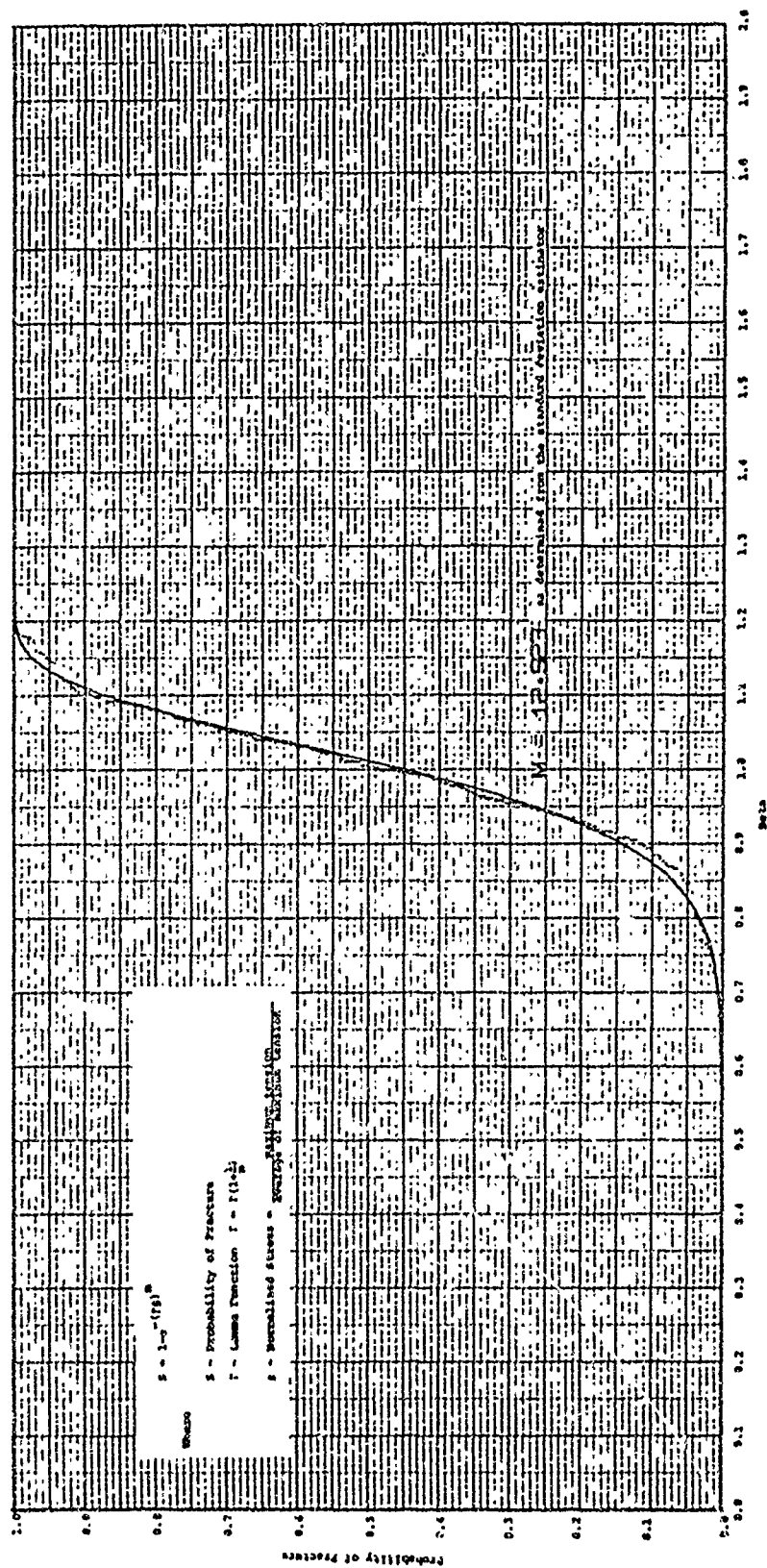


Figure 83. Probability of Fracture versus Normalized Stress  $\beta$  for the Macroflexural Specimens

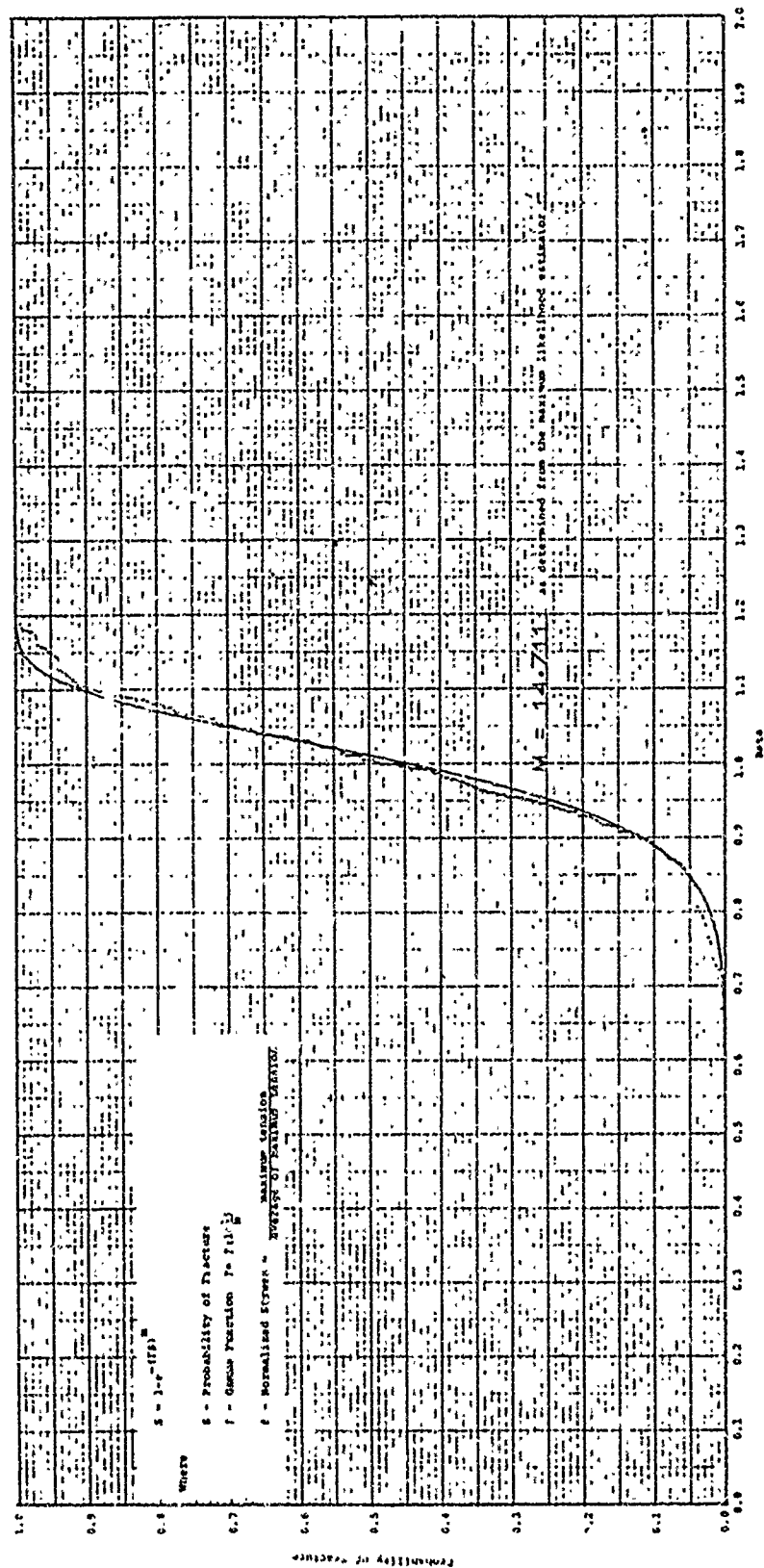


Figure 84. Probability of Fracture versus Normalized Stress  $\beta$  for the Macroflexural Specimens

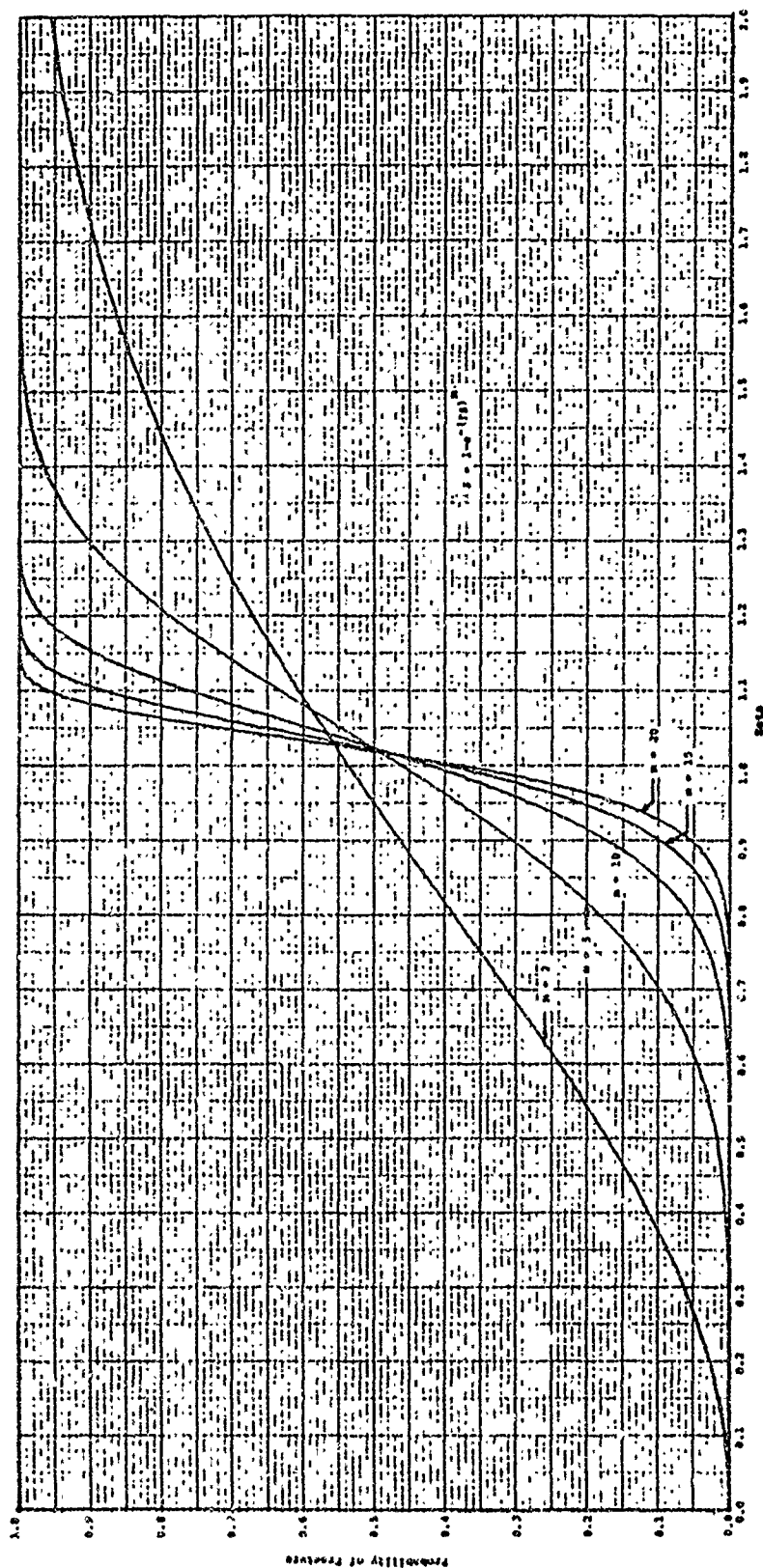


Figure 85. Family of Weibull Distribution



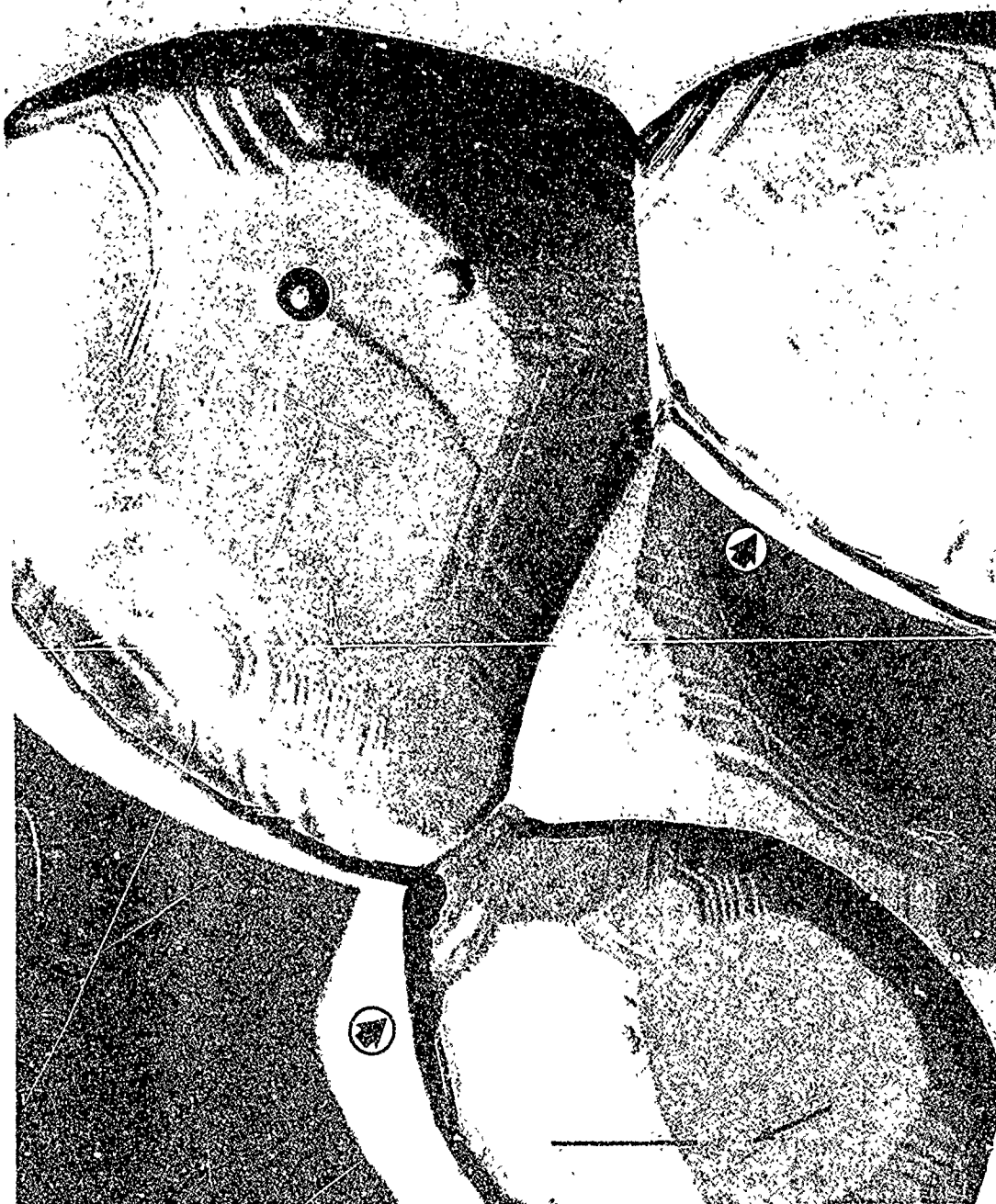


Figure 86. Electron Photomicrograph - Illustration of Black Line Artifact. Fiducial Bar Equals 0.5 micron



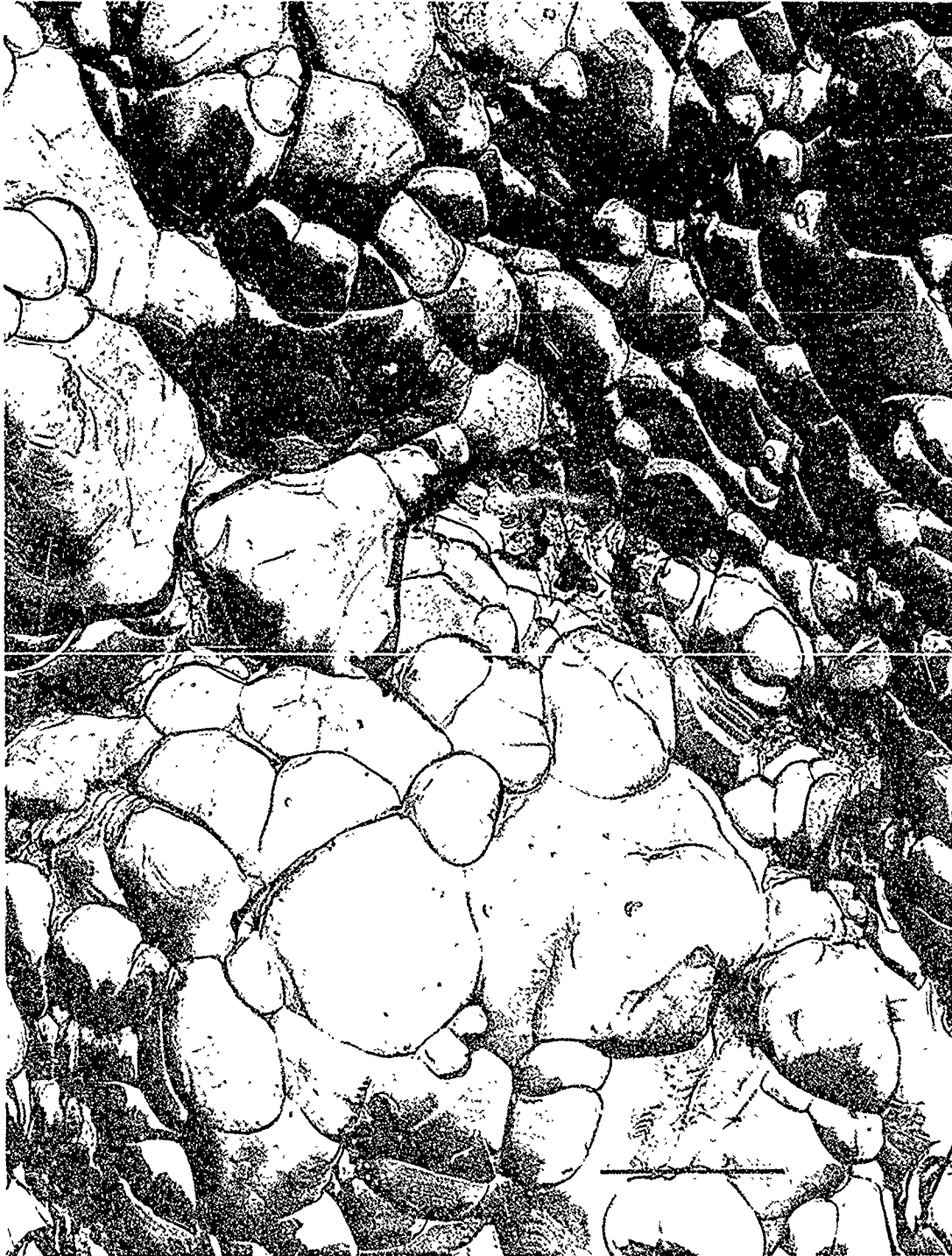


Figure 87. Electron Photomicrograph - As-Received Surface, Pressed and Fired. Fiducial Bar Equals 5.0 microns



Figure 88. Electron Photomicrograph - As-Received Surface, Pressed, Green Machined, and Fired. Fiducial Bar Equals 5.0 microns



Figure 89. Electron Photomicrograph - Surface Created by Cutting with a 100-Grit Diamond Wheel. Fiducial Bar Equals 5.0 microns



Figure 90. Electron Photomicrograph - 15-rms Surface Created by Standard Shop Surface Grinding. Fiducial Bar Equals 5.0 microns

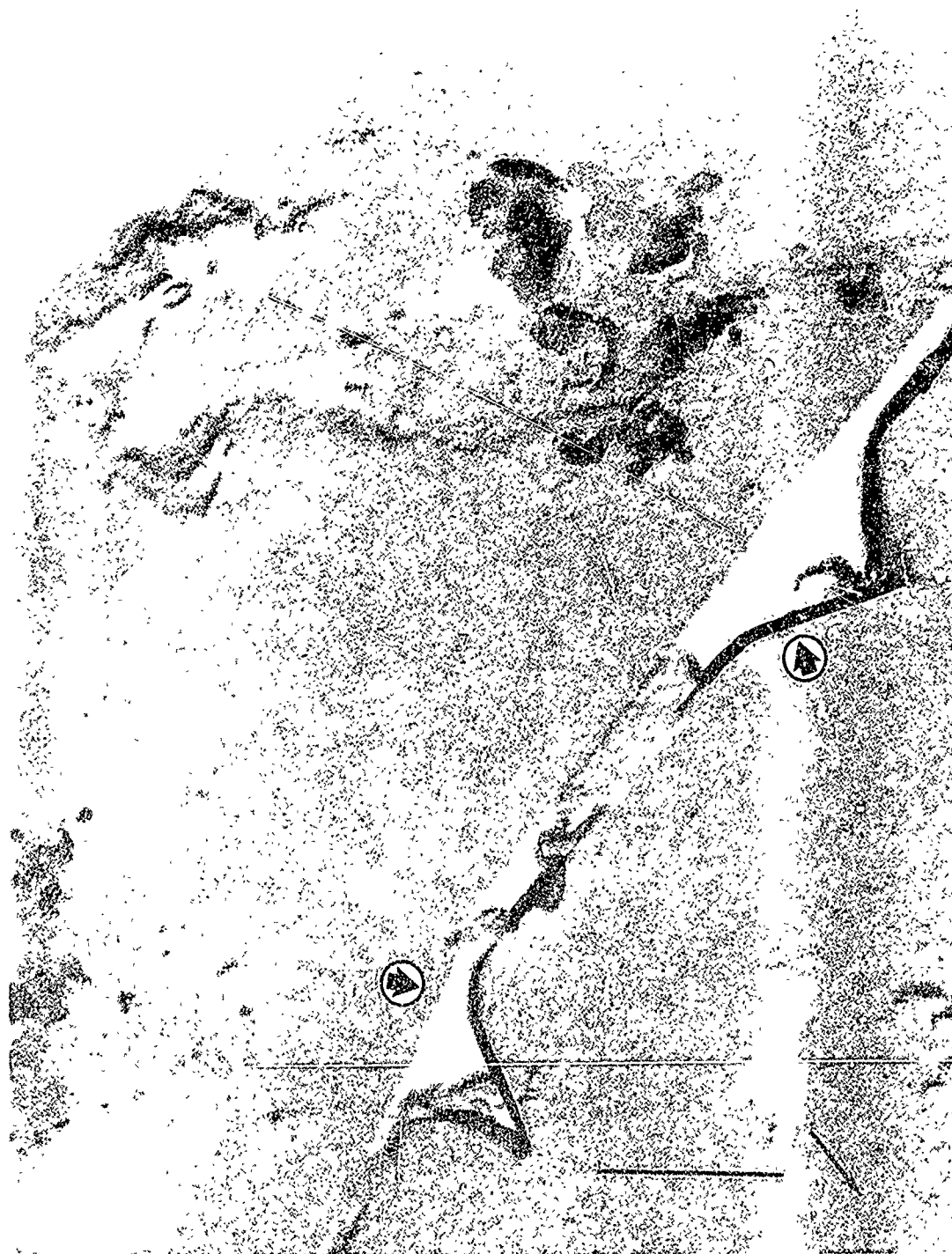


Figure 91. Electron Photomicrograph - 15-rms Surface Created by Standard Shop Surface Grinding - Illustration of Surface Crack. Fiducial Bar Equals 0.5 micron





Figure 92    Electron Photomicrograph - 5-rms Surface Developed  
Using Abernathy Lap.    Fiducial Bar Equals 5.0 microns



Figure 93. Electron Photomicrograph -  $<1$ -rms Surface Developed Using Metallurgical Laboratory Lapping Techniques. Fiducial Bar Equals 5.0 microns

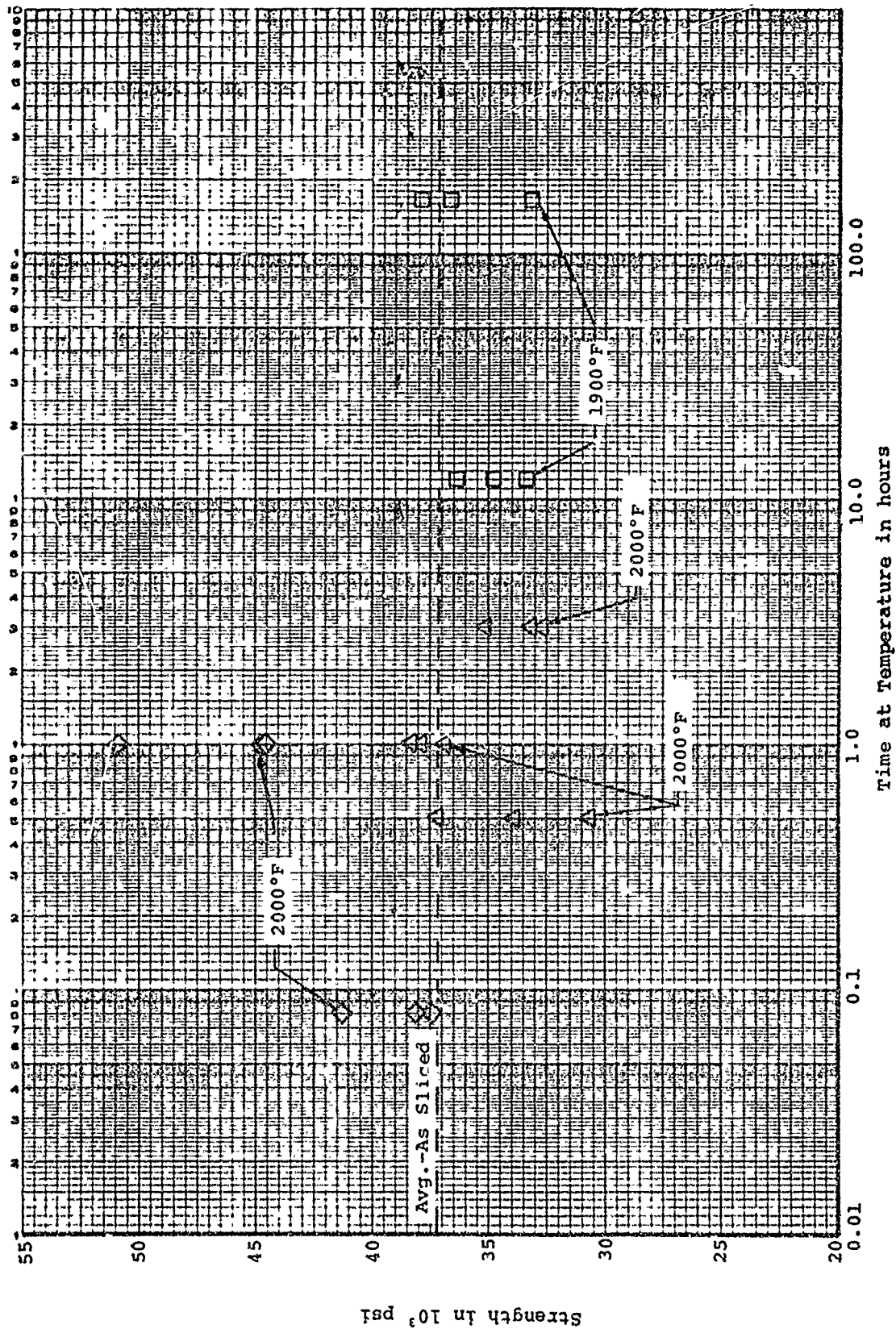


Figure 94. Effects of Thermal Treatment on Strength of Sliced Macroflexure Specimens



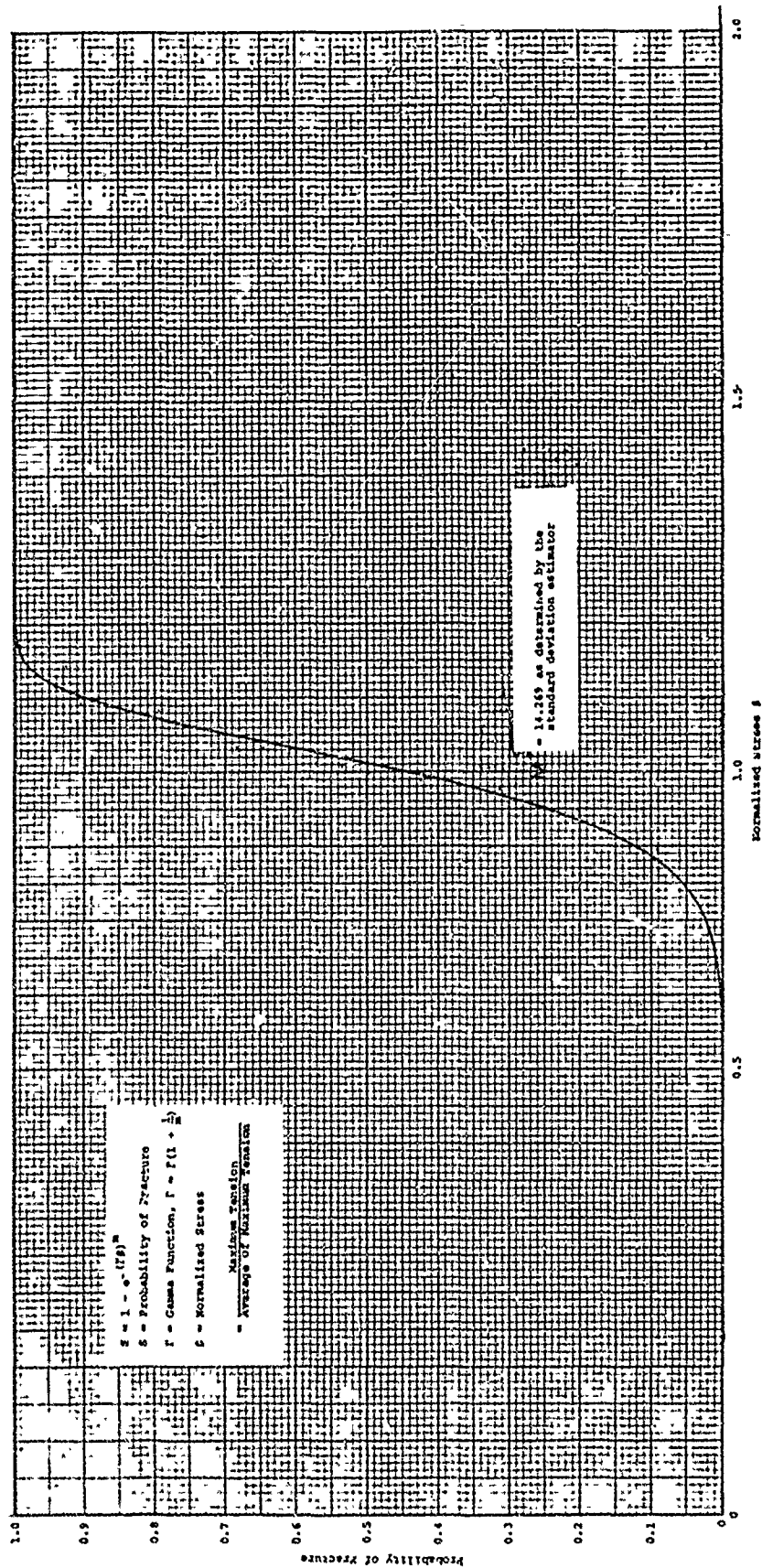


Figure 95. Probability of Fracture versus Normalized Stress  $S$  for the Macroflexure Specimens Machined by Southern Research Institute

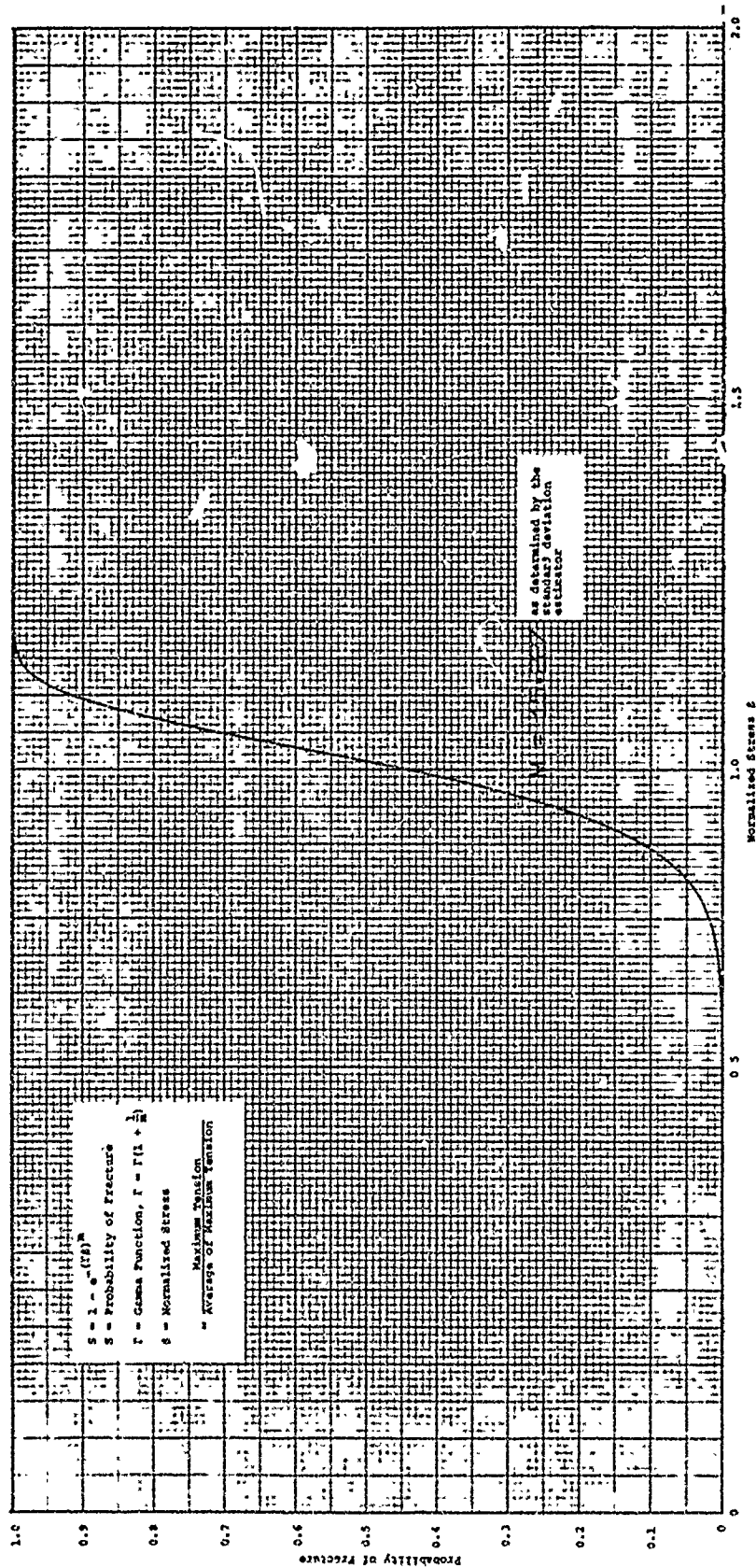


Figure 96. Probability of Fracture versus Normalized Stress  $\delta$  for the Macroflaxure 3, which was machined by Coors Porcelain Company

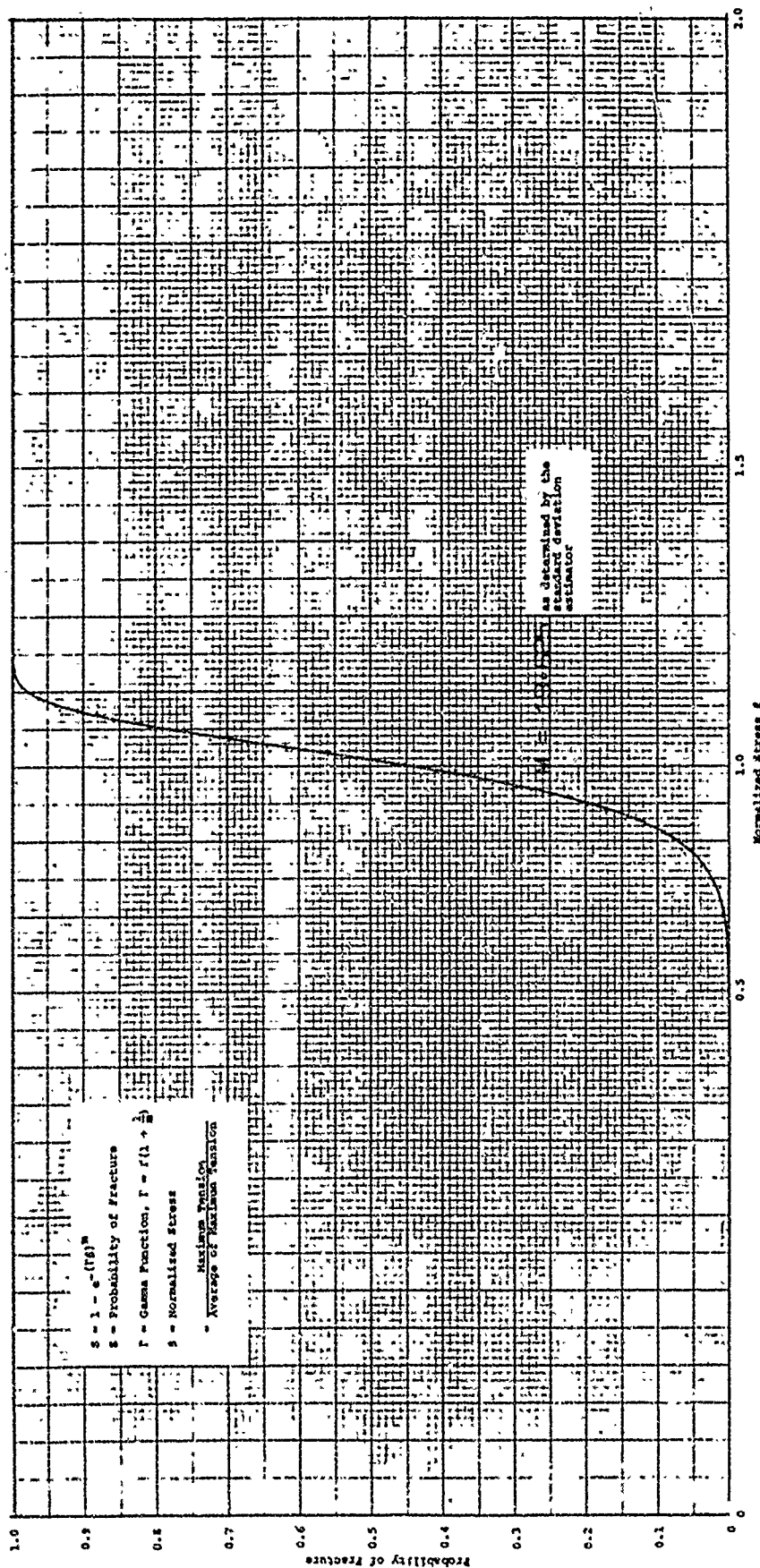


Figure 97. Probability of Fracture versus Normalized Stress  $s$  for the Microfissure Specimens Machined by R and W Products

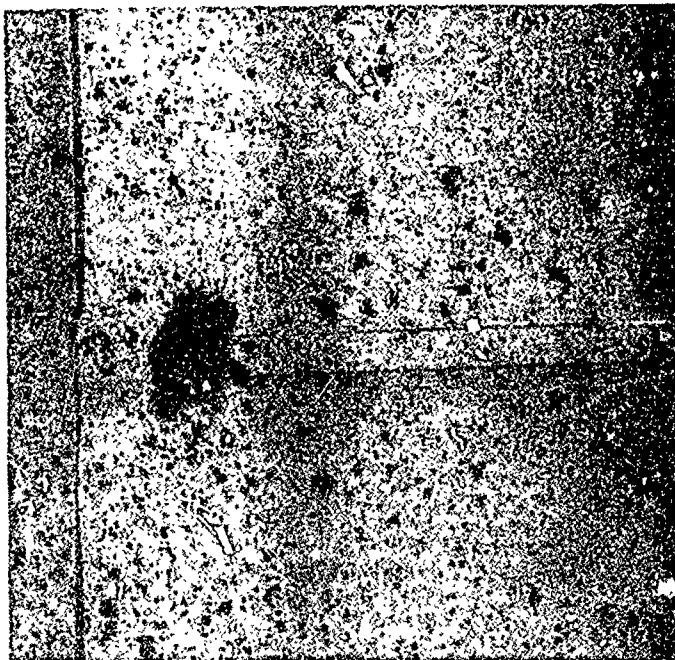


Figure 98a

Tensile Face of Flexure  
Specimen 3A09-084-24A,  
Shop Ground and Metal-  
lurgically Lapped, before  
Refire, Showing 0.0075-  
inch Void, 50X

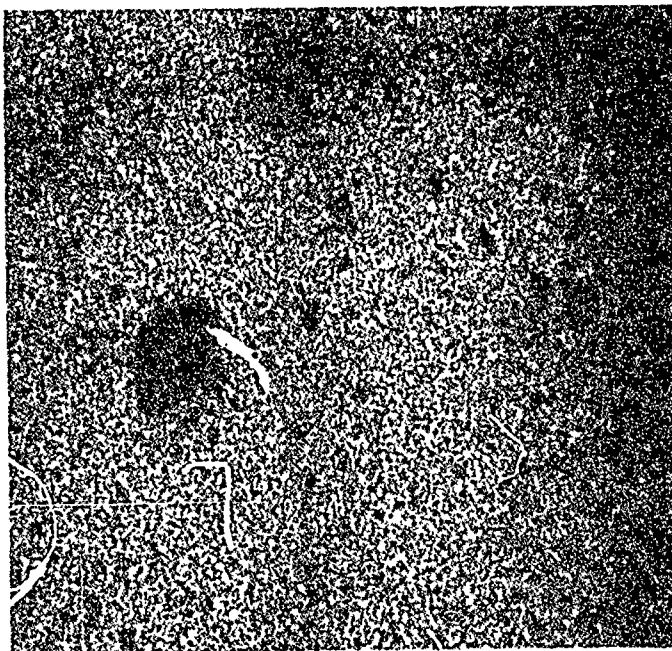
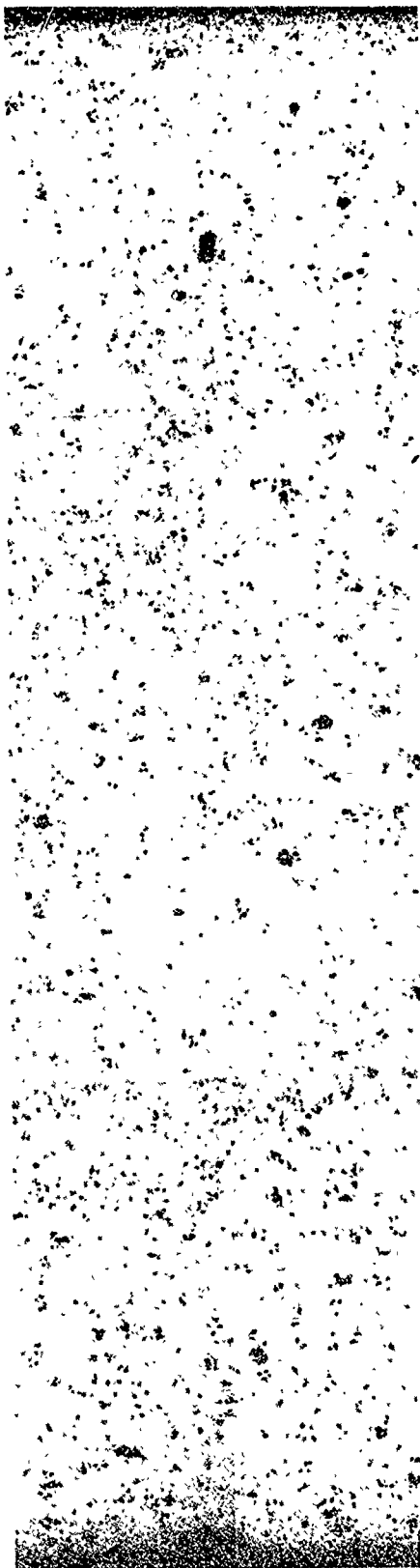
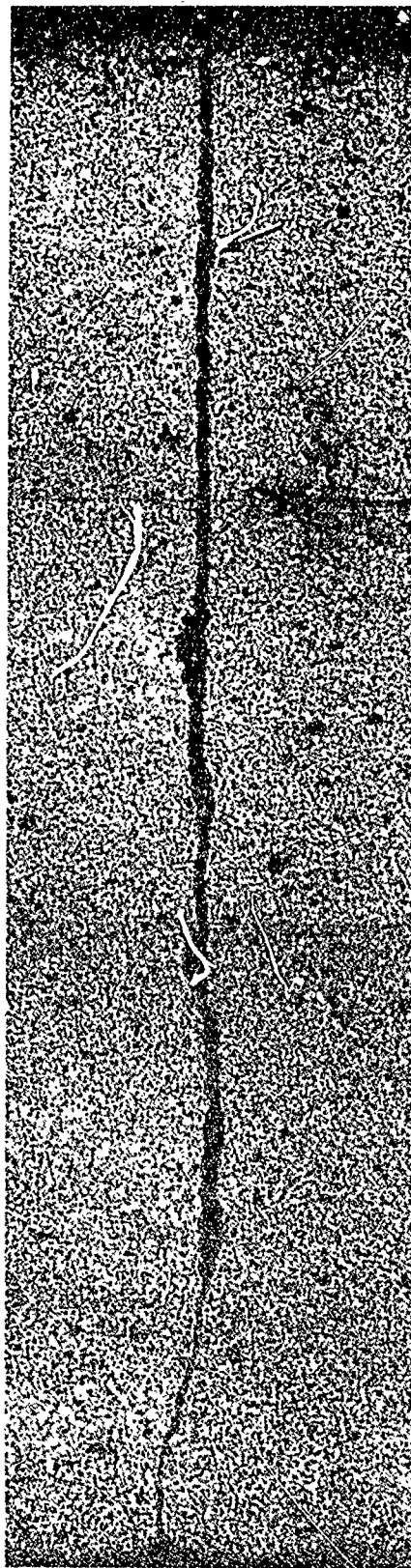


Figure 98b

Tensile Face of Flexure  
Specimen 3A09-084-24A,  
Shop Ground and Metal-  
lurgically Lapped, after  
Refire, Showing 0.0075-  
inch Void, 50X



Before Refire



After Refire

Figure 99. Tensile Face of Flexural Specimen 3A09-084-24A, Shop Ground and Metal-lurgically Lapped, before Refire and after Refire and Fracture. Arrow on Lower Photomicrograph Points to the 0.002 x 0.004-inch Void. 50X

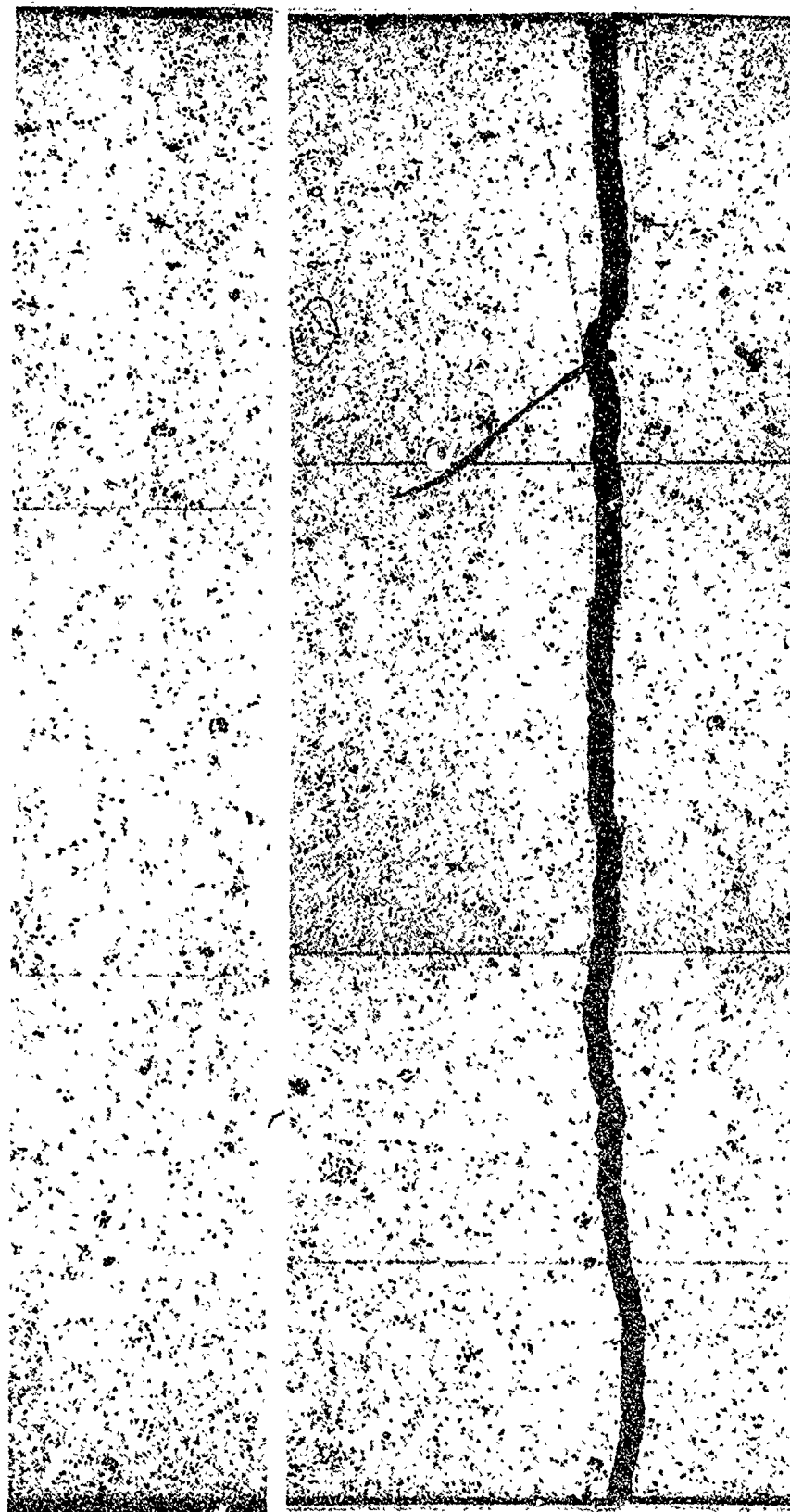
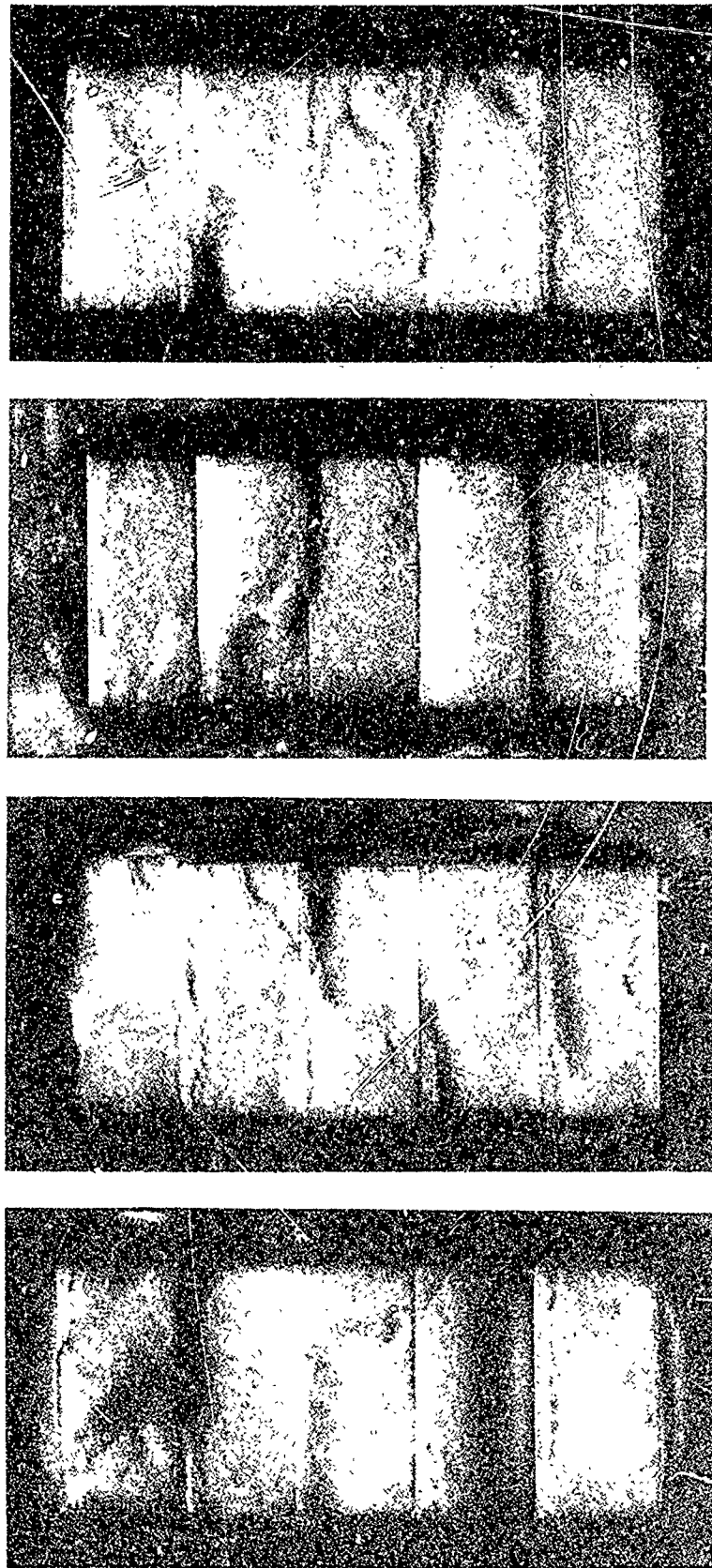


Figure 100. Tensile Face of Flexural Specimen 3A10-088-C12A, Shop Ground and Metallurgically Lapped, 50X, before and after Fracture. \*Artifact-Lint





#### No Treatment

3A09-081-14A  
52,480 psi  
3A09-084-12B  
50,020 psi  
3A09-084-23C  
48,860 psi  
3A09-084-24C  
47,750 psi  
3A09-081-14B  
43,250 psi

#### H<sub>2</sub> Refired

3A09-082-23C  
51,330 psi  
3A09-082-23A  
48,100 psi  
3A09-081-23B  
45,160 psi  
3A09-084-21A  
44,760 psi  
3A09-084-12C  
41,460 psi

#### Lapped/H<sub>2</sub> Refired

3A09-084-21C  
51,710 psi  
3A09-081-24C  
48,900 psi  
3A09-081-11C  
45,450 psi  
3A09-082-23B  
41,120 psi  
3A09-084-12A  
35,560 psi

#### O<sub>2</sub> Refired

3A09-081-11B  
47,520 psi  
3A09-084-24B  
45,550 psi  
3A09-082-11B  
44,210 psi  
3A09-082-22C  
42,490 psi  
3A09-084-13C  
38,720 psi

Figure 101. Fracture Faces of Selected Flexural Specimens from Refiring Study. Lower Edge of Each Fracture Face is the Tension Side. Specimen Numbers and Flexural Strengths are in the Same Order as the Specimens Appear in the Photographs. 7.3X

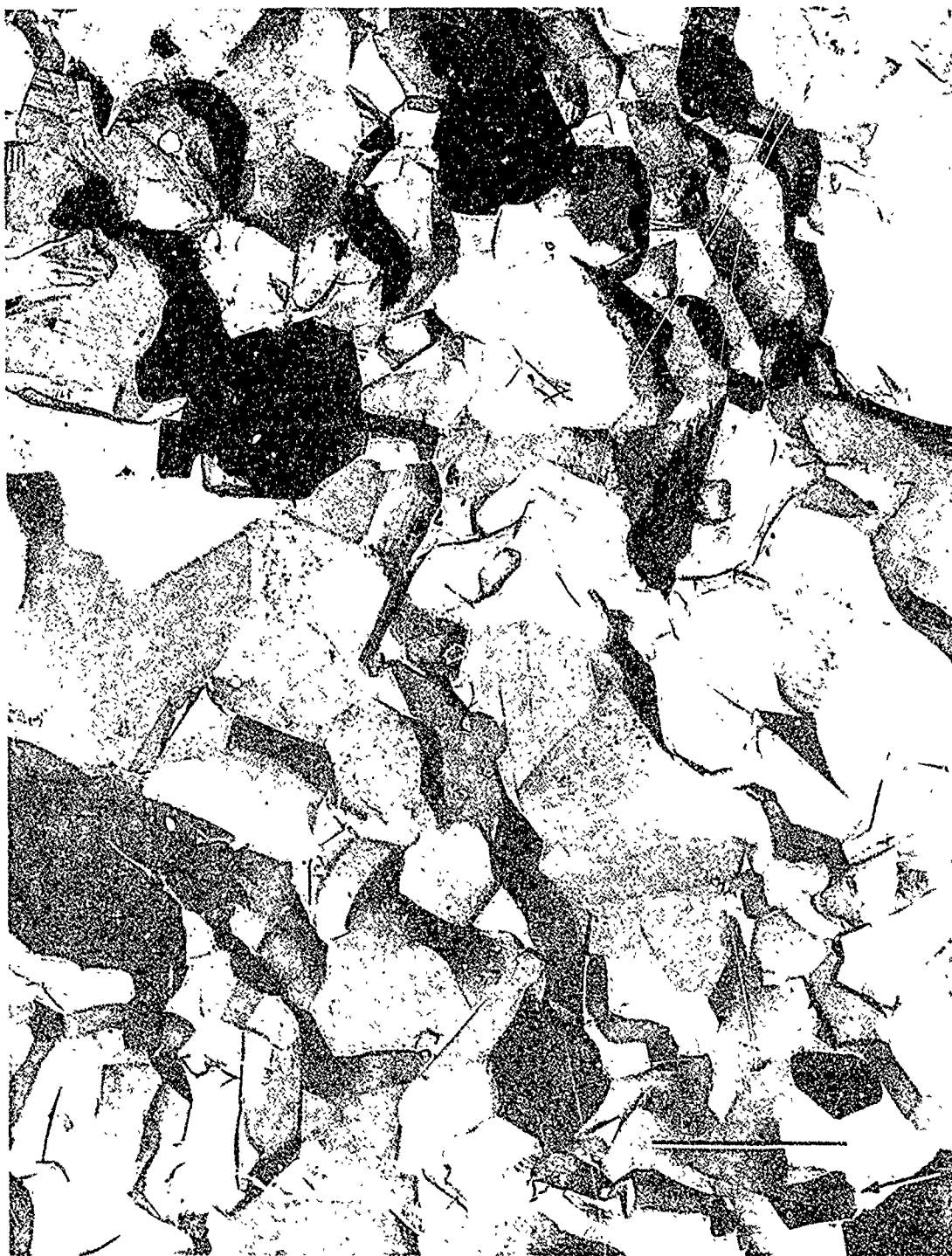


Figure 102. Electron Photomicrograph - Surface of Specimen 3A09-084-13A - Shop Ground. Fiducial Bar Equals 5.0 microns. Arrow Gives Shadowing Direction





Figure 103. Electron Photomicrograph - Surface of Specimen 3A09-084-21A, Shop Ground, Surface Hydrogen Refired to 1550°C. Fiducial Bar Equals 5.0 microns. Arrow Gives Direction of Shadowing

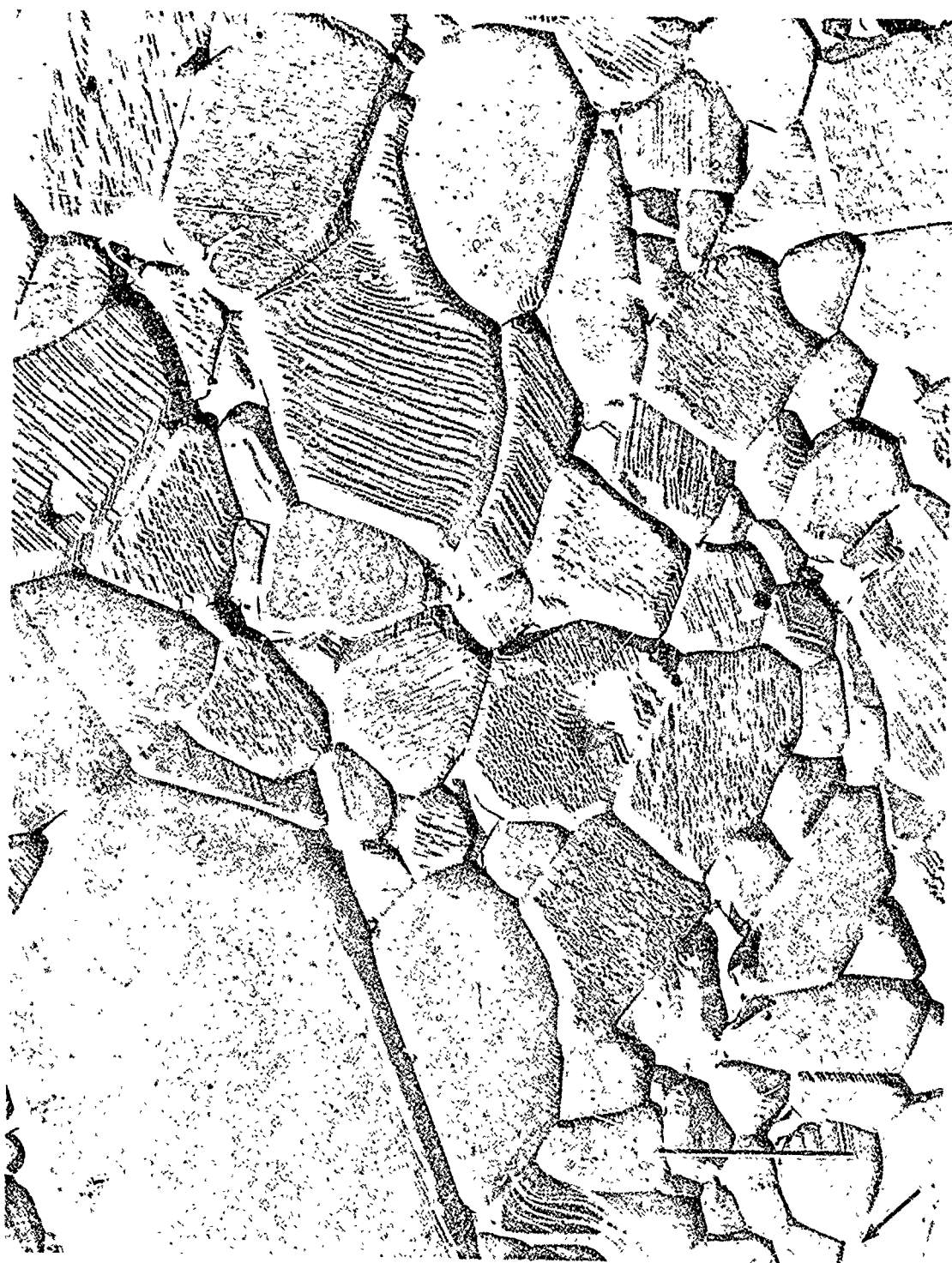


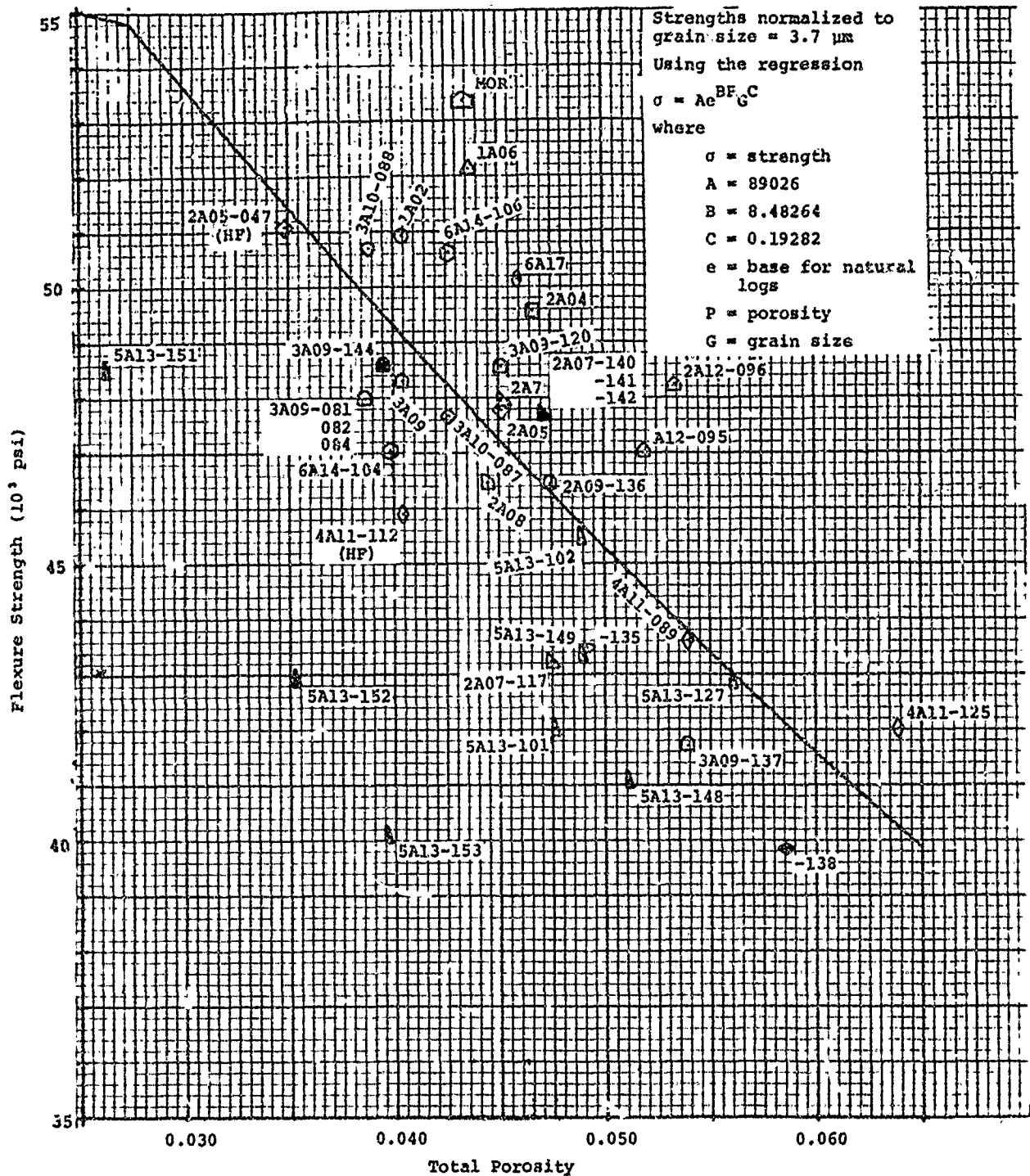
Figure 104. Electron Photomicrograph - Surface of Specimen 3A09-084-24A, Shop Ground, Metallurgically Lapped, and Hydrogen Refired to 1550°C. Fiducial Bar Equals 5.0 microns. Arrow Gives Direction of Shadowing



Figure 105. Electron Photomicrograph -- Surface of Specimen 3A09-084-24B, Shop Ground and Air Refired to 1570°C. Fiducial Bar Equals 5.0 microns. Arrow Gives Direction of Shadowing









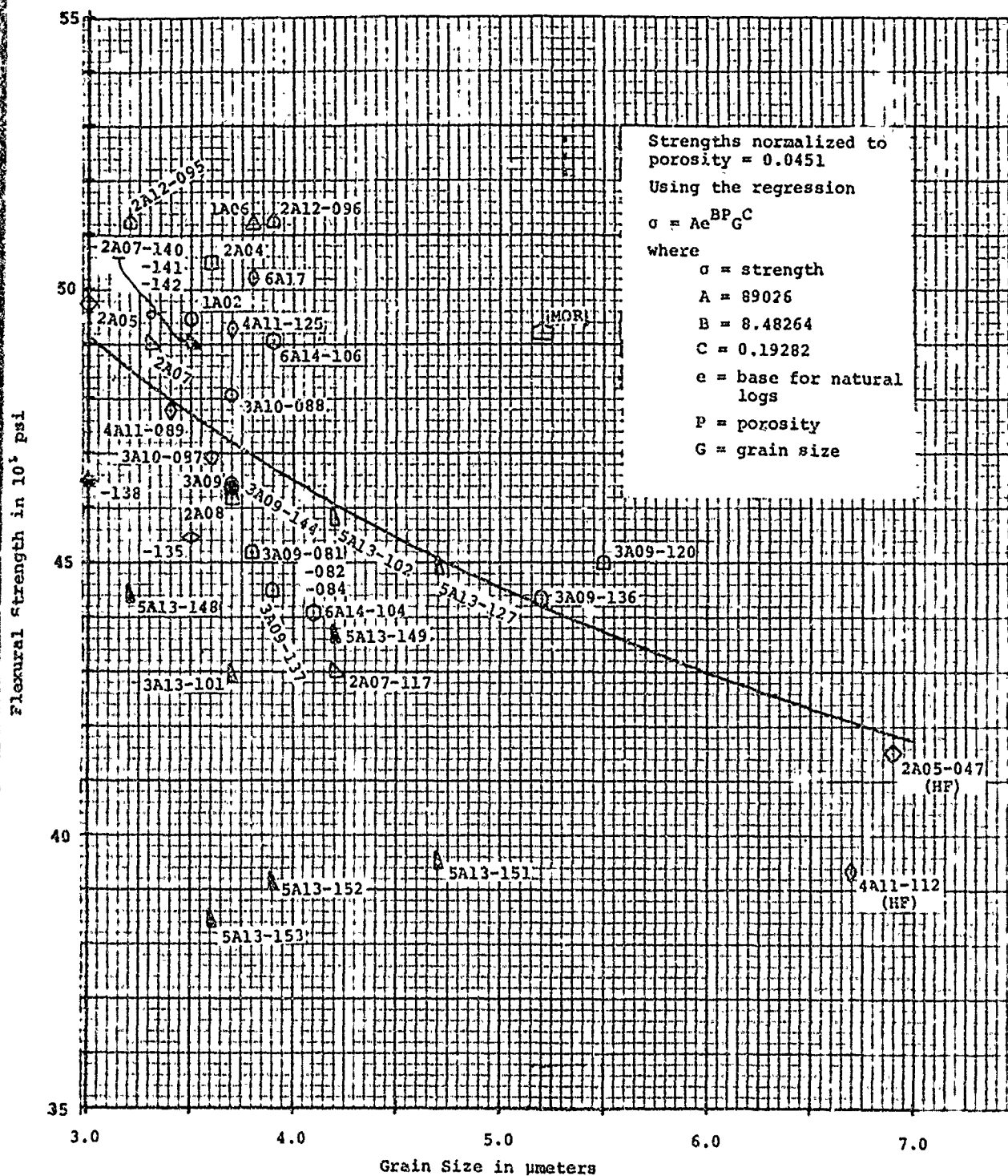


Figure 109. Grain Size versus Normalized Flexure Strength

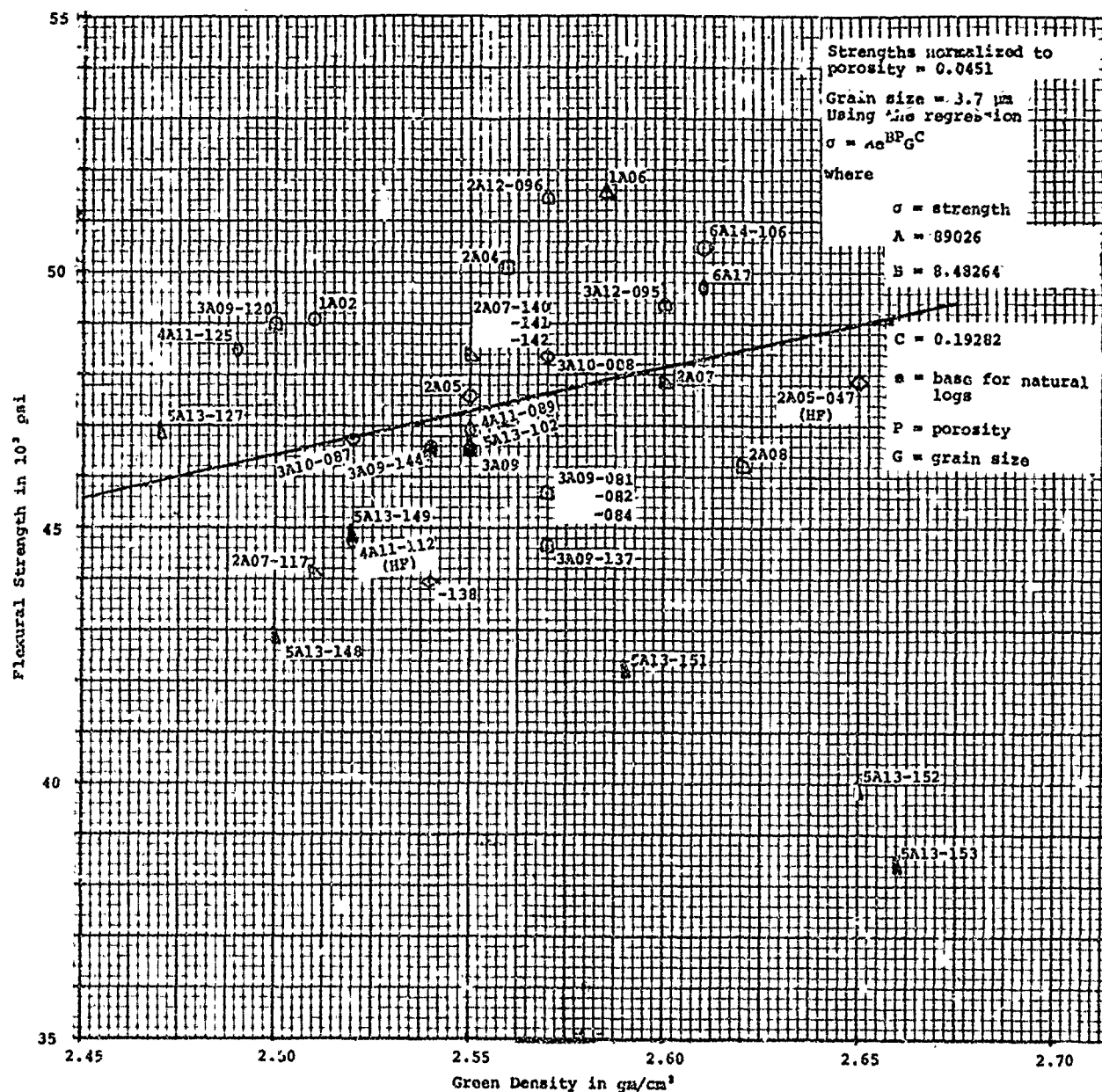


Figure 110. Green Density versus Normalized Flexural Strength



TABLE I

FIRING ANALYSIS DATA Southern Research Institute PO 16-07476

Specimen No.	Specimen Number	SRI Part No. (No./Order)	Date Fired	1-33 Kiln Car No.	Location on Kiln Car and Bung No.	No. of Planural Specimens	No. of Tensile Specimens	Comments	Cone Deformation	Fired Density	X-Ray	Photomicrographs See Figure	Crystal Size Range, Average	Vacuum*	Steel Shell	Pressing Caps	Tool Bit No.
1	53	1831-A-3 (29)	9/26	9	R 28	2	2		B 31 at 1:00		Good			No	Yes	Steel	1
2	61	"	"	"	R 29	"	"		B 31 at 1:30		"			"	"	"	"
3	62	"	"	"	R 30	"	"		B 31 at 2:00	3.85	Void			"	"	"	"
4	63	"	"	"	R 31	"	"		B 31 at 2:30		Good			"	"	"	"
5	76	"	"	"	R 32	"	"		B 31 at 3:00		"			"	"	"	"
6	78	"	"	"	R 33	"	"		B 31 at 4:00		"			"	"	"	"
7	84	"	"	"	R 34	"	"		B 31 at 5:00		"			"	"	"	"
8	86	"	"	"	RC 19	"	"		B 31 at 1:00		"			"	"	"	"
9	90	"	"	"	RC 20	"	"		B 31 at 1:00		"			"	"	"	"
10	91	"	"	"	RC 21	"	"		B 31 at 1:00		"			"	"	"	"
11	92	"	"	"	RC 22	"	"		B 31 at 2:30	3.87	Void			"	"	"	"
12	93	"	"	"	RC 23	"	"		B 31 at 2:30		Good			"	"	"	"
13	94	"	"	"	RC 24	"	"		B 31 at 2:30		"			"	"	"	"
14	95	"	"	"	LC 11	"	"		B 31 at 1:00		"			"	"	"	"
15	103	"	"	"	LC 12	"	"		B 31 at 1:00		"			"	"	"	"
16	104	"	"	"	LC 13	"	"		B 31 at 1:30		"			"	"	"	"
17	105	"	"	"	LC 14	"	"		B 31 at 1:30		"			"	"	"	"
18	125	"	"	"	LC 15	"	"		B 31 at 1:30	3.85	"			"	"	"	"
19	136	"	"	"	LC 16	"	"		B 31 at 3:00	3.87	"			"	"	"	"
20	137	"	"	"	L 5	"	"		B 31 at 3:00		"			"	"	"	"
21	138	"	"	"	L 7	"	"		B 31 at 3:00		"			"	"	"	"
22	150	"	"	"	L 6	"	"		B 31 at 3:00	3.88	Photo- micro	35	3-25	12	"	"	"
23	152	"	"	"	L 8	"	"		B 31 at 3:00		"			"	"	"	"
24	44	1831-A-4 (10)	9/14	13	R 31	2	2		B 31 at 6:00	3.84	"			"	"	"	2
25	107	"	"	"	L 6	"	"		B 31 at 5:30	3.86	Low Den	37	2-25	8	"	"	"
26	108	"	"	"	LC 11	4	4		B 31 at 12:30	3.84	Good			"	"	"	"
27	110	"	"	"	LC 12	"	"		B 31 at 12:30		"			"	"	"	"
28	111	"	"	"	LC 13	"	"		B 31 at 1:00		"			"	"	"	"
29	112	"	"	"	LC 14	"	"		B 31 at 1:00		"			"	"	"	"
30	113	"	"	"	LC 15	"	"		B 31 at 3:00		"			"	"	"	"
31	115	"	"	"	R 28	"	"		B 31 at 3:00		"			"	"	"	"
32	118	"	"	"	R 29	"	"		B 31 at 4:00		"			"	"	"	"
33	119	"	"	"	R 30	"	"		B 31 at 5:00		"			"	"	"	"
34	131	"	"	"	LC 16	"	"		B 31 at 1:30		"			"	"	"	"
35	161	"	9/26	35	L 2	4	4		B 31 at 3:00		"			"	"	"	"

TABLE I (CONTINUED)

Item No.	Coor Spect- men Number	SHI Part No. (No./Order)	Date Fired	Car No. L-33 Kiln	Location on Kiln Car and Bung No.	No. of Flexural Specimens	No. of Tensile Specimens	Comments	Deformation Cone A	Fired Density	X-Ray	Photomicrographs See Figure	Crystal Size Range	Average	Vacuum*	Steel Shell	Pressing Caps	Tool Set No.
36	46	1831-A-5	9/12	13	O	2	2		B 31 at 5:00		Good				No	Yes	Steel	2
37	75	"	"	"	L 2				(B 31 at 5:30)		"				"	"	"	"
38	80	"	"	"	L 3				(B 31 at 6:00)	3.84	"				"	"	"	"
39	81	"	"	"	L 4	2	2		(B 31 at 6:30)		"				"	"	"	"
40	83	"	"	"	L 5				(B 31 at 5:00)		"				"	"	"	"
41	88	"	"	"	L 6				(B 31 at 4:00)		"				"	"	"	"
42	89	"	"	"	L 7				(B 31 at 3:00)		"				"	"	"	"
43	96	"	"	"	L 8	4			B 31 at 1:00	3.84	"				"	"	"	"
44	158	"	9/26	6	LC 11	2	2		(B 31 at 3:00)		"				"	"	"	"
45	159	"	"	"	L 2				(B 31 at 3:00)		"				"	"	"	"
46	160	"	"	"	L 3	2	2		(B 31 at 3:00)		"				"	"	"	"
47	169	"	10/2	22	L 4	2	2		(B 31 at 3:00)	3.88	"				"	"	"	"
48	170	"	"	8	L 6	2	2		T 33 at 1:30		"				"	"	"	"
49	171	"	"	9	L 6				B 33 at 2:00	3.88	"				"	"	"	"
					LC 14				T 33 at 12:30	3.87	"				"	"	"	"
					R 32				B 33 at 1:30		"				"	"	"	"
									B 33 at 2:30		"				"	"	"	"
50	133-1	1831-A-6	9/12	13	RC 18	2			T 31 at 2:00	3.84	"				"	"	"	1
51	133-2	"	"	"	RC 19	2			T 31 at 2:00	3.84	"				"	"	"	"
52	133-3	"	"	"	RC 19	2			T 31 at 2:00	3.84	"				"	"	"	"
53	134-1	"	"	"	RC 19	2			B 31 at 1:45		"				"	"	"	"
54	134-2	"	"	"	RC 19	2			B 31 at 1:45		"				"	"	"	"
55	134-3	"	"	"	RC 19	2			B 31 at 1:45	3.86	"				"	"	"	"
56	135-1	"	"	"	RC 20	2			(T 31 at 1:30)	3.86	"				"	"	"	"
57	135-2	"	"	"	RC 20	2			(T 31 at 1:30)	3.86	"				"	"	"	"
58	135-3	"	"	"	RC 20	2			(T 31 at 1:30)	3.86	"				"	"	"	"
59	119-1	1831-A-7	9/12	13	LC 14	4			(T 31 at 1:00)	3.84	"				"	"	"	2
60	119-2	"	"	"	LC 14				(T 31 at 1:00)	3.84	"				"	"	"	"
61	119-3	"	"	"	LC 14	4			(B 31 at 1:00)	3.84	"				"	"	"	"
62	120-1	"	"	"	LC 14	4			(B 31 at 1:00)		"				"	"	"	"
63	120-2	"	"	"	LC 15	2			(T 31 at 2:00)	3.84	"				"	"	"	"
64	121-1	"	"	"	LC 15	4			(T 31 at 2:00)	3.84	"				"	"	"	"
65	121-2	"	"	"	LC 15	4			(B 31 at 2:00)	3.84	"				"	"	"	"
66	121-3	"	"	"	LC 15	4			(B 31 at 2:00)	3.85	"				"	"	"	"
67	122-1	"	"	"	LC 16	4			T 31 at 3:00	3.85	"				"	"	"	"
68	122-2	"	"	"	LC 16	2			T 31 at 3:00	3.85	"				"	"	"	"
69	122-3	"	"	"	LC 16				(B 31 at 3:00)	3.85	"				"	"	"	"

Table 1 (Continued)

Item No.	Coarse Specimen Number	SRI Part No. (No./Order)	Date Fired	Car No. Kiln	Location on Kiln Car and Bung No.	No. of Flexural Specimens	No. of Tensile Specimens	Comments	Green Density	Cone Deformation	Fired Density by Coarse	X-Ray	Photomicrographs See Figure	Crystalline Size Average	Vacuum	Steel Shell	Pressing Caps	Tool Set No.
70	136-1	1831-A-8	9/12	13	O R 31	2	3		2.62	T 31 at 200	3.86	Good			No	Yes	Steel	2
71	136-2	(8)	"	"	R 31	6			2.62	T 31 at 200	3.86	"			"	"	"	"
72	136-3	"	"	"	R 31	3			2.62	T 31 at 130	3.86	"			"	"	"	"
73	137-1	"	"	"	R 31	3			2.62	T 31 at 130	3.86	"			"	"	"	"
74	137-2	"	"	"	R 32				2.65	T 31 at 230	3.86	"			"	"	"	"
75	137-3	"	"	"	R 32				2.65	T 31 at 200	3.86	"			"	"	"	"
76	138-1	"	"	"	R 32				2.65	T 31 at 200	3.86	"			"	"	"	"
77	138-2	"	"	"	R 33	6			2.65	T 31 at 200	3.86	"			"	"	"	"
78	138-3	"	"	"	R 33	3			2.65	T 31 at 200	3.86	"			"	"	"	"
79	141-1	"	"	"	R 33				2.65	T 31 at 200	3.86	"			"	"	"	"
80	141-2	"	"	"	R 33				2.65	T 31 at 200	3.86	"			"	"	"	"
81	146	1831-A-9	9/28	35	L 3				2.55	B 31 at 300	3.86	"			"	"	"	3
82	147	(5)	"	"	L 4				2.55	B 31 at 230	3.86	"			"	"	"	"
83	150-1	"	"	"	L 5	6			2.55	B 31 at 230	3.86	"			"	"	"	"
84	150-2	"	"	"	L 6				2.55	B 31 at 230	3.86	"			"	"	"	"
85	151-1	"	"	"	L 7	8			2.55	B 31 at 200	3.86	"			"	"	"	"
86	151-2	"	"	"	L 8	8			2.55	B 31 at 150	3.86	"			"	"	"	"
110	195	" (24)	11/1	33	Center				2.55	B 31 at 150	3.86	"			"	"	"	"
87	145	1831-A-10	9/14	13	L 2	29			2.52	B 31 at 500	3.86	"			"	"	"	"
88	148	(2)	"	"	L 4				2.57	B 31 at 500	3.86	"			"	"	"	"
89	153	1831-A-11	9/22	25	Center	20	20		2.55	B 31 at 150	3.86	Crack			"	"	"	4
90	153	(2)	9/28	35	Center				2.52	B 31 at 150	3.86	Crack			"	"	"	"
91	178	"	10/17	7	Center				2.52	B 31 at 150	3.86	Crack			"	"	"	"
92	179	"	10/17	7	Center				2.49	B 31 at 150	3.86	Crack			"	"	"	"
93	180	"	10/17	7	Center				2.49	B 31 at 150	3.86	Crack			"	"	"	"
94	181	"	10/19	7	Center				2.49	B 31 at 150	3.86	Crack			"	"	"	"
111	201	"	11/10	23	Center				2.49	B 31 at 150	3.86	Crack			"	"	"	"
112	202	"	"	"	Center				2.49	B 31 at 150	3.86	Crack			"	"	"	"
113	203	"	"	"	Center				2.49	B 31 at 150	3.86	Crack			"	"	"	"
114	204	"	"	"	Center				2.49	B 31 at 150	3.86	Crack			"	"	"	"
95	165	1831-A-12	9/28	35	L 11	7	7		2.60	B 31 at 230	3.86	Crack			"	"	"	2
96	167	(2)	"	"	L 12	13	1		2.57	B 31 at 230	3.86	Crack			"	"	"	"
97	168	"	10/2	32	L 5				2.45	B 31 at 130	3.86	Crack			"	"	"	"
98	172	"	"	"	L 13				2.45	B 31 at 130	3.86	Crack			"	"	"	"
99	173	"	"	"	RC 22				2.62	T 33 at 200	3.86	Crack			"	"	"	"
100	174	"	"	"	R 31				2.59	T 33 at 200	3.86	Crack			"	"	"	"

TABLE I (CONTINUED)

Item No.	Cores Specimen Number	SRI Part No. (No./Order)	Date Fired	Car N. L-35 Kilm	Location on Kilm Car and Bung No.	No. of Flexural Specimens	No. of Tensile Specimens	Comments	Green Density	Cone Deformation	Density by Cores	X-ray	Photomicrographs See Figure	Crystal Size Range	Average	Vacuum	Steel Shell	Pressing Caps	Tool Set No.
101	70	1831-A-13	9/14	13	L 5	7	5		2.55	(B 31) at 5:00	2.85	Good							
102	71	" (3)	"	"	L 6	7	5		2.54	(B 31) at 5:00	2.84	"						"	
103	72	"	"	"	L 7	7	5			(B 31) at 5:30		"					"	"	
104	67	1831-A-14	9/12	13	R 29	6	8		2.63	(B 31) at 1:30	2.88	"						"	
105	68	" (3)	"	"	R 30	13	4		2.61	(B 31) at 1:30	2.88	"					"	"	
106	69	"	"	"	R 30	13	4			(B 31) at 1:30		"					"	"	
107	65	1831-A-17	"	"	R 28	7	7		2.62	(T 31) at 2:00	2.85	"					"	"	
108	66	" (3)	"	"	R 28	7	7		2.59	(B 31) at 1:30	2.85	"					"	"	
109	74	"	"	"	R 29	7	7			(T 31) at 2:00		"		30	2-25	8	"	"	

T &amp; B Designate the Top or Bottom of the block when it was pressed.

\*\* Designates samples cut from the fired part.

⊗ Fired in L-32 kiln (80° higher temperature than L-33).

⊙ Vacuum was used with rubber shell only.

O, N, RC, LC and L designate right, right center, left center, and left. Refer to Figures 26 through 33.

Δ B and M designate the bottom or middle of bungs.

() Designates estimated cone deformations from cores in same area.

Note: All parts were pressed at 30,000 psi.

Fired densities were taken on a 4AQL, Level II per MIL Std. 103D.

Photomicrographs were made one per kiln car.

For defective X-rayed parts, see Figure 43, Specimens 63 and 93.

47, 107

48, 122

49, 153

50, 178

51, 180

TABLE II

RESULTS OF FLEXURAL EVALUATIONS OF PHASE I MACRO SPECIMENS

SRI Run Number	Specimen	Temperature °F	Bulk Density (Mechanics Section) gm/cm <sup>3</sup>	Stress Rate psi/sec	Load at Fracture lbc	Fracture Stress psi	Fracture Location (inches from midspan)	Strain Velocity in./in./sec	Remarks
1	1A02-002-1	70	3.830	5000	96.25	54140	0.35-0.375		
2	-003-2		3.830		83.75	52730	0.48-0.375		
3	-004-1		3.827		93.75	52730	0.25		
4	-004-2		3.833		83.25	52450	0.3		
5	-005-1		3.838		83.25	45370	0.05		
6	-005-2		3.822		100.75	58670	0.0		
7	-006-1		3.824		90.00	55650	0.05		
8	-006-2		3.831		88.00	47810	0.35		
9	-007-1		3.828		84.00	47250	0.3		
10	-007-2		3.838		78.25	44020	0.05		
11	-011-1		3.827		88.75	42800	0.35		
12	-011-2		3.812		96.25	54.50	0.0		
13	-016-1		3.822		81.50	47.40	0.0		
14	-016-2		3.834		90.25	50770	0.25		
15	-017-1		3.814		82.00	51750	0.0		
16	-017-2		3.828		93.50	52500	0.35		
17	-020-1		3.849		95.75	53800	0.25		
18	-020-2		3.839		93.50	52500	0.25		
19	-023-1		3.833		92.75	53170	0.15		
20	-023-2		3.835		100.75	56670	0.2		
Mean Value						51450			
Standard Deviation						3540			
Coefficient of Variation						0.0706			
21	2A04-024-1		3.833		89.25	50200	0.3		
22	-024-2		3.825		89.25	55330	0.25		
23	-025-1		3.830		35.00	47810	0.25		
24	-025-2		3.830		86.25	48620	0.25-0.375		
25	-028-1		3.789		97.00	54550	0.375-0.375		
26	-028-2		3.760		80.50	45280	0.0		
27	-026-3		3.804		32.00	43130	0.3		
28	-026-4		3.787		35.00	52310	0.2		
29	-028-1		3.802		77.75	43730	0.05		
30	-028-2		3.805		85.75	45330	0.1		
31	-030-1		3.783		98.00	56130	0.3		
32	-030-2		3.791		75.50	44160	0.2		
33	-030-3		3.789		93.25	52450	0.375		
34	-030-4		3.811		91.50	51470	0.0		
35	-031-1		3.819		90.00	50630	0.1		
36	-031-2		3.818		95.00	53440	0.25		
37	-035-1		3.799		81.00	45310	0.35		Specimen length = 1.592
38	-035-2		3.794		75.00	42190	0.375		
39	-035-3		3.803		91.25	51330	0.2		
40	-035-4		3.804		102.00	57380	0.3-0.35		
Mean Value			3.804			49810			
Standard Deviation			0.020			4390			
Coefficient of Variation						0.0881			
41	2A05-043-1		3.786		87.25	49080	0.35-0.375	0.4355	
42	-043-2		3.793		92.25	51890	0.375	0.4509	
43	-043-3		3.797		95.50	53710	0.10	0.4501	
44	-043-4		3.797		94.00	52880	0.375-0.375	0.4396	
45	-036-1								Broken during grinding
46	-036-2		3.794		33.00	47810	0.35	0.4507	
47	-039-1		3.809		65.50	48090	0.25	0.4431	
48	-039-2		3.818		62.75	52170	0.375	0.4386	
49	-044-1		3.831		85.00	47810	0.375	0.4546	
50	-044-2		3.820		81.50	45840	0.375	0.4453	
51	-046-1		3.808		85.25	47950	0.20	0.4371	
52	-046-2		3.814		89.75	45620	0.25	0.4431	
53	-047-1		3.829		80.25	45140	0.20	0.4423	Fired at 60°C higher temperature
54	-047-2		3.850		80.75	45420	0.00	0.4496	Fired at 60°C higher temperature
Mean Value			3.810			49740			
Standard Deviation			0.017			2650			
Coefficient of Variation						0.0513			
187	1A06-051-1		3.781		86.75	49920	0.00	0.4147	
188	-051-2		3.803		91.35	51350	0.00	0.4156	
189	-052-1		3.825		89.75	50480	0.10	0.4122	
170	-052-2		3.821		55.25	52450	0.10	0.4150	
171	-053-1		3.811		75.50	44160	0.20	0.4234	
172	-053-2		3.809		101.25	56950	0.10	0.4128	
173	-054-1		3.822		95.00	54000	0.10	0.4193	
174	-054-2		3.830		75.75	44300	0.20	0.4203	
175	-055-1		3.805		100.25	56350	0.20	0.4277	
176	-055-2		3.802		88.25	55370	0.10	0.4241	
177	-056-1		3.824		101.00	56810	0.20	0.4237	
178	-056-2		3.833		98.50	54280	0.20	0.4309	
179	-057-1		3.832		94.50	53100	0.20	0.4191	
180	-057-2		3.834		82.00	48130	0.10	0.4173	
Mean Value			3.818			51830			
Standard Deviation			0.016			4390			
Coefficient of Variation						0.0618			

TABLE II (CONTINUED)

SPI Run Number	Specimen	Temperature °F	Bulk Density (Mechanics Section) gm/cm <sup>3</sup>	Stress Rate psi/sec	Load at Fracture lbs	Fracture Stress psi	Fracture Location (Inches from midspan)	Sonic Velocity in./μsec	Remarks
55	2A07-058-1	70	3.806	5000	88.00	48380	0.05	0.3964	
56	-058-2		3.813		76.50	43330	0.15	0.3661	
57	-058-3		3.810		92.50	50300	0.20	0.3932	
58	-058-4		3.805		85.00	47810	0.40	0.3913	
59	-062-1		3.808		91.00	51190	0.1	0.3925	
60	-062-2		3.806		83.50	52550	0.3	0.3893	
61	-062-3		3.814		92.50	52030	0.0	0.3979	
62	-062-4		3.802		81.00	45500	0.20	0.3904	
63	-064-1		3.803		37.75	42500	0.15	0.3364	
64	-064-2		3.811		91.75	51610	0.0	0.3911	
66	-065-2		3.813		83.50	52550	0.3	0.3830	
67	-065-3		3.810		81.00	51190	0.15	0.3941	
68	-065-4		3.819		81.75	45980	0.0	0.3953	
69	-066-1		3.819		39.00	50080	0.2	0.3952	
70	-065-2		3.817		89.75	50480	0.3	0.3955	
71	-066-3		3.815		83.25	48630	0.15	0.3861	
72	-066-4		3.820		89.75	50480	0.06	0.3910	
73	-067-1		3.813		85.25	47250	0.35	0.3988	
74	-067-2		3.811		74.75	42050	0.0	0.3037	
75	-067-3		3.808		80.00	45000	0.25-0.45	0.3928	
76	-067-4		3.808		86.00	48380	0.2	0.3975	
77	-068-1		3.787		91.50	53160	0.05	0.3986	
78	-068-2		3.784		89.00	52310	0.12	0.3952	
83	-069-1		3.821		82.00	48150	0.25	0.3928	
Mean Value			3.810			49010			
Standard Deviation			0.008			3170			
Coefficient of Variation						0.0647			
79	2A08-070-1		3.815		80.75	45420	0.375	0.3952	
80	-070-2		3.808		84.50	47530	0.3	0.3928	
81	-070-3		3.817		65.00	38500	0.3	0.3979	
82	-071-1		3.820		83.25	49040	0.15	0.3944	
83	-071-2		3.811		86.50	48580	0.15	0.3964	
84	-071-3		3.816		72.50	40780	0.3	0.3860	
85	-071-4		3.807		82.0	46410	0.25	0.4018	
86	-071-5		3.793		81.0	45580	0.3	0.4043	
87	-071-6		3.797		92.00	51750	0.25	0.4020	
88	-073-1		3.821		80.75	45420	0.25	0.3962	
89	-073-2		3.816		91.25	51320	0.2	0.3308	
90	-073-3		3.822		83.75	47110	0.05	0.3933	
91	-073-4		3.832		79.50	44720	0.2	0.3897	
92	-073-5		3.819		91.00	51180	0.3	0.3917	
93	-073-6		3.791		77.75	43730	0.35	0.3523	
94	-073-7		3.820		76.75	43170	0.05	0.3869	
95	-073-8		3.818		88.25	49640	0.05	0.3938	
96	-073-9		3.820		92.00	51750	0.25	0.3944	
97	-080-1		3.811		73.00	41000	0.05	0.2950	
98	-080-2		3.812		86.75	48800	0.1	0.3857	
99	-080-3		3.811		80.00	45000	0.3	0.3884	
Mean Value			3.813			46440			
Standard Deviation			0.010			4000			
Coefficient of Variation						0.0851			
100	3A02-083-1		3.834		91.25	49700	0.2	0.4020	14 RMS
101	-083-2		3.835		91.25	51330	0.05	0.4042	
102	-083-3		3.836		83.75	52730	0.1	0.4013	
103	-083-4		3.841		82.00	50830	0.1	0.4041	
104	-083-5		3.837		85.00	47810	0.15	0.4009	
105	-083-6		3.847		59.50	48680	0.15	0.4042	
106	-085-1		3.818		81.75	54750	0.0	0.4090	13 RMS
107	-085-2		3.818		92.50	52330	0.3	0.4117	
108	-085-3		3.840		81.50	45840	0.38	0.4120	
109	-085-4		3.828		87.75	45980	0.15	0.4083	
110	-085-5		3.819		76.50	43580	0.3	0.4053	
111	-085-6		3.824		86.00	48380	0.25	0.4068	
112	-085-7		3.824		92.75	52170	0.05	0.4068	
113	-085-8		3.838		82.00	50000	0.3	0.4153	
114	-085-9		3.822		85.00	47810	0.05	0.4371	
115	-086-2		3.826		82.25	51890	0.2	0.4352	
116	-086-3		3.821		91.00	51180	0.05	0.4298	
117	-086-4		3.820		80.75	51050	0.3	0.4340	
118	-086-5		3.842		79.00	44440	0.3	0.4425	
119	-086-6		3.820		83.25	49040	0.2	0.4333	
Mean Value			3.829			48263			
Standard Deviation			0.010			4210			
Coefficient of Variation						0.0673			
120	3A10-087-1		3.825		80.50	49220	0.35	0.4113	
121	-087-2		3.841		83.75	47110	0.2	0.4119	
122	-087-3		3.827		88.00	49500	0.375	0.4117	
123	-087-4		3.824		88.50	55410	0.375-0.375	0.4120	
124	-087-5		3.848		86.50	48600	0.1	0.4132	
125	-087-6		3.820		87.50	49220	0.3	0.4084	15 RMS
126	-087-7		3.823		93.25	52450	0.2	0.4108	
127	-087-8		3.822		83.25	47530	0.1	0.4101	
128	-087-9		3.811		84.50	47530	0.25	0.4072	
129	-087-10		3.816		82.25	46270	0.05	0.4119	
130	-087-11		3.816		86.50	48680	0.05	0.4119	
131	-087-12		3.809		74.50	41810	0.0	0.4120	
132	-087-13		3.822		81.75	45980	0.2	0.4094	
133	-087-14		3.823		75.00	42190	0.1	0.4100	
134	-087-15		3.825		84.00	47250	0.3	0.4102	
135	-087-16		3.824		74.25	41788	0.05	0.4084	
136	-087-17		3.816		77.75	43730	0.1	0.4099	
137	-087-18		3.817		91.50	51470	0.3	0.4119	

TABLE II (CONTINUED)

SRI Run Number	Specimen	Temperature °F	Bulk Density (Mechanics Section) gm/cm <sup>3</sup>	Stress Rate: psi/sec	Load at Fracture lbs	Fracture Stress psi	Fracture Location inches from midspan	Sonic Velocity in./μsec	Remarks
138	3A10-087-19	70	3.771	5000	75.75	42810	0.25	0.4037	Weak back echo
139	-087-20		3.818		80.00	45000	0.15	0.4087	
140	-087-21		3.797		82.75	43790	0.35-0.35	0.4111	
141	-087-22		3.823		88.00	44380	0.05	0.4137	
142	-087-23		3.825		83.75	45020	0.25	0.4130	
143	-087-24		3.823		81.00	45560	0.15	0.4117	
144	-087-25		3.834		84.00	52890	0.1	0.4123	
145	-087-26		3.811		82.00	46130	0.05	0.4136	
221	-088-A1		3.841		101.00	56790	0.20	0.4037	3 RMS
222	-088-A2		3.834		93.50	52530	0.00	0.3988	
223	-088-A3		3.817		94.50	53110	0.375-0.375	0.4029	
224	-088-A4		3.842		82.50	46450	0.375	0.4033	
225	-088-A5		3.856		88.50	43810	0.30	0.4072	
226	-088-B1		3.857		104.75	58950	0.00	0.4067	
227	-088-B2		3.823		84.50	53110	0.00	0.4051	
228	-088-B3		3.825		100.00	55620	0.25	0.4037	
229	-088-B4		3.825		85.00	47770	0.375	0.4041	4 RMS
230	-088-B5		3.830		89.00	50100	0.10	0.4024	
231	-088-B6		3.852		81.75	53200	0.18	0.4042	
232	-088-B7		3.838		80.25	50150	0.375-0.375	0.4037	
233	-088-B8		3.806		84.25	47380	0.05	0.4022	
234	-088-B9		3.842		82.00	50020	0.20	0.4036	
235	-088-B10		3.841		83.25	52410	0.20	0.3945	
236	-088-B11		3.851		80.75	51000	0.375	0.4052	4 RMS
237	-088-B12		3.841		84.00	52520	0.15	0.4048	
238	-088-B13		3.843		85.50	49740	0.10	0.4042	
239	-088-B14		3.844		100.50	56430	0.00	0.4019	
240	-088-B15		3.872		85.75	48190	0.375	0.4028	
241	-088-C1		3.842		89.75	51200	0.15	0.4050	
242	-088-C2		3.821		79.50	48950	0.10	0.4051	
243	-088-C3		3.836		82.50	47050	0.15	0.4081	3 RMS
244	-088-C4		3.850		85.50	53810	0.25	0.4074	
245	-088-C5		3.854		76.25	42200	0.10	0.4029	
246	-088-C6		3.821		82.50	51990	0.20	0.4021	
247	-088-C7		3.821		84.00	52220	0.10	0.4036	
248	-088-C8		3.854		84.25	52970	0.10	0.4033	
249	-088-D1		3.843		80.25	55060	0.20	0.4065	3 RMS
250	-088-D2		3.827		84.75	48100	0.20	0.4030	
251	-088-D3		3.818		78.50	44500	0.10	0.4045	
252	-088-D4		3.844		101.75	57180	0.00	0.4040	
253	-088-D5		3.835		91.50	51420	0.10	0.4037	
254	-088-D6		3.840		77.75	43700	0.00	0.4037	
255	-088-D7		3.841		84.50	53110	0.10	0.4019	
256	-088-D8		3.821		84.50	53110	0.10	0.4016	
Mean Value			3.827			49220			
Standard Deviation						4360			
Coefficient of Variation						0.0885			
213	4A11-089-A1		3.732		58.25	49040	0.2		
214	-089-A2		3.787		89.00	50080	0.05		
215	-089-A3		3.755		83.75	47110	0.375		
216	-089-A4		3.786		81.00	43580	0.25		
217	-089-A5		3.786		79.25	44560	0.25		
218	-089-A6		3.791		81.75	45980	0.1		
219	-089-B1		3.744		66.50	36530	0.2		
220	-089-B2		3.822		79.50	44720	0.2		
221	-089-B3		3.790		89.50	50340	0.15		
222	-089-B4		3.765		69.25	38940	0.45		
223	-089-B5		3.776		68.00	38250	0.1		
224	-089-B6		3.773		72.50	40760	0.3		
225	-089-B7		3.788		89.00	50080	0.2		
226	-089-B8		3.725		87.00	37690	0.0		
227	-089-B9		3.791		86.50	43640	0.1		
228	-089-B10		3.768		63.00	35440	0.05		
229	-089-B11		3.768		77.75	42610	0.15		
230	-089-B12		3.789		74.25	41770	0.2		
231	-089-B13		3.775		82.50	46410	0.25		
232	-089-B14		3.787		87.50	49220	0.35		
Mean Value			3.775			44320			
Standard Deviation			0.019			4780			
Coefficient of Variation						0.1078			
240	2A12-095-1		3.772		83.75	47110	0.2		
241	-095-2		3.792		87.50	49220	0.05		
242	-095-3		3.779		90.75	51030	0.2		
243	-095-4		3.763		84.00	52580	0.2-0.2		
244	-095-5		3.777		81.50	42340	0.5		
245	-095-6		3.753		79.75	46800	0.375		
246	-095-7		3.794		84.25	47390	0.2		
247	-095-8		3.770		85.50	48090	0.3		
248	-095-9		3.789		91.25	51530	0.35		
249	-095-10		3.774		80.00	45000	0.3		
250	-095-11		3.788		83.75	48330	0.1		
251	-095-12		3.773		85.50	48060	0.15		
252	-095-13		3.785		89.50	50340	0.05		
253	-095-14		3.771		83.00	46690	0.2		
254	-095-15		3.789		85.00	47810	0.0		
255	-095-16		3.781		87.75	49330	0.2		
256	-095-17		3.791		85.25	47990	0.0		
257	-095-18		3.798		87.50	49110	0.3		
258	-095-19		3.776		82.25	46370	0.1		
259	-095-20		3.778		77.50	43590	0.15		
Mean Value			3.779			47680			
Standard Deviation			0.008			4671			
Coefficient of Variation						0.0092			

TABLE II (CONTINUED)

SRM Run Number	Specimen	Temperature °F	Bulk Density (Mechanics Section) gm/cm <sup>3</sup>	Stress Rate psi/sec	Load at Fracture lbs	Fracture Stress psi	Fracture Location inches from midspan	Sonic Velocity in./msec	Remarks
224	5A13-101-1	70	3.802	5000	73.50	41340	0.05		
226	-101-2		3.807		71.50	40220	0.0		
230	-101-3		3.787		77.00	43310	0.0		
245	-101-4		3.800		78.00	42730	0.375		
195	-101-5		3.787		69.00	38810	0.3		
246	-101-6		3.600		78.50	44180	0.3-0.375		
227	-101-7		3.799		77.50	43590	0.375		
207	-102-1		3.773		75.50	42470	0.375		
239	-102-2		3.781		82.25	45140	0.3		
231	-102-3		3.768		83.25	45580	0.3-0.35		
215	-102-4		3.771		77.50	43590	0.35		
220	-102-5		3.767		77.75	43730	0.25		
254	-102-6		3.765		89.50	50340	0.0		
242	-102-7		3.773		75.50	42470	0.1		
300	-102-10		3.607		78.50	44115	0.20	0.4050	
313	-102-11		3.815		83.00	48330	0.375-0.375	0.4052	
312	-102-12		3.816		82.75	49880	0.15	0.4052	
311	-102-13		3.815		67.75	37800	0.375	0.4042	
310	-102-14		3.816		87.25	49040	0.05	0.4043	
309	-102-15		3.812		83.50	48930	0.10	0.4033	
305	-102-16		3.807		85.25	47910	0.10	0.4034	
302	-102-17		3.813		88.75	49680	0.05	0.4061	
292	-102-18		3.816		57.25	32190	0.05	0.4061	
187	-103-1		3.787		88.00	48380	0.3		
217	-103-2		3.788		77.00	43310	0.2		
189	-103-3		3.787		79.50	44720	0.15		
255	-103-4		3.786		80.00	45000	0.15		
259	-103-5		3.794		76.50	43030	0.2		
183	-103-6		3.785		81.25	45700	0.2		
238	-103-7		3.789		78.50	44160	0.05		
309	-103-10		3.819		81.75	45940	0.10	0.4049	
306	-103-11		3.819		78.50	44120	0.05	0.4055	
304	-103-12		3.826		88.00	49460	0.15	0.4092	
303	-103-13		3.817		89.00	50020	0.15	0.4093	
301	-103-14		3.817		82.75	48510	0.15	0.4045	
297	-103-15		3.817		87.50	49180	0.375	0.4085	
307	-103-16		3.810		85.00	47770	0.375-0.375	0.4088	
299	-103-17		3.807		79.50	44680	0.30	0.4054	
314	-103-18		3.811		81.50	45800	0.20	0.4036	
Mean Value			3.789			44650			
Standard Deviation						4320			
Coefficient of Variation						0.0900			
146	6A14-104-1		3.637		88.50	49780	0.20	0.4114	
147	-104-2		3.625		87.50	49220	0.10	0.4125	
148	-104-3		3.632		88.25	49640	0.20	0.4145	
149	-104-4		3.629		81.75	45980	0.30	0.4230	
150	-104-5		3.632		74.50	41810	0.10	0.4082	
151	-104-6		3.636		95.00	52310	0.20	0.4033	
152	-104-7		3.631		62.25	35020	0.10	0.4033	
153	-104-8		3.630		80.00	45000	0.375	0.4088	
154	-106-1		3.814		85.50	48090	0.10	0.4130	
155	-106-2		3.803		94.50	53100	0.375	0.4102	
156	-106-3		3.830		99.00	55690	0.05	0.4076	
157	-106-4		3.823		88.75	49820	0.10	0.4068	
158	-106-5		3.822		84.75	47670	0.05	0.4110	
159	-106-6		3.823		85.00	47810	0.10	0.4070	
160	-106-7		3.802		88.50	49780	0.20	0.4117	
161	-106-8		3.817		88.50	49780	0.375	0.4091	
162	-106-9		3.812		74.00	41630	0.20	0.4118	
163	-106-10		3.812		63.00	32310	0.05	0.4073	
164	-106-11		3.821		90.25	50770	0.05	0.4074	
165	-106-12		3.830		100.50	58530	0.375-0.375	0.4099	
165	-106-13		3.836		85.50	48090	0.35	0.4060	Spore from scrap
Mean Value			3.824			46580			
Standard Deviation			0.010			4580			
Coefficient of Variation						0.1001			
244	6A17-107-1		3.819		98.50	65410	0.15		
181	-107-2		3.812		85.50	48090	0.2		
256	-107-3		3.811		90.25	50770	0.3		
184	-107-4		3.812		85.00	47810	0.35		
249	-107-5		3.814		90.25	50770	0.375		
197	-107-6		3.812		93.50	52590	0.2		
247	-107-7		3.812		94.75	53100	0.375-0.375		
271	-108-1		3.799		63.50	32490	0.3		
253	-108-2		3.794		83.50	46790	0.15		
203	-108-3		3.803		90.50	45280	0.25		
194	-108-4		3.803		90.50	50910	0.25		
233	-108-5		3.803		87.50	49220	0.3		
210	-108-6		3.805		84.75	53100	0.375		
203	-108-7		3.803		90.00	50430	0.35		
222	-109-1		3.808		90.25	50770	0.1		
224	-109-2		3.802		88.00	49300	0.3		
241	-109-3		3.806		85.50	46900	0.2		
237	-109-4		3.803		84.50	46970	0.2		
221	-109-5		3.806		79.50	44720	0.1		
235	-109-6		3.808		94.25	53020	0.375-0.375		
230	-109-7		3.813		82.75	48350	0.1		
Mean Value			3.807			48870			
Standard Deviation			0.008			2910			
Coefficient of Variation						0.0583			



TABLE III

TABLE OF MEAN STRESSES, STANDARD DEVIATIONS, AND  
COEFFICIENTS OF VARIATION FOR PHASE I  
FLEXURAL DATA ON MACRO SPECIMENS

Specimen Blank Type	Number of Specimens	Mean Fracture Stress	Standard Deviation	Coefficient of Variation
A2	20	51450	3640	0.0706
A4	19	49810	4390	0.0881
A5	13	49050	2870	0.0585
A6	14	51830	4390	0.0846
A7	24	49010	3170	0.0647
A8	21	46440	4000	0.0861
A9	20	48280	4210	0.0673
A10	62	49520	4380	0.0885
A11	20	44320	4780	0.1078
A12	20	47060	4670	0.0992
A13	39	44650	4020	0.0900
A14	21	48580	4860	0.1001
A17	21	49870	2910	0.0583
Total Population	314	48290	4160	0.0954

**TABLE IV**  
RESULTS OF TENSILE EVALUATIONS OF PHASE I MACRO SPECIMENS

SRI Run Number	Specimen	Temperature °F	Bulk Density (Mechanics Section) g/cc	Stress Rate psi/sec	Load at Fracture lbs	Fracture Stress psi	Fracture Location Inches from midspan	Sonic Velocity in./µsec	Remarks
T-15	1A03-001-1T	70	3.845	5000	342.3	48390	R	0.3788*	Fracture stress base on gage diameter 0.004 diameter
T-5	-001-2T		3.849		285.8	43770	C	0.3800*	
T-6	-003-1T		3.831		303.8	43770	C	0.3793*	
T-10	-003-2T		3.827		279.0	40200	G	0.3778*	
T-11	-010-1T		3.815		308.0	42090	G	0.3750*	
T-9	-010-2T		3.818		324.8	46790	G	0.3762*	
T-13	-021-1T		3.832		330.0	47550	G	0.3778*	
T-16	-021-2T		3.836		329.3	47440	R-O, 1010	0.3779*	
Mean Value			3.832			45450			
Standard Deviation						2940			
Coefficient of Variation						0.0641			
T-16	2A04-024-1T		3.845		351.0	50580	G	0.3741*	
T-2	-024-2T		3.845		241.0	34730	R-O, 1065	0.3859*	
T-17	-025-1T		3.827		335.3	48310	G	0.3808*	
T-4	-025-2T		3.806		348.0	50140	G	0.3811*	
T-20	-028-1T		3.823		319.5	45170	R-O, 0978	0.3835*	
T-7	-028-2T		3.827		309.8	43770	R-O, 1060	0.3821*	
T-22	-031-1T		3.842		356.8	48520	G	0.3842*	
T-14	-031-2T		3.851		348.5	50250	G	0.3863*	
Mean Value			3.834			46430			
Standard Deviation						5390			
Coefficient of Variation						0.1148			
T-21	2A05-036-1T		3.821		305.3	43030	G	0.3838*	
T-82	-036-2T		3.818		240.0	34580	R-O, 0995	-----	Broken in handling
	-039-1T		-----		-----	-----	G	-----	
T-83	-039-2T		3.822		342.8	42390	G	-----	
T-60	-044-1T		3.784		325.3	46580	G	0.3943*	
T-3	-044-2T		3.841		309.0	44520	G	0.3881*	
T-8	-046-1T		3.835		330.0	47950	G	0.3921*	
T-19	-046-2T		3.846		317.5	45710	G	0.3928*	
T-12	-047-1T		3.869		158.5	22400	G	0.3953*	
T-1	-047-2T		3.865		324.0	46540	G	-----	Fired at 80°C higher temperature Fired at 80°C higher temperature
Mean Value			3.845			44620			
Standard Deviation						4790			
Coefficient of Variation						0.1070			
T-94	2A07-060-1T		3.786		264.5	52520	G	0.4025	
T-68	-060-2T		3.787		317.3	45710	G	0.4200	
T-71	-060-3T		3.786		380.0	51870	G	0.4107	
T-78	-060-4T		3.786		330.0	47550	G	0.4099	Spare
T-95	-064-1T		3.797		338.3	48740	G	0.4120	
T-107	-064-2T		3.798		327.0	47120	R-O, 1065	0.4150	Spare
T-75	-066-1T		3.783		307.5	44310	G	0.4095	
T-29	-068-2T		3.788		306.0	44090	G	0.4115	Spare
T-47	-069-1T		3.793		318.5	45810	G	0.4086	
T-113	-069-2T		3.801		345.0	50140	G	0.4061	
T-27	-069-3T		3.797		339.8	48950	R-O, 0985	0.4058	
	-049-4T		3.802		-----	-----	G	0.4058	Spare broken during gluing
Mean Value			3.793			47870			
Standard Deviation						3870			
Coefficient of Variation						0.0808			
T-59	2A08-070-1T		3.801		282.5	42150	G	0.4144	
T-72	-070-2T		3.801		339.8	48960	G	0.4128	
T-49	-070-3T		3.749		321.0	46260	G	0.4159	
T-79	-073-1T		3.794		348.5	49930	G	0.4076	
T-101	-073-2T		3.800		348.8	50250	G	0.4151	
T-108	-073-3T		3.803		300.0	43230	G	0.4111	
T-67	-080-1T		3.800		344.3	48610	G	0.4114	
T-31	-080-2T		3.789		291.6	42040	R-O, 0985	0.4095	
T-115	-080-3T		3.798		315.0	45300	G	0.4112	
Mean Value			3.794			46420			
Standard Deviation						5400			
Coefficient of Variation						0.0731			
T-70	3A09-083-1T		3.842		338.3	48740	G	0.4135	
T-112	-083-2T		3.836		284.2	40860	G	0.4156	
T-97	-083-3T		3.841		309.8	44030	G	0.4149	
T-89	-083-4T		3.861		364.3	52840	G	0.4177	
T-60	-083-5T		3.840		343.5	49500	G	0.4160	
T-65	-083-6T		3.845		309.0	44530	G	0.4120	
T-24	-085-1T		3.837		300.8	43340	G	0.4151	
T-34	-085-2T		3.835		336.0	48420		0.4175	
Mean Value			3.851			46590			
Standard Deviation						3840			
Coefficient of Variation						0.0626			
T-120	3A10-087-1T		3.833		-----	-----		0.4124	Broken in handling
T-118	-087-2T		3.824		331.5	47770	R-O, 125	0.4088	
T-121	-087-3T		3.833		342.8	49390	G	0.4143	
T-121	-087-4T		3.831		322.5	46470	G	0.4158	
T-35	-087-5T		3.834		322.5	46470	G	0.4118	
T-96	-087-6T		3.837		339.0	48850	G	0.4126	
T-98	-087-7T		3.847		375.0	54040	R-C, 1002	0.4145	
T-77	-087-8T		3.840		304.5	43860	G	0.4262	
T-61	-087-9T		3.837		345.8	49820	G	0.4118	
T-36	-087-10T		3.833		338.6	48520	G	0.4118	
T-91	-087-11T		3.852		381.0	54900	G		Spare
T-26	-087-12T		3.818		304.0	44090	G	0.4110	Spare
Mean Value			3.833			48560			
Standard Deviation						3320			
Coefficient of Variation						0.0724			

TABLE IV (CONTINUED)

SRI Run Number	Specimen	Temperature °F	Bulk Density (Mechanics Section) gm/cm <sup>3</sup>	Stress Rate psi/sec	Load at Fracture lbs	Fracture Stress psi	Fracture Location inches from midspan	Sonic Velocity in./μsec	Remarks
T-37	4A11-089-A1T	70	3.726	9000	-----	-----	-----	-----	Broken during gluing
T-44	-089-A2T		3.775		298.8	41180	G		
T-129	-089-A3T		3.743		308.0	41530	G		
T-130	-089-A4T		3.697		344.8	35230	G		
T-131	-089-A5T		3.738		250.5	40420	G		
T-133	-089-B1T		3.716		342.6	43390			
T-51	-089-B1T		3.668		308.0	44530	G		
T-134	-089-C1T		3.814		308.8	44200	G		
T-103	-089-C2T		3.714		279.0	40200	G		
T-80	-089-C3T		3.794		275.0	39840	G		
T-119	-089-C4T		3.683		278.8	39880	G		
T-62	-089-C5T		3.732		370.0	38910	G		
T-132	-089-C6T		3.714		308.3	43560	G		
T-55	-089-C7T		3.725		340.8	34500	G		Spare
T-66	-089-D1T		3.678		384.0	39020	G		
T-66	-089-E1T		3.739		312.8	48170	R-O, 1008		
	-089-E2T		3.733		-----	-----	-----		Broken during grinding
Y-48	-089-E3T		3.725		318.0	48820	R-O, 1036		
T-73	-089-E4T		3.780		277.5	39990	G		
T-42	-089-E5T		3.742		346.6	49230	R-O, 1033		
T-128	-089-E6T		3.706		321.8	48300	G		
Mean Value			3.730			43170			
Standard Deviation						4270			
Coefficient of Variation						0.1013			
T-84	2A12-095-1T		3.757		324.0	49690	R-O, 1000		
T-125	-095-2T		3.760		348.8	49030	G		
T-117	-095-3T		3.782		344.3	49610	G		
T-87	-095-4T		3.761		348.8	49330	G		
T-106	-095-5T		3.759		338.3	47460	G		
T-127	-095-6T		3.759		325.5	48600	G		
	-095-7T		3.754		-----	-----	-----		Broken in handling
T-49	-095-1T		3.714		312.8	45070	G		
Mean Value			3.753			47880			
Standard Deviation						1820			
Coefficient of Variation						0.0380			
Y-80	5A13-101-1T		3.787		392.5	42180	R-O, 1038		
Y-111	-101-2T		3.677		301.6	43430	R-O, 1046		
T-126	-101-3T		3.784		398.5	43010	G		
T-93	-101-4T		3.760		271.5	39120	G		
	-101-5T		3.747		-----	-----	-----		Broken in handling
T-85	-102-1T		3.733		298.5	43610	R-O, 1044		
T-92	-102-2T		3.788		391.8	43040	G		
T-104	-102-3T		3.781		307.5	44510	G		
T-108	-102-4T		3.786		299.8	43120	R-O, 1000		
T-110	-102-5T		3.783		272.3	39250	R-O, 0965		
T-148	-102-6T		3.794		392.5	42160	G		
	-102-7T		3.794		-----	-----	-----		Broken
T-146	-102-8T		3.791		288.0	41500	G		
Y-145	-102-9T		3.786		252.8	28430	G		
T-147	-102-10T		3.794		381.3	40620	G		
T-99	-103-1T		3.791		296.3	42960	G		
T-118	-103-2T		3.810		339.8	48960	G		
T-64	-103-3T		3.788		302.3	44420	G		
T-124	-103-4T		3.808		237.3	34260	G		
T-81	-103-5T		3.787		288.3	42980	G		
T-139	-103-6T		3.800		278.3	40090	G		
T-128	-103-7T		3.803		240.9	34700	G		
T-137	-103-8T		3.802		295.5	42580	G		
	-103-9T		3.794		-----	-----	-----		Broken in grinder
	-103-10T		3.801		-----	-----	-----		Broken in grinder
Mean Value			3.781			41450			
Standard Deviation						3350			
Coefficient of Variation						0.0811			
T-58	6A19-104-1T		3.837		321.8	48500	G	0.4544	
T-45	-104-2T		3.821		384.0	51010	G	0.4160	
T-43	-104-3T		3.840		323.3	48580	G	0.4082	
T-36	-104-4T		3.838		351.0	50580	G	0.4112	
T-30	-104-5T		3.828		366.0	52760	G	0.4037	
T-23	-104-6T		3.838		378.8	54580	G	0.4101	
T-25	-104-7T		3.839		384.0	51010	G	0.4120	
T-26	-104-8T		3.835		345.0	49710	G	0.4028	
T-63	-106-1T		3.827		346.0	49710	G	0.4054	
T-57	-106-2T		3.861		327.8	47230	R-O, 1004	0.4108	
T-84	-106-3T		3.883		374.3	53930	G	0.4089	
T-62	-106-4T		3.882		344.2	49810	R-O, 1023	0.4003	
Mean Value			3.843			50150			
Standard Deviation						2070			
Coefficient of Variation						0.0521			

TABLE IV (CONTINUED)

SRI Run Number	Specimen	Temperature °F	Bulk Density (Mechanics Section) gm/cm <sup>3</sup>	Stress Rate psi/sec	Load at Fracture lbs	Fracture Stress psi	Fracture Location inches from midspan	Sonic Velocity in./μsec	Remarks
T-35	6A17-107-1T	70	3.806	5000	386.6	41280	G		
T-127	-107-3T		3.804		351.3	50690	G		
T-135	-107-3T		3.807		384.0	55350	G		
T-136	-107-4T		3.807		369.0	44550	G		
T-106	-107-5T		3.806		328.5	47340	R-0.1000		
T-74	-107-6T		3.803		351.0	50580	G		
T-32	-107-7T		3.808		342.8	46320	G		
T-114	-108-1T		3.810		330.0	48850	G		
T-122	-108-2T		3.810		362.3	52200	G		
-----	-108-3T		3.837		-----	-----			Broken during gluing
T-102	-108-4T		3.832		314.3	45260	G		
T-100	-108-5T		3.831		309.8	44630	G		
T-78	-108-6T		3.814		338.3	48740	G		
T-86	-108-7T		3.807		330.8	47660	G		
T-33	-109-1T		3.788		352.5	50780	R-0.1157		
T-30	-109-2T		3.784		351.8	50690	G		
T-46	-109-3T		3.791		345.0	49710	G		
T-41	-109-4T		3.787		346.5	49950	G		
T-65	-108-5T		3.789		345.0	49710	G		
T-99	-109-6T		3.789		311.3	44850	G		
T-53	-108-7T		3.793		331.5	47770	G		
Mean Value			3.806			48500			
Standard Deviation						3200			
Coefficient of Variation						0.0659			

\* Specimen ends camfered (Signal weak due to reduced area causing difficulty in reading output. The values shown should not be used to compare with uncamfered specimens).

\*\* G denotes specimen fractured within the uniform diameter gage section.

-R-0.1010 denotes that the specimen failed in the breakdown radius and the fracture cross section was 0.1010 inches in diameter.

TABLE V

TABLE OF MEAN STRESSES, STANDARD DEVIATIONS, AND  
COEFFICIENTS OF VARIATION FOR PHASE I  
TENSILE DATA ON MACRO SPECIMENS

Specimen Blank Type	Number of Specimens	Mean Fracture Stress	Standard Deviation	Coefficient of Variation
A2	8	45830	2940	0.0641
A4	8	46430	5330	0.1148
A5	9	44620	4790	0.107
A6	--	-----	-----	-----
A7	11	47870	2870	0.0598
A8	9	46420	3400	0.0731
A9	8	46590	3840	0.0824
A10	11	48560	3520	0.0724
A11	19	42170	4270	0.1013
A12	7	47860	1820	0.0380
A13	21	41450	3360	0.0811
A14	12	50250	2670	0.0531
A17	20	48500	3200	0.0659
Total Population	143	46300	4330	0.0935

TABLE VI

SUMMARY OF TENSILE AND FLEXURAL RESULTS ON RADIO SPECIMENS

Specimen Type	Block Type or Drawing No. (Tool Set)	Sonic Velocity (in./in./sec)	No. of Tensile Specimens	Mechanics Bulk Density of Tensile Specimens g./cm <sup>3</sup>	Tensile Strength Standard Deviation Coefficient of Variation	Extrema Values Low and High psi	No. of Flexural Specimens	Mechanics Bulk Density of Flexural Specimens g./cm <sup>3</sup>	Modulus of Rupture Standard Deviation Coefficient of Variation	Extrema Values Low and High psi
I-Tensile	A2 (1)	0.3773 <sup>1</sup>	8	3.83	45,830 2,840 0.064	40,300 49,300	20	3.838	91,450 3,640 0.071	44,020 56,870
II-Tensile	A4 (2)	0.3655 <sup>2</sup>	8	3.83	46,340 5,350 0.115	34,730 59,580	19	3.80	49,810 4,390 0.088	42,160 57,360
III-Tensile	A5 <sup>3</sup> (3)	0.4287 <sup>4</sup>	7	3.85	44,630 4,760 0.107	34,580 49,290	11	3.81	49,740 2,550 0.051	45,840 53,710
I-Compressive	A6 (1)	0.4104 <sup>4</sup>	-	----	-----	-----	14	3.82	51,850 4,390 0.082	44,160 56,650
II-Compressive	A7 (2)	0.3931	11	3.79	47,870 2,870 0.060	44,090 52,520	24	3.81	49,010 3,170 0.065	42,050 53,180
III-Compressive	A8 (3)	0.3977	9	3.79	46,430 5,400 0.073	42,040 59,250	31	3.81	46,440 4,000 0.086	38,680 51,150
I-Flexural	A9 (3)	0.4152	8	3.85	46,590 3,840 0.082	40,980 52,630	20	3.83	48,280 4,210 0.087	34,720 52,730
II-Flexural	A10 (3)	0.4110	11	3.83	48,860 3,550 0.072	43,890 54,900	22	3.83	45,520 4,180 0.089	41,770 58,860
III-Flexural	A11 (4)	-----	19	3.73	42,170 4,270 0.101	34,930 59,930	20	3.78	44,320 4,780 0.108	35,460 59,340
II-Diametral Compression	A12 (2)	-----	7	3.75	47,860 1,820 0.038	45,070 49,950	20	3.78	47,080 4,670 0.098	29,610 52,880
III-Diametral Compression	A13 (5)	-----	21	3.78	41,450 2,390 0.061	34,260 48,960	39	3.80	44,660 4,020 0.090	32,160 50,020
Thin Ring	A14 (6)	0.4109	12	3.84	50,250 2,870 0.053	46,320 54,580	21	3.82	46,530 4,180 0.100	35,020 59,530
Thick Ring	A17 (6)	-----	20	3.81	48,500 3,200 0.064	41,280 55,330	21	3.81	49,870 3,210 0.064	44,720 55,410
			141		46,300 4,390 0.0935	34,360 55,350	312		48,290 4,610 0.0854	29,810 57,380

<sup>1</sup> Tensile specimens only. Specimen ends were cambered. The reduced area weakened the signal causing difficulty in reading in output.

<sup>2</sup> The values shown should not be compared with other groups.

<sup>3</sup> Tensile and Flexural Specimens, but the ends of the tensile specimens were cambered. See Note 1

<sup>4</sup> Tensile specimens only

<sup>5</sup> Thin Tensile and Flexural specimens fired at 60°C higher temperature are not included in values shown. One of the Tensile specimens had a strength of 22,000 psi. Other strength values were nominal

TABLE VII  
RANK CORRELATION TESTS

Test No.	Items Tested	Number of Samples	Z	Correlation Indicated			Confidence Level
				Positive	Negative	Indication Too Weak	
RC 1	Green Density vs Sonic Velocity	42	-1.801		X		92.82%
	(a) Tensile (b) Flexural	158	-6.273		X		>99.99%
RC 2	Green Density vs Cone Angle	45	-0.598			X	
RC 3	Green Density vs Tensile Strength						
	(a) All Blanks	98	3.089	X			99.8%
	(b) Less 11,12,13	55	0.354			X	
(c)	Blanks 11,12,13	43	3.271	X			99.9%
RC 4	Green Density vs Flexural Strength						
	(a) All Blanks	242	3.431	X			99.94%
	(b) Less 11,12,13	188	0.504			X	
(c)	Blanks 11,12,13	54	2.844	X			99.5%
RC 5	Green Density vs Fired Density	37	-1.628			X	
RC 6	Cone Angle vs Sonic Velocity						
	(a) Tensile (b) Flexural	73 191	1.095 -0.520			X X	
RC 7	Cone Angle vs Tensile Strength	122	-4.219		X		>99.99%
RC 8	Cone Angle vs Flexural Strength	293	-8.560		X		>99.99%
RC 9	Cone Angle vs Fired Density						
	(a) Tensile (b) Flexural	130 293	-0.290 18.691	X		X	>99.99%
RC 10	Sonic Velocity vs Tensile Strength	71	0.355			X	
RC 11	Sonic Velocity vs Flexural Strength	193	1.653	X			90.16
RC 12	Sonic Velocity vs Fired Density						
	(a) Tensile (b) Flexural	73 193	0.548 1.680	X		X	90.70
RC 13	Sonic Velocity vs Minimum Thickness						
	(a) Tensile (b) Flexural	73 182	1.043 1.416			X X	
RC 14	Fired Density vs Tensile Strength						
	(a) All Blanks	141	4.085	X			>99.99%
	(b) Less 11,12,13	94	-0.017			X	
(c)	Blanks 11,12,13	47	-0.822			X	
RC 15	Fired Density vs Flexural Strength						
	(a) All Blanks	315	8.681	X			>99.99%
	(b) Less 11,12,13	236	2.421	X			98.4%
(c)	Blanks 11,12,13	79	0.907			X	
RC 16	Minimum Thickness vs Tensile Strength	141	-6.748		X		>99.99%
RC 17	Minimum Thickness vs Flexural Strength	304	-13.530		X		>99.99%
RC 18	Minimum Thickness vs Fired Density	64	-3.727		X		>99.98%

TABLE VIII

## RANK TESTS

Test No	Description	Degrees of Freedom	Statistic	Inference	Confidence Level
RT 1	Tool set effects on green density	5	$\chi^2=22.46$	There are differences in green density due to tool sets	99.5%
RT 2	Reproducibility of Tensile Strength between Blank Types for a given Tool Set				
(a)	Tool Set 2 (Blank Types 4,5,7,8,12)	4	$\chi^2=3.181$	Cannot conclude differences in strength exist	-----
(b)	Tool Set 2 (Blank Types 4,5,7,8)	3	$\chi^2=2.388$	Cannot conclude differences in strength exist	-----
(c)	Tool Set 3 (Blank Types 9 & 10)	8,11	$U=32.0$	Cannot conclude differences in strength exist	-----
(d)	Tool Set 6 (Blank Types 14 & 17)	12,20	$U=82.5$	There are differences in tensile strength of different Blank Types produced from Tool Set 6	90-95%
RT 3	Reproducibility of Flexural Strength between Blank Types for a given Tool Set				
(a)	Tool Set 1 (Blank Types 2 & 6)	14,20	$U=138.5$	Cannot conclude differences in strength exist	-----
(b)	Tool Set 2 (Blank Types 4,5,7,8,12)	4	$\chi^2=11.47$	There are differences in flexural strength of different Blank Types produced from Tool Set 2	97.5-99%
(c)	Tool Set 2 (Blank Types 4,5,7,8)	3	$\chi^2=9.23$	There are differences in flexural strength of different Blank Types produced from Tool Set 2	95-97.5%
(d)	Tool Set 3 (Blank Types 9 & 10)	>20	$z=-1.02$	Cannot conclude differences in strength exist	-----
(e)	Tool Set 6 (Blank Types 14 & 17)	>20	$z=-0.805$	Cannot conclude differences in strength exist	-----
RT 4	Blank type effects on tensile strength				
(a)	All Blanks	11	$\chi^2=62.7$	There are differences in tensile strength between Blank Types	99.5%
(b)	All Blanks less 11,12,13	8	$\chi^2=16.8$	There are differences in tensile strength between blank types	95-97.5%
RT 5	Blank type effects on flexural strength				
(a)	All Blanks	12	$\chi^2=69.9$	There are differences in flexural strength between Blank Types	>99.5%
(b)	All Blanks less 11,12,13	9	$\chi^2=21.0$	There are differences in flexural strength between Blank Types	97.5-99%
RT 6	Blank type effects on fired density				
(a)	All Tensile	11	$\chi^2=111.5$	There are differences in fired density between Blank Types	>>99.5%
(b)	All Tensile less 11,12,13	8	$\chi^2=67.9$		
(c)	All Flexural	12	$\chi^2=197.0$		
(d)	All Flexural less 11,12,13	9	$\chi^2=105.9$		
RT 7	Reproducibility of tensile strength of items within a given blank type				
(a)	A13 Blanks	2	$\chi^2=0.179$	Cannot conclude differences in strength exist	-----
(b)	A17 Blanks	2	$\chi^2=1.08$		
RT 8	Reproducibility of flexural strength of items within a given blank type				
(a)	A02 Blanks	9	$\chi^2=8.38$	Cannot conclude differences in strength exist	-----
(b)	A04 Blanks	6	$\chi^2=3.93$		
(c)	A05 Blanks	4	$\chi^2=7.41$		
(d)	A06 Blanks	6	$\chi^2=5.54$		
(e)	A07 Blanks	6	$\chi^2=9.07$		
(f)	A08 Blanks	4	$\chi^2=2.22$		
(g)	A09 Blanks	2	$\chi^2=1.28$		
(h)	A10 Blanks	26,36	$z=2.60$		
(i)	A12 Blanks	7,13	$U=41.00$		
(j)	A13 Blanks	2	$\chi^2=8.11$		
(k)	A14 Blanks	8,13	$U=28.50$	There are differences in strength between items within Blank Type A14	98%
(l)	A17 Blanks	2	$\chi^2=2.83$	Cannot conclude differences in strength exist	95%
RT 9	Uniformity within Blank 3A-10-088				
(a)	Sections A,B,C,D	3	$\chi^2=1.94$	Cannot conclude differences in strength exist	-----
(b)	Sections A,D	5,5	$U=11$		
(c)	Sections B,C	5,5	$U=11$		
(d)	Sections (A+D), (B+C)	10,10	$U=33$		
				There are differences in strength between ends and center of blank	90.0%



TABLE IX  
FRACTURE STRESS, DENSITY, AND MICROSTRUCTURAL DATA FOR SELECTED MACRO SPECIMENS

WEAR/STRONG STUDY

FLEXURAL SPECIMENS

Specimen No.	Description	FRACTURE STRESS, psi x 10 <sup>-3</sup>			DENSITY, g/cc				CHAIN SIZE			SECOND PHASE		POROSITY FEATURES			
		Individual	Average for Group	Low, High for Group	Average for Group	Individual	Small Piece Vol. Measured	Individual	Average	Largest Grain	% Area Fraction	Average Site Fraction	% Area Fraction	Average Pore Size Microns	Maximum Pore Size Microns	Minimum Pore Size Microns	
FLEXURAL SPECIMENS																	
1	3A09-085-2	52	48	35.53	3.83	3.82	3.82	3.86	3.86	3.1	15-20	5.1	1.9	5.6	1.5	27	220
2	6A14-106-12	57	49	35.57	3.82	3.85	3.84	3.87	3.87	2.8	15-20	6.4	2.0	5.0	1.1	59	830
3	6A14-104-7	35	49	35.57	3.82	3.80	3.84	3.87	3.87	2.9	10-15	6.7	2.0	5.6	1.3	43	430
4	5A13-102-6	50	43	35.50	3.79	3.77	3.81	3.83	3.83	3.3	20-25	4.9	1.9	10.5	1.6	43	1500
5	2A12-096-11	30	47	30.53	3.78	3.77	3.80	3.84	3.84	2.8	10-15	7.7	2.2	6.0	1.1	18	250
6	3A09-085-1	35	48	35.53	3.83	3.82	3.85	3.87	3.87	3.2	20-25	6.4	2.4	5.4	1.2	84	1100
7	4A11-089B-1	38	44	35.50	3.78	3.73	3.80	3.80	3.80	3.1	10-15	7.2	1.7	10.4	1.4	32	450

TENSILE SPECIMENS

Specimen No.	Description	Individual	Average for Group	Low, High for Group	Average for Group	Individual	Small Piece Vol. Measured	Individual	Average	Largest Grain	% Area Fraction	Average Site Fraction	% Area Fraction	Average Pore Size Microns	Maximum Pore Size Microns	Minimum Pore Size Microns
1	5A13-101-4T	39	42	34.49	3.77	3.68	3.81	3.76	-	3.85	3.4	20-25				
2	2A12-085-3T	50	48	45.50	3.75	3.71	3.76	3.78	-	3.84	3.1	15-20				
3	2A05-047-2T	47	45**	25.49	3.83	3.78	3.97	3.87	-	3.86	6.0***	30-35				
4	2A05-047-1T	23	45**	23.49	3.83	3.75	3.87	3.87	-	3.88	6.2***	30-35				
5	4A11-089C-2T	40	42	35.50	3.73	3.67	3.81	3.71	-	3.82	3.0	-				
6	3A09-085-2T	45	47	41.55	3.85	3.84	3.88	3.86	-	3.86	3.6	-				
7	3A10-087-2T	48	49	44.55	3.83	3.82	3.85	3.82	-	3.84	3.6	-				
8	4A11-089A-6T	43	42	35.50	3.73	3.67	3.81	3.73	-	3.80	3.2	-				

NOTES:  
 \* Values taken from Coor's final report, 11-7-57.  
 \*\* Figure 23, Item 154.  
 \*\*\* Does not include 23,000 psi specimen.  
 \*\*\*\* Higher-than-normal firing technique.

NOTES:  
\* Values taken from Coor's final report, 11-7-67,  
Figure 21, Item 164.  
\*\* Does not include 25,000 psi specimen.  
\*\*\* Higher-than-normal firing technique.

TABLE X  
AVERAGE GRAIN INTERCEPT SIZE FOR SELECTED SPECIMENS

Specimen	Fracture Stress $\times 10^{-3}$ psi	Density-gm/cm <sup>3</sup>		Minimum Fired Section in.	Cone 31-1/2 Deformation	Average Grain Intercept Size Microns
		Green	Fired			
1A02-011-1	49	2.52	3.83	0.35	12:30	3.3
1A02-007-1	47	2.52	3.83	0.35	5:00	3.7
1A06-051-2	51	2.60	3.80	0.32	2:00	3.8
2A04-024-1	50	2.59	3.83	0.55	6:00	3.8
2A04-026-2	45	2.55	3.76	0.55	12:30	3.5
2A05-043-1	49	2.53	3.79	0.67	1:00	2.9
2A05-039-2	52	2.57	3.82	0.67	6:30	3.1
2A07-059-1	48	2.61	3.81	0.49	1:00	3.3
2A08-070-2	48	2.62	3.81	0.75	2:00	3.7
2A12-095-3T	50	2.60	3.76	0.88	12:30	3.2
2A12-096-11	30	2.57	3.80	0.88	12:30	3.9
3A09-085-2T	48	2.55	3.86	0.32	2:00	3.6
3A09-085-1	35	2.55	3.82	0.32	2:00	3.8
3A09-085-2	52	2.55	3.82	0.32	2:00	3.8
3A10-087-2T	48	2.52	3.82	1.11	5:00	3.6
3A10-088 (avg.)	48	2.57	3.84	1.11	5:00	3.7
4A11-089A-6T	49	2.55	3.72	1.11	-----	3.5
4A11-089D-1	38	2.55	3.73	1.11	-----	3.7
4A11-089C-2T	40	2.55	3.71	1.11	-----	3.0
5A13-101-4T	39	-----	3.76	1.34	5:00	3.7
5A13-102-6	50	2.55	3.77	1.34	5:00	4.2
6A14-104-7	35	-----	3.83	0.17	1:30	4.1
6A14-106-12	57	2.61	3.83	0.17	1:30	3.9

TABLE XIa  
SPECIMEN DENSITIES  
BLANK 1831-A11-112 SECTION A

Section A - Specimen "Wet" Densities				
3.890	3.877	3.840	3.800	3.888
3.876	3.864	3.853	3.846	3.878
3.822	3.861	3.834	3.844	3.872
3.873	3.836	3.841	3.877	3.876
3.881	3.872	3.864	3.867	3.890

Section A - Specimen "Dry" Densities				
3.858	3.838	3.807	3.851	3.863
3.840	3.826	3.822	3.827	3.846
3.843	3.816	3.807	3.814	3.846
3.839	3.807	3.794	3.846	3.830
3.853	3.843	3.832	3.845	3.857

"Wet"  
Mean = 3.866 gm/cm<sup>3</sup>  
S.D. = .017  
C.O.V. = 0.44%

"Dry"  
Mean = 3.834 gm/cm<sup>3</sup>  
S.D. = 0.018  
C.O.V. = 0.48%

TABLE XIb  
SPECIMEN DENSITIES  
BLANK 1831-A.1-112 SECTION C

Section C - Specimen "Wet" Densities				
3.889	3.868	3.872	3.876	3.890
3.873	3.846	3.842	3.842	3.867
3.868	3.822	3.805	3.824	3.872
3.870	3.818	3.771	3.811	3.867
3.886	3.866	3.845	3.862	3.882

Section C - Specimen "Dry" Densities				
3.854	3.840	3.837	3.840	3.861
3.844	3.813	3.809	3.818	3.843
3.837	3.790	3.775	3.791	3.843
3.835	3.781	3.736	3.785	3.835
3.848	3.835	3.815	3.836	3.856

"Wet"  
Mean = 3.853 gm/cm<sup>3</sup>  
S.D. = 0.030  
C.O.V. = 0.78%

"Dry"  
Mean = 3.823  
S.D. = 0.030  
C.O.V. = 0.79%

TABLE XII

## RESULTS OF FLEXURAL EVALUATION OF "IMPROVED" ALL BLANK

GRI Run Number	Specimen	Temp. °P	Bulk Density gm/cm <sup>3</sup>	Stress Rate psi/sec	Load At Fracture lbs	Fracture Stress psi	Strength Rank**	Fracture Location in. from midspan	Sonic Velocity in./u sec	Remarks
345	4A11-112-A11	70	3.858	5000	69.25	38,800	37	0.00	0.4043	7x5 mil void in fracture.
346	-112-A12		3.858		83.25	47,740		0.03	0.4043	
347	-112-A13		3.857		69.75	38,983		0.15	0.3983	
348	-112-A14		3.857		90.75	45,960		0.20	0.4037	
349	-112-A15		3.863		75.00	42,020	24	0.20	0.4044	Disparate in fracture.
350	-112-A21		3.860		78.00	43,700		0.25	0.4001	
351	-112-A22		3.826		69.00	38,600		0.15	0.3934	
352	-112-A23		3.826		62.00	34,120		0.08	0.3968	Disparate in fracture.
353	-112-A24		3.827		70.00	39,080		0.30	0.4001	
354	-112-A25		3.846		79.75	44,680		0.30	0.4033	
355	-112-A31		3.843		92.00	44,530		0.30	0.4033	
356	-112-A32		3.857		73.25	41,960	31	0.25	0.3985	Disparate in fracture.
357	-112-A33		3.857		51.75	28,240		0.25	0.3964	
358	-112-A34		3.846		81.75	45,000		0.04	0.4010	
359	-112-A35		3.839		82.75	46,380		0.27	0.4005	
360	-112-A41		3.857		76.75	42,910		0.00	0.3985	
361	-112-A42		3.857		66.50	36,320		0.35	0.3959	
362	-112-A43		3.857		69.75	39,610	34	0.33	0.4044	Disparate in fracture.
363	-112-A44		3.839		52.25	34,880		0.12	0.4035	
364	-112-A45		3.843		79.50	44,450	45	0.30	0.4032	12x4 mil void in fracture.
365	-112-A51		3.832		68.50	38,340		0.35	0.3996	
366	-112-A52		3.832		74.50	41,700		0.20	0.4031	
367	-112-A53		3.857		73.75	41,320		0.14	0.4066	
368	-112-A54		3.857							
369	-112-A55		3.857							
Section A										
Mean Value			3.834			41,850			0.4007	
Standard Deviation			0.019			4,290			0.0034	
Coefficient of Variation			0.005			0.1046			0.0084	
374	4A11-112-C11		3.854		83.25	46,590		0.22	0.4075	
375	-112-C12		3.840		65.75	36,970		0.30	0.4036	
376	-112-C13		3.837		75.25	42,700	41	0.10	0.4030	Fracture at location of 5x2 mil void. Void not visible after fracture.
377	-112-C14		3.861		73.75	41,360		0.18	0.4018	
378	-112-C15		3.860		82.50	46,200		0.35	0.4061	
379	-112-C21		3.844		72.25	40,540		0.08	0.4044	
380	-112-C22		3.813		73.00	41,560		0.20	0.4027	
381	-112-C23		3.809		64.50	36,210		0.375	0.3989	
382	-112-C24		3.818		66.50	37,370		0.00	0.4010	Fracture at location of 4 mil surface discontinuity. Discontinuity not visible after fracture.
383	-112-C25		3.843		85.75	48,110	47	0.12	0.4020	
384	-112-C31		3.837		60.75	34,100		0.18	0.4010	
385	-112-C32		3.790		78.50	44,130		0.15	0.3965	
386	-112-C33		3.775		73.75	41,400	27	0.20	0.3970	
387	-112-C34		3.791		76.00	43,830		0.35	0.3994	
388	-112-C35		3.843		78.50	44,050		0.35	0.4043	
389	-112-C41		3.835		76.25	43,990		0.35	0.4027	
390	-112-C42		3.791		64.50	36,230		0.18	0.4004	
391	-112-C43		3.736		53.25	36,560		0.35	0.3979	
392	-112-C44		3.785		78.00	43,740		0.30	0.4013	
393	-112-C45		3.835		76.25	42,680		0.15	0.4038	
394	-112-C51		3.848		80.25	44,920		0.18	0.4091	
395	-112-C52		3.835		75.00	42,230		0.30	0.4020	
396	-112-C53		3.815		48.50	27,160	50	0.375	0.4037	Porous area in fracture.
397	-112-C54		3.836		60.00	33,720		0.15	0.4056	
398	-112-C55		3.856		78.75	44,080	13	0.25	0.4078	High density spot on x-ray.
Section C										
Mean Value			3.823			40,800			0.4024	
Standard Deviation			0.030			4,860			0.0032	
Coefficient of Variation			0.008			0.1194			0.0082	
Combined										
Mean Value			3.829			40,920			0.4016	
Standard Deviation			0.026			4,550			0.0035	
Coefficient of Variation			0.007			0.1111			0.0087	

\* Dimensions of dispartes are nominal and were measured prior to failure.  
 \*\* Strength rank lowest for highest strength. Shown only for specimens which had corresponding dispartes and fracture location.

TABLE XIII

RESULTS OF FLEXURAL EVALUATIONS ON MACHO SPECIMENS FROM BLANK 3A10-088 (SURFACE FINISH)

SRH Run Number	Specimen	Temp. °F	Bulk Density (Mechanics Section) gm/cm <sup>3</sup>	Stress Rate psi/sec	Load at Fracture lbs.	Fracture Stress psi	Fracture Location in. from midspan	Sonic Velocity in./sec	Remarks
316	3A10-088-C11F-A	70		5000	166.3	49220	0.19	} 0.4012	Polished
315	-C11F-B				180.0	53290	0.19		} Polished
312	-C13F-A				167.0	49440	0.0		
317	-C12F-B				166.0	49150	0.0	} 0.4010	} Polished
320	-C13F-A				181.8	53810	0.06		
319	-C13F-B				180.3	53360	0.09	0.4040	Polished
286	-A4				82.5	48450	0.375	} 0.4033	3 RMS
287	-B5				88.0	50100	0.10		4 RMS
292	-C1				89.8	51200	0.15		4 RMS
286	-C2				79.5	45950	0.10	0.4051	3 RMS
294	-C3				82.5	47050	0.15	0.4051	3 RMS
291	-D1				86.3	55050	0.20	0.4055	3 RMS
295	-D2				84.3	45050	0.20	0.4030	3 RMS
293	-D3				78.5	44500	0.10	0.4045	3 RMS
321	-A6		3.856		69.3	38933	0.1	0.4092	} Tension Surface as fired
322	-A7		3.765		72.3	40641	0.15	0.4048	
323	-A8		3.808		81.3	45703	0.375-0.375	0.4045	
324	-A9		3.778		67.5	37969	0.375-0.375	0.4036	

TABLE XIV  
RESULTS OF TENSILE EVALUATIONS OF POLISHED MACRO SPECIMENS REMOVED FROM B'ANK 3A10-088

SRI Run Number	Specimen	Temperature °F	Bulk Density gm/cm <sup>3</sup>	Stress Rate psi/sec	Load at Fracture lbs	Fracture Stress psi	Fracture Location in.	Sonic Velocity in./microsec	Remarks
—	3A10-088-C4	70	3.809	5000	—	—	—	0.4004	3-4 rms
141	-C5		3.812		315.0	45880	0.1	0.4028	"
140	-C14		3.774		319.5	46040	0.1	0.4032	"
142	-C15		3.791		338.0	49760	0.15	0.4004	"
144	-D4		3.802		298.5	43480	0.1	0.3979	"
143	-D5		3.815		318.8	45930	0.1	0.3979	"

Mean Stress = 46220  
Standard Deviation = 2250  
Coefficient of Variation = 0.0487

TABLE XV

## RESULTS OF SURFACE FINISH STUDY ON MACRO SPECIMENS

Surface Condition	Remarks	Flexure psi	Tension psi
pressed and fired (150-175 rms)	Blank 3A10-088	40,820	—
pressed, green machined, and fired	Blank 3A09-085	43,240	—
Ground surface (15 rms) (shop ground)	Blank 3A10-087	47,890	48,560
	Blank 3A10-088	50,620	
Polished surface (3-4 rms) (shop polish)	Blank 3A10-088	48,420	46,220
Polished surface (lapped) (Metallurgically Lapped)	Blank 3A10-088 One-inch specimens taken from two-inch specimen. Alternate ends were evaluated as ground. MOR = 51,930 psi.	50,820	—





**TABLE XVII**  
**RESULTS OF VARIOUS TREATMENTS**

SRI Run No.	Specimen Number	Treatment	Strength psi	Average Strength psi	t	Confidence Level	Inference
P-379 381 383 431 421 419	4A11-112-26 4A11-112-52 4A11-112-27 4A11-112-103 4A11-112-86 4A11-112-73	As Sliced	38,520 39,975 36,710 34,150 35,440 37,960	Avg.=37,125 S.D.=2,127 C.O.V.=0.0573	-3.511 <sup>1</sup>	99(+)%	Strengths differ
P-375 377 380	4A11-112-14 4A11-112-22 4A11-112-37	Modified "Deep Lap"	43,150 40,030 25,275	36,150	-1.12	<80%	Cannot conclude that strengths differ
P-493 490 503 492 489	4A11-112-114 4A11-112-115 4A11-112-116 4A11-112-117 4A11-112-118	Slow Machining Rate (Sliced)	35,395 36,950 33,320 31,330 40,020	37,400	0.21 <sup>2</sup>	<<80%	Cannot conclude that strengths differ
P-487 506 507	4A11-112-143 4A11-112-144 4A11-112-147	Intermediate Machining Rate (Sliced)	38,570 32,140 39,410	35,710	-0.28 <sup>2</sup>	<<80%	Cannot conclude that strengths differ
P-509 502 485	4A11-112-123 4A11-112-124 4A11-112-136	Sand blast Machined	38,950 35,020 33,150	35,710	-0.94 <sup>2</sup>	<85%	Cannot conclude that strengths differ
P-467 468 469 482 470 476 474 480	4A11-112-151 4A11-112-152 4A11-112-153 4A11-112-154 4A11-112-155 4A11-112-156 4A11-112-157 4A11-112-158	Sliced with tangent to wheel normal to specimen centerline	36,390 37,620 32,290 37,750 35,235 36,140 39,830 39,330	36,850	-0.24 <sup>2</sup>	<<80%	Cannot conclude that strengths differ
P-504 488 505 500 503	3A10-088-A10 3A10-088-A11 3A10-088-A12 3A10-088-A13 3A10-088-A14	Sliced "good" material	44,900 47,400 50,520 45,490 43,110	46,280 S.D.=2,280 C.O.V.=0.0609	2.06 <sup>3</sup>	97.5%	Strengths differ
P-471 473 472 475 478 477 479 481	3A10-088-1S 3A10-088-2S 3A10-088-3S 3A10-088-4S 3A10-088-5S 3A10-088-6S 3A10-088-7S 3A10-088-8S	"Good" material sliced with tangent to wheel normal to specimen centerline	35,240 43,990 34,200 43,350 36,150 36,920 35,270 38,635	37,970	-9.34 <sup>4</sup> -4.53 <sup>1</sup>	99(+)% 99%	Strengths differ Strengths differ
P-436 437 435	4A11-112-64 4A11-112-94 4A11-112-84	Etched for 1 hour in hydrofluoric acid (-10 mils deep)	27,650 25,090 25,480	26,070	-7.350 <sup>2</sup>	99(+)%	Strengths differ
P-439 440 441	4A11-112-56 4A11-112-98 4A11-112-83	Etched for 10 minutes in hydrofluoric acid (-5 mils deep)	35,950 31,510 36,660	34,710	-1.461 <sup>2</sup>	80%	Cannot conclude that strengths differ
P-515 513 514	4A11-112-128 4A11-112-131 4A11-112-132	Etched -5 mils and machined -4 mils All over	40,780 35,420 43,210	39,803	1.78 <sup>2</sup> -0.41 <sup>1</sup>	93% <<80%	Strengths differ Cannot conclude that strengths differ
P-512 511 510	4A11-112-113 4A11-112-126 4A11-112-142	Borax machined 2 minutes at 1550°F	36,860 40,435 39,750	39,750	1.74 <sup>2</sup>	92%	Strengths differ
P-516 518 517	3A10-087-A21 3A10-087-B71 3A10-087D13	"Good" specimens and material. Borax machined 2 minutes at 1550°F	42,840 47,010 46,060	45,300	-1.12 <sup>7</sup>	<80%	Cannot conclude that strengths differ
P-376 384 385	4A11-112-17 4A11-112-51 4A11-112-35	Torch "Refire" to ~2000°F	41,200 39,740 35,290	38,740	1.86 <sup>2</sup>	87.5%	Cannot conclude that strengths differ

TABLE XVII (CONTINUED)

SKY Run. No.	Specimen Number	Treatment	Strength psi	Average Strength psi	t	Confidence Level	Inference
P-397 401 395	4A11-112-13 4A11-112-15 4A11-112-54	Torch "Refire" to -2900°F	30,550 35,180 25,640	30,640	-7.68 <sup>1</sup>	99+	Strengths differ
P-387 388 389	4A11-112-46 4A11-112-24 4A11-112-34	2000°F in Air for 5 minutes, furnace cool	37,400 41,300 38,085	38,920	2.08 <sup>2</sup>	91%	Strengths differ
P-486 499 497	4A11-112-122 4A11-112-137 4A11-112-138	2000°F in Air for 1/2 hour, furnace cool	33,950 30,790 37,350	34,030	-2.06 <sup>2</sup>	90%	Strengths differ
P-378 382 386	4A11-112-25 4A11-112-56 4A11-112-55	2000°F in Air for 1 hour, furnace cool	50,960 44,610 44,720	46,760	11.10 <sup>2</sup>	99+	Strengths differ
P-495 496 501	4A11-112-121 4A11-112-125 4A11-112-135	2000°F in Air for 1 hour, furnace cool, (repeat)	37,830 34,430 38,260	36,840	-0.19 <sup>2</sup>	-----	Cannot conclude that strengths differ
P-432 426 418	4A11-112-104 4A11-112-81 4A11-112-92	2000°F in Air for 3 hours, furnace cool	32,700 33,130 35,050	33,620	-2.32 <sup>2</sup>	93%	Strengths differ
P-428 424 420	4A11-112-97 4A11-112-77 4A11-112-82	1900°F in Air for 12 hours, furnace cool	34,830 36,450 33,400	34,900	-1.48 <sup>2</sup>	80%	Cannot conclude that strengths differ
P-433 423 422	4A11-112-74 4A11-112-106 4A11-112-67	1900°F in Air for 168 hours, furnace cool	37,965 36,600 33,210	35,925	-0.80 <sup>2</sup>	<80%	Cannot conclude that strengths differ
P-429 427 423	4A11-112-105 4A11-112-107 4A11-112-87	2000°F in vacuum for 1 hour, furnace cool	32,690 38,490 38,720	36,630	-0.33	<<80%	Cannot conclude that strengths differ
	4A11-112-75 4A11-112-95 4A11-112-85	1750°F in Air for 1 hour. Placed in vacuum hot. Vacuum soaked 24 hrs and broken in vacuum -10 <sup>-6</sup> torr	37,165 32,730 29,860	34,950	-1.25 <sup>2</sup>	<80%	Cannot conclude that strengths differ
	4A11-112-145	660°F in vacuum for 2 hours, soak in vacuum 24 hours -10 <sup>-6</sup> torr	46,435		3.55 <sup>2</sup>	99(+)%	Strengths differ
P-391 400 392	4A11-112-33 4A11-112-32 4A11-112-44	2000°F in vacuum for 1 hr with cyclic longitudinal compressive load	36,320 36,390 34,360	35,660	-1.69 <sup>2</sup>	84%	Cannot conclude that strengths differ
P-498 492 494	3A09-085-9 3A09-085-10 3A09-085-11	Green machined and fired surface	44,400 47,485 41,830	43,240	-0.87 <sup>2</sup>	-----	Cannot conclude that strengths differ

## Notes:

1. Value of t computed using average and standard deviation of ground specimens from this blank. (average strength = 40,920 psi, S.D. = 4550 psi, 50 specimens).
2. Average of t computed using average and standard deviation of as-sliced specimens.
3. 8 mil void in fracture. Strength not included in average.
4. Value of t computed using average strength = 50,680 psi, S.D. = 4460 psi for 36 specimens.
5. Value of t computed using average strength = 48,600 psi, S.D. = 5690 psi for 8 specimens.
6. Value of t computed using average strength = 46,200 psi, S.D. = 2820 psi for 5 specimens.
7. Value of t computed using average strength = 47,890 psi, S.D. 3783 psi for 26 specimens.

TABLE XVIII

## RESULTS OF MACHINING STUDY

SRI RUN NUMBER	SPECIMEN NUMBER	TEST TEMP DEGR F	STRESS RATE PSI/SEC	BULK DENSITY GM/CM <sup>3</sup>	SONIC VELOCITY IN/MICRO SEC	LOAD AT FRACTURE POUNDS	FRACTURE STRESS PSI	FRACTURE LOCATION IN. FROM MIDSPAN	REMARKS
MACHINED BY SRI									
F-634	2A04-031-A01	70	5000	3.818	0.3967	47.00	37690.	0.050	Debris and deviation of crack but no flaw
F-636	2A04-031-A02			3.815	0.3958	92.75	31980.	0.300	20-26 rms surface finish
F-637	2A04-031-A03			3.810	0.3968	76.00	42730.	0.200	4x3.4 subsurface void
F-639	2A04-031-A04			3.815	0.3983	84.00	47200.	0.350	3 mil subsurface void
F-643	2A04-031-A05			3.813	0.3938	83.50	48940.	0.250	2 mil void
F-667	2A04-031-A06			3.817	0.3936	83.75	47200.	0.375	
F-674	2A04-031-A07			3.815	0.3965	83.75	48110.	0.150	
F-696	2A04-031-A08			3.815	0.3980	84.00	47130.	0.375	
F-699	2A04-031-A09			3.817	0.3987	87.25	48980.	0.100	
F-709	2A04-031-A10			3.818	0.3983	70.25	39420.	0.150	
F-721	2A04-031-A11			3.810	0.3971	93.25	50760.	0.050	2 mil void
F-642	2A04-031-A12			3.815	0.3985	87.75	51830.	0.350	20-23 rms surface finish
F-637	2A04-031-A13			3.824	0.3991	74.75	56220.	0.350	
F-656	2A04-031-A14			3.813	0.3965	83.75	52150.	0.100	4 mil void - 2 mils deep
F-647	2A04-035-A01			3.804	0.3981	91.75	51710.	0.050	
F-650	2A04-035-A02			3.805	0.3991	95.00	53500.	0.001	4 mil void
F-651	2A04-035-A03			3.804	0.3997	87.00	50110.	0.300	3x3 mil void - 4 mils deep
F-711	2A04-035-A04			3.800	0.4000	77.25	44980.	0.375	
F-702	2A04-035-A06			0.000	0.0000	0.00	0.	0.000	Broken in handling
F-700	2A04-035-A07			3.805	0.3940	76.50	43010.	0.350	
F-695	2A04-035-A08			3.808	0.4015	82.75	46820.	0.050	2 mil void - 4 mils deep
F-693	2A04-035-A09			3.797	0.4000	55.50	49340.	0.150	
F-687	2A04-035-A10			3.800	0.4000	80.25	46340.	0.150	
F-684	2A04-035-A11			3.809	0.4001	87.75	48330.	0.050	
F-678	2A04-035-A12			3.802	0.4001	82.50	47610.	0.350	
F-682	2A04-035-A13			3.796	0.4012	79.50	45810.	0.150	4x3 mil void - 3 mils deep
F-639	2A04-035-A14			3.810	0.3998	80.75	45330.	0.350	3x2 mil subsurface void - 1 mil below tension surface
				3.809	0.4009	83.50	49349.	0.200	

AVERAGE VALUE	3.809	0.3980	47763.
STANDARD DEVIATION	0.009	0.0023	4098.
COEFFICIENT OF VARIATION	0.002	0.005	0.008

## SPECIMENS FROM BLANK 2A04-031

AVERAGE VALUE	3.815	0.3947	47737.
STANDARD DEVIATION	0.005	0.0017	5086.
COEFFICIENT OF VARIATION	0.001	0.004	0.106

## SPECIMENS FROM BLANK 2A04-035

AVERAGE VALUE	3.803	0.3994	47802.
STANDARD DEVIATION	0.004	0.0021	2928.
COEFFICIENT OF VARIATION	0.001	0.005	0.061

Comparing average strengths  
of specimens from-031 and-035  
 $t = 0.026$   
• Cannot conclude average  
strengths are different

TABLE XVIII (CONTINUED)

SRI RUN NUMBER	SPECIMEN NUMBER	TEST TEMP DEGR F	5 HESS RATE PSI/SEC	BULK DENSITY GM/CM <sup>3</sup>	VELOCITY IN/MICRO SEC	LOAD AT FRACTURE POUNDS	FRACTURE STRESS PSI	FRACTURE LOCATION IN. FROM HIDE PAN	REMARKS
MACHINED BY COORS USING SRI SPECIFICATIONS									
F-714	2A04-024-C01	70	5000	3.807	0.3996	79.78	45220.	0.001	
F-663	2A04-024-C02			3.812	0.3988	92.50	51720.	0.250-0.375	(shallow 4 mil void) <sup>1</sup>
F-668	2A04-024-C03			3.811	0.3979	85.75	48260.	0.375	2 mil void - subsurface
F-677	2A04-024-C04			3.812	0.3978	63.25	35510.	0.001	3x4 mil void - 4 mils deep (strength not in-
F-680	2A04-024-C05			3.814	0.3935	79.50	44560.	0.300	3 mil void - 4 mils deep (cluded in average)
F-681	2A04-024-C06			3.819	0.3994	82.25	46170.	0.200	
F-686	2A04-024-C07			3.812	0.3972	90.50	50400.	0.100	
F-665	2A04-025-C01			3.811	0.4009	80.00	50170.	0.390	25-28 rms surface finish
F-664	2A04-025-C02			3.816	0.4038	75.00	42170.	0.290	(3 mil void)
F-661	2A04-025-C03			3.823	0.4046	90.25	50590.	0.500	
F-660	2A04-025-C04			3.813	0.4000	86.75	48580.	0.100	
F-652	2A04-025-C05			3.814	0.3993	87.50	48830.	0.150	(5 mil void)
F-721	2A04-026-C06			3.816	0.4016	93.50	52330.	0.230	
F-638	2A04-026-C07			3.813	0.3979	83.50	49200.	0.100	3x2 mil void - 3 mils deep
F-644	2A04-026-C01			3.792	0.3973	88.50	52380.	0.290	
F-643	2A04-026-C02			3.789	0.3962	88.75	52740.	0.390	2 mil void
F-722	2A04-026-C03			3.800	0.3986	90.00	50430.	0.250	(3 mil void on chamfer)
F-689	2A04-026-C04			3.797	0.3876	83.75	46970.	0.250	(3x2 mil void)
F-690	2A04-026-C05			3.792	0.3992	83.50	46550.	0.130	23-25 rms surface finish
F-691	2A04-026-C06			3.800	0.3948	78.75	44160.	0.100	
F-675	2A04-026-C07			3.791	0.3973	84.75	47240.	0.375	2 mil void and porous area <sup>2</sup> (3 mil void)
AVERAGE VALUE				3.807	0.3989		48439.		
STANDARD DEVIATION				0.011	0.0027		3004.		
COEFFICIENT OF VARIATION				0.003	0.006		0.082		
MACHINED BY COORS USING OWN SPECIFICATIONS									
F-716	2A04-024-C08	70	5000	3.821	0.3952	75.00	42400.	0.150	
F-697	2A04-024-C09			3.820	0.3989	81.25	45620.	0.375	4 mil void - 3 mils deep
F-698	2A04-024-C10			3.822	0.3903	76.50	43120.	0.001	3 mil void - low on chamfer
F-713	2A04-024-C11			3.821	0.4014	94.25	53590.	0.390	
F-705	2A04-024-C12			3.817	0.4050	76.75	43430.	0.001	
F-717	2A04-024-C13			3.807	0.3982	89.25	50500.	0.330	(3 mil void) 22-25 rms surface finish
F-669	2A04-024-C14			3.817	0.4047	80.25	45390.	0.100	3x2 mil void - 4 mils deep
F-670	2A04-025-C08			3.822	0.4000	83.75	47990.	0.130	(3 mil void)
F-676	2A04-025-C09			3.825	0.4016	86.75	48850.	0.250	(4x3 mil void)
F-679	2A04-025-C10			3.824	0.4026	71.25	40800.	0.300	
F-685	2A04-025-C11			3.818	0.4035	72.00	40820.	0.200	2 mil void near chamfer
F-682	2A04-025-C12			3.818	0.3992	91.25	51740.	0.300	
F-653	2A04-025-C13			3.827	0.4045	35.25	48360.	0.200	
F-641	2A04-025-C14			3.819	0.3982	92.75	53590.	0.290	28-30 rms surface finish
F-648	2A04-026-C09			3.792	0.4009	76.00	41830.	0.375	3 mil subsurface void 0.01 from fracture site
F-718	2A04-026-C10			3.802	0.3950	93.00	51740.	0.390-0.375	
F-719	2A04-026-C11			3.796	0.3974	88.25	49170.	0.150	(2 mil void)
F-706	2A04-026-C12			3.787	0.3996	98.00	55040.	0.050	
F-707	2A04-026-C13			3.787	0.3980	79.00	46500.	0.290	
F-708	2A04-026-C14			3.792	0.3973	87.50	49270.	0.001	
AVERAGE VALUE				3.812	0.3998		47614.		Compared to specimens machined
STANDARD DEVIATION				0.013	0.0031		4623.		by Coors using SRI specifica-
COEFFICIENT OF VARIATION				0.003	0.007		0.097		tions
SPECIMENS FROM BLANK 2A04-024									
AVERAGE VALUE				3.813	0.3989		48136.		t = 0.665
STANDARD DEVIATION				0.006	0.0030		4989.		* Cannot conclude average
COEFFICIENT OF VARIATION				0.001	0.007		0.099		* strengths are different
SPECIMENS FROM BLANK 2A04-025									
AVERAGE VALUE				3.818	0.4014		49324.		Comparing average strengths
STANDARD DEVIATION				0.006	0.0029		4936.		of specimens from 024 and 025
COEFFICIENT OF VARIATION				0.001	0.006		0.089		t = 0.903 $\phi$ = 25
SPECIMENS FROM BLANK 2A04-026									
AVERAGE VALUE				3.784	0.3976		48772.		* Cannot conclude average
STANDARD DEVIATION				0.006	0.0019		3711.		* strengths are different
COEFFICIENT OF VARIATION				0.001	0.004		0.076		t = 1.277 $\phi$ = 25
ALL SPECIMENS MACHINED BY COORS									
AVERAGE VALUE				3.809	0.3993		47719.		Confidence level <90%
STANDARD DEVIATION				0.013	0.0029		4294.		* Cannot conclude average
COEFFICIENT OF VARIATION				0.003	0.007		0.089		* strengths are different
Compared to specimens machined by SRI									
t = 0.257 $\phi$ = 63									
* Cannot conclude average									
* strengths are different									

TABLE XVIII (CONTINUED)

SRI RUN NUMBER	SPECIMEN NUMBER	TEST TEMP DEGR F	STRESS RATE PSI/SEC	BULK DENSITY GM/CM**3	SONIC VELOCITY IN/MICRO SEC	LOAD AT FRACTURE POUNDS	FRACTURE STRESS PSI	FRACTURE LOCATION IN. FROM MIDSPAN	REMARKS
MACHINED BY R AND W PRODUCTS USING SRI SPECIFICATIONS									
F-775	2A04-RW-S01	70	3000	3.802	0.4044	44.25	40090.	0.300	2 mil void Near cheafer
F-800	2A04-RW-S02			3.824	0.4070	79.28	47925.	0.200	
F-802	2A04-RW-S03			3.826	0.4069	64.75	39030.	0.350	
F-770	2A04-RW-S04			3.827	0.4044	70.78	42810.	0.100	
F-768	2A04-RW-S05			3.802	0.4081	75.00	45640.	0.350	
F-789	2A04-RW-S06			3.817	0.4107	73.78	44900.	0.400	4 mil void - .4 mils deep
F-783	2A04-RW-S07			3.809	0.4024	69.50	41940.	0.050	9-12 rms Surface finish
F-782	2A04-RW-S08			3.792	0.4061	82.73	49940.	0.050	
F-774	2A04-RW-S09			3.820	0.4121	73.78	44600.	0.200	2 mil A void
F-776	2A04-RW-S10			3.798	0.4075	80.00	48460.	0.200-0.400	
F-785	2A04-RW-S11			3.805	0.4038	72.00	43520.	0.150	
F-773	2A04-RW-S12			3.826	0.4063	79.28	48030.	0.150	
F-797	2A04-RW-S13			3.795	0.4038	51.00	30860.	0.400	28 mil Irregular void - strength not
F-794	2A04-RW-S14			3.819	0.4075	74.73	43210.	0.375	{ included in average }
F-779	2A04-RW-S15			3.823	0.4097	78.25	47350.	0.100	
F-772	2A04-RW-S16			3.815	0.4099	77.25	46720.	0.400	
F-791	2A04-RW-S17			3.824	0.4094	82.00	49590.	0.001	10-12 rms Surface finish
F-790	2A04-RW-S18			3.817	0.4074	77.73	47120.	0.250	
F-787	2A04-RW-S19			3.825	0.4080	69.25	41790.	0.150	
F-784	2A04-RW-S20			3.823	0.4079	80.00	48460.	0.250	2 mil Subsurface void
AVERAGE VALUE				3.814	0.4072		45431.		
STANDARD DEVIATION				0.012	0.0024		3191.		
COEFFICIENT OF VARIATION				0.003	0.006		0.070		

MACHINED BY R AND W PRODUCTS USING OWN SPECIFICATIONS

F-778	2A04-R-W-M-01	70	3000	3.792	0.4060	80.23	44920.	0.150	
F-793	2A04-R-W-M-02			3.806	0.4049	81.23	45640.	0.300	
F-799	2A04-R-W-M-03			3.818	0.4059	77.75	43490.	0.150	Shallow 4 mil void
F-795	2A04-R-W-M-04			3.820	0.4044	82.00	46150.	0.350	
F-781	2A04-R-W-M-05			3.810	0.4053	77.50	43380.	0.260	11-13 rms Surface finish
F-796	2A04-R-W-M-06			3.814	0.4078	86.25	48570.	0.300	
F-780	2A04-R-W-M-07			3.806	0.4056	82.73	46320.	0.100	
F-788	2A04-R-W-M-08			3.811	0.4072	81.50	46050.	0.200	
F-786	2A04-R-W-M-09			3.783	0.4014	83.25	46780.	0.001	3 mil void
F-777	2A04-R-W-M-10			3.790	0.4021	86.00	49330.	0.030	
F-792	2A04-R-W-M-11			3.808	0.4078	82.25	46130.	0.150	3 mil void - 1.5 Below tension
F-801	2A04-R-W-M-12			3.807	0.4079	82.75	46390.	0.350/0.375	[surface]
F-798	2A04-R-W-M-13			3.802	0.4071	81.50	45330.	0.001	3x2 mil void - 2 mils deep
F-771	2A04-R-W-M-14			3.796	0.4059	67.00	37400.	0.100	Debris & deviation of crack but
F-769	2A04-R-W-M-15			3.808	0.4117	80.50	45150.	0.250	no flaw
F-747	2A04-R-W-M-16			3.773	0.4080	79.00	43700.	0.300	2 mil void
F-766	2A04-R-W-M-17			3.795	0.4083	79.00	44220.	0.150	13-15 rms Surface finish
F-785	2A04-R-W-M-18			3.822	0.4107	73.25	42370.	0.350	4x3 mil void - 4 mils deep
F-764	2A04-R-W-M-19			3.826	0.4090	71.00	39900.	0.150	[5x8 mil void on tension surface]
F-763	2A04-R-W-M-20			3.821	0.4110	73.00	41240.	0.200	[max dimension 17 mils subsurface]
									[strength not included in average]
AVERAGE VALUE				3.805	0.4068		44664.		Compared to average strength of specimens
STANDARD DEVIATION				0.014	0.0026		2517.		machined by R & W Products using GRZ speci-
COEFFICIENT OF VARIATION				0.003	0.006		0.036		fications:

ALL SPECIMENS MACHINED BY R AND W PRODUCTS

AVERAGE VALUE	3.809	0.0070	4463%	Compared to average strength of specimens
STANDARD DEVIATION	0.019	0.0025	3661.	machined by Coors (same fired blanks)
COEFFICIENT OF VARIATION	0.003	0.006	0.061	$t = 3.751$ ; $\phi = 76$ ; confidence level > 99%
				$\therefore$ Average strengths are different

Compared to average strength of specimens machined by SRI (different  $f'$  + blanks)  
 $t = 2.605$ ;  $df = 64$ ; confidence level = 90%  
 $\therefore$  Average strengths are different

**Note:**

1. Flaw description enclosed in parentheses refer to the largest flaws found at locations within the region of high stress, but away from fractures. All others were on fracture faces.

**TABLE XIX**  
**RESULTS OF REFIRING STUDY**

SRI RUN NUMBER	SPECIMEN NUMBER	TEST TEMP DEGR F	STRESS RATE PST/SEC	BULK DENSITY GN/CM <sup>3</sup>	SONIC VELOCITY IN/MICRO SEC	LOAD AT FRACTURE POUNDS	FRACTURE STRESS PSI	FRACTURE LOCATION IN. FROM MIDSPAN	REMARKS
<b>NO TREATMENT</b>									
F-454	3A09-081-14A	70	5000	3.838	0.4101	92.00	52480.	0.150	
F-458	3A09-081-14B			3.847	0.4101	77.50	43250.	0.150	
F-464	3A09-081-13C			3.830	0.3933	90.75	50670.	0.050	
F-457	3A09-082-14A			3.835	0.4041	89.50	47040.	0.100	
F-446	3A09-082-12B			3.835	0.4035	86.50	47910.	0.300	
F-443	3A09-082-14C			3.846	0.4033	89.00	49640.	0.350	
F-463	3A09-084-13A			3.802	0.4031	69.50	39510.	0.350	G.S. = 3.9 μ
F-466	3A09-084-12B			3.839	0.3996	90.00	50020.	0.150	
F-451	3A09-084-23C			3.839	0.3957	88.00	48860.	0.200	
F-448	3A09-084-24C			3.848	0.4041	86.00	47750.	0.375	
AVERAGE VALUE				3.835	0.4026		47712.		
STANDARD DEVIATION				0.016	0.0054		3784.		
COEFFICIENT OF VARIATION				0.003	0.013		0.079		
<b>LAPPED PRIOR TO HYDROGEN REFIRING</b>									
F-452	3A09-081-24A	70	5000	3.845	0.4071	57.00	37370.	0.250	{3 x 6 mil void in Fracture, Strength not included in averages.}
F-414	3A09-081-11C			3.844	0.4008	67.50	45480.	0.100	
F-449	3A09-081-14C			3.849	0.4008	64.50	43900.	0.100	{6-8 rms Surface finish after refiring 1-2 rms before refiring}
F-415	3A09-081-24C			3.845	0.4055	74.25	46900.	0.300	
F-408	3A09-082-11A			3.844	0.4025	75.25	49660.	0.100	
F-467	3A09-082-27A			3.826	0.4063	69.00	46200.	0.200	
F-406	3A09-082-23B			3.830	0.4036	61.50	41120.	0.350	5-7 rms Surface finish after refiring
F-413	3A09-084-24A			3.853	0.3953	59.50	38790.	0.100	{G.S. = 3.8 μ, 2x4 mil void in fracture}
F-444	3A09-084-12A			3.848	0.4035	54.00	35560.	0.150	{7.5 mil void in high stress region}
F-461	3A09-084-21C			3.850	0.4033	77.50	51710.	0.200	
AVERAGE VALUE				3.843	0.4028		43839.		
STANDARD DEVIATION				0.009	0.0034		5309.		
COEFFICIENT OF VARIATION				0.002	0.008		0.125		Compared to Specimens with No Treatment t = -1.473, φ = 17 Cannot Conclude Average Strengths Are Different
<b>HYDROGEN REFIED</b>									
F-447	3A09-081-21A	70	5000	3.846	0.4059	75.00	41850.	0.150	
F-453	3A09-081-23B			3.831	0.3988	80.25	45160.	0.000	
F-411	3A09-081-21C			3.845	0.4053	78.75	44090.	0.150	
F-412	3A09-082-17A			3.824	0.4043	85.00	47500.	0.250	
F-450	3A09-082-23A			3.834	0.4033	86.25	48100.	0.100	
F-402	3A09-082-24A			3.841	0.4025	73.75	41280.	0.250	{Large Chip on Edge, Strength not Included in Averages}
F-410	3A09-082-23C			3.830	0.4013	91.50	51330.	0.200	G.S. = 3.9 μ
F-405	3A09-084-21A			3.852	0.3992	79.75	44760.	0.000	
F-416	3A09-084-23B			3.840	0.4033	85.75	48160.	0.200	
F-416	3A09-084-12C			3.829	0.3997	74.00	41450.	0.050	
AVERAGE VALUE				3.837	0.4019		45368.		
STANDARD DEVIATION				0.010	0.0032		3363.		
COEFFICIENT OF VARIATION				0.002	0.008		0.074		Compared to Specimens with No Treatment t = -1.173, φ = 17 Cannot Conclude Average Strengths Are Different
<b>OXYGEN REFIED</b>									
F-403	3A09-081-12A	70	5000	3.831	0.3996	84.00	47060.	0.200	
F-404	3A09-081-11B			3.840	0.4025	84.75	47520.	0.150	
F-456	3A09-081-12B			3.838	0.4005	86.25	48180.	0.250	
F-459	3A09-082-11B			3.844	0.4043	79.50	44210.	0.100	
F-417	3A09-082-13C			3.834	0.4079	81.50	49520.	0.150	
F-435	3A09-082-22C			3.830	0.4031	76.00	42490.	0.050	
F-445	3A09-084-13B			3.841	0.3980	75.50	41820.	0.250	
F-445	3A09-084-14B			3.853	0.4051	78.00	43440.	0.050	
F-407	3A09-084-24B			3.848	0.4027	81.75	45550.	0.000	
F-409	3A09-084-13C			3.840	0.3976	89.50	58720.	0.150	G.S. = 3.8 μ
AVERAGE VALUE				3.839	0.4021		44452.		
STANDARD DEVIATION				0.008	0.0032		2928.		
COEFFICIENT OF VARIATION				0.002	0.008		0.065		Compared to Specimens with No Treatment t = -2.151, φ = 18 Average Strengths Are Different, Confidence Level = 95%
<b>ALL SPECIMENS FROM BLANK 3A09-081</b>									
AVERAGE VALUE				3.840	0.4030		49813.		
STANDARD DEVIATION				0.006	0.0048		3975.		
COEFFICIENT OF VARIATION				0.002	0.012		0.086		Comparing Specimens from 081 and 082 t = 0.167, φ = 22 Cannot Conclude Average Strengths are Different
<b>ALL SPECIMENS FROM BLANK 3A09-082</b>									
AVERAGE VALUE				3.834	0.4038		48310.		
STANDARD DEVIATION				0.009	0.0017		3285.		
COEFFICIENT OF VARIATION				0.002	0.004		0.070		Comparing Specimens from 082 and 084 t = 1.732, φ = 24 Average Strengths are Different, Confidence level 90%
<b>ALL SPECIMENS FROM PLANK 3A09-084</b>									
AVERAGE VALUE				3.841	0.4004		44009.		
STANDARD DEVIATION				0.014	0.0035		4896.		
COEFFICIENT OF VARIATION				0.003	0.008		0.111		Comparing Specimens from 081 and 084 t = 1.566, φ = 24 Confidence level = 85% Cannot Conclude Average Strengths are Different

**TABLE XX**  
**RESULTS OF ENVIRONMENT STUDY**

SRI RUN NUMBER	SPECIMEN NUMBER	TEST TEMP DEGR F	STRESS RATE PSI/SEC	BULK DENSITY GM/CM <sup>3</sup>	SONIC VELOCITY IN/MICRO SEC	LOAD AT FRACTURE POUNDS	FRACTURE STRESS PSI	FRACTURE LOCATION IN. FROM MIDSPAN	REMARKS
VACUUM DRIED AT 2000 DEGREES F AND TESTED DRY									
F-736	3A10-087-A12	70	5000	3.825	0.4000	73.00	40800.	0.100	3 mil porous area
F-742	3A10-087-A22			3.830	0.4016	89.75	50980.	0.090	6 x 4 mil void on chamfer
F-725	3A10-087-A31			3.832	0.3998	91.25	51100.	0.430	3 mil porous area
F-734	3A10-087-A41			3.848	0.4016	83.75	46800.	0.300	porous area
F-723	3A10-087-B14			3.843	0.4035	109.50	60500.	0.390+0.460	2 mil void at each fracture
F-724	3A10-087-B21			3.832	0.4025	74.25	41290.	0.200	5 mil porous area
F-731	3A10-087-B22			3.828	0.4019	95.50	53320.	0.090	2 mil void
F-737	3A10-087-B24			3.833	0.4022	94.00	52120.	0.300	2 mil void 1/2 mil below tension surface
F-732	3A10-087-B32			3.827	0.4027	87.50	44640.	0.050	2 x 3 mil void
F-728	3A10-087-B33			3.830	0.4005	98.75	54860.	0.050	
F-740	3A10-087-B42			3.826	0.4030	90.50	50580.	0.200	
F-730	3A10-087-B43			3.829	0.4001	102.50	57480.	0.200	
F-729	3A10-087-B51			3.842	0.4039	90.75	50970.	0.430	6 x 3 glassy incl and porous area
F-726	3A10-087-B62			3.832	0.4025	97.75	54570.	0.150	
F-734	3A10-087-C23			3.831	0.4000	74.75	41840.	0.030	3 x 2 void
F-727	3A10-087-C33			3.832	0.4008	94.00	52640.	0.300	debris at fracture site but no identifiable flaw
F-735	3A10-087-C41			3.832	0.4000	94.00	52510.	0.200	3 mil void
F-735	3A10-087-D12			3.832	0.4000	94.00	52510.	0.150	3 x 2 mil void
F-741	3A10-087-D42			3.824	0.4000	101.50	56160.	0.100	Shallow 5 x 4 mil void
F-739	3A10-087-D51			3.848	0.4032	100.75	56350.	0.200	3 mil void - 1 mil below tension surface
AVERAGE VALUE				3.832	0.4016		50757.		
STANDARD DEVIATION				0.009	0.0016		5382.		
COEFFICIENT OF VARIATION				0.002	0.004		0.109		
VACUUM DRIED AT 2000 DEGREES F, STORED 2 WEEKS, AT 100 RH									
F-749	3A10-087-A24	70	5000	3.833	0.4030	87.25	48420.	0.300	
F-746	3A10-087-A33			3.830	0.4001	85.00	47830.	0.100	
F-748	3A10-087-A42			3.843	0.4030	95.75	53540.	0.150	
F-744	3A10-087-A43			3.838	0.4037	81.00	45980.	0.200	porous area(?)
F-753	3A10-087-B44			3.832	0.3998	84.50	46870.	0.420	2 - 3 mil crack(?)
F-747	3A10-087-B54			3.830	0.4030	79.25	43960.	0.250	6 mil irregular void
F-751	3A10-087-B64			3.825	0.3999	76.25	42700.	0.250	porous area(?)
F-761	3A10-087-C11			3.841	0.4035	80.75	45130.	0.375	
F-756	3A10-087-C14			3.847	0.4035	91.75	51200.	0.300	
F-760	3A10-087-C24			3.836	0.4032	83.25	46410.	0.150	2 mil void
F-750	3A10-087-C32			3.829	0.4017	77.00	43640.	0.300	4 mil void just below chamfer
F-754	3A10-087-C61			3.852	0.4035	86.75	48690.	0.420	
F-745	3A10-087-C63			3.851	0.4032	86.00	48160.	0.200	2 mil void near chamfer
F-755	3A10-087-D11			3.840	0.4017	82.00	43800.	0.200	6 x 4 void at chamfer
F-758	3A10-087-D21			3.838	0.4014	84.25	47060.	0.300	5 mil porous area(?)
F-762	3A10-087-D22			3.825	0.4012	75.50	42170.	0.150	6 mil porous area
F-743	3A10-087-D23			3.830	0.4025	70.75	39500.	0.300	3 mil void tangent to surface
F-757	3A10-087-D31			3.839	0.4027	80.50	49120.	0.350	3 mil porous area
F-752	3A10-087-D33			3.832	0.4024	85.25	46970.	0.250	
F-759	3A10-087-D52			3.846	0.4037	83.75	46940.	0.250	4 mil irregular void
AVERAGE VALUE				3.836	0.4023		46229.		
STANDARD DEVIATION				0.009	0.0014		3120.		
COEFFICIENT OF VARIATION				0.002	0.003		0.067		
VACUUM DRIED, ULTRASONICALLY CLEANED AND OVEN DRIED									
F-645	3A10-087-A44	70	5000	3.849	0.4035	77.00	44895.	0.300	2 mil void - 3 mils deep
F-672	3A10-087-B52			3.827	0.4030	79.00	44040.	0.150	
F-710	3A10-087-C12			3.837	0.4032	81.50	45920.	0.150	
F-658	3A10-087-C22			3.828	0.4024	75.25	42100.	0.150	3 mil void - 4 mils deep
F-712	3A10-087-C34			3.830	0.4030	76.25	42830.	0.350	3 mil void at chamfer
F-704	3A10-087-C42			3.828	0.4000	60.00	44800.	0.200	
F-673	3A10-087-C53			3.828	0.4001	70.00	39140.	0.150	
F-671	3A10-087-C54			3.834	0.4025	85.25	47600.	0.100	4 x 3 mil void - 2 mils deep
F-646	3A10-087-D43			3.827	0.4030	76.50	42820.	0.200	4 x 3 mil void - 2 mils deep
F-720	3A10-087-D53			3.844	0.4033	68.75	49550.	0.200	
AVERAGE VALUE				3.833	0.4023		44359.		
STANDARD DEVIATION				0.008	0.0013		2929.		
COEFFICIENT OF VARIATION				0.002	0.003		0.066		
VACUUM DRIED AND STORED AT ROOM CONDITIONS FOR 2 WEEKS									
F-640	3A10-087-A13	70	5000	3.828	0.4003	72.00	42940.	0.300	4 x 2 mil void - 4 mils deep
F-703	3A10-087-A14			3.833	0.4004	79.75	44220.	0.150	4 mil void - 2 mils deep
F-683	3A10-087-A34			3.834	0.4020	52.00	45370.	0.375	
F-649	3A10-087-B15			3.839	0.4037	77.75	43260.	0.375	2 mil void at chamfer
F-688	3A10-087-B23			3.830	0.4030	85.75	47990.	0.200	
F-715	3A10-087-B34			3.831	0.4030	74.00	41030.	0.300	4 mil porous area - Crack (?)
F-655	3A10-087-B41			3.838	0.4016	87.75	46890.	0.150	
F-607	3A10-087-C54			3.839	0.4008	89.00	49610.	0.200	
F-694	3A10-087-C52			3.829	0.4003	73.75	41220.	0.100	3 mil subsurface void
F-652	3A10-087-C64			3.833	0.4035	83.75	46690.	0.350	
AVERAGE VALUE				3.839	0.4018		45073.		
STANDARD DEVIATION				0.008	0.0014		3129.		
COEFFICIENT OF VARIATION				0.002	0.003		0.069		

TABLE XXI  
ENVIRONMENT STUDY STATISTICAL COMPARISONS

Treatment No.	Treatment Description	No. of spec	Average strength, psi	Standard deviation
1	Previous evaluations from this blank	26	47,890	3,783
2	Dried in vacuum (2.1 $\mu$ ) at 1800°F for 2 hours stored in desiccator with relative humidity >0.2% for two weeks. Evaluated in dry nitrogen atmosphere	20	50,798	5,581
3	Dried in vacuum as above. Stored in desiccator with relative humidity = 100% for two weeks. Removed from desiccator one at a time and evaluated at lab conditions.	20	46,230	3,119
4	Dried in vacuum as above. Ultrasonically cleaned and oven dried at 235°F (usual lab procedure)	10	44,359	2,929
5	Dried in vacuum as above. Stored at room conditions for two weeks and evaluated	10	45,074	3,129

Treatments compared	Student's t	Degrees of freedom, $\phi$	Confidence level	Inference
1 and 2	+2.003	44	95%	Averages are different
1 and 3	-1.630	44	89%	Cannot conclude averages differ
1 and 4	-2.975	34	99% (+)	Averages are different
1 and 5	-2.277	34	97%	Averages are different
2 and 3	-3.195	38	99% (+)	Averages are different
2 and 4	-4.143	28	99% (+)	Averages are different
2 and 5	-3.594	28	99% (+)	Averages are different
3 and 4	-1.614	28	<88%	Cannot conclude averages differ
3 and 5	-0.955	28	--	Cannot conclude averages differ
4 and 5	+0.528	18	--	Cannot conclude averages differ
3 and 4, 5 lumped	1.541	37	<84%	Cannot conclude averages differ



TABLE XXII

FIRING ANALYSIS DATA - SOUTHERN RESEARCH INSTITUTE PO-16-91551

Item No.	Coors Specimen Number	SR: Part No. (No./Order)	Date fired	L-33/Min Car No.	Location on Loin Car and Bung No.	Green Density g/cm <sup>3</sup>	Core Deformation		Core Fired Density	SR: Piecewise Specimen Density	X ray	Coors Crystal Size		SR: Piecewise Avg. Grain Size, $\mu$	Vacuum	Pressing <sup>a</sup>		Tool Set No.	No. of Piecewise Specimens
							314	32				Range	Average			Steel	Caps		
115	12-2	1831-A-7	10-16-70	16	R-30	2.52	T	4.00	1.30	3.85	Good	2-25	4-6		No	Yes	Steel	2	
116	13-1	1831-A-7	10-16-70	16	R-30	2.50	T	4.00	1.30	3.84	Good	2-25	4-6		No	Yes	Steel	2	
117	14-1	1831-A-7	10-16-70	16	R-32	2.51	T	3.15	1.15	3.84	Good	2-20	5-7	6.2	No	Yes	Steel	2	4
118	14-2	1831-A-7	10-16-70	16	R-31	2.52	T	2.45	1.09	3.85	Good	2-25	4-6		No	Yes	Steel	2	
119	24-2	1831-A-7	10-16-70	16	R-33	2.51	T	3.00	1.15	3.85	Good	2-25	4-6		No	Yes	Steel	1	5
120	16-1	1831-A-9	10-16-70	16	L-7	2.50	B	9.00	7.00	3.84	Good	2-30	5-7	5.3	No	Yes	Steel	3	
121	19-1	1831-A-9	10-16-70	16	L-8	2.53	B	9.00	7.00	3.86	Low Density	2-25	5-7		No	Yes	Steel	3	
122	18	1831-A-10	10-16-70	16	L-4	2.51	B	9.00	7.00	3.84	Good	2-30	5-7		No	Yes	Steel	3	
123	28	1831-A-11	10-20-70	16	Center	2.53	EC	2.00	12.30	3.83	Low Density	2-30	5-7		No	Yes	Rubber	4	
124	29	1831-A-11	10-20-70	16	Center	2.52	EC	2.00	12.30	3.84	Good	2-30	5-7		No	Yes	Rubber	4	
125	30	1831-A-11	10-20-70	16	Center	2.49	EC	2.00	12.30	3.83	Low Density	2-25	3-5	1.7	No	Yes	Rubber	4	5
126	21	1831-A-13	10-20-70	15	L-6	2.53	B	9.00	7.15	3.84	Good	2-25	5-7		Yes	No	Rubber	5	
127	22	1831-A-13	10-20-70	16	L-4	2.47	B	9.00	7.00	3.84	Good	2-30	5-7	4.7	Yes	No	Rubber	5	5
128	1-11	MOR Bars Green Mach.	10-16-70	16	LC-12		T	3.30	1.30	3.88	3.832				No	Yes	Steel	-	2
129	12-25	MOR Bars Green Mach.	10-16-70	16	RC-21		T	2.15	1.15		3.816				No	Yes	Steel	-	1
130	26-40	MOR Bars Green Mach.	10-16-70	16	LC-13		T	3.00	1.15		3.828				No	Yes	Steel	-	2
131	41-55	MOR Bars as pressed	10-16-70	16	RC-22		T	3.15	1.15		3.823				No	Yes	Steel	-	2
132	56-58	MOR Bars as pressed	10-16-70	16	LC-14		T	2.45	1.30		3.825			5.2	No	Yes	Steel	-	1
133	69-83	MOR Bars Green Mach.	10-21-70	15	Ref. Left Rear V		FV	0.00	1.00		3.867				No	Yes	Steel	-	5
134	84-97	MOR Bars as pressed	10-21-70	15	Ref. Left Rear V		TV	9.00	5.00	No. 97				5.2	No	Yes	Steel	-	6
135	157							12.30		3.838				3.5					2
136	20-1	1831-A-9						9.00		3.859				5.2					3
137		1831-A-9		(L-29)		2.57		3.18		3.851				3.4	3.9				3
138	4 <sup>a</sup>		2-13-71	(L-50)		2.54		4.00		3.810				2.6	3.0				3
139	13-1 <sup>a</sup>	1831-A7-2	2-24-71	(L-50)				2.00			Visual Crack								2
140	14-1 <sup>a</sup>	1831-A7-3	2-24-71	(L-50)				6.00						3.6					2
141	15-1 <sup>a</sup>	1831-A7-4	2-24-71	(L-50)		2.55		2.00						3.4					2
142	16-1 <sup>a</sup>	1831-A7-5	2-24-71	(L-50)				1.00		3.839				3.5					2
143	16-1 <sup>a</sup>	1831-A9	2-24-71	(L-50)				5.30		3.870									3
144	16-2 <sup>a</sup>	1831-A9	2-24-71	(L-50)		2.54		5.30		3.839				3.8	3.5				3
145	16-3 <sup>a</sup>	1831-A9	2-24-71	(L-50)				4.30		3.863									3
146	16-4 <sup>a</sup>	1831-A9	2-24-71	(L-50)				2.00		3.861									3
147	16-19	1831-A13	2-24-71	(L-50)				1.00		3.803									5
148	16-21	1831-A13	2-24-71	(L-50)		2.50		5.30		3.847				2.8	3.1				5
149	16-23	1831-A13	4-02-71			2.52		2.00	12.30	3.871				3.63	4.2				5
150	16-24	1831-A13	4-02-71			2.54		6.00	12.30	3.889				3.65					5
151	16-52	1831-A25				2.59		1.30		3.800				3.8	4.7				5
152	16-53	1831-A26				2.65		1.00		3.856				3.7	6.2				5
153	16-54	1831-A27				3.64		1.00		3.871				3.5	3.6				5

## Notes:

- Vacuum was used with rubber shell only
- R, RC, LC, L, designates right, right center, left center, and left
- B, BC, BCP, BCL, T, designates bottom bottom center, bottom center front, bottom center rear, and top
- FV, RV, TV, cones placed and read in this order: in front of V refractory on bottom, to rear of V refractory on bottom, and on top of V refractory stack on top of car
- Density tests run on a piece cut-off from the part after firing, except on 1831-A-7, a small disc was fired along with the part
- All parts pressed at 30,000 psi
- Density by weight and micrometer measurements, except as noted by 7
- Density by immersion
- KAD997B material, which is a mixture of 3 parts of KAD997A and 2 parts of PS-144-1
- KAD997C material, which is a mixture of 2 parts of KAD997A and 3 parts of PS-144-1
- Mixture of 1 part of KAD997A and 4 parts of PS-144-1
- Mixture of 1 part each of PS-144-1 and PS-176-5
- 100% PS-144-1
- PS-144-1 and PS-176-5 were made from the identical powder used for KAD997A, but used different binders

**TABLE XXIII**  
FLEXURE STRENGTH OF FIRED TO SIZE MACRO SPECIMENS

SRI RUN NUMBER	SPECIMEN NUMBER	TEST TEMP DEGR F	STRESS RATE PSI/SEC	BULK DENSITY GM/CM**3	SONIC VELOCITY IN/MICRO SEC	LOAD AT FRACTURE POUNDS	FRACTURE STRESS PSI	FRACTURE LOCATION IN. FROM MIDSPAN	REMARKS
AS PRESSED FIRST FIRING, AS FIRED SURFACE									
F-519	MOR-131-49	70	5000	3.852	0.3962	75.50	34690.	0.300+0.350	
F-520	MOR-131-65			3.859	0.3972	60.75	27520.	0.300	
AVERAGE VALUE				3.855	0.3967		31084.		
STANDARD DEVIATION				0.005	0.0007		5041.		
COEFFICIENT OF VARIATION				0.001	0.001		0.162		
GREEN MACHINED FIRST FIRING, AS FIRED SURFACE									
F-524	MOR-128-04	70	5000	3.869	0.4036	68.00	36470.	0.150	
F-523	MOR-129-24			3.866	0.4049	90.50	41730.	0.350	
F-528	MOR-130-37			3.857	0.4033	77.00	39700.	0.000	
AVERAGE VALUE				3.857	0.4039		39299.		
STANDARD DEVIATION				0.012	0.0008		2652.		
COEFFICIENT OF VARIATION				0.003	0.002		0.067		
AS PRESSED SECOND FIRING, AS FIRED SURFACE									
F-521	MOR-134-86	70	5000	3.894	0.4048	53.00	28975.	0.200	
F-525	MOR-134-88			3.892	0.4000	73.00	34260.	0.100	G.S. = 5.2 μ
F-522	MOR-134-92			3.895	0.4025	67.25	34590.	0.350	
AVERAGE VALUE				3.893	0.4036		32608.		
STANDARD DEVIATION				0.002	0.0016		3152.		
COEFFICIENT OF VARIATION				0.000	0.004		0.096		
GREEN MACHINED SECOND FIRING, AS FIRED SURFACE									
F-526	MOR-133-72	70	5000	3.899	0.4125	84.50	43840.	0.200	
F-527	MOR-133-83			3.903	0.4043	70.00	37900.	0.000	
AVERAGE VALUE				3.900	0.4083		40870.		
STANDARD DEVIATION				0.004	0.0058		4200.		
COEFFICIENT OF VARIATION				0.001	0.014		0.102		
GREEN MACHINED FIRST FIRING, MACHINED ALL OVER									
F-585	MOR-128-06	70	5000	3.826	0.4060	64.20	46340.	0.200	
F-585	MOR-130-33			3.829	0.3987	70.00	50640.	0.200	
AVERAGE VALUE				3.827	0.4023		46490.		
STANDARD DEVIATION				0.003	0.0051		3040.		
COEFFICIENT OF VARIATION				0.000	0.012		0.062		
AS PRESSED FIRST FIRING, MACHINED ALL OVER									
F-579	MOR-131-52	70	5000	3.814	0.3952	69.80	50660.	0.250	
F-569	MOR-132-51			3.820	0.3987	68.00	49190.	0.050	G.S. = 5.2 μ
AVERAGE VALUE				3.816	0.3969		49925.		
STANDARD DEVIATION				0.003	0.0024		1039.		
COEFFICIENT OF VARIATION				0.001	0.006		0.020		
GREEN MACHINED SECOND FIRING, MACHINED ALL OVER									
F-591	MOR-133-75	70	5000	3.866	0.4093	41.80	44730.	0.400	
F-570	MOR-133-78			3.858	0.4021	67.60	48920.	0.250	
F-592	MOR-133-82			3.871	0.4035	64.60	46800.	0.100	
AVERAGE VALUE				3.864	0.4050		46816.		
STANDARD DEVIATION				0.007	0.0039		2095.		
COEFFICIENT OF VARIATION				0.001	0.009		0.044		
AS PRESSED SECOND FIRING, MACHINED ALL OVER									
F-583	MOR-134-85	70	5000	3.845	0.4037	57.20	41420.	0.300	
F-588	MOR-134-91			3.866	0.4048	72.00	52260.	0.180	
F-594	MOR-134-96			3.861	0.4101	57.80	41970.	0.000	
AVERAGE VALUE				3.857	0.4061		45216.		
STANDARD DEVIATION				0.011	0.0034		4106.		
COEFFICIENT OF VARIATION				0.002	0.008		0.135		

**TABLE XXIV**  
RESULTS OF LOT-TO-LOT REPRODUCIBILITY AND UPGRADE STUDY

SRI RUN NUMBER	SPECIMEN NUMBER	TEST TEMP DEGR F	STRESS RATE PSI/SEC	BULK DENSITY G/CM <sup>3</sup>	SONIC VELOCITY IN/MICRO SEC	LOAD-AT FRACTURE POUNDS	FRACTURE STRESS PSI	FRACTURE LOCATION IN. FROM MIDSPAN	REMARKS
F-544	2A07-117-01	70	5000	3.794	0.3963	76.00	42355.	0.350	
F-546	2A07-117-02			3.798	0.3971	76.00	42320.	0.350	
F-547	2A07-117-03			3.810	0.3998	66.00	36775.	0.400	
F-545	2A07-117-04			3.804	0.3979	84.50	47175.	0.200	G.S. = 4.2 μ
AVERAGE VALUE				3.800	0.3977		42176.		
STANDARD DEVIATION				0.007	0.0015		4255.		
COEFFICIENT OF VARIATION				0.002	0.003		0.100		
F-608	2A07-140-01	70	5000	3.807	0.3995	84.75	47940.	0.050	
F-604	2A07-140-02			3.808	0.3932	83.00	50020.	0.300	G.S. = 3.6 μ
F-614	2A07-140-03			3.810	0.3908	81.25	46140.	0.050	
F-609	2A07-140-04			3.809	0.3969	38.50	33345.	0.100	Flaw very strongly suspected but was not detectable in the fracture.
AVERAGE VALUE				3.808	0.3950		44371.		
STANDARD DEVIATION				0.003	0.0038		7318.		
COEFFICIENT OF VARIATION				0.000	0.009		0.169		
F-560	2A07-141-01	70	5000	3.804	0.3937	66.80	38170.	0.300	6 mil void in fracture. Strength not included in average.
F-562	2A07-141-02			3.799	0.3933	85.40	48520.	0.050	
F-556	2A07-141-03			3.792	0.3930	66.20	46440.	0.350	G.S. = 3.4 μ
F-563	2A07-141-04			3.798	0.3952	68.50	41500.	0.180	
AVERAGE VALUE				3.799	0.3937		45419.		
STANDARD DEVIATION				0.004	0.0010		3716.		
COEFFICIENT OF VARIATION				0.001	0.002		0.081		
F-611	2A07-142-02	70	5000	3.803	0.3972	93.25	52555.	0.300	G.S. = 3.5 μ
F-613	2A07-142-01			3.795	0.3997	84.00	47725.	0.200	
F-601	2A07-142-03			3.801	0.3959	93.25	53210.	0.040	
F-605	2A07-142-04			3.799	0.3921	73.50	41980.	0.300	6 mil void in fracture. Strength not included in average.
AVERAGE VALUE				3.798	0.3962		51096.		
STANDARD DEVIATION				0.005	0.0031		2951.		
COEFFICIENT OF VARIATION				0.001	0.008		0.037		Average strength for -140, -141, and -142.
F-530	3A09-120-12	70	5000	3.796	0.4042	45.50	36310.	0.250	5 mil void in fracture G.S. = 5.5 μ
F-531	3A09-120-13			3.798	0.4044	81.75	45330.	0.375	
F-529	3A09-120-21			3.826	0.4050	83.50	44590.	0.100	
F-532	3A09-120-23			3.805	0.4032	85.25	47525.	0.100	
F-533	3A09-120-24			3.826	0.4013	87.75	48920.	0.150	
AVERAGE VALUE				3.810	0.4056		44974.		
STANDARD DEVIATION				0.015	0.0014		5001.		
COEFFICIENT OF VARIATION				0.004	0.003		0.111		
F-593	-135-01	70	5000	3.796	0.3998	76.20	42730.	0.300	
F-547	-135-02			3.801	0.3955	71.40	39510.	0.000	4 mil subsurface void in cleavage area.
F-576	-135-03			3.804	0.3995	74.00	40940.	0.100	
F-571	-135-04			3.800	0.4000	82.00	45125.	0.200	G.S. = 3.5 μ
F-590	-135-05			3.782	0.4003	81.80	45200.	0.300	
F-578	-135-06			3.782	0.3997	90.20	50130.	0.000	
AVERAGE VALUE				3.796	0.3989		43939.		
STANDARD DEVIATION				0.010	0.0018		2779.		
COEFFICIENT OF VARIATION				0.002	0.004		0.086		
F-597	3A09-136-01	70	5000	3.804	0.4061	80.75	45135.	0.250	
F-573	3A09-136-02			3.801	0.4033	69.60	38725.	0.150	G.S. = 5.2 μ
F-569	3A09-136-03			3.799	0.3998	80.80	44865.	0.150	
F-575	3A09-136-04			3.798	0.4076	83.60	48610.	0.050	
F-598	3A09-136-05			3.807	0.4011	75.60	42020.	0.400	
AVERAGE VALUE				3.801	0.4035		43470.		
STANDARD DEVIATION				0.004	0.0035		3130.		
COEFFICIENT OF VARIATION				0.001	0.008		0.072		
F-584	3A09-137-01	70	5000	3.794	0.4204	80.20	44350.	0.200	
F-582	3A09-137-02			3.779	0.3988	67.60	37180.	0.300	
F-565	3A09-137-03			3.781	0.4001	74.00	40545.	0.000	
F-579	3A09-137-04			3.782	0.3972	73.40	40575.	0.250	
F-581	3A09-137-05			3.761	0.3998	79.20	41510.	0.350	
F-599	3A09-137-06			3.774	0.4008	78.00	43500.	0.050	G.S. = 3.9 μ
AVERAGE VALUE				3.775	0.3988		41276.		
STANDARD DEVIATION				0.013	0.0020		2540.		
COEFFICIENT OF VARIATION				0.003	0.005		0.061		
F-580	-138-A01	70	5000	3.754	0.3940	74.40	41225.	0.100	
F-586	-138-A02			3.752	0.3934	72.00	40020.	0.100	
F-577	-138-A03			3.764	0.3940	77.40	42825.	0.050	
F-587	-138-A04			3.752	0.3937	77.60	42850.	0.350	
F-595	-138-B01			3.758	0.3933	64.60	35650.	0.250	4 mil void in fracture.
F-588	-138-B02			3.753	0.3937	73.00	40210.	0.200	G.S. 3.0
F-596	-138-B03			3.754	0.3961	67.40	37510.	0.350	4x8 mil void in fracture
F-574	-138-B04			3.765	0.3968	75.40	41680.	0.100	
AVERAGE VALUE				3.756	0.3946		41488.		
STANDARD DEVIATION				0.006	0.0014		1228.		
COEFFICIENT OF VARIATION				0.001	0.003		0.029		

TABLE XXIV (CONTINUED)

SRI RUN NUMBER	SPECIMEN NUMBER	TEST TEMP DEGR F	STRESS RATE SI/SEC	BULK DENSITY GM/CM <sup>3</sup>	SONIC VELOCITY IN/MICRO SEC	LOAD AT FRACTURE POUNDS	FRACTURE STRESS PSI	FRACTURE LOCATION IN. FROM MIDSPAN	REMARKS
F-530	3A09-144-11	70	5000	3.840	0.3968	92.80	51450.	0.100	
F-531	3A09-144-12			3.801	0.3932	93.40	52120.	0.150	
F-532	3A09-144-13			3.839	0.3968	80.20	44350.	0.090	
F-533	3A09-144-14			3.847	0.3968	85.80	47570.	0.230	
F-534	3A09-144-21			3.832	0.3968	81.40	45220.	0.130	
F-534	3A09-144-22			3.831	0.3952	94.40	52200.	0.330+0.400	
F-549	3A09-144-23			3.828	0.3955	88.40	48910.	0.300	G.S. = 3.7 $\mu$
F-555	3A09-144-24			3.942	0.3967	84.20	48560.	0.250	
AVERAGE VALUE				3.832	0.3959		48572.		
STANDARD DEVIATION				0.014	0.0013		5083.		
COEFFICIENT OF VARIATION				0.003	0.003		0.063		
F-529	4A11-125-01	70	5000	3.805	0.3972	84.30	47390.	0.000	
F-540	4A11-125-02			3.710	0.3856	77.00	43030.	0.200	
F-541	4A11-125-03			3.718	0.3860	71.25	39720.	0.250	
F-542	4A11-125-04			3.721	0.3867	72.25	40540.	0.300+0.350	
F-543	4A11-125-05			3.721	0.3874	70.00	39350.	0.350	
AVERAGE VALUE				3.734	0.3869		42006.		
STANDARD DEVIATION				0.039	0.0048		3333.		
COEFFICIENT OF VARIATION				0.010	0.012		0.079		
F-534	5A13-127-01	70	5000	3.774	0.3921	79.00	41090.	0.230	
F-535	5A13-127-02			3.752	0.3951	70.00	39020.	0.375	
F-536	5A13-127-03			3.749	0.3935	69.60	38410.	0.500	
F-537	5A13-127-04			3.756	0.3928	75.00	40775.	0.350	
F-538	5A13-127-05			3.795	0.3949	81.25	45430.	0.130	
AVERAGE VALUE				3.763	0.3936		40944.		
STANDARD DEVIATION				0.019	0.0013		2752.		
COEFFICIENT OF VARIATION				0.005	0.003		0.067		
F-558	5A13-148-01	70	5000	3.781	0.3872	79.40	42160.	0.150	G.S. = 3.1 $\mu$
F-561	5A13-148-02			3.792	0.3865	77.80	40700.	0.150	
F-564	5A13-148-03			3.785	0.3861	72.20	40270.	0.350	G.S. = 3.2 $\mu$
F-559	5A13-148-04			3.746	0.3879	60.80	45000.	0.250	
F-557	5A13-148-05			3.782	0.3882	77.40	42990.	0.200	
AVERAGE VALUE				3.785	0.3871		42224.		
STANDARD DEVIATION				0.005	0.0009		1900.		
COEFFICIENT OF VARIATION				0.001	0.002		0.043		
F-600	5A13-149-B21	70	5000	3.799	0.3937	74.50	41600.	0.400	
F-602	5A13-149-B22			3.795	0.3933	79.00	40775.	0.300	
F-607	5A13-149-B23			3.791	0.3918	71.50	39640.	0.200	
F-606	5A13-149-B24			3.803	0.3935	74.50	41825.	0.400	
F-610	5A13-149-B25			3.792	0.3931	75.00	41870.	0.300	
F-612	5A13-149-B26			3.790	0.3951	80.25	44690.	0.350+0.400	
F-603	5A13-149-B27			3.798	0.3946	81.00	45290.	0.350	
AVERAGE VALUE				3.795	0.3938		42301.		
STANDARD DEVIATION				0.006	0.0015		1983.		
COEFFICIENT OF VARIATION				0.001	0.004		0.046		
F-623	5A13-151-01	70	5000	3.907*	0.4177*	70.75	40200.	0.350	
F-629	5A13-151-02			3.874	0.4148	79.75	43510.	0.350	
F-615	5A13-151-03			3.875	0.4152	88.25	48680.	0.350	
F-632	5A13-151-04			3.876	0.4149	79.75	45220.	0.050	
F-610	5A13-151-05			3.873	0.4140	84.25	47580.	0.375	
F-618	5A13-151-06			3.884	0.4144	81.25	46350.	0.200	
F-619	5A13-151-07			3.908	0.4165	58.50	80710.	0.350	
AVERAGE VALUE				3.885	0.4153		46321.		
STANDARD DEVIATION				0.016	0.0013		3344.		
COEFFICIENT OF VARIATION				0.004	0.003		0.072		
F-616	5A13-152-01	70	5000	3.884*	0.4150*	71.50	40280.	0.050	
F-625	5A13-152-02			3.881	0.4095	77.75	43840.	0.340	
F-634	5A13-152-03			3.879	0.4079	70.50	39840.	0.250	
F-624	5A13-152-04			3.843	0.4085	80.50	45550.	0.250	
F-631	5A13-152-05			3.837	0.4076	67.75	38320.	0.100	
F-620	5A13-152-06			3.827	0.4088	75.00	42290.	0.350	
F-627	5A13-152-07			3.880	0.4145	83.75	47320.	0.150	
AVERAGE VALUE				3.866	0.4102		42491.		
STANDARD DEVIATION				0.023	0.0031		3262.		
COEFFICIENT OF VARIATION				0.006	0.007		0.076		
F-635	5A13-153-01	70	5000	3.863*	0.4122*	69.00	38980.	0.250	
F-621	5A13-153-02			3.822	0.4078	70.00	39710.	0.250	
F-633	5A13-153-03			3.814	0.4070	70.00	39790.	0.250	
F-622	5A13-153-04			3.823	0.4059	75.25	42850.	0.000	
F-626	5A13-153-05			3.820	0.4071	18.50	38625.	0.100	
F-617	5A13-153-06			3.821	0.4079	12.25	40660.	0.100	
F-624	5A13-153-07			3.865	0.4113	14.00	41730.	0.200	
AVERAGE VALUE				3.832	0.4085		40287.		
STANDARD DEVIATION				0.022	0.0023		1430.		
COEFFICIENT OF VARIATION				0.005	0.005		0.035		

\*Fairly strong density and velocity gradients from outer (Specimens 1 and 7) to inner material.

TABLE XXV

AVERAGE DATA FOR REGRESSION ANALYSIS OF STRENGTH VERSUS POROSITY, GRAIN SIZE, AND GREEN DENSITY

Blank	No. Spec.	Green Density	Firing Parameters	Fired Density	Porosity	Grain Size	Average Flexure Strength	Strength Normalised to G.S. = 3.7 $\mu$	Strength Normalised to Porosity = 0.0451	Strength Normalised to G.S. = 3.7 $\mu$ and Porosity = 0.0451
1A02	20	2.51	314 @ 2:00	3.329	0.0404	3.5	51,450	50,901	49,439	48,912
2A04	20	2.56	314 @ 2:45	3.804	0.0466	3.6	49,810	49,547	53,448	50,382
2A05	11	2.55	314 @ 4:00	3.810	0.0451	3.0	49,740	47,768	49,768	47,768
2A05-G47(HF)	2	2.65	33 @ 2:00	3.851	0.0348	6.9	45,280	51,061	51,491	46,789
1A06	14	2.585	314 @ 1:45	3.816	0.0436	3.8	51,830	52,097	51,174	51,438
2A07	24	2.60	314 @ 2:00	3.810	0.0451	3.3	49,010	47,940	49,010	47,940
2A07-117	4	2.51	314 @ 3:15	3.801	0.0474	4.2	42,176	43,219	43,007	44,071
2A07-140 <sup>1</sup>	9	2.55	31 @ 3:00	3.802	0.0471	3.5	48,130	47,674	49,012	48,490
-141										
-142										
2A08	21	2.62	314 @ 2:30	3.813	0.0444	3.7	46,440	46,440	46,165	46,165
3A09	20	2.55	314 @ 2:00	3.829	0.0404	3.7	48,283	48,283	46,396	46,395
3A09-081 <sup>1</sup>	20	2.57	314 @ 2:30	3.836	0.0386	3.8	47,710	47,956	45,150	45,383
-082										
-084										
3A09-120	5	2.50	31 @ 9:00	3.810	0.0451	5.5	44,975	48,547	44,975	48,547
3A09-144 <sup>2</sup>	8	2.54	31 @ 5:30	3.832	0.0395	3.7	48,572	48,572	46,318	46,318
-135	6	-----	314 @ 12:30	3.754	0.0491	3.5	43,939	43,471	45,455	44,971
3A09-136	5		314 @ 9:00	3.801	0.0474	5.2	43,470	46,418	44,326	47,332
3A09-137	5	2.57	31 @ 1:00	3.775	0.0539	3.9	41,276	41,697	44,475	44,928
-138 <sup>2</sup>	8	2.54	31 @ 4:00	3.756	0.0586	3.0	41,468	39,824	46,499	44,656
3A10-087	26	2.52	314 @ 5:00	3.820	0.0426	3.6	47,990	47,638	46,885	46,638
3A10-088	36	2.57	314 @ 5:00	3.835	0.0388	3.7	50,678	50,678	49,040	49,040
4A11-089	20	2.55	---	1.775	0.0539	3.4	44,320	43,603	47,755	46,982
4A11-112(HF)	50	2.52	33 @ 1:30	3.829	0.0404	6.7	40,920	45,884	39,320	44,090
4A11-125	5	2.49	314 @ 2:15	3.735	0.0639	3.7	42,010	42,010	49,273	49,273
2A12-095	7	2.60	314 @ 12:30	3.783	0.0519	3.2	48,336	47,001	51,206	49,752
2A12-096	13	2.57	314 @ 12:30	3.777	0.0534	3.9	47,729	48,216	51,210	51,733
5A13-101	7	-----	314 @ 5:00	3.800	0.0476	3.7	42,026	42,026	42,927	42,926
5A13-102	16	2.55	314 @ 5:00	3.795	0.0489	4.2	44,337	45,434	45,789	46,922
5A13-103	16	2.54	314 @ 5:30	3.804	0.0466	---	46,111	---	---	---
5A13-127	5	2.47	314 @ 9:00	3.766	0.0561	4.7	40,944	42,877	44,948	47,070
5A13-148 <sup>1</sup>	5	2.50	31 @ 5:30	3.786	0.0511	3.2	42,225	41,059	44,430	43,203
5A13-149 <sup>1</sup>	7	2.52	31 @ 2:00	3.795	0.0489	4.2	42,301	43,347	43,687	44,767
5A13-151 <sup>1</sup>	7	2.59	314 @ 1:30	3.885	0.0263	4.7	46,321	48,508	39,492	41,357
5A13-152 <sup>1</sup>	7	2.65	314 @ 1:00	3.849	0.0353	3.9	42,491	42,924	39,101	39,500
5A13-153 <sup>1</sup>	7	2.66	314 @ 1:00	3.832	0.0396	3.6	40,288	40,175	38,451	38,249
6A14-104	8	-----	314 @ 1:30	3.831	0.0398	4.1	46,107	47,028	44,080	44,961
6A14-106	12	2.61	314 @ 1:30	3.820	0.0426	3.9	50,095	50,606	49,044	49,544
6A17	21	2.61	314 @ 2:00	3.807	0.0459	3.8	49,870	50,127	50,269	50,468
MOR	2	-----	314 @ 3:00	3.817	0.0434	5.2	49,925	53,311	49,210	52,547

## Notes:

1. Includes only those specimen that were not refired
2. Parts pressed from a body called XAD997B which was a mixture 3 parts of the original body (XAD997A) and 2 parts of a new body (PS-144-1) from identical powder but different binder
3. Part pressed from a mixture of 1 part each of PS-144-1 and PS-176-5, also from identical powder but different binder
4. Part pressed from a mixture of 2 parts XAD997A and 3 parts PS-144-1
5. Part pressed from 100% PS-144-1

## APPENDIX

### THE STATISTICS OF FRACTURE

The statistics of fracture and the Weibull Distribution was examined. For this purpose, the Weibull Distribution function was used in the following form:

$$S = \exp \left[ - \int_V \left( \frac{\sigma}{\sigma_o} \right)^m dV \right]$$

where

- S = survival probability
- $\sigma$  = tensile stress of arbitrary spatial distribution
- $\sigma_o$  = constant
- m = Weibull Modulus
- V = volume subject to tension

The question of probability of fracture within some specified region of a test specimen relates the relative size of the region in question to the total specimen volume. For a simple example, the probability of fracture within a given region of a specimen subject to uniform tension is found by the ratio of the given region's volume to that of the whole specimen. This process may be generalized for any given stress distribution by finding the size of the specimen having the same probability of fracture but subject to uniform tension only. The ratios of such "equivalent" volumes represent the relative frequency of fracture expected to occur in the respective volumes.

#### Fracture Source Distribution

Beginning with the Weibull Distribution

$$S = \exp \left[ - \int_V \left( \frac{\sigma}{\sigma_o} \right)^m dV \right]$$

this can be altered by choosing normalized variables describing the stress distribution and the volume.

$$\sigma = \sigma_T \cdot f(\xi)$$

$$dV = C V_T d\xi$$

where

$\sigma_T$  = reference stress, usually maximum tension  
 $V_T$  = volume in tension  
 $C$  = constant  
 $\xi$  = normalized position variable

thus

$$S = \exp \left[ - \left( \frac{\sigma_T}{\sigma_0} \right)^m V_T \int_{\xi_1}^{\xi_2} C f(\xi)^m d\xi \right]$$

This integral is a function of the Weibull Modulus  $m$  and the limits of integration  $\xi_1$  and  $\xi_2$

$$\int_{\xi_1}^{\xi_2} C f(\xi)^m d\xi = G(\xi_1, \xi_2, m)$$

so that

$$S = \exp \left[ - \left( \frac{\sigma_T}{\sigma_0} \right)^m V_T \cdot G(\xi_1, \xi_2, m) \right]$$

This equation represents a portion of a specimen whose overall distribution integral  $G_T$  is given by the total limits as  $G(u, v, m)$ . Using  $\sigma_T$  as a convenient reference stress, the volume subject to a uniform tension  $\sigma_T$  having the same probability of failure as the whole specimen is given by

$$S = \exp \left[ - \left( \frac{\sigma_T}{\sigma_0} \right)^m G_T V_T \right] = \exp \left[ - \left( \frac{\sigma_T}{\sigma_0} \right)^m V_{EQ_T} \right]$$

For a subsidiary portion within the limits  $(\xi_1, \xi_2)$  the same process yields

$$S_S = \exp \left[ - \left( \frac{\sigma_T}{\sigma_0} \right)^m V_T G(\xi_1, \xi_2, m) \right] = \exp \left[ - \left( \frac{\sigma_T}{\sigma_0} \right)^m V_{EQ_S} \right]$$

The probability,  $F_S$ , that fracture will initiate in the subsidiary volume is simply the ratio of its "equivalent" volume  $V_{EQS}$  to the equivalent volume of the whole specimen  $V_{EQ_T}$  or

$$F_S = \frac{V_{EQS}}{V_{EQ_T}} = \frac{G(\xi_1, \xi_2, m)}{G(u, v, m)}$$

For a rectangular flexural specimen the dimensionless functions are

$$\sigma = \sigma_T \xi, \quad f(\xi) = \xi$$

where  $\xi$  is the dimensionless transverse distance from the neutral plane and the volume under tension is

$$dV = V_T d\xi$$

$$G(\xi_1, \xi_2, m) = \int_{\xi_1}^{\xi_2} \xi^m d\xi$$

Putting in limits for the whole specimen  $0 \leq \xi \leq 1$  gives

$$G_T(0, 1, m) = \int_0^1 \xi^m d\xi = \frac{1}{m+1}$$

and for a subsidiary portion  $0 \leq \xi \leq \xi$

$$G_S = (0, \xi, m) = \int_0^{\xi} \xi^m d\xi = \frac{\xi^{m+1}}{m+1}$$

Now the probability of fracture initiating between the neutral axis and the fraction  $\xi$  of the beam half-height is

$$F = \frac{G_S}{G_T} = \frac{\xi^{m+1}}{\frac{1}{m+1}} \cdot \frac{m+1}{1} = \xi^{m+1}$$



For a specimen subjected to uniform tension

$$\sigma = \sigma_T, f(\xi) = 1$$

$$dV = 2V_T \cdot \xi d\xi$$

so that

$$G(\xi_1, \xi_2, m) = \int_{\xi_1}^{\xi_2} 2\xi d\xi$$

For the whole specimen

$$G_T(0, 1, m) = 2 \int_0^1 \xi d\xi = 2 \left[ \frac{\xi^2}{2} \right]_0^1 = 1$$

and for a subsidiary portion

$$G_B(0, \xi, m) = 2 \int_0^\xi \xi d\xi = \xi^2$$

and the probability of fracture is given by

$$F = \frac{G_S}{G_T} = \xi^2$$

which is independent of m.

#### Comparisons Between Specimens

For a group of specimens with a particular form of stress distribution the Weibull Distribution function reduces to

$$S = \exp \left[ - \left( \frac{\sigma_T}{\sigma_0} \right)^m V_{EQ_T} \right]$$

where

- S = specimen survival probability
- $\sigma_T$  = a convenient reference stress such as the maximum stress in the specimen
- $\sigma_0$  = constant
- $V_{EQ_T}$  = equivalent volume in tension
- m = Weibull modulus

The differential of S is

$$dS = \exp\left[-\left(\frac{\sigma_T}{\sigma_0}\right)^m V_{EQ_T}\right] \left[ -m \left(\frac{\sigma_T}{\sigma_0}\right)^{m-1} \frac{V_{EQ_T}}{\sigma_0} \right] d\sigma_T$$

The mean failing stress  $\bar{\sigma}_T$  is given by

$$\begin{aligned} \bar{\sigma}_T &= \frac{\int_{S=0}^1 \sigma_T dS}{\int_{S=0}^1 dS} = \int_{S=0}^1 \sigma_T dS \\ &= \sigma_0 \left( V_{EQ_T} \right)^{1/m} \int_{\sigma_T=0}^{\infty} \exp\left[-\left(\frac{\sigma_T}{\sigma_0}\right)^m V_{EQ_T}\right] \left[ \frac{\sigma_T}{\sigma_0} \left( V_{EQ_T} \right)^{1/m} \right] \left[ m \left(\frac{\sigma_T}{\sigma_0}\right)^{m-1} \frac{V_{EQ_T}}{\sigma_0} \right] d\sigma_T \end{aligned}$$

Remembering that the Gamma Function is defined as

$$\Gamma(m) = \int_0^{\infty} e^{-x} x^{m-1} dx$$

and

$$\Gamma(1+1/m) = \int_0^{\infty} e^{-x} x^{1/m} dx$$

The mean stress integral is of this latter form when  $x = \left(\frac{\sigma_T}{\sigma_0}\right)^m V_{EQ_T}$  and therefore

$$\bar{\sigma}_T = \sigma_0 (V_{EQ_T})^{-1/m} \Gamma(1+1/m)$$

Substitution into the reduced form of the Weibull Distribution function yields

$$S = \exp\left[\beta^m \Gamma^m\right]$$

where

$$\beta = \text{normalized stress} = \frac{\sigma_T}{\bar{\sigma}_T}$$

$$\Gamma = \Gamma(1+1/m)$$

The same transformation can also be made in the same way if

$$S = \exp \left[ - \int_A \left( \frac{\sigma_T}{\sigma_0} \right)^m dA \right]$$

where

$\int_A$  is an area integral instead of a volume integral.

If the sample average  $\bar{\sigma}_T$  is accepted ( $\beta = \sigma_T / \bar{\sigma}_T$ ) the transformed form of the distribution shows that there is only one parameter left to define the distribution, the Weibull Modulus  $m$ . Intuitively, it would be expected that the value of  $m$  for a surface effect would be different from one for a volume effect.

Recall that the reduced form of the Weibull Distribution function for any particular form of stress is:

$$S = \exp \left[ - \left( \frac{\sigma_T}{\sigma_0} \right)^m V_{EQ_T} \right]$$

where

- $S$  = specimen survival probability
- $\sigma_T$  = a convenient reference stress such as the maximum stress in the specimen
- $\sigma_0$  = a constant
- $V_{EQ_T}$  = equivalent volume in tension
- $m$  = Weibull modulus

Two different volumes having the same probability of survival are related as

$$S = \exp \left[ - \left( \frac{\sigma_{T1}}{\sigma_{01}} \right)^{m_1} V_{EQ_{T1}} \right] = \exp \left[ - \left( \frac{\sigma_{T2}}{\sigma_{02}} \right)^{m_2} V_{EQ_{T2}} \right]$$

$$\left( \frac{\sigma_{T1}}{\sigma_{01}} \right)^{m_1} V_{EQ_{T1}} = \left( \frac{\sigma_{T2}}{\sigma_{02}} \right)^{m_2} V_{EQ_{T2}}$$

If the forms of the distribution are the same, then  $\sigma_{O_1} = \sigma_{O_2}$  and  $m_1 = m_2$  and

$$\left( \frac{\sigma_{T_1}}{\sigma_{T_2}} \right)^m = \frac{V_{EQ_{T_2}}}{V_{EQ_{T_1}}} \quad \text{or}$$

$$\frac{\sigma_{T_1}}{\sigma_{T_2}} = \left( \frac{V_{EQ_{T_2}}}{V_{EQ_{T_1}}} \right)^{1/m}$$

For uniform tension,  $V_{EQ_T} = V_T$ . Then comparing two different volumes in uniform tension gives

$$\frac{\sigma_{T_1}}{\sigma_{T_2}} = \left( \frac{V_{T_2}}{V_{T_1}} \right)^{1/m}$$

For a rectangular beam in pure bending,  $V_{EQ_T} = V_F \frac{1}{m+1}$ . Comparing a volume in uniform tension and a volume of a rectangular beam in pure bending gives

$$\frac{\sigma_T}{\sigma_F} = \left[ \frac{V_F}{V_T} \cdot \frac{1}{m+1} \right]^{1/m}$$